doi : 10.17596/0003215

R/V *Mirai* Cruise Report

MR09-01

Subtropical Ocean in the South Pacific

10th April – 3rd July

Japan Agency for Marine-Earth Science and Technology

(JAMSTEC)

Cruise Report ERRATA of the Nutrients part

page	Error	Correction
116	potassium nitrate CAS No. 7757-91-1	potassium nitrate CAS No. 7757-79-1

Content

I. Introduction

It is well known that climate changes of a timescale more than a decade are influenced by changes of oceanic conditions. Among a lot of oceanic changes, we focus on transport and accumulation of anthropogenic CO_2 and heat in the ocean, both of which are important for global warming. Accordingly we are aimed at clarifying temporal changes of the transport and accumulation quantitatively. In doing so, we pay a special attention to water masses of the Southern Ocean's origin, which play an important role in transporting anthropogenic CO_2 and heat into the ocean's interior. With this purpose, we have so far re-occupied historical observation lines, mainly in the Pacific Ocean.

This cruise is a reoccupation of the hydrographic section called 'WHP-P21', which was observed by an ocean science group of United States of America (USA) in 1994 as a part of World Ocean Circulation Experiment (WOCE). The dataset is included in the data base of Climate Variability and Predictability (CLIVAR) and Carbon Hydrographic Data Office (http://whpo.ucsd.edu/). We will compare physical and chemical properties along section WHP-P21 with those obtained in 1994 to detect and evaluate long-term changes of the marine environment in the Pacific.

Reoccupations of the WOCE hydrographic sections are now in progress by international cooperation in ocean science community, under the framework of CLIVAR, which is as part of World Climate Research Programme (WCRP) and International Ocean Carbon Coordination Project (IOCCP). Our research is planned as a contribution to this international projects supported by World Meteorological Organization (WMO), International Council for Science (ICSU) / Scientific Committee on Oceanic Research (SCOR) and United Nations Educational, Scientific and Cultural Organization (UNESCO)/Intergovernmental Oceanographic Commission (IOC), and the results and data will be published by 2010 for worldwide use.

The other purposes of this cruise are as follows:

1) to observe surface meteorological and hydrological parameters as a basic data of meteorology and oceanography such as studies on flux exchange, air-sea interaction and so on,

2) to observe sea bottom topography, gravity and magnetic fields along the cruise track to understand the dynamics of ocean plate and accompanying geophysical activities,

3) to observe biogeochemical parameters to study material (carbon, nitrate, etc) cycle in the ocean,

4) to observe greenhouse gases in the atmosphere and the ocean to study their cycle from bio-geochemical aspect.

5) to estimate diapycnal diffusitivity in the deep ocean.

II. Observation

1. Cruise Narrative

Akihiko Murata (RIGC/JAMSTEC)

Hiroshi Uchida (RIGC/JAMSTEC)

Kenichi Sasaki (MIO/JAMSTEC)

1.1. Basic Information

Cruise track:	Figs. 1.1.1 and 1.1.2
Cruise code:	MR09-01
Expocode	49NZ20090410
GHPO section designation:	P21
Ship name:	R/V Mirai
Ports of call:	Leg 1, Valparaiso, Chile - Papeete, Tahiti Leg 2a, Papeete, Tahiti - Papeete, Tahiti Leg 2b, Papeete, Tahiti - Brisbane, Australia Leg 3, Brisbane, Australia - Moji, Japan
Cruise date:	Leg 1, April 10, 2009 - May 19, 2009 Leg 2a, May 21, 2009 - May 24, 2009 Leg 2b, May 25, 2009 - June 19, 2009 Leg 3, June 20, 2009 - July 3, 2009
Chief scientists:	Leg 1, Akihiko Murata Leg 2, Hiroshi Uchida Leg 3, Kenichi Sasaki
	Ocean Climate Change Research Program Research Institute for Global Change (RIGC) Japan Agency for Marine-Earth Science and Technology (JAMSTEC)

Number of Stations: Leg 1, 140 Stations
Leg 2a, 8 Stations
Leg 2b, 109 Stations
Leg 3, 0 Station

Geographic Boundaries (for hydrographic stations):
24-59.81S - 15-29.52S
153-44.52E - 75-09.86W

Floats and drifters deployed: 5 floats

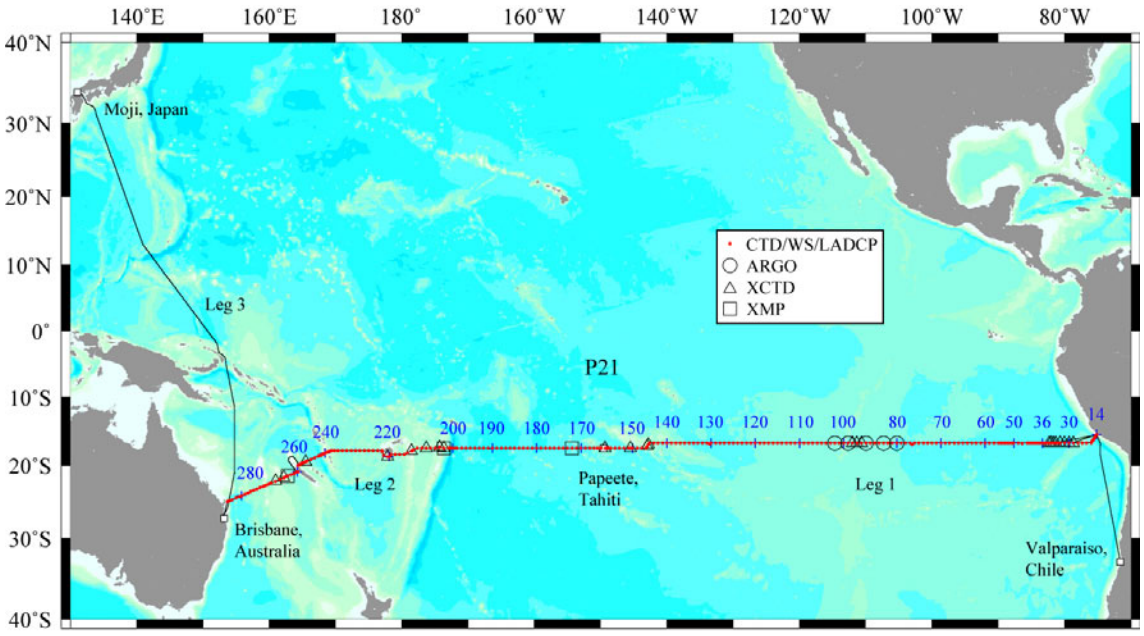

Fig. 1.1.1 Station map.

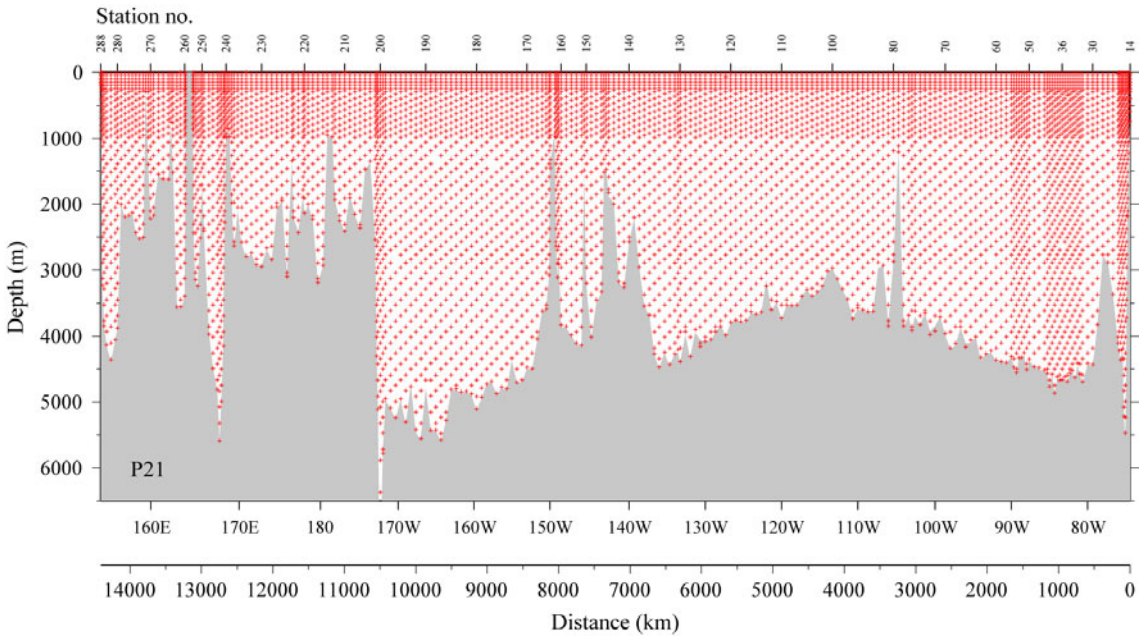

Fig. 1.1.2 Water sampling positions.

1.2. List of Cruise Participants

List of Participants for leg 1

Akihiko Murata	Chief scientist/carbon/water sampling	RIGC/JAMSTEC
Hiroshi Uchida	CTD/water sampling	RIGC/JAMSTEC
Sinya Kouketsu	LADCP/ADCP/water sampling	RIGC/JAMSTEC
Yuichiro Kumamoto	DO/thermosalinograph /$\Delta^{14}C$	RIGC/JAMSTEC
Kenichi Sasaki	CFCs	MIO/JAMSTEC
Hirokatsu Uno	CTD/water sampling	MWJ
Kenichi Katayama	CTD/water sampling	MWJ
Shinsuke Toyoda	CTD/water sampling	MWJ
Hiroyuki Hayashi	CTD/water sampling	MWJ
Tatsuya Tanaka	Salinity	MWJ
Akira Watanabe	Salinity	MWJ
Fuyuki Shibata	DO/water sampling	MWJ
Miyo Ikeda	DO/water sampling	MWJ
Misato Kuwahara	DO/water sampling	MWJ
Shinichiro Yokogawa	Nutrients	MWJ
Ayumi Takeuchi	Nutrients	MWJ
Kohei Miura	Nutrients	MWJ
Kenichiro Sato	Chief technologist/nutrients/water sampling	MWJ

Ai Ueda	Water sampling	MWJ
Yuichi Sonoyama	CFCs	MWJ
Katsunori Sagishima	CFCs	MWJ
Shoko Tatamisashi	CFCs	MWJ
Tomonori Watai	pH/total alkalinity	MWJ
Ayaka Hatsuyama	pH/total alkalinity	MWJ
Minoru Kamata	DIC	MWJ
Yoshiko Ishikawa	DIC	MWJ
Shinya Okumura	Meteorology/geophysics/ADCP/XCTD	GODI
Ryo Kimura	Meteorology/geophysics/ADCP/XCTD	GODI
Yosuke Yuki	Meteorology/geophysics/ADCP/XCTD	GODI
Takuhei Shiozaki	Biology/water sampling	The University of Tokyo
Satoshi Kitajima	Biology/water sampling	The University of Tokyo
Taketoshi Kodama	Biology/water sampling	The University of Tokyo
Hiroyuki Kurotori	Biology/water sampling	The University of Tokyo
Osamu Yoshida	CH_4 and N_2O/water sampling	Rakuno Gakuen University
Sho Imai	CH_4 and N_2O/water sampling	Rakuno Gakuen University
Chiho Kubota	CH_4 and N_2O/water sampling	Rakuno Gakuen University
Wolfgang Schneider	CTD/water sampling	COPAS/Universidad de Concepcion, Chile
Lorena Graciela Márquez Ismodes	Observer	Peruvian Navy

List of Participants for leg 2a

Hiroshi Uchida	Chief Scientist/CTD/water sampling	RIGC/JAMSTEC
Shinya Kouketsu	LADCP/ADCP/water sampling	RIG C/JAMSTEC
Yuichiro Kumamoto	DO/thermosalinograph /$\Delta^{14}C$	RIGC/JAMSTEC
Toshimasa Doi	LADCP /water sampling	RIGC/JAMSTEC
Katsuro Katsumata	XMP/LADCP/water sampling	RIGC/JAMSTEC
Kenichi Sasaki	CFCs	MIO/JAMSTEC
Hirokatsu Uno	CTD/water sampling	MWJ
Kenichi Katayama	CTD/water sampling	MWJ
Shinsuke Toyoda	CTD/water sampling	MWJ
Hiroyuki Hayashi	CTD/water sampling	MWJ

Tatsuya Tanaka	Salinity	MWJ
Akira Watanabe	Salinity	MWJ
Fuyuki Shibata	DO/water sampling	MWJ
Miyo Ikeda	DO/water sampling	MWJ
Misato Kuwahara	DO/water sampling	MWJ
Shinichiro Yokogawa	Nutrients	MWJ
Ayumi Takeuchi	Nutrients	MWJ
Kohei Miura	Nutrients	MWJ
Kenichiro Sato	Chief technologist/nutrients/water sampling	MWJ
Ai Ueda	Water sampling	MWJ
Yuichi Sonoyama	CFCs	MWJ
Katsunori Sagishima	CFCs	MWJ
Shoko Tatamisashi	CFCs	MWJ
Tomonori Watai	pH/total alkalinity	MWJ
Ayaka Hatsuyama	pH/total alkalinity	MWJ
Minoru Kamata	DIC	MWJ
Yoshiko Ishikawa	DIC	MWJ
Shinya Okumura	Meteorology/geophysics/ADCP/XCTD	GODI
Ryo Kimura	Meteorology/geophysics/ADCP/XCTD	GODI
Yosuke Yuki	Meteorology/geophysics/ADCP/XCTD	GODI
Takuhei Shiozaki	Biology/water sampling	The University of Tokyo
Satoshi Kitajima	Biology/water sampling	The University of Tokyo
Taketoshi Kodama	Biology/water sampling	The University of Tokyo
Hiroyuki Kurotori	Biology/water sampling	The University of Tokyo
Sho Imai	CH_4 and N_2O/water sampling	Rakuno Gakuen University
Chiho Kubota	CH_4 and N_2O/water sampling	Rakuno Gakuen University
Wolfgang Schneider	CTD/water sampling	COPAS/Universidad de Concepcion, Chile
Camillia Pauline Garae	Observer	Department of Geology Mines and Water Resources, Vanuatu
Harish Pratap	Observer	Fiji Meteorological Services, Fiji

List of Participants for leg 2b

Hiroshi Uchida	Chief scientist/CTD/water sampling	RIGC/JAMSTEC
Yuichiro Kumamoto	DO/thermosalinograph/$\Delta^{14}C$	RIGC/JAMSTEC
Toshimasa Doi	LADCP/water sampling	RIGC/JAMSTEC
Katsuro Katsumata	XMP/LADCP/water sampling	RIGC/JAMSTEC
Kenichi Sasaki	CFCs	MIO / JAMSTEC
Fujio Kobayashi	Salinity	MWJ
Akira Watanabe	Salinity	MWJ
Miyo Ikeda	DO/water sampling	MWJ
Misato Kuwahara	DO/water sampling	MWJ
Masanori Enoki	DO/water sampling	MWJ
Ayumi Takeuchi	Nutrients	MWJ
Kohei Miura	Nutrients	MWJ
Junji Matsushita	Nutrients	MWJ
Satoshi Ozawa	Chief technologist /CTD/water Sampling	MWJ
Ai Ueda	Water sampling	MWJ
Yuichi Sonoyama	CFCs	MWJ
Katsunori Sagishima	CFCs	MWJ
Shoko Tatamisashi	CFCs	MWJ
Yoshiko Ishikawa	pH/total alkalinity	MWJ
Ayaka Hatsuyama	pH/total alkalinity	MWJ
Minoru Kamata	DIC	MWJ
Yasuhiro Arii	DIC	MWJ
Tomoyuki Takamori	CTD/water sampling	MWJ
Hiroshi Matsunaga	CTD/water sampling	MWJ
Masayuki Fujisaki	CTD/water sampling	MWJ
Shungo Oshitani	CTD/water sampling	MWJ
Tatsuya Ando	Water sampling	MWJ
Tomomi Watanabe	Water sampling	MWJ
Kanako Yoshida	Water sampling	MWJ
Mami Kawai	Water sampling	MWJ
Hideki Yamamoto	Water sampling	MWJ
Satoshi Okumura	Meteorology/geophysics/ADCP/XCTD	GODI
Kazuho Yoshida	Meteorology/geophysics/ADCP/XCTD	GODI
Harumi Ota	Meteorology/geophysics/ADCP/XCTD	GODI
Takuhei Shiozaki	Biology/water sampling	The University of Tokyo
Satoshi Kitajima	Biology/water sampling	The University of Tokyo

Taketoshi Kodama	Biology/water sampling	The University of Tokyo
Hiroyuki Kurotori	Biology/water sampling	The University of Tokyo
Sho Imai	CH_4 and N_2O/water sampling	Rakuno Gakuen University
Chiho Kubota	CH_4 and N_2O/water sampling	Rakuno Gakuen University
Wolfgang Schneider	CTD/water sampling	COPAS / Universidad de Concepcion, Chile
Camillia Pauline Garae	Observer	Department of Geology Mines and Water Resources, Vanuatu
Harish Pratap	Observer	Fiji Meteorological Services, Fiji
Sakae Toyoda	CH_4 and N_2O/water sampling	TIT
Taku Watanabe	CH_4 and N_2O/water sampling	TIT

List of Participants for leg 3

Kenichi Sasaki	Chief scientist	MIO/JAMSTEC
Fujio Kobayashi	Technician	MWJ
Sinsuke Toyoda	Technician	MWJ
Fuyuki Shibata	Technician	MWJ
Sinichiro Yokogawa	Technician	MWJ
Shoko Tatamisashi	Technician	MWJ
Hideki Yamamoto	Technician	MWJ
Hironori Sato	Technician	MWJ
Yasuhiro Arii	Technician	MWJ
Ryo Kimura	Meteorology/geophysics/ADCP/XCTD	GODI
Soichiro Sueyoshi	Meteorology/geophysics/ADCP/XCTD	GODI
Takuhei Shiozaki	Biology	The University of Tokyo
Satoshi Kitajima	Biology	The University of Tokyo
Taketoshi Kodama	Biology	The University of Tokyo

Hiroyuki Kurotori	Biology	The University of Tokyo
Taku Watanabe	CH_4 and N_2O	TIT
Sho Imai	CH_4 and N_2O	Rakuno Gakuen University
Chiho Kubota	CH_4 and N_2O	Rakuno Gakuen University
Hiroshi Furutani	Air sampling	ORI/The University of Tokyo
Jinyoung Jung	Air sampling	ORI/The University of Tokyo

2. Underway Observation

2.1 Navigation

(1) Personnel

Shinya Okumura	***(GODI)***	***: Leg1***
Satoshi Okumura	***(GODI)***	***: Leg2***
Souichiro Sueyoshi	***(GODI)***	***: Leg3***
Ryo Kimura	***(GODI)***	***: Leg1, Leg3***
Yousuke Yuuki	***(GODI)***	***: Leg1***
Kazuho Yoshida	***(GODI)***	***: Leg2***
Harumi Ota	***(GODI)***	***: Leg2***

(2) Overview of the equipment

Ship's position, speed and course were provided by Radio Navigation System on R/V MIRAI. The system integrates GPS position, Log speed, Gyro heading and other basic data on a workstation. Ship's course and speed over ground are calculated from GPS position. The workstation clock is synchronized to reference clock using NTP (Network Time Protocol). Navigation data, called "SOJ data", is distributed to client computer every second, and recorded every 60 seconds.

Navigation devices are listed below.

1. GPS receiver (2sets): Trimble DS-4000 9-channel receiver, the antennas are located on Navigation deck, port and starboard side. GPS position from each receiver is converted to the position of radar mast.
2. Doppler log: Furuno DS-30, which use three acoustic beam for current measurement
3. Gyrocompass: Tokimec TG-6000, sperry mechanical gyrocompass
4. Reference clock: Symmetricom TymServ2100, GPS time server
5. Workstation Hewlett-Packard ZX2000 running HP-UX ver.11.22

(3) Data period

MR09-01 Leg1: 17:58UTC 09 Apr. 2009 to 23:59 UTC 19 May. 2009 (UTC)
MR09-01 Leg2: 00:00 UTC 21 May. 2009 to 02:00 UTC 19 Jun. 2009 (UTC)
MR09-01 Leg3: 22:50 UTC 19 Jun. 2009 to 00:00 UTC 03 Jul. 2009 (UTC)

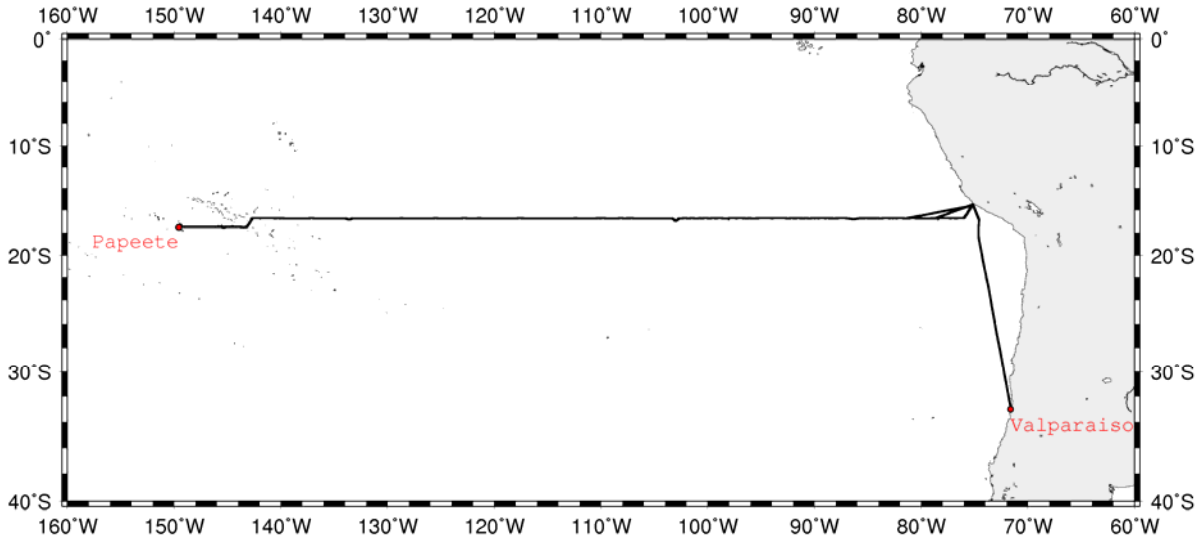

Fig.2.1-1 Cruise Track of MR09-01 Leg1

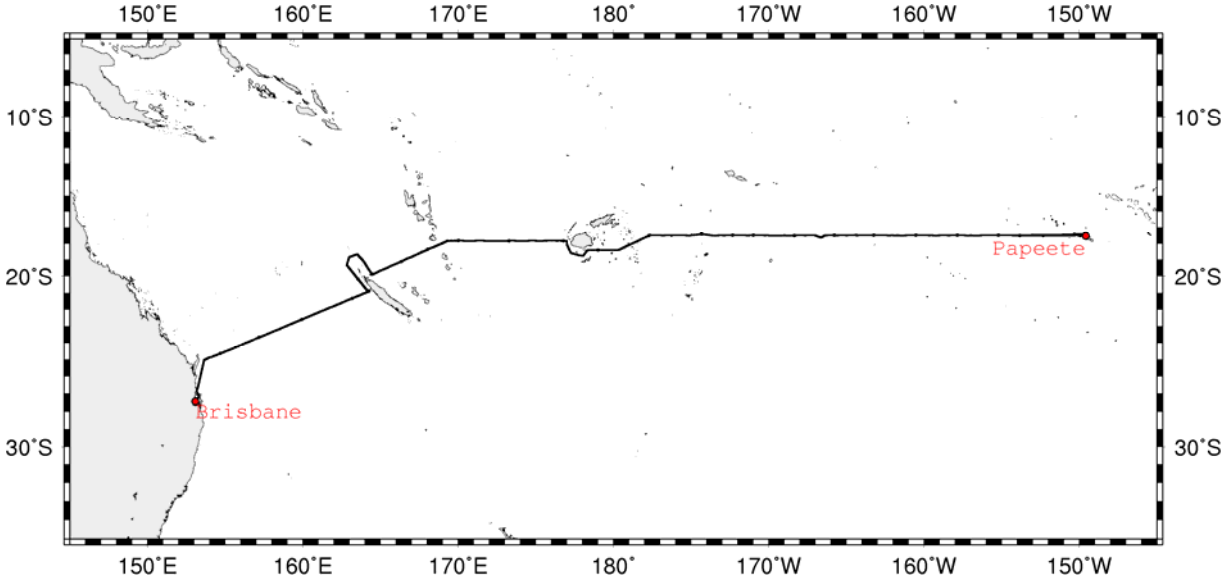

Fig.2.1-2 Cruise Track of MR09-01 Leg2

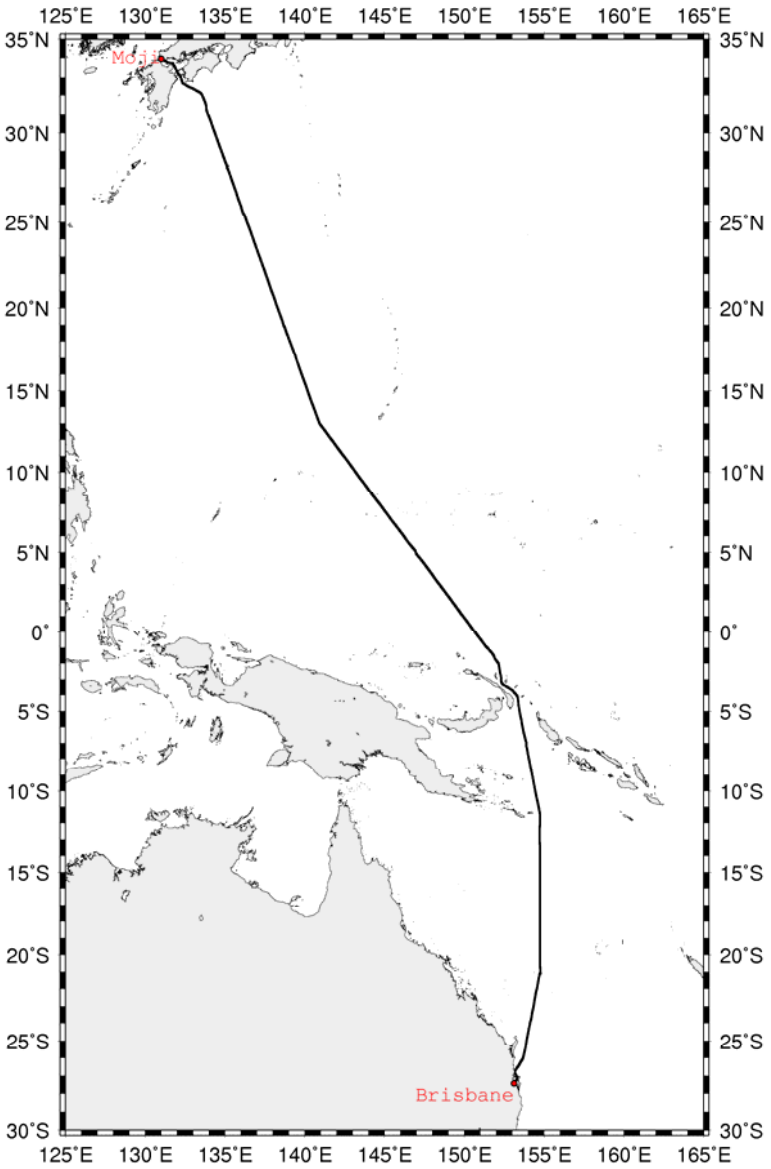

Fig.2.1-3 Cruise Track of MR09-01 Leg3

2.2 Bathymetry

(1) Personnel

Takeshi Matsumoto	*(University of the Ryukyus)*	*: Principal investigator / Not on-board*
Masao Nakanishi	*(Chiba University)*	*: Principal investigator / Not on-board*
Shinya Okumura	*(GODI): Leg1*	
Satoshi Okumura	*(GODI)*	*: Leg2*
Souichiro Sueyoshi	*(GODI)*	*: Leg3*
Ryo Kimura	*(GODI)*	*: Leg1, Leg3*
Yousuke Yuuki	*(GODI)*	*: Leg1*
Kazuho Yoshida	*(GODI)*	*: Leg2*
Harumi Ota	*(GODI)*	*: Leg2*

(2) Overview of the equipments

R/V MIRAI equipped with a Multi Beam Echo Sounding system (MBES), SEABEAM 2112.004 (SeaBeam Instruments Inc.) The main objective of MBES survey is collecting continuous bathymetry data along ship's track to make a contribution to geological and geophysical investigations and global datasets. Data interval along ship's track was max 17 seconds at 6,000 m. To get accurate sound velocity of water column for ray-path correction of acoustic multibeam, we used Surface Sound Velocimeter (SSV) data to get the sea surface (6.2m depth) sound velocity, and the deeper depth profiles were calculated using temperature and salinity profiles from the nearest CTD data by the equation in Mackenzie (1981).

System configuration and performance of SEABEAM 2112.004,

Frequency:	12 kHz
Transmit beam width:	2 degree
Transmit power:	20 kW
Transmit pulse length:	3 to 20 msec.
Depth range:	100 to 11,000 m
Beam spacing:	1 degree athwart ship
Swath width:	150 degree (max)
	120 degree to 4,500 m
	100 degree to 6,000 m
	90 degree to 11,000 m
Depth accuracy:	Within < 0.5% of depth or +/-1m, whichever is greater, over the entire swath.
	(Nadir beam has greater accuracy; typically within < 0.2% of depth or +/-1m, whichever is greater)

(3) Data Period

MR09-01 Leg1:	P21-029 on 14 April 2009 to P21-033 on 16 April. 2009,
	P21-014 on 17 April 2009 to P21-156 on 18 May 2009
MR09-01 Leg2:	P21-157 on 21 May 2009 to P21-288 on 17 June 2009
MR09-01 Leg3:	20 June 2009 to 1 July 2009
	(except for the territorial waters of Papua New Guinea)

(4) Data processing

i. Sound velocity correction

The continuous bathymetry data are split into small areas around each CTD station. For each small area, the bathymetry data are corrected using a sound velocity profile calculated from the CTD data in the area. The equation of Mackenzie (1981) is used for calculating sound velocity. The data processing is carried out using "mbbath" command of MBsystem.

ii. Editing and Gridding

Gridding for the bathymetry data are carried out using the HIPS software version 6.1 Service Pack 2 (CARIS, Canada). Firstly, the bathymetry data during Ship's turning is basically removed before "BASE surface" is made. A spike noise of each swath data is also removed using "swath editor" and "subset editor". Then the bathymetry data are gridded by "Interpolate" function of the software with following parameters.

BASE surface resolution:	50m
Interpolate matrix size:	5 x 5
Minimum number of neighbors for interpolate:	10

Finally, raw data and interpolated data are exported as ASCII data, and converted to 150m grid data using "xyz2grd" utility of GMT (Generic Mapping Tool) software.

(5) Data Archive

Bathymetry data obtained during this cruise was submitted to the Data Integration and Analysis Group (DIAG) of JAMSTEC, and archived there.

(6) Tectonic history of the Pacific Plate

The Pacific Plate is the largest oceanic lithospheric plate on the Earth. The Pacific Plate was born around 190 Ma, Middle Jurassic (Nakanishi et al., 1992). The tectonic history of the Pacific Plate has been exposed by many studies based on magnetic anomaly lineations. However, the tectonic history in some periods is still obscure because of lack of geophysical data. To reveal the entire tectonic history of the Pacific Plate from Middle Jurassic to the present, increase in geophysical data is indispensable.

Identification of magnetic anomaly lineations has been the most common method for tectonic studies of oceanic plates. After improvement of the multi-narrow beam echo sounder, we become able to describe lineated abyssal hills for the tectonic studies in detail. Abyssal hills are related to the nature of the mid-ocean ridges at which they form (e.g. Goff et al., 1997). For example, abyssal hills heights and widths tend to correlate inversely with spreading rates. Abyssal hills also change morphology depending on crustal thickness and magma supply, factors which can vary within a single ridge segment and/or can vary from one ridge segment to another. Abyssal hills are therefore an off-axis indicator of mid-ocean ridge spreading history.

We collected bathymetric data using SeaBeam 2112 during the cruise. Figures 2.2.1 and 2.2.2 show examples of abyssal hills. Figure 2.2.1 is the bathymetric map near the East Pacific Rise (EPR). The crest of the EPR has about 2600m depth and about 350 m higher than its foot. The depth of the seafloor near the edges of Figure 2.2.1a is about 3500 m. Most of the abyssal hills have the similar strike as the EPR, but some have different strikes from the EPR. The height of abyssal hills is 50 m near the EPR and is more than 200 m around 114°W.

Figure 2.2.2 is the bathymetric map of the seafloor south of the Manihiki Plateau and crosses the East Manihiki Scarp, which is a remarkably linear feature extending more than 700 km from the northeastern corner of the Manihiki plateau. Previous works (e.g., Viso et al., 2005; Downey et al., 2007) show the existence of the abyssal hills with an E-W strike in this

area. The abyssal hills originate from the Pacific-Phoenix Ridge in the mid-Cretaceous. The abyssal hills with an E-W strike exist west of 164°W (Figure 2.2.2b). The height of the abyssal hills is ~100 m. Several knolls with depression exist around 165°15'W. The height of the knolls is about 600 m. The abyssal hills east of the East Manihiki Scarp (EMS) have an NE-SW strike (Figure 2.2.2a, c). The height of abyssal hills is more than 100 m. The pattern of the abyssal hills near the EMS is similar to that around 2.5°S reported by Viso et al. (2005). They interpret these abyssal hills as intratransform spreading centers resulting from transtensional strain across the EMS. Thus, the abyssal hills east of the EMS in Figure 2.2.2(c) derive from the same mechanism.

References

Downey, N. J., J. M. Stock, R. W. Clayton, and S. C. Cande, 2007: History of the Cretaceous Osbourn spreading center, *J. Geophys. Res*., 112, B04102, doi:10.1029/2006JB004550.

Goff, J. A., Y. Ma, A. Shah, J.R. Cochran, and J.-C. Sempere, 1997, Stochastic analysis of seafloor morphology on the flank of the Southeast Indian Ridge: The influence of ridge morphology on the formation of abyssal hills, *J. Geophys. Res*., 102, 15,521-15,534.

Mackenzie, K.V. (1981): Nine-term equation for the sound speed in the oceans, J. Acoust. Soc. Am., 70 (3), pp 807-812.

Nakanishi, M., K. Tamaki, and K. Kobayashi, 1992, A new Mesozoic isochron chart of the whole western Pacific Ocean: Paleomagnetic and tectonic implications, *Geophys. Res. Lett*., 19, 693-696.

Searle, R., 1984, GLORIA survey of the East Pacific Rise Near 3.5°S: Tectonic and volcanic characteristics of a fast spreading mid-ocean rise, *Tectonophysics*, 101, 319-344.

Viso, R. F., R. L. Larson, and R. A. Pockalny, 2005: Tectonic evolution of the Pacific–Phoenix–Farallon triple junction in the South Pacific Ocean, *Earth Planet. Sci. Lett.*, 233, 179-194.

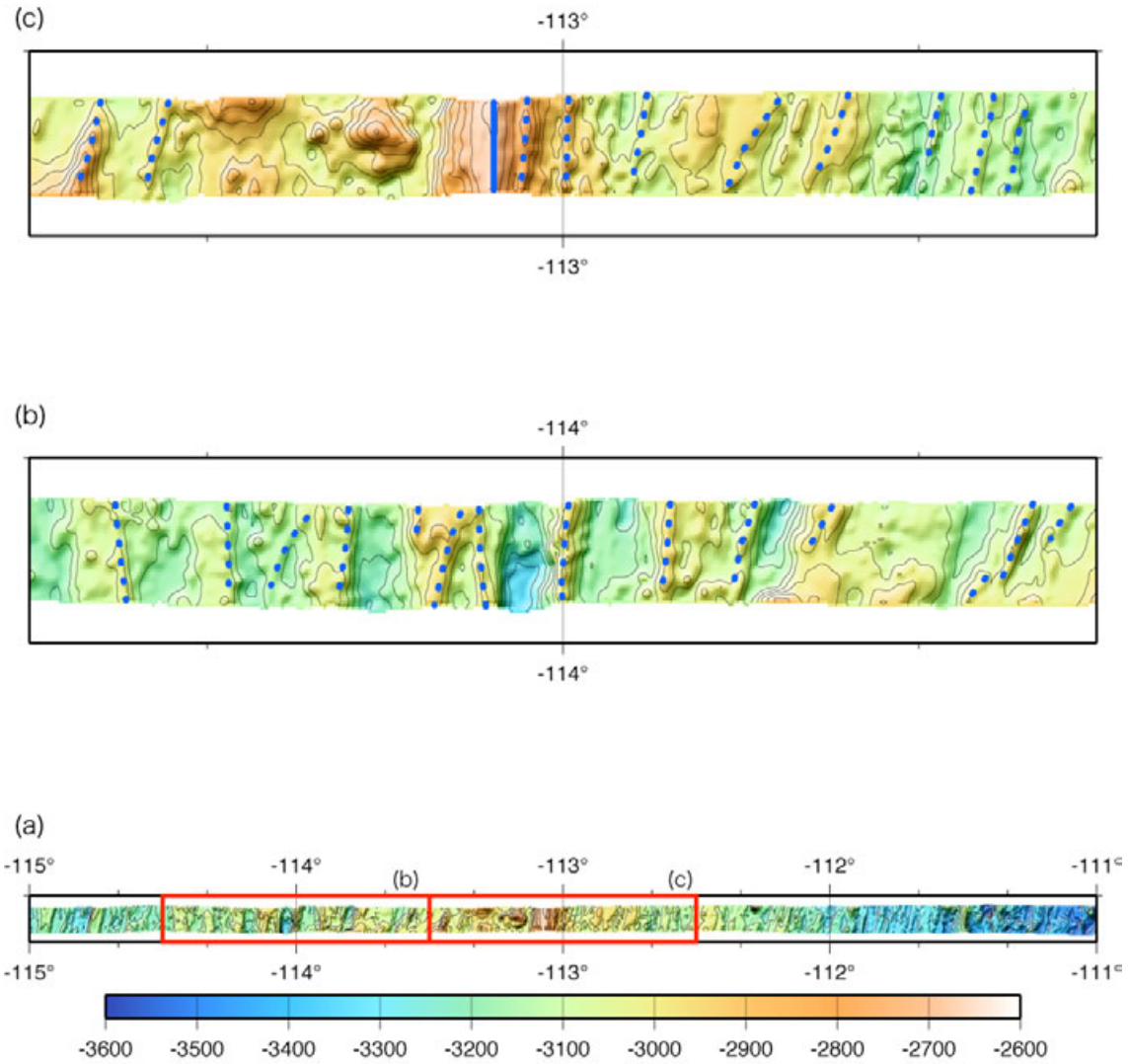

Figure 2.1.1 Bathymetric Map around the East Pacific Rise. Contour interval is 50 m. Bathymetry is illuminated from the northwest. Red rectangles in (a) represent the areas of (b) and (c). Blue dotted lines represent abyssal hills. A blue line shows the crest of the East Pacific Rise.

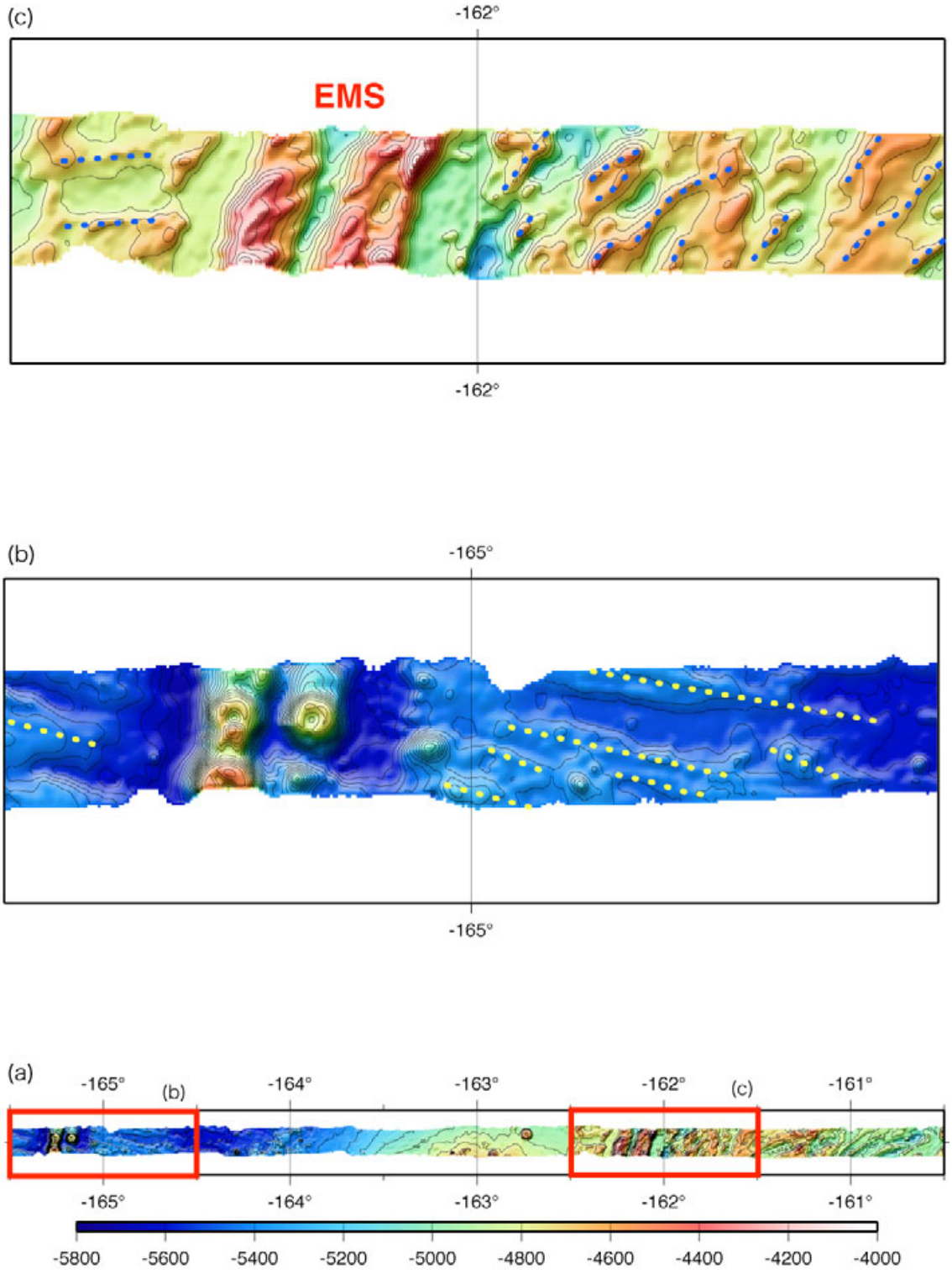

Figure 2.1.2 Bathymetric Map of the seafloor south of the Manihiki Plateau. Contour interval is 50 m. Bathymetry is illuminated from the northwest. Red rectangles in (a) represent the areas of (b) and (c). Yellow and blue dotted lines represent abyssal hills. EMS represents the East Manihiki Scarp.

2.3 Surface Meteorological Observation

(1) Personnel

Kunio Yoneyama	*(JAMSTEC) : Principal Investigator / Not on-board*	
Shinya Okumura	*(GODI): Leg1*	
Satoshi Okumura	*(GODI)*	*: Leg2*
Souichiro Sueyoshi	*(GODI)*	*: Leg3*
Ryo Kimura	*(GODI)*	*: Leg1, Leg3*
Yousuke Yuuki	*(GODI)*	*: Leg1*
Kazuho Yoshida	*(GODI)*	*: Leg2*
Harumi Ota	*(GODI)*	*: Leg2*

(2) Objectives

The surface meteorological parameters are observed as a basic dataset of the meteorology. These parameters bring us the information about the temporal variation of the meteorological condition surrounding the ship.

(3) Methods

The surface meteorological parameters were observed throughout the MR09-01 cruise. During this cruise, we used two systems for the observation.

i. MIRAI Surface Meteorological observation (SMET) system
ii. Shipboard Oceanographic and Atmospheric Radiation (SOAR) system

i. MIRAI Surface Meteorological observation (SMET) system

Instruments of SMET system are listed in Table 2.3-1 and measured parameters are listed in Table 2.3-2. Data were collected and processed by KOAC-7800 weather data processor made by Koshin-Denki, Japan. The data set consists of 6-second averaged data.

ii. Shipboard Oceanographic and Atmospheric Radiation (SOAR) system

SOAR system designed by BNL (Brookhaven National Laboratory, USA) consists of major three parts.

a) Portable Radiation Package (PRP) designed by BNL – short and long wave downward radiation.
b) Zeno Meteorological (Zeno/Met) system designed by BNL – wind, air temperature, relative humidity, pressure, and rainfall measurement.
c) Scientific Computer System (SCS) designed by NOAA (National Oceanic and Atmospheric Administration, USA) – centralized data acquisition and logging of all data sets.

SCS recorded PRP data every 6 seconds, Zeno/Met data every 10 seconds. Instruments and their locations are listed in Table 2.3-3 and measured parameters are listed in Table 2.3-4.

We have checked the following sensors, before and after the cruise for the quality control as post processing.

a) Young Rain gauge (SMET and SOAR)

Inspect of the linearity of output value from the rain gauge sensor to change Input value by adding fixed quantity of test water.

b) Barometer(SMET and SOAR)

Comparison with the portable barometer value, PTB220CASE, VAISALA.

c) Thermometer (air temperature and relative humidity) (SMET and SOAR)

Comparison with the portable thermometer value, HMP41/45, VAISALA.

(4) Preliminary results

Fig.2.3-1 show the time series of the following parameters;

Wind (SOAR)
Air temperature (SOAR)
Relative humidity (SOAR)
Precipitation (SOAR, Optical rain gauge)
Short/long wave radiation (SOAR)
Pressure (SOAR)
Sea surface temperature (SMET)
Significant wave height (SMET)

(5) Data archives

These meteorological data will be submitted to the Data Integration and Analysis Group (DIAG) of JAMSTEC just after the cruise. Corrected data sets will be available from K. Yoneyama of JAMSTEC.

(6) Remarks

i. SST (Sea Surface Temperature) data are available in the following periods.

12:40UTC 14 Apr. 2009 – 05:30UTC 16 Apr. 2009
00:15UTC 21 Apr. 2009 – 07:06UTC 18 May. 2009
20:18UTC 25 May. 2009 – 17:08UTC 13 Jun. 2009
17:17UTC 13 Jun. 2009 – 19:36UTC 17 Jun. 2009
09:30UTC 20 Jun. 2009 – 23:00UTC 23 Jun. 2009
14:06UTC 24 Jun. 2009 – 04:24UTC 01 Jul. 2009

ii. PRP data of SOAR system are not available due to the maintenance in the following periods.

14:23UTC 17 Apr. 2009 – 14:58UTC 17 Apr. 2009 (PRP was replaced on S/N 11 to S/N 07)
08:26UTC 22 Apr. 2009 – 09:19UTC 22 Apr. 2009
20:43UTC 13 May. 2009 – 21:28UTC 13 May. 2009 (PRP was replaced on S/N 07 to S/N 11)

iii. SOAR sensor cleaning

(PRP) 15:30UTC 12 Apr. 2009, 19:35UTC 28 May. 2009, 05:31UTC 19 Jun. 2009
(ORG) 15:30UTC 12 Apr. 2009, 01:56UTC 21 May. 2009, 19:34UTC 28 May. 2009, 05:38UTC 19 Jun. 2009

Table 2.3-1 Instruments and installations of MIRAI Surface Meteorological observation system

Sensors	Type	Manufacturer	Location (altitude from surface)
Anemometer	KE-500	Koshin Denki, Japan	foremast (24 m)
Tair/RH	HMP45A	Vaisala, Finland	
with 43408 Gill aspirated radiation shield		R.M. Young, USA	compass deck (21 m)
			starboard side and port side
Thermometer: SST	RFN1-0	Koshin Denki, Japan	4th deck (-1m, inlet -5m)
Barometer	AP370	Koshin Denki, Japan	captain deck (13 m)
			weather observation room
Rain gauge	50202	R. M. Young, USA	compass deck (19 m)
Optical rain gauge	ORG-815DR	Osi, USA	compass deck (19 m)
Radiometer (short wave)	MS-801	Eiko Seiki, Japan	radar mast (28 m)
Radiometer (long wave)	MS-202	Eiko Seiki, Japan	radar mast (28 m)
Wave height meter	MW-2	Tsurumi-seiki, Japan	bow (10 m)

Table 2.3-2 Parameters of MIRAI Surface Meteorological observation system

	Parameter	Units	Remarks
1	Latitude	degree	
2	Longitude	degree	
3	Ship's speed	knot	Mirai log, DS-30 Furuno
4	Ship's heading	degree	Mirai gyro, TG-6000, Tokimec
5	Relative wind speed	m/s	6sec./10min. averaged
6	Relative wind direction	degree	6sec./10min. averaged
7	True wind speed	m/s	6sec./10min. averaged
8	True wind direction	degree	6sec./10min. averaged
9	Barometric pressure	hPa	adjusted to sea surface level
			6sec. averaged
10	Air temperature (starboard side)	degC	6sec. averaged
11	Air temperature (port side)	degC	6sec. averaged
12	Dewpoint temperature (starboard side)	degC	6sec. averaged
13	Dewpoint temperature (port side)	degC	6sec. averaged
14	Relative humidity (starboard side)	%	6sec. averaged
15	Relative humidity (port side)	%	6sec. averaged
16	Sea surface temperature	degC	6sec. averaged
17	Rain rate (optical rain gauge)	mm/hr	hourly accumulation
18	Rain rate (capacitive rain gauge)	mm/hr	hourly accumulation
19	Down welling shortwave radiation	W/m^2	6sec. averaged
20	Down welling infra-red radiation	W/m^2	6sec. averaged
21	Significant wave height (bow)	m	hourly
22	Significant wave height (aft)	m	hourly
23	Significant wave period (bow)	second	hourly
24	Significant wave period (aft)	second	hourly

Table 2.3-3 Instruments and installation locations of SOAR system

Sensors(*Zeno/Met*)	Type	Manufacturer	Location (altitude from surface)
Anemometer	05106	R.M. Young, USA	foremast (25 m)
Tair/RH	HMP45A	Vaisala, Finland	
with 43408 Gill aspirated radiation shield		R.M. Young, USA	foremast (23 m)
Barometer	61201	R.M. Young, USA	
with 61002 Gill pressure port	R.M. Young, USA		foremast (22 m)
Rain gauge	50202	R.M. Young, USA	foremast (24 m)
Optical rain gauge	ORG-815DA	Osi, USA	foremast (24 m)

Sensors (*PRP*)	Type	Manufacturer	Location (altitude from surface)
Radiometer (short wave)	PSP	Epply Labs, USA	foremast (24 m)
Radiometer (long wave)	PIR	Epply Labs, USA	foremast (24m)
Fast rotating shadowband radiometer		Yankee, USA	foremast (24 m)

Table 2.3-4 Parameters of SOAR system

	Parameter		Units	Remarks
1	Latitude		degree	
2	Longitude		degree	
3	SOG		knot	
4	COG		degree	
5	Relative wind speed		m/s	
6	Relative wind direction		degree	
7	Barometric pressure		hPa	
8	Air temperature	degC		
9	Relative humidity		%	
10	Rain rate (optical rain gauge)		mm/hr	
11	Precipitation (capacitive rain gauge)	mm		reset at 50 mm
12	Down welling shortwave radiation	W/m^2		
13	Down welling infra-red radiation		W/m^2	
14	Defuse irradiance		W/m^2	

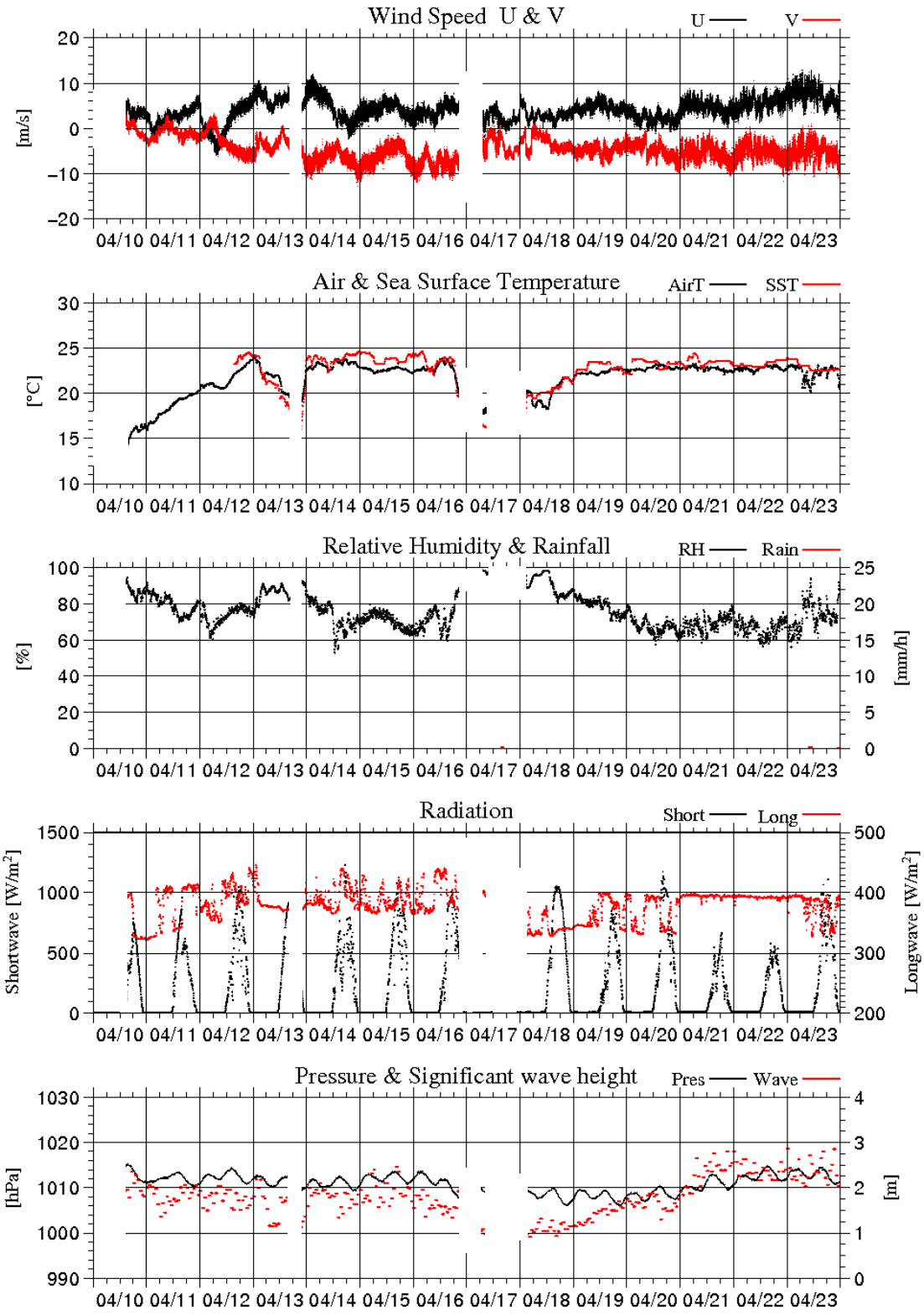

Fig.2.3-1 Time series of surface meteorological parameters during the MR09-01 cruise

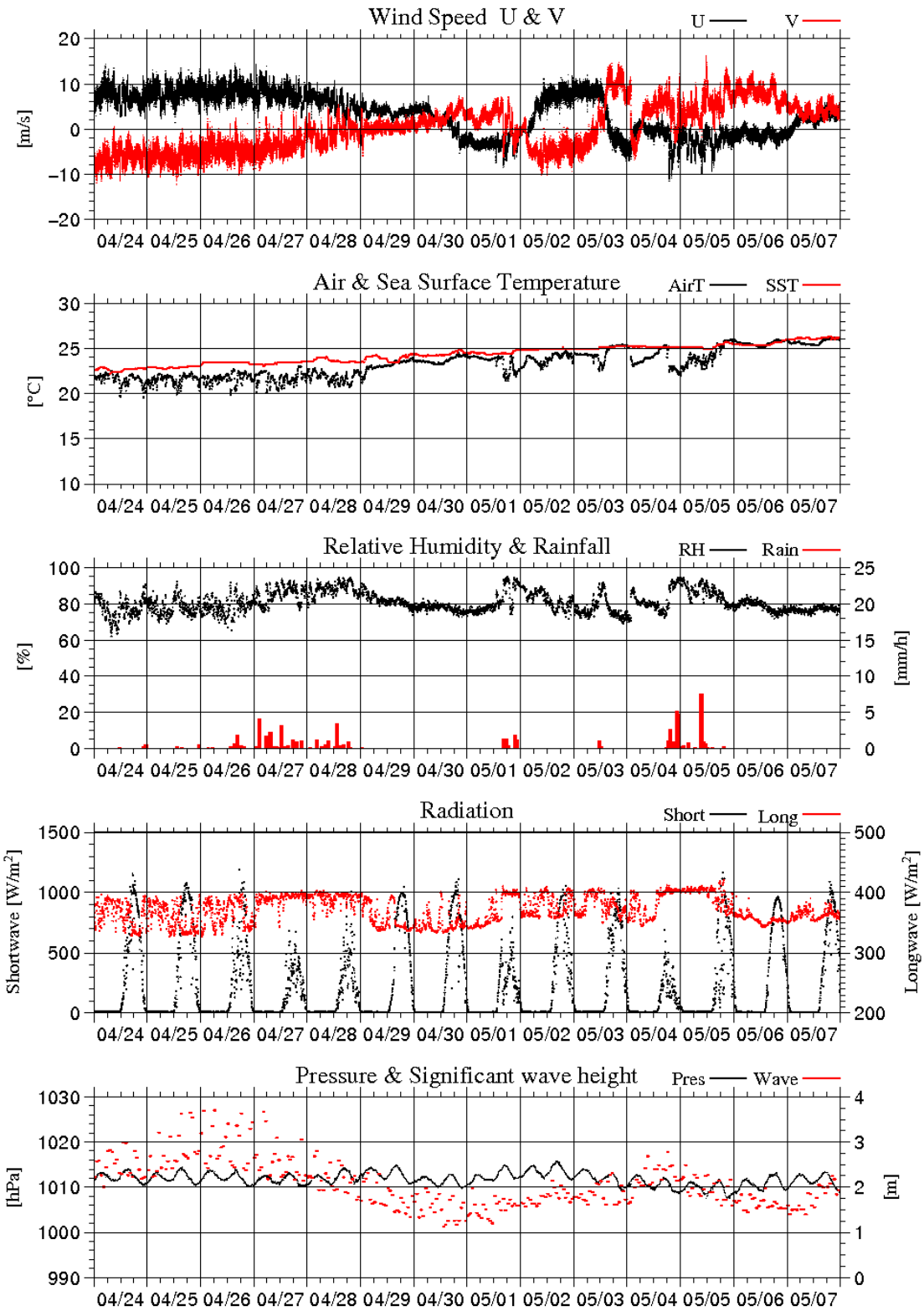

Fig.2.3-1 (Continued)

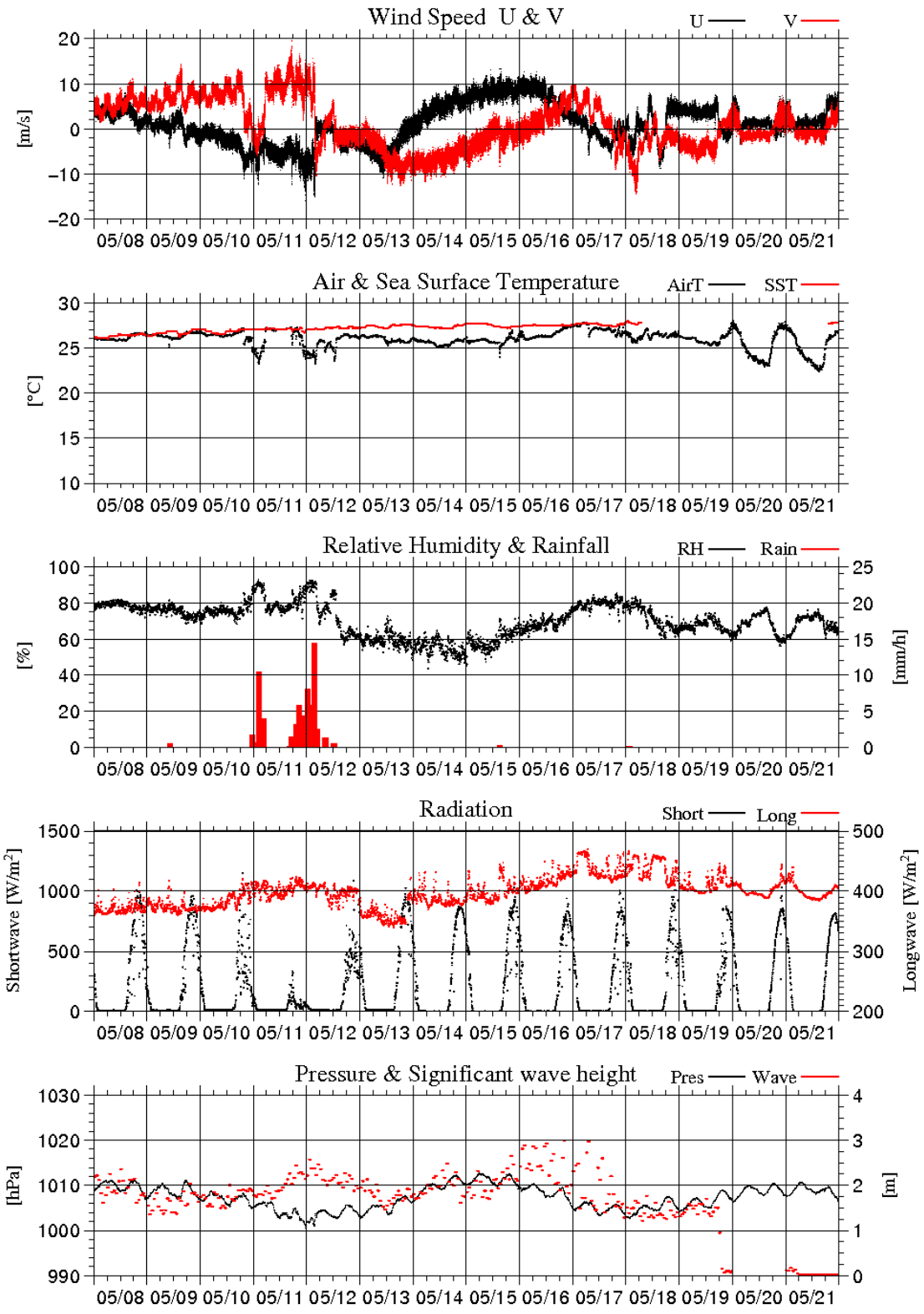

Fig.2.3-1 (Continued)

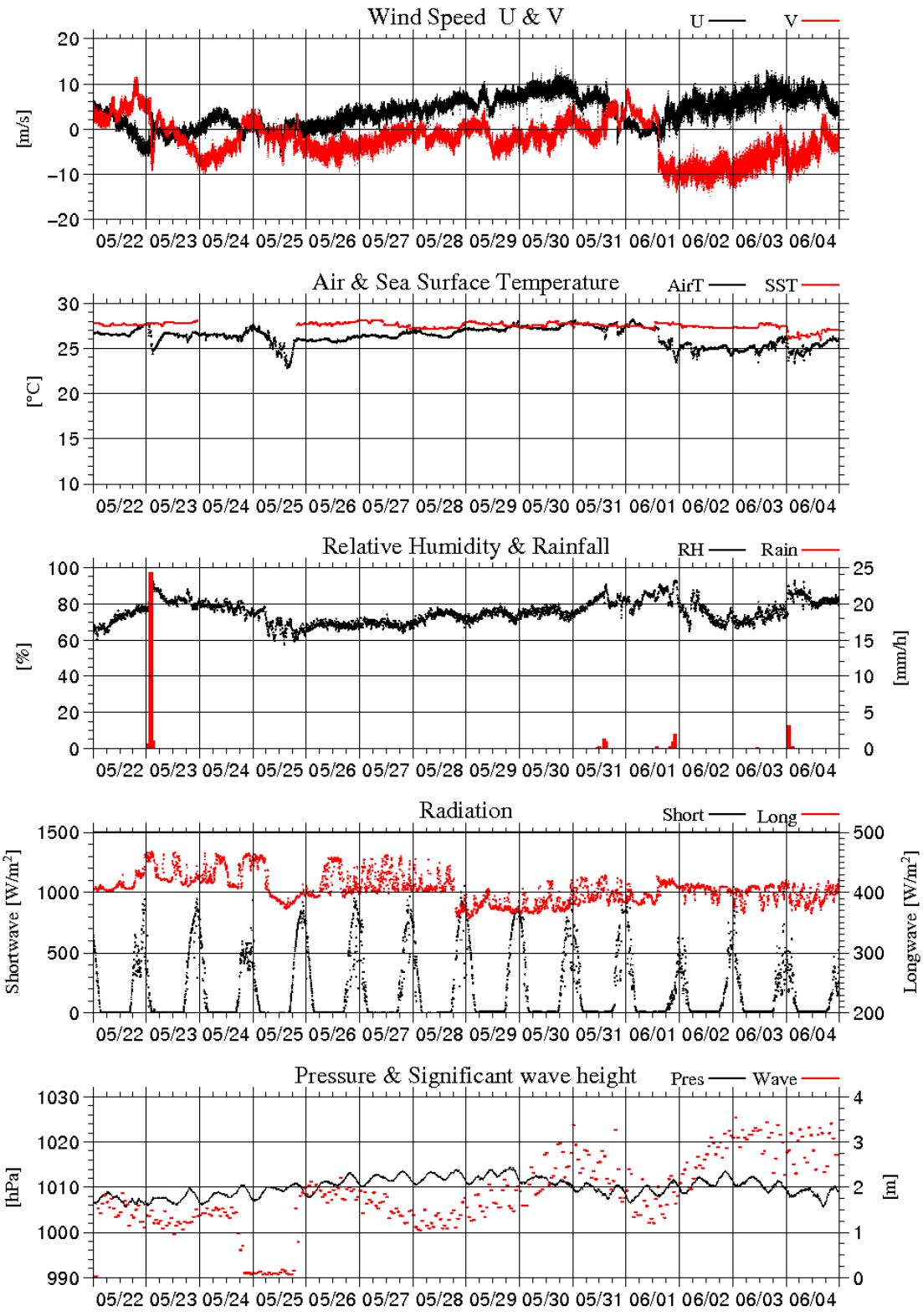

Fig.2.3-1 (Continued)

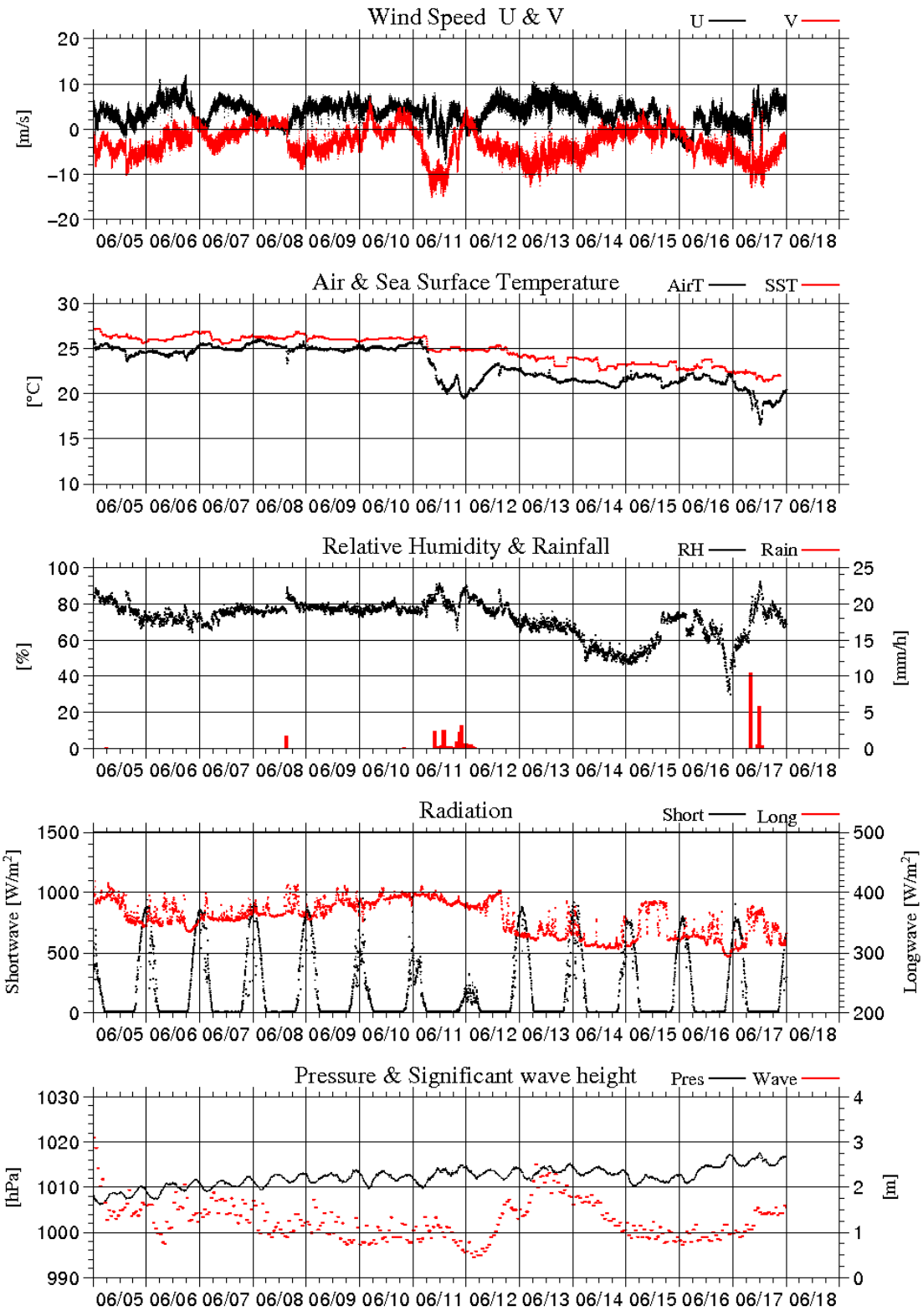

Fig.2.3-1 (Continued)

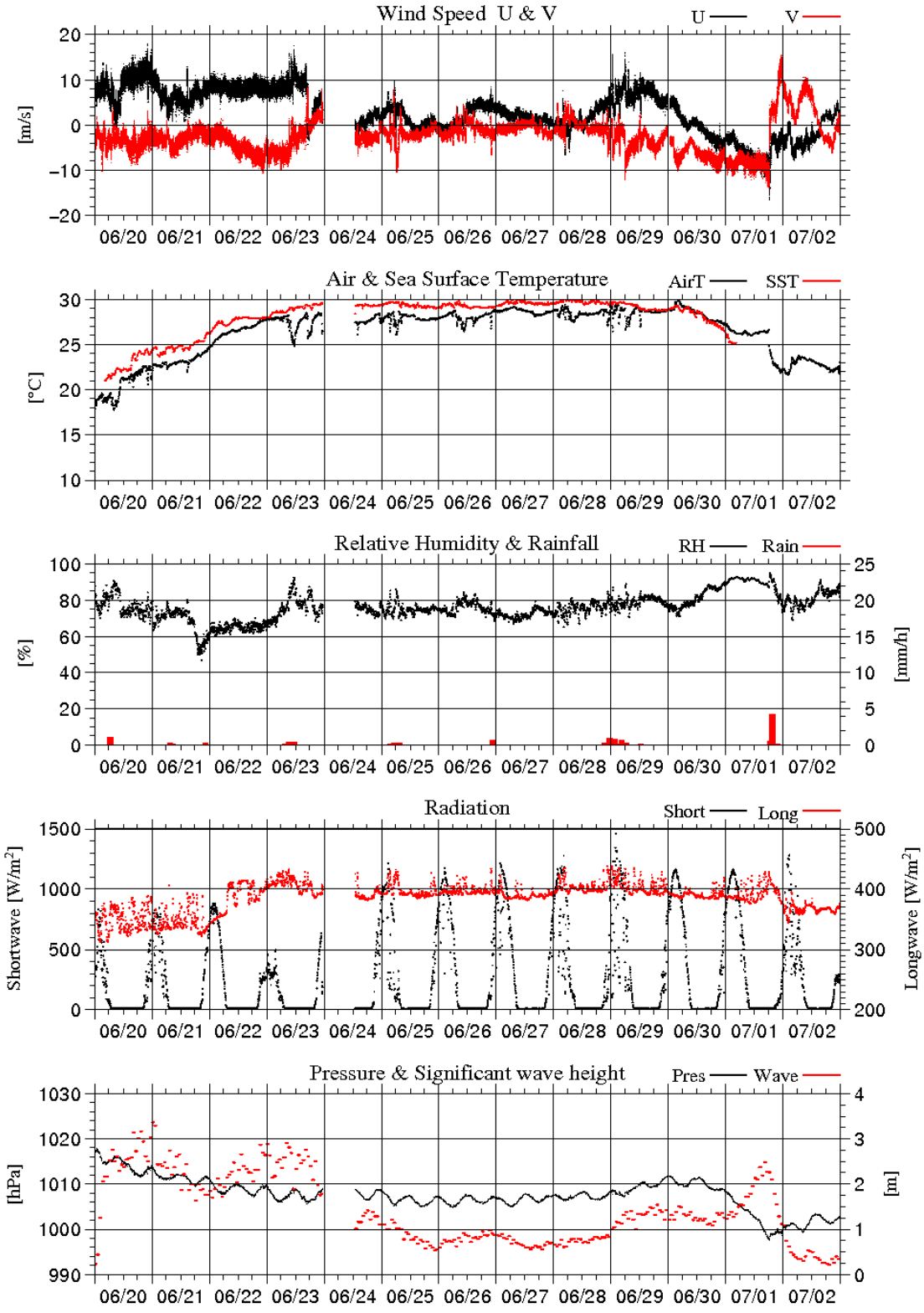

Fig.2.3-1 (Continued)

2.4 Thermo-salinograph and related measurements

June 06, 2009

(1) Personnel

Yuichiro KUMAMOTO [1)]**,**
Miyo IKEDA [2)]**,**
Fuyuki SHIBATA [2)]**,**
Masanori ENOKI [2)]
Misato KUWAHARA [2)]

1) Japan Agency for Marine Earth Science and Technology (JAMSTEC)
2) Marine Works Japan Co. Ltd

(2) Objective

Our purpose is to obtain salinity, temperature, dissolved oxygen, and fluorescence data continuously in near-sea surface water during MR09-01 cruise.

(3) Methods

The Continuous Sea Surface Water Monitoring System (Nippon Kaiyo Co. Ltd.), including the thermo-salinograph, has five sensors and automatically measures salinity, temperature, dissolved oxygen, and fluorescence in near-sea surface water every one minute. This system is located in the sea surface monitoring laboratory and connected to shipboard LAN system. Measured data, time, and location of the ship were displayed on a monitor and stored in a data management PC (IBM NetVista 6826-CBJ). The near-surface water was continuously pumped up to the laboratory from about 4 m water depth and flowed into the system through a vinyl-chloride pipe. The flow rate of the surface seawater was controlled by several valves and adjusted to be 12 dm^3/min except for a fluorometer (about 0.5 dm^3/min). The flow rate was measured by two flow meters. Specifications of the each sensor in this system are listed below.

a) Temperature and salinity sensors

SEACAT THERMOSALINOGRAPH

Model:	SBE-21, SEA-BIRD ELECTRONICS, INC.
Serial number:	2126391-3126
Measurement range:	Temperature −5 to +35°C (ITS-90), Salinity 0 to 7.0 S m^{-1}
Accuracy:	Temperature 0.01°C $6month^{-1}$, Salinity 0.001 S m^{-1} $month^{-1}$
Resolution:	Temperatures 0.001°C, Salinity0.0001 S m^{-1}

b) Bottom of ship thermometer (RMT)

Model:	SBE 3S, SEA-BIRD ELECTRONICS, INC.
Serial number:	032175
Measurement range:	−5 to +35°C (ITS-90)
Resolution:	±0.001°C
Stability:	0.002°C $year^{-1}$

c) Dissolved oxygen sensor

Model:	2127A, HACH ULTRA ANALYTICS JAPAN, INC.
Serial number:	47477
Measurement range:	0 to 14 ppm
Accuracy:	±1% at 5°C of correction range
Stability:	1% $month^{-1}$

d) Fluorometer

Model: 10-AU-005, TURNER DESIGNS

Serial number: 5562 FRXX

Detection limit: 5 ppt or less for chlorophyll-a

Stability: 0.5% month^{-1} of full scale

e) Flow meter

Model: EMARG2W, Aichi Watch Electronics LTD.

Serial number: 8672

Measurement range: 0 to 30 l min^{-1}

Accuracy: ±1%

Stability: ±1% day^{-1}

(4) Measurements

Periods of measurement, maintenance, and problems during MR09-01 are listed in Table 2.4.1.

Table 2.4.1 Events list of the thermo-salinograph during MR09-01

System Date [UTC]	System Time [UTC]	Events	Remarks
09-Apr.-14	12:47	All the measurements started.	Leg-1 start
09-Apr.-15	23:59	All the measurements stopped due to entering in the Peruvian EEZ.	
09-Apr.-18	00:02		
09-Apr.-18	02:35	All the measurements stopped due to failure of operation.	
09-Apr.-18	05:18		
09-Apr.-22	01:40	Lost of all the data due to reboot of the data management PC.	
09-Apr.-22	02:04		
09-May-18	07:06	All the measurements stopped.	Leg-1 finish
09-May-21	20:18	All the measurements started.	Leg-2a start
09-May-23	20:44	All the measurements stopped.	Leg-2a finish
09-May-25	20:19	All the measurements started.	Leg-2b start
09-Jun.-13	17:07	Lost of all the data due to error on program.	
09-Jun.-13	17:18		
09-Jun.-17	19:36	All the measurements stopped.	Leg-2b finish
09-Jun.-20	10:01	All the measurements started.	Leg-3 start
09-Jun.-23	22:59	Lost of all the data	
09-Jun.-24	14:03		
09-Jul.-01	04:23	All the measurements stopped.	Leg-3 finish

(5) Calibrations

i. Comparison with bottle salinity data

We collected the surface seawater samples for salinity sensor calibration during Leg-1 and Leg-2 (Table 2.4.2). The seawater was collected approximately twice a day using a 250ml brown grass bottle. The samples were stored in the sea surface monitoring laboratory and then measured using the Guildline 8400B at the end of the legs after all the measurements of the hydrocast bottle samples.

Table 2.4.2 Comparison of the sensor salinity with the bottle salinity

Date [UTC]	Time [UTC]	Latitude	Longitude	Sensor salinity [PSS-78]	Bottle salinity [PSS-78]	Difference [Sen. - Bot.]
2009/4/14	13:48	16-44.97580S	078-42.43970W	35.4984	35.4950	0.0034
2009/4/14	21:56	16-45.17830S	079-19.83920W	35.5812	35.5769	0.0043
2009/4/15	8:56	16-44.40370S	080-39.63650W	35.5748	35.5725	0.0023
2009/4/15	22:04	16-40.73990S	080-59.80990W	35.4099	35.4083	0.0016
2009/4/21	8:19	16-44.92050S	080-25.69800W	35.4962	35.4981	-0.0019
2009/4/21	21:10	16-44.52540S	082-00.27190W	35.5029	35.5088	-0.0059
2009/4/22	10:00	16-44.93300S	082-59.85970W	35.5844	35.5889	-0.0045
2009/4/22	10:02	16-44.91210S	082-59.85080W	35.5842	35.5890	-0.0048
2009/4/22	21:29	16-45.09040S	083-40.05760W	35.5448	35.5507	-0.0059
2009/4/23	8:51	16-44.56640S	084-20.09390W	35.6529	35.6570	-0.0041
2009/4/23	21:08	16-45.11350S	085-19.65940W	35.5000	35.5058	-0.0058
2009/4/24	9:52	16-49.99990S	086-23.16600W	35.7428	35.7466	-0.0038
2009/4/24	21:11	16-44.71580S	087-40.33490W	35.7371	35.7444	-0.0073
2009/4/25	10:36	16-45.00120S	088-39.82020W	35.7708	35.7750	-0.0042
2009/4/25	10:38	16-45.00260S	088-39.84800W	35.7718	35.7744	-0.0026
2009/4/25	20:55	16-44.78260S	089-20.05120W	35.7637	35.7691	-0.0054
2009/4/26	10:09	16-44.73750S	090-08.14720W	35.7523	35.7574	-0.0051
2009/4/26	21:41	16-44.78340S	091-28.27440W	35.7917	35.7951	-0.0034
2009/4/27	9:19	16-44.80660S	092-49.23870W	35.8304	35.8362	-0.0058
2009/4/27	21:37	16-43.85810S	094-21.16550W	35.8251	35.8318	-0.0067
2009/4/28	9:21	16-45.33650S	095-47.60370W	35.8719	35.8724	-0.0005
2009/4/28	9:23	16-45.34400S	095-48.13740W	35.8679	35.8707	-0.0028
2009/4/28	21:52	16-44.73560S	097-20.31890W	35.8107	35.8161	-0.0054
2009/4/29	9:38	16-44.79350S	098-40.12210W	35.9412	35.9454	-0.0042
2009/4/29	22:07	16-44.05720S	100-00.30900W	36.0435	36.0471	-0.0036
2009/4/30	10:07	16-44.61130S	101-28.24690W	35.9749	35.9805	-0.0056

Table 2.4.2 (continued)

Date [UTC]	Time [UTC]	Latitude	Longitude	Sensor salinity [PSS-78]	Bottle salinity [PSS-78]	Difference [Sen. - Bot.]
2009/4/30	10:09	16-44.62880S	101-28.76720W	35.9771	35.9820	-0.0049
2009/4/30	21:57	16-59.19030S	102-58.24090W	35.9857	35.9880	-0.0023
2009/5/1	11:09	16-45.46850S	104-00.09040W	36.0785	36.0822	-0.0037
2009/5/1	23:39	16-45.03880S	106-00.04450W	36.0361	36.0432	-0.0071
2009/5/2	11:08	16-44.97480S	106-54.64000W	36.0931	36.0988	-0.0057
2009/5/3	1:48	16-45.49220S	107-15.05250W	36.1222	36.1272	-0.0050
2009/5/3	10:31	16-44.96970S	107-37.76710W	36.1409	36.1453	-0.0044
2009/5/3	23:03	16-45.14510S	109-19.99040W	36.1931	36.1985	-0.0054
2009/5/3	23:04	16-45.14910S	109-19.98920W	36.1924	36.1974	-0.0050
2009/5/4	11:33	16-45.13740S	110-40.38760W	36.2194	36.2242	-0.0048
2009/5/4	23:32	16-45.29100S	112-00.07440W	36.1544	36.1630	-0.0086
2009/5/5	10:47	16-45.25910S	113-37.45760W	36.3165	36.3205	-0.0040
2009/5/5	21:52	16-45.46490S	115-13.33820W	36.2483	36.2538	-0.0055
2009/5/6	11:27	16-44.98470S	116-42.80650W	36.3767	36.3807	-0.0040
2009/5/6	23:06	16-45.17100S	118-25.21730W	36.2563	36.2622	-0.0059
2009/5/7	11:36	16-45.09820S	120-00.16570W	36.2863	36.2924	-0.0061
2009/5/7	11:38	16-45.10700S	120-00.17050W	36.2868	36.2924	-0.0056
2009/5/8	7:21	16-45.09310S	122-39.65920W	36.2948	36.3001	-0.0053
2009/5/8	11:20	16-44.85160S	122-57.81300W	36.3801	36.3857	-0.0056
2009/5/8	23:17	16-45.11080S	124-39.69490W	36.4907	36.4951	-0.0044
2009/5/9	10:59	16-45.02640S	126-00.21060W	36.3923	36.3965	-0.0042
2009/5/9	23:45	16-45.30990S	127-20.52890W	36.3225	36.3272	-0.0047
2009/5/10	12:35	16-45.01200S	129-05.41100W	36.3609	36.3641	-0.0032
2009/5/10	12:37	16-45.01500S	129-05.91430W	36.3552	36.3591	-0.0039
2009/5/11	2:11	16-45.46310S	130-39.68820W	36.3718	36.3788	-0.0070
2009/5/11	12:12	16-45.05740S	131-59.97770W	36.4767	36.4823	-0.0056
2009/5/12	2:21	16-45.29710S	133-20.19320W	36.3381	36.3432	-0.0051
2009/5/12	11:51	16-45.56450S	134-00.34900W	36.2077	36.2137	-0.0060
2009/5/13	11:58	16-45.31040S	136-39.87070W	36.4252	36.4293	-0.0041
2009/5/13	12:00	16-45.30590S	136-39.85740W	36.4246	36.4307	-0.0061
2009/5/13	17:28	16-44.96630S	137-20.15810W	36.3616	36.3693	-0.0077
2009/5/14	0:08	16-45.09200S	138-22.38950W	36.3073	36.3105	-0.0032
2009/5/14	12:56	16-44.92430S	140-02.89960W	36.3949	36.4020	-0.0071
2009/5/15	0:27	16-44.56690S	141-43.14970W	36.2809	36.2862	-0.0053

Table 2.4.2 (continued)

Date [UTC]	Time [UTC]	Latitude	Longitude	Sensor salinity [PSS-78]	Bottle salinity [PSS-78]	Difference [Sen. - Bot.]
2009/5/15	14:26	17-18.00390S	143-01.90900W	36.2908	36.2964	-0.0056
2009/5/16	0:40	17-29.56580S	144-09.39550W	36.3152	36.3204	-0.0052
2009/5/16	14:32	17-29.82400S	145-44.07210W	36.3189	36.3234	-0.0045
2009/5/16	14:34	17-29.85300S	145-44.45950W	36.3190	36.3243	-0.0053
2009/5/17	1:06	17-29.80410S	146-55.62150W	36.3267	36.3310	-0.0043
2009/5/17	12:53	17-30.21460S	148-28.58790W	36.2912	36.2957	-0.0045
2009/5/18	2:28	17-30.00190S	149-10.30590W	36.2251	36.2292	-0.0041
2009/5/18	7:03	17-29.95660S	149-19.96200W	36.2223	36.2345	-0.0122
2009/5/22	0:57	17-29.84320S	150-05.34030W	36.1993	36.1916	0.0077
2009/5/22	13:27	17-29.91300S	151-16.85460W	36.1192	36.1159	0.0033
2009/5/23	1:14	17-30.41760S	152-43.27130W	36.038	36.0309	0.0071
2009/5/23	13:20	17-30.39290S	154-03.86520W	35.9694	35.9629	0.0065
2009/5/23	19:06	17-30.73690S	154-19.15890W	35.9772	35.9698	0.0074
2009/5/26	0:33	17-30.27460S	150-56.34070W	36.148	36.1428	0.0052
2009/5/26	7:46	17-28.15840S	152-47.88450W	36.0207	36.0145	0.0062
2009/5/26	7:48	17-28.15860S	152-48.39390W	36.0187	36.0123	0.0064
2009/5/27	2:22	17-29.71150S	155-39.65110W	35.935	35.9279	0.0071
2009/5/27	12:43	17-30.14850S	156-59.98330W	35.9856	35.9789	0.0067
2009/5/28	2:43	17-30.05130S	158-21.80860W	35.6579	35.6521	0.0058
2009/5/28	13:17	17-29.60850S	159-40.16600W	35.7293	35.7217	0.0076
2009/5/29	3:15	17-29.62850S	161-00.53220W	35.7593	35.7527	0.0066
2009/5/29	12:44	17-29.84780S	162-20.19010W	35.5213	35.5153	0.0060
2009/5/29	12:46	17-29.84070S	162-20.19980W	35.5218	35.5148	0.0070
2009/5/30	0:51	17-29.71710S	163-40.22410W	35.5298	35.5240	0.0058
2009/5/30	13:14	17-29.86090S	165-00.09660W	35.658	35.6523	0.0057
2009/5/31	2:37	17-29.50610S	166-20.56290W	35.3233	35.3168	0.0065
2009/5/31	12:34	17-29.75890S	167-19.39840W	35.2629	35.2559	0.0070
2009/6/1	2:10	17-30.02270S	168-57.87450W	35.1326	35.1238	0.0088
2009/6/1	2:12	17-30.01870S	168-58.38400W	35.1286	35.1222	0.0064
2009/6/1	13:19	17-30.12720S	169-57.96900W	35.6192	35.6121	0.0071
2009/6/2	2:06	17-30.09560S	171-19.29490W	35.3532	35.3447	0.0085
2009/6/2	13:53	17-29.47620S	172-09.08020W	35.3759	35.3695	0.0064
2009/6/3	2:19	17-29.86830S	172-39.93180W	35.3979	35.3921	0.0058
2009/6/3	13:42	17-29.76370S	172-59.95610W	35.4848	35.4781	0.0067

Table 2.4.2 (continued)

Date [UTC]	Time [UTC]	Latitude	Longitude	Sensor salinity [PSS-78]	Bottle salinity [PSS-78]	Difference [Sen. - Bot.]
2009/6/4	1:57	17-29.15390S	174-53.24790W	35.1388	35.1300	0.0088
2009/6/4	2:00	17-29.24690S	174-54.02150W	35.1391	35.1312	0.0079
2009/6/4	14:06	17-29.84240S	176-29.21680W	35.4266	35.4206	0.0060
2009/6/5	1:48	17-45.08660S	178-15.00220W	35.5201	35.5144	0.0057
2009/6/5	14:08	18-24.86800S	179-39.44760W	35.0543	35.0458	0.0085
2009/6/6	4:37	18-25.14400S	178-19.77450E	34.7175	34.7105	0.0070
2009/6/6	15:05	18-34.43890S	177-15.01060E	34.8111	34.8052	0.0059
2009/6/7	3:07	17-49.80500S	176-20.13720E	34.8422	34.8366	0.0056
2009/6/7	3:09	17-49.80020S	176-20.14540E	34.8446	34.8362	0.0084
2009/6/7	14:51	17-49.96720S	174-30.44490E	34.7476	34.7396	0.0080
2009/6/8	3:29	17-50.20620S	172-57.74250E	34.7886	34.7854	0.0032
2009/6/8	16:16	17-50.03360S	171-00.02810E	34.8332	34.8284	0.0048
2009/6/9	3:14	17-49.98500S	169-39.81200E	34.8549	34.8498	0.0051
2009/6/9	14:51	18-08.76050S	168-35.87720E	34.8734	34.8673	0.0061
2009/6/9	14:54	18-08.72630S	168-35.86890E	34.8733	34.8673	0.0060
2009/6/10	3:33	18-28.98480S	167-48.94890E	34.8825	34.8751	0.0074
2009/6/10	15:10	18-41.83330S	167-18.97920E	34.668	34.6618	0.0062
2009/6/11	4:30	19-09.22850S	166-15.30210E	34.6166	34.6111	0.0055
2009/6/11	15:48	19-35.14790S	165-13.44460E	34.8688	34.8621	0.0067
2009/6/12	4:20	19-55.09680S	164-26.87740E	34.7665	34.7596	0.0069
2009/6/12	4:23	19-55.03730S	164-27.09530E	34.7686	34.7604	0.0082
2009/6/12	14:15	18-41.18910S	163-27.76470E	34.7966	34.7912	0.0054
2009/6/13	5:09	20-52.28470S	164-12.34210E	34.9014	34.8964	0.0050
2009/6/13	15:40	20-58.30450S	164-05.86780E	35.1654	35.1531	0.0123
2009/6/14	4:12	21-28.99900S	162-45.98240E	34.894	34.8870	0.0070
2009/6/14	15:44	22-05.92740S	161-12.07260E	35.2426	35.2314	0.0112
2009/6/15	4:55	22-43.07240S	159-39.05030E	35.2074	35.1999	0.0075
2009/6/15	4:57	22-43.07120S	159-39.05450E	35.2077	35.2009	0.0068
2009/6/15	15:44	23-15.94420S	158-15.27150E	35.2435	35.2369	0.0066
2009/6/16	4:18	23-52.07610S	156-43.12080E	35.3243	35.3164	0.0079
2009/6/16	16:06	24-20.93430S	155-30.04440E	35.2284	35.2212	0.0072
2009/6/17	5:24	24-46.82500S	154-19.41980E	35.437	35.4248	0.0122
2009/6/17	18:53	25-02.01130S	153-38.93560E	35.3601	35.3536	0.0065

ii. Sensor calibrations

The sensors for temperature and salinity were calibrated before the cruise. After the cruise the sensors will be calibrated again in order to evaluate drifts of measurements during the cruise.

(6) Date archive

Quality controlled data of temperature, salinity, dissolved oxygen, and fluorescence will be available via the JAMSTEC MIRAI DATA Web.

2.5. pCO_2

(1) Personnel

Akihiko Murata (JAMSTEC)
Minoru Kamata (MWJ)
Yoshiko Ishikawa (MWJ)
Yasuhiro Arii (MWJ)

(2) Objective

Concentrations of CO_2 in the atmosphere are now increasing at a rate of 1.9 ppmv y^{-1} owing to human activities such as burning of fossil fuels, deforestation, and cement production. It is an urgent task to estimate as accurately as possible the absorption capacity of the oceans against the increased atmospheric CO_2, and to clarify the mechanism of the CO_2 absorption, because the magnitude of the anticipated global warming depends on the levels of CO_2 in the atmosphere, and because the ocean currently absorbs 1/3 of the 6 Gt of carbon emitted into the atmosphere each year by human activities.

In this cruise, we were aimed at quantifying how much anthropogenic CO_2 were absorbed in the surface ocean in the South Pacific. For the purpose, we measured pCO_2 (partial pressure of CO_2) in the atmosphere and surface seawater along the WHP P21 line at 17°S.

(3) Apparatus

Concentrations of CO_2 in the atmosphere and the sea surface were measured continuously during the cruise using an automated system with a non-dispersive infrared (NDIR) analyzer (BINOS^{TM}). The automated system was operated by one and a half hour cycle. In one cycle, standard gasses, marine air and an air in a headspace of an equilibrator were analyzed subsequently. The concentrations of the standard gas were 270.21, 330.42, 359.98 and 420.30 ppmv. The standard gases will be recalibrated after the cruise.

The marine air taken from the bow was introduced into the NDIR by passing through a mass flow controller, which controlled the air flow rate at about 0.5 L/min, a cooling unit, a perma-pure dryer (GL Sciences Inc.) and a desiccant holder containing $Mg(ClO_4)_2$.

A fixed volume of the marine air taken from the bow was equilibrated with a stream of seawater that flowed at a rate of 5-6L/min in the equilibrator. The air in the equilibrator was circulated with a pump at 0.7-0.8L/min in a closed loop passing through two cooling units, a perma-pure dryer (GL Science Inc.) and a desiccant holder containing $Mg(ClO_4)_2$.

(4) Results

Concentrations of CO_2 (xCO_2) of marine air and surface seawater are shown in Fig. 2.5.1.

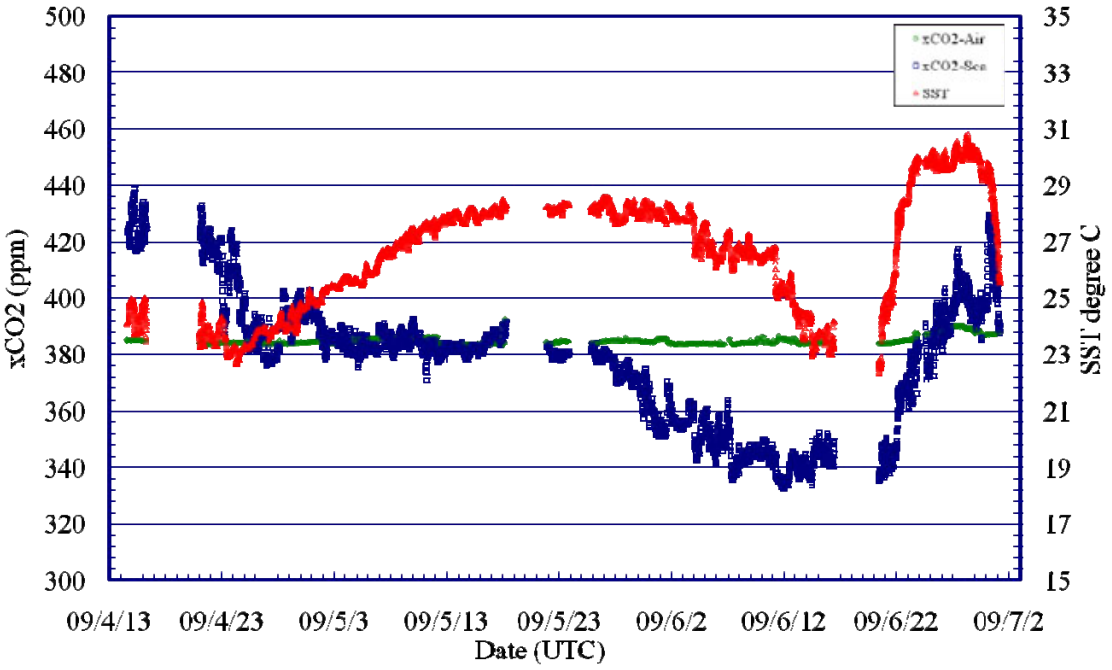

Fig. 2.5.1. Concentrations of CO_2 (xCO_2) in atmosphere (green) and surface seawater (blue), and SST (red).

2.6 Acoustic Doppler Current Profiler (ADCP)

(1)Personnel

Shinya Kouketsu	***(JAMSTEC)***	
Shinya Okumura	***(Global Ocean Development Inc., GODI)***	***-leg1-***
Ryo Kimura	***(GODI)***	***-leg1, 3-***
Yousuke Yuki	***(GODI)***	***-leg1-***
Satoshi Okumura	***(GODI)***	***-leg2-***
Kazuho Yoshida	***(GODI)***	***-leg2-***
Harumi Ohta	***(GODI)***	***-leg2-***
Souichiro Sueyoshi	***(GODI)***	***-leg3-***

(2)Objective

To obtain continuous measurement of the current profile along the ship's track.

(3)Methods

Upper ocean current measurements were made throughout MR09-01 cruise, using the hull mounted Acoustic Doppler Current Profiler (ADCP) system. For most of its operation, the instrument was configured for water-tracking mode recording. Bottom-tracking mode, interleaved bottom-ping with water-ping, was made in shallower water region to get the calibration data for evaluating transducer misalignment angle.

The system consists of following components;

1) R/V MIRAI has installed the Ocean Surveyor for vessel-mount (acoustic frequency 75 kHz; Teledyne RD Instruments). It has a phased-array transducer with single ceramic assembly and creates 4 acoustic beams electronically. We mounted the transducer head rotated to a ship-relative angle of 45 degrees azimuth from the keel.
2) For heading source, we use ship's gyro compass (Tokimec, Japan), continuously providing heading to the ADCP system directory. Additionally, we have Inertial Navigation System (INS) which provide high-precision heading, attitude information, pitch and roll, are stored in ".N2R" data files with a time stamp.
3) GPS navigation receiver (Trimble DS4000) provides position fixes.
4) We used VmDas version 1.4.2 (TRD Instruments) for data acquisition.
5) To synchronize time stamp of ping with GPS time, the clock of the logging computer is adjusted to GPS time every 1 minute.
6) The sound speed at the transducer does affect the vertical bin mapping and vertical velocity measurement, is calculated from temperature, salinity (constant value; 35.0 psu) and depth (6.5 m; transducer depth) by equation in Medwin (1975).

The data was configured for 4 m processing bin, 4 m intervals and starting 20 m below the surface. Every ping was recorded as raw ensemble data (.ENR). Also, 60 seconds and 300 seconds averaged data were recorded as short term average (.STA) and long term average (.LTA) data, respectively. We changed the major parameters, and showed the date and time that we changed command file.

(4)Data archive

These data obtained in this cruise will be submitted to the Data Integration and Analysis Group (DIAG) of JAMSTEC, and will be opened to the public via "R/V MIRAI Data Web Page" in JAMSTEC home page.

(5)Remarks

The profile with bad quality is included between 200m in depth and 400m while in this cruise corresponding to weak echo intensities (Fig 2.6.1. causes of the weak echo intensity may be considered during data processing after cruise).

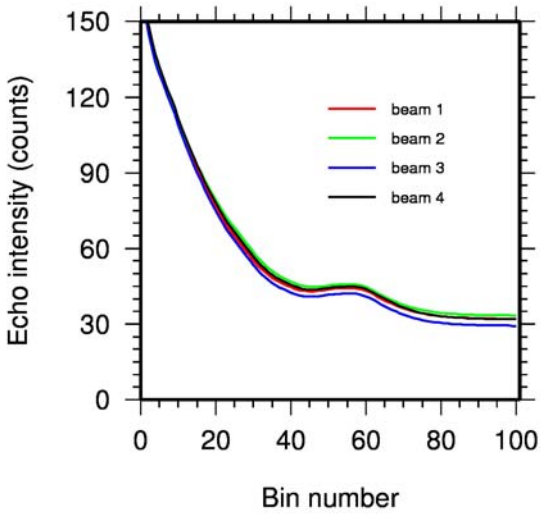

Fig. 2.6.1. Cruise-averaged echo intensities.

2.7 Ceilometer Observation

(1) Personnel

Kunio Yoneyama	***(JAMSTEC)***	***: Principal Investigator / Not on-board***
Shinya Okumura	***(GODI): Leg1***	
Satoshi Okumura	***(GODI): Leg2***	
Souichiro Sueyoshi	***(GODI): Leg3***	
Ryo Kimura	***(GODI): Leg1, Leg3***	
Yousuke Yuuki	***(GODI): Leg1***	
Kazuho Yoshida	***(GODI): Leg2***	
Harumi Ota	***(GODI): Leg2***	

(2) Objectives

The information of cloud base height and the liquid water amount around cloud base is important to understand the process on formation of the cloud. As one of the methods to measure them, the ceilometer observation was carried out.

(3) Parameters

1. Cloud base height [m].
2. Backscatter profile, sensitivity and range normalized at 30 m resolution.
3. Estimated cloud amount [oktas] and height [m]; Sky Condition Algorithm.

(4) Methods

We measured cloud base height and backscatter profile using ceilometer (CT-25K, VAISALA, Finland) throughout the MR09-01 cruise.

Major parameters for the measurement configuration are as follows;

Laser source:	Indium Gallium Arsenide (InGaAs) Diode
Transmitting wavelength:	905±5 mm at 25 degC
Transmitting average power:	8.9 mW
Repetition rate:	5.57 kHz
Detector:	Silicon avalanche photodiode (APD)
	Responsibility at 905 nm: 65 A/W
Measurement range:	0 ~ 7.5 km
Resolution:	50 ft in full range
Sampling rate:	60 sec
Sky Condition	0, 1, 3, 5, 7, 8 oktas (9: Vertical Visibility)
	(0: Sky Clear, 1:Few, 3:Scattered, 5-7: Broken, 8: Overcast)

On the archive dataset, cloud base height and backscatter profile are recorded with the resolution of 30 m (100 ft).

(5) Preliminary results

Fig.2.7-1 to Fig.2.7-3 shows the time series of the lowest, second and third cloud base height during the cruise.

(6) Data archives

The raw data obtained during this cruise will be submitted to the Data Integration and Analysis Group (DIAG) in JAMSTEC.

(7) Remarks

1. We did not collect data in the territorial waters and the EEZ at following terms.

The territorial waters and the EEZ of Peru:	00:00UTC 13 Apr. 2009 to 12:40UTC 14 Apr. 2009
	06:00UTC 16 Apr. 2009 to 00:15UTC 21 Apr. 2009
The territorial waters of Papua New Guinea:	23:10UTC 23 Jun. 2009 to 13:06UTC 24 Jun. 2009

2. Window cleaning;

15:08UTC 14 Apr. 2009
06:43UTC 26 Apr. 2009
10:26UTC 27 Apr. 2009
14:51UTC 29 Apr. 2009
12:30UTC 05 May. 2009
10:51UTC 07 May. 2009
01:54UTC 21 May. 2009
02:17UTC 27 May. 2009
01:20UTC 01 Jun. 2009
02:10UTC 03 Jun. 2009
03:16UTC 08 Jun. 2009
05:45UTC 14 Jun. 2009
05:26UTC 19 Jun. 2009
01:34UTC 30 Jun. 2009

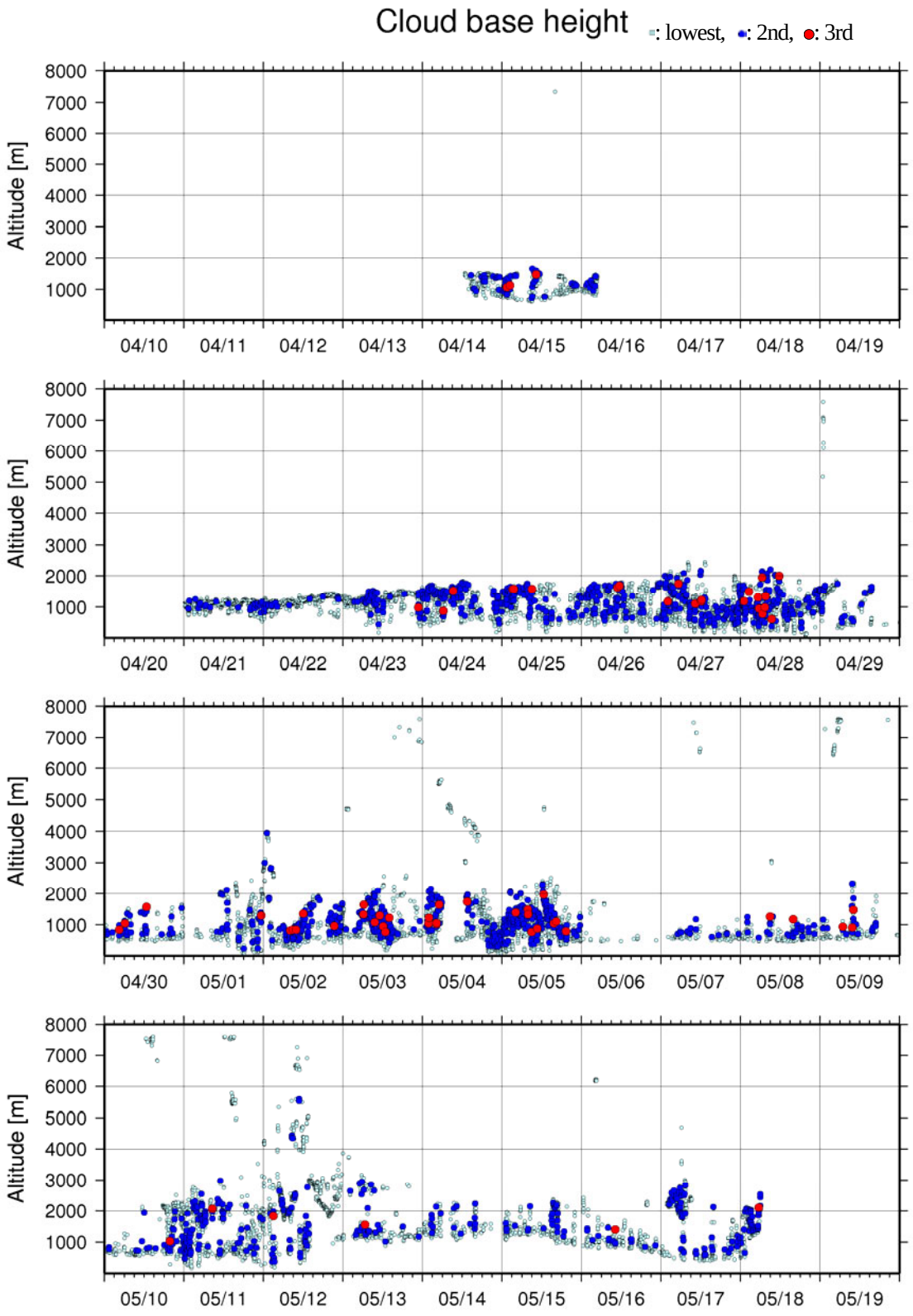

Fig.2.7-1 Lowest, 2nd and 3rd cloud base height during the MR09-01 Leg1 cruise

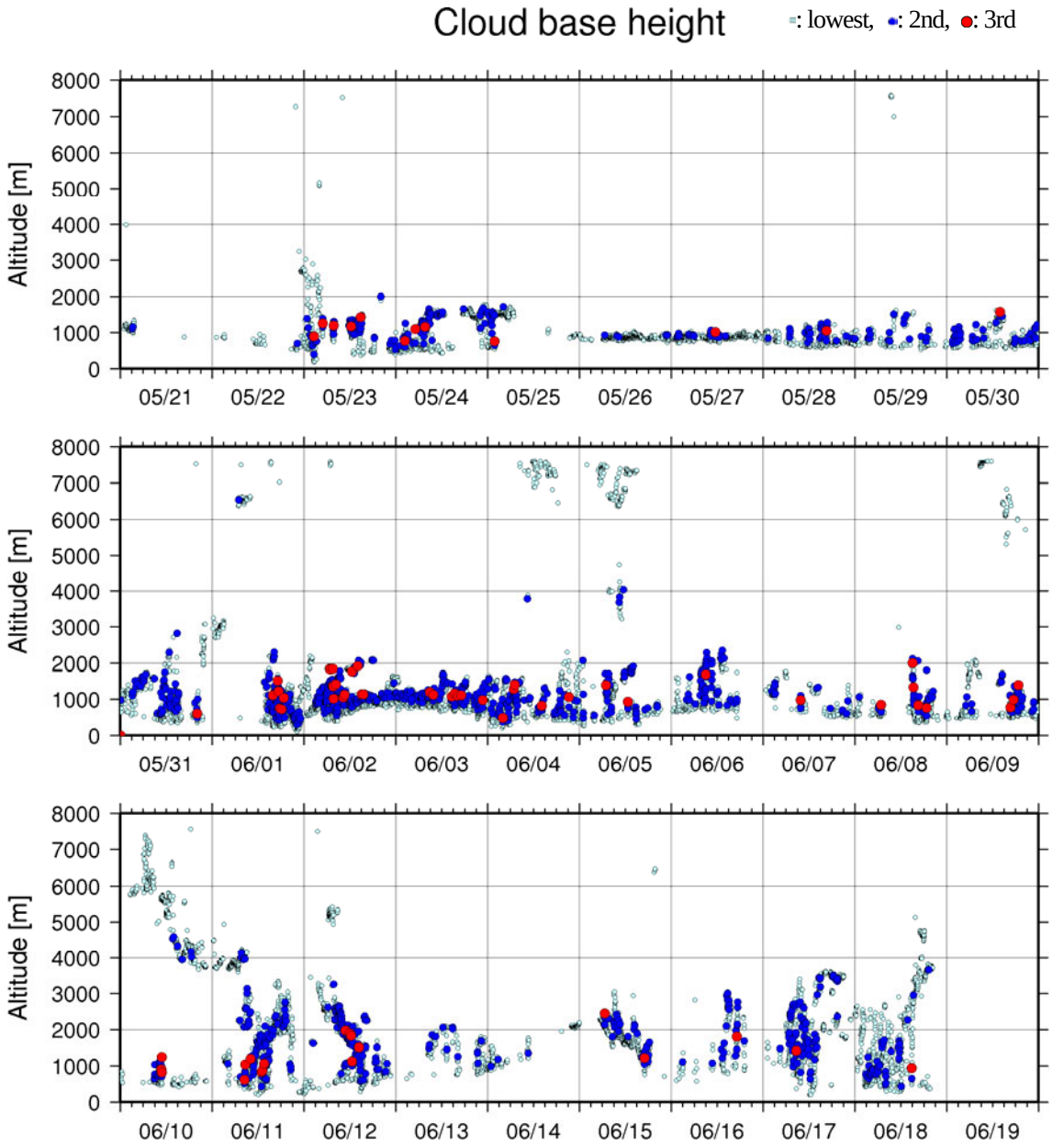

Fig.2.7-2 Lowest, 2nd and 3rd cloud base height during the MR09-01 Leg2 cruise

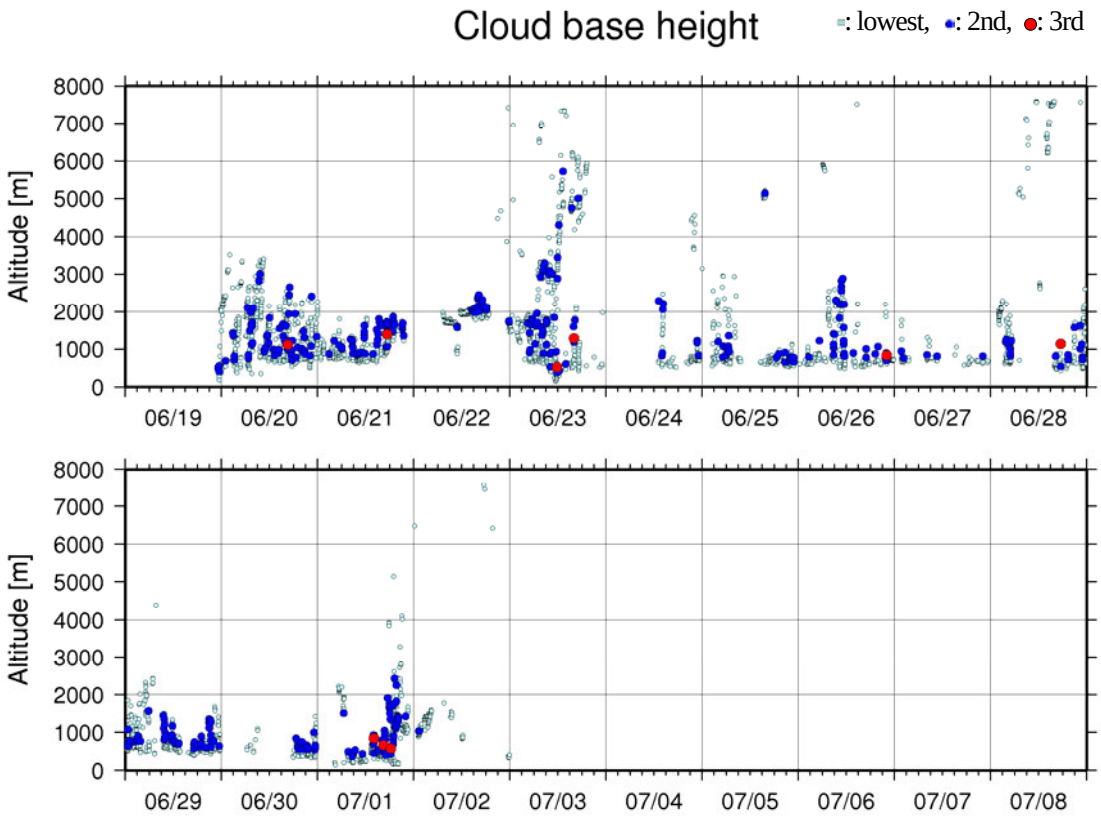

Fig.2.7-3 Lowest, 2nd and 3rd cloud base height during the MR09-01 Leg3 cruise

2.8 Air-sea surface eddy flux measurement

(1) Personnel

Osamu Tsukamoto	(Okayama University) Principal Investigator	* not on board
Fumiyoshi Kondo	(University of Tokyo)	* not on board
Hiroshi Ishida	(Kobe University)	* not on board
Satoshi Okumura	(Global Ocean Development Inc. (GODI))	

(2) Objective

To better understand the air-sea interaction, accurate measurements of surface heat and fresh water budgets are necessary as well as momentum exchange through the sea surface. In addition, the evaluation of surface flux of carbon dioxide is also indispensable for the study of global warming. Sea surface turbulent fluxes of momentum, sensible heat, latent heat, and carbon dioxide were measured by using the eddy correlation method that is thought to be most accurate and free from assumptions. These surface heat flux data are combined with radiation fluxes and water temperature profiles to derive the surface energy budget.

(3) Instruments and Methods

The surface turbulent flux measurement system (Fig. 2.8-1) consists of turbulence instruments (Kaijo Co., Ltd.) and ship motion sensors (Kanto Aircraft Instrument Co., Ltd.). The turbulence sensors include a three-dimensional sonic anemometer-thermometer (Kaijo, DA-600) and an infrared hygrometer (LICOR, LI-7500). The sonic anemometer measures three-dimensional wind components relative to the ship. The ship motion sensors include a two-axis inclinometer (Applied Geomechanics, MD-900-T), a three-axis accelerometer (Applied Signal Inc., QA-700-020), and a three-axis rate gyro (Systron Donner, QRS-0050-100). LI7500 is a CO_2/H_2O turbulence sensor that measures turbulent signals of carbon dioxide and water vapor simultaneously. These signals are sampled at 10 Hz by a PC-based data logging system (Labview, National Instruments Co., Ltd.). By obtaining the ship speed and heading information through the Mirai network system it yields the absolute wind components relative to the ground. Combining wind data with the turbulence data, turbulent fluxes and statistics are calculated in a real-time basis. These data are also saved in digital files every 0.1 second for raw data and every 1 minute for statistic data.

(4) Observation log

The observation was carried out throughout this cruise.

(5) Data Policy and citation

All data are archived at Okayama University, and will be open to public after quality checks and corrections. Corrected data will be submitted to JAMSTEC Marine-Earth Data and Information Department.

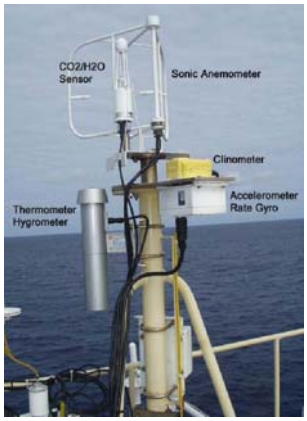

Fig. 2.8-1 Turbulent flux measurement system on the top deck of the foremast.

2.9 Lidar observations of clouds and aerosols

(1) Personnel

Nobuo Sugimoto (National Institute for Environmental Studies, NIES), not on board

Ichiro Matsui (NIES), not on board

Atsushi Shimizu (NIES), not on board

Tomoaki Nishizawa (NIES), not on board

Lidar operation was supported by Global Ocean Development Inc.

(2) Objectives

Objectives of the observations in this cruise is to study distribution and optical characteristics of ice/water clouds and marine aerosols using a two-wavelength lidar.

(3) Measured parameters

- Vertical profiles of backscattering coefficient at 532 nm
- Vertical profiles of backscattering coefficient at 1064 nm
- Depolarization ratio at 532 nm

(4) Method

Vertical profiles of aerosols and clouds were measured with a two-wavelength lidar. The lidar employs a Nd:YAG laser as a light source which generates the fundamental output at 1064 nm and the second harmonic at 532 nm. Transmitted laser energy is typically 30 mJ per pulse at both of 1064 and 532 nm. The pulse repetition rate is 10 Hz. The receiver telescope has a diameter of 20 cm. The receiver has three detection channels to receive the lidar signals at 1064 nm and the parallel and perpendicular polarization components at 532 nm. An analog-mode avalanche photo diode (APD) is used as a detector for 1064 nm, and photomultiplier tubes (PMTs) are used for 532 nm. The detected signals are recorded with a transient recorder and stored on a hard disk with a computer. The lidar system was installed in a container which has a glass window on the roof, and the lidar was operated continuously regardless of weather. Every 10 minutes vertical profiles of four channels (532 parallel, 532 perpendicular, 1064, 532 near range) are recorded.

(5) Results

Figures 1 and 2 show vertical distributions of clouds and aerosols detected by the lidar during Leg1 and Leg2/3, respectively. Top panel indicates the intensity of backscatter at visible wavelength (532nm). Cloud base is indicated red color in the panel, and blue or green colors correspond to aerosols. Light blue color indicate weak scattering from molecules. In the former half of Leg1 clouds appeared continuously

around 1 – 2 km height, and higher altitude were obscured by these clouds. We observed some high clouds in May, and they showed greater depolarization ratio (middle panel) which means the particles have irregular (non spherical) shape. Scattering at the beginning of Leg2 was very weak, it means that the atmosphere was very clean near the sea surface. In the middle of Leg2 surface aerosol layer height was greater than the bottom height of cumulus. To interpret it, long range transport of aerosols must be considered. Mineral dust layer, which shows non-zero depolarization ratio, was obeserved around April 18. Several ground based lidars in Japan detected similar dust layers same time.

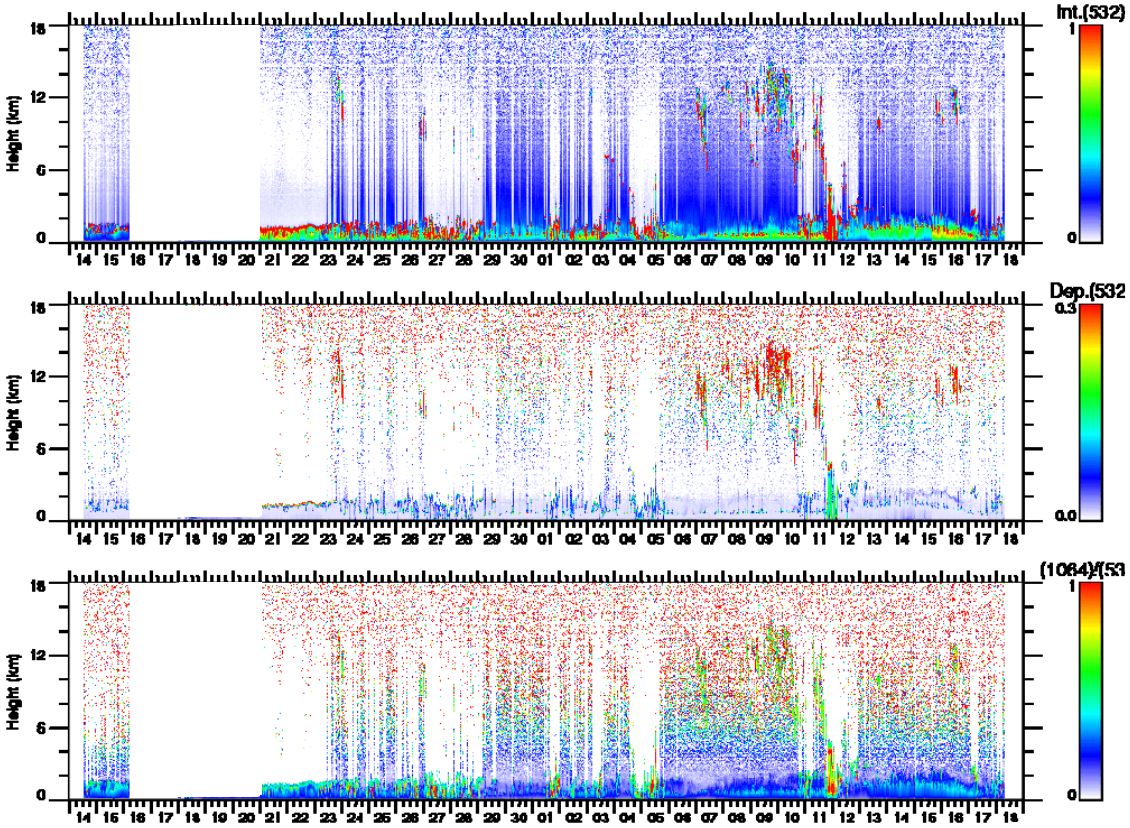

Figure 1: Time-height sections of (top) backscatter intensity at 532 nm, (middle) depolarization ratio at 532 nm, and (bottom) ratio of backscatter intensities at 1064nm and 532 nm, during April 14 and May 18, 2009.

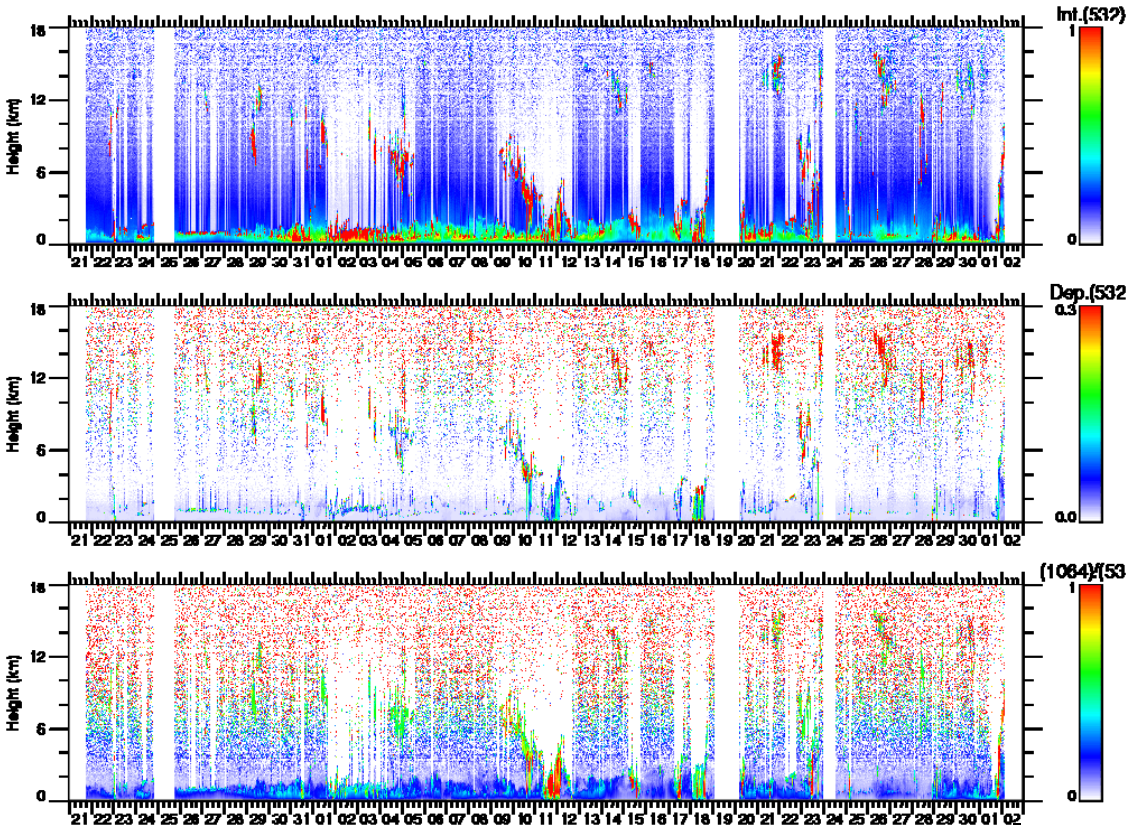

Figure 2: Same as Fig.1, but for the period during May 21 and July 2, 2009.

(6) Data archive

- raw data

  lidar signal at 532 nm

  lidar signal at 1064 nm

  depolarization ratio at 532 nm

  temporal resolution 10min/ vertical resolution 6 m

  data period (UTC): April 14 – July 2, 2009

- processed data (plan)

  cloud base height, apparent cloud top height

  phase of clouds (ice/water)

  cloud fraction

  boundary layer height (aerosol layer upper boundary height)

  backscatter coefficient of aerosols

  particle depolarization ratio of aerosols

(7) Data policy and Citation

Contact NIES lidar team (nsugimot/i-matsui/shimizua/nisizawa) to utilize lidar data for productive use.

2.10 Water isotopes in atmospheric vapor, precipitation, and sea surface water

(1) Personnel

Naoyuki Kurita (JAMSTEC), Principal Investigator
Ryu Uemura (LSCE/CEA)
Kimpei Ichiyanagi (Kumamoto Univ.)
Hironori Fudeyasu (Hawaii Univ.)

(2) Objective

It is well known that the variability of stable water isotopes (HDO and $H_2{}^{18}O$) is closely related with the moisture origin and hydrological processes during the transportation from the source region to deposition site. Thus, water isotope tracer is recognized as the powerful tool to study of the hydrological cycles in the atmosphere. However, oceanic region is one of sparse region of the isotope data, it is necessary to fill the data to identify the moisture sources by using the isotope tracer. In this study, to fill this sparse observation area, intense water isotopes observation was conducted along the cruise track of MR-09-01.

(3) Method

Following observation was carried out throughout this cruise.

- Atmospheric moisture sampling:

  Water vapor was sampled from the height about 20m above the sea level. The air was drawn at rate of 1.5-2L/min through a plastic tube attached to top of the compass deck. The flow rate is regulated according to the water vapor content to collect the sample amount 15-30ml. The water vapor was trapped in a glass trap submerged into a ethanol cooled to 100 degree C by radiator, and then they are collected every 12 hour during the cruise. After collection, water in the trap was subsequently thawed and poured into the 6ml glass bottle.

- Rainwater sampling

  Rainwater samples gathered in rain collector were collected just after precipitation events have ended. The collected sample was then transferred into glass bottle (6ml) immediately after the measurement of precipitation amount.

- Surface seawater sampling

  Seawater sample taken by the pump from 4m depth were collected in glass bottle (6ml) around the noon at the local time. The surface water taken by bucket from the deck was also sampled in case the bucket water sampling has carried out to compare the 4m depth samples.

(4) Results

Sampling of water vapor for isotope analysis is summarized in Table 2.10-1 (148 samples). The detail of rainfall sampling (38 samples) is summarized in Table 2.10-2. Described rainfall amount is calculated from the collected amount of precipitation. Sampling of surface seawater taken by pump from 4m depths is summarized in Table 2.10-3 (68 samples). And, surface sea water samples taken by bucket sampling is summarized in Table 2.10-4 (54 samples).

(5) Data archive

Isotopes (HDO, $H_2{}^{18}O$) analysis will be done at IORGC/JAMSTEC, and then analyzed isotopes data will be submitted to JAMSTEC Data Management Office.

Table 2.10-1 Summary of water vapor sampling for isotope analysis.

Sample	Date	Time (UT)	Date	Time (UT)	Lon	Lat	Total (m^3)	MASS (ml)
V-L1-1	14-Apr	12:50	15-Apr	00:01	079-50W	16-45S	1.52	18.0
V-L1-2	15-Apr	00:05	15-Apr	12:00	080-59W	16-44S	1.62	22.0
V-L1-3	15-Apr	12:04	16-Apr	00:00	080-30W	16-35S	1.61	20.0
V-L1-4	16-Apr	00:04	16-Apr	05:35	079-04W	16-20S	0.75	8.0
V-L1-11	21-Apr	00:15	21-Apr	12:00	081-19W	16-44S	1.43	18.0
V-L1-12	21-Apr	12:04	22-Apr	00:00	082-20W	16-45S	1.44	18.8
V-L1-13	22-Apr	00:03	22-Apr	12:00	082-59W	16-44S	1.45	18.0
V-L1-14	22-Apr	12:04	23-Apr	00:00	083-49W	16-45S	1.44	18.0
V-L1-15	23-Apr	00:04	23-Apr	12:01	084-40W	16-45S	1.44	17.8
V-L1-16	23-Apr	12:03	24-Apr	00:00	085-19W	16-44S	1.44	20.0
V-L1-17	24-Apr	00:03	24-Apr	12:01	086-26W	16-49S	1.45	18.8
V-L1-18	24-Apr	12:06	25-Apr	00:00	087-51W	16-45S	1.44	20.0
V-L1-19	25-Apr	00:03	25-Apr	12:00	088-39W	16-44S	1.45	18.4
V-L1-20	25-Apr	12:04	26-Apr	00:00	089-23W	16-44S	1.44	20.0
V-L1-21	26-Apr	00:03	26-Apr	12:01	090-38W	16-45S	1.45	18.6
V-L1-22	26-Apr	12:07	27-Apr	00:00	092-00W	16-45S	1.47	21.0
V-L1-23	27-Apr	00:04	27-Apr	12:00	093-20W	16-45S	1.47	22.0
V-L1-24	27-Apr	12:04	28-Apr	00:00	094-40W	16-45S	1.47	22.8
V-L1-25	28-Apr	00:03	28-Apr	12:00	096-00W	16-45S	1.47	22.8
V-L1-26	28-Apr	12:03	29-Apr	00:00	097-20W	16-43S	1.47	24.0
V-L1-27	29-Apr	00:03	29-Apr	12:00	098-46W	16-44S	1.47	24.0
V-L1-28	29-Apr	12:03	30-Apr	00:00	100-24W	16-45S	1.47	24.0
V-L1-29	30-Apr	00:03	30-Apr	12:00	101-58W	16-45S	1.47	22.0
V-L1-30	30-Apr	12:03	1-May	00:00	103-00W	17-00S	1.47	21.8
V-L1-31	1-May	00:04	1-May	12:00	104-09W	16-45S	1.47	22.0
V-L1-32	1-May	12:03	2-May	00:00	106-00W	16-45S	1.47	24.0
V-L1-33	2-May	00:04	2-May	12:00	106-57W	16-45S	1.47	24.2
V-L1-34	2-May	12:02	3-May	00:02	107-17W	16-45S	1.48	24.2
V-L1-35	3-May	00:05	3-May	12:00	108-00W	16-45S	1.47	22.4
V-L1-36	3-May	12:04	4-May	00:00	109-20W	16-45S	1.46	24.8
V-L1-37	4-May	00:06	4-May	12:00	110-40W	16-45S	1.47	22.8
V-L1-38	4-May	12:02	5-May	00:00	112-01W	16-45S	1.47	24.0

V-L1-39	5-May	00:02	5-May	12:01	113-57W	16-45S	1.48	24.8
V-L1-40	5-May	12:03	6-May	00:00	115-20W	16-45S	1.46	28.0
V-L1-41	6-May	00:03	6-May	12:00	116-51W	16-45S	1.46	27.0
V-L1-42	6-May	12:03	7-May	00:00	118-38W	16-45S	1.47	26.0
V-L1-43	7-May	00:02	7-May	12:00	120-00W	16-45S	1.47	25.0
V-L1-44	7-May	12:02	8-May	00:00	121-23W	16-45S	1.46	26.0
V-L1-45	8-May	00:02	8-May	12:00	123-08W	16-45S	1.47	27.0
V-L1-46	8-May	12:04	9-May	00:00	124-40W	16-45S	1.46	26.8
V-L1-47	9-May	00:02	9-May	12:01	126-00W	16-45S	1.47	24.6
V-L1-48	9-May	12:04	10-May	00:00	127-20W	16-45S	1.47	26.0
V-L1-49	10-May	00:02	10-May	12:00	128-56W	16-45S	1.47	26.0
V-L1-50	10-May	12:02	11-May	00:00	130-30W	16-45S	1.46	26.8
V-L1-51	11-May	00:04	11-May	12:00	131-59W	16-45S	1.47	27.0
V-L1-52	11-May	12:04	12-May	00:00	133-20W	16-45S	1.46	24.0
V-L1-53	12-May	00:04	12-May	12:02	134-00W	16-45S	1.45	26.0
V-L1-54	12-May	12:05	13-May	00:00	135-19W	16-45S	1.47	24.0
V-L1-55	13-May	00:02	13-May	12:00	136-40W	16-45S	1.47	20.0
V-L1-56	13-May	12:01	14-May	00:00	138-20W	16-45S	1.49	20.0
V-L1-57	14-May	00:02	14-May	12:00	139-59W	16-45S	1.50	20.0
V-L1-58	14-May	12:02	15-May	00:00	141-36W	16-45S	1.53	18.0
V-L1-59	15-May	00:03	15-May	12:00	142-56W	17-09S	1.54	20.0
V-L1-60	15-May	12:02	16-May	00:00	143-58W	17-29S	1.54	23.0
V-L1-61	16-May	00:02	16-May	12:00	145-30W	17-30S	1.54	20.0
V-L1-62	16-May	12:02	17-May	00:00	146-38W	17-30S	1.52	26.0
V-L1-63	17-May	00:02	17-May	12:00	148-15W	17-30S	1.50	30.0
V-L1-64	17-May	12:02	18-May	00:00	149-00W	17-30S	1.50	30.0
V-L1-65	18-May	00:02	18-May	07:02	149-20W	17-30S	0.88	16.0
V-L2-66	21-May	17:50	22-May	00:00	150-04W	17-30S	0.79	12.0
V-L2-67	22-May	00:02	22-May	12:00	151-00W	17-30S	1.47	24.0
V-L2-68	22-May	12:02	23-May	00:00	152-24W	17-30S	1.47	28.0
V-L2-69	23-May	00:02	23-May	12:00	153-44W	17-30S	1.47	28.0
V-L2-70	23-May	12:03	24-May	00:04	153-23W	17-30S	1.47	28.0
V-L2-71	24-May	00:06	24-May	12:00	150-57W	17-27S	1.44	28.0
V-L2-72	24-May	12:02	24-May	19:45	149-34W	17-32S	0.95	18.0

V-L2-73	24-May	19:49	25-May	18:09	149-34W	17-32S	2.40	40.5
V-L2-74	25-May	18:12	26-May	00:00	150-48W	17-30S	0.69	9.2
V-L2-75	26-May	00:03	26-May	12:00	153-52W	17-30S	1.43	20.0
V-L2-76	26-May	12:11	27-May	00:10	155-40W	17-30S	1.44	23.8
V-L2-77	27-May	00:13	27-May	12:02	156-00W	17-30S	1.42	21.5
V-L2-78	27-May	12:10	28-May	00:01	158-20W	17-30S	1.42	22.6
V-L2-79	28-May	00:05	28-May	12:00	159-40W	17-30S	1.43	21.3
V-L2-80	28-May	12:05	29-May	00:03	161-00W	17-30S	1.43	26.2
V-L2-81	29-May	00:08	29-May	12:09	162-20W	17-30S	1.44	26.4
V-L2-82	29-May	12:14	30-May	00:00	163-40W	17-30S	1.39	27.0
V-L2-83	30-May	00:04	30-May	12:00	164-53W	17-30S	1.29	24.2
V-L2-84	30-May	12:03	31-May	00:17	166-07W	17-30S	1.32	26.0
V-L2-85	31-May	00:20	31-May	12:00	167-11W	17-30S	1.26	25.0
V-L2-86	31-May	12:02	1-Jun	00:00	168-25W	17-30S	1.29	25.8
V-L2-87	1-Jun	00:03	1-Jun	12:00	169-41W	17-30S	1.29	25.0
V-L2-88	1-Jun	12:02	2-Jun	00:04	170-59W	17-30S	1.30	25.0
V-L2-89	2-Jun	00:07	2-Jun	12:21	172-00W	17-29S	1.32	22.5
V-L2-90	2-Jun	12:24	3-Jun	00:08	172-20W	17-29S	1.27	19.8
V-L2-91	3-Jun	00:10	3-Jun	12:01	173-00W	17-30S	1.28	19.0
V-L2-92	3-Jun	12:04	4-Jun	00:06	174-25W	17-26S	1.30	22.2
V-L2-93	4-Jun	00:09	4-Jun	12:00	176-20W	17-30S	1.28	22.8
V-L2-94	4-Jun	12:02	5-Jun	00:02	177-57W	17-37S	1.44	26.2
V-L2-95	5-Jun	00:04	5-Jun	12:00	179-37W	18-24S	1.44	26.2
V-L2-96	5-Jun	12:03	6-Jun	00:00	179-00E	18-25S	1.43	23.8
V-L2-97	6-Jun	00:01	6-Jun	12:00	177-40E	18-42S	1.37	20.2
V-L2-98	6-Jun	12:01	7-Jun	00:00	176-46E	17-50S	1.37	20.5
V-L2-99	7-Jun	00:02	7-Jun	12:00	157-00E	17-50S	1.37	22.0
V-L2-100	7-Jun	12:02	7-Jun	23:57	173-17E	17-50S	1.33	22.2
V-L2-101	8-Jun	00:00	8-Jun	12:01	171-40E	17-50S	1.30	22.0
V-L2-102	8-Jun	12:03	9-Jun	00:00	171-01E	17-50S	1.29	23.0
V-L2-103	9-Jun	00:02	9-Jun	12:00	168-50E	18-03S	1.36	23.0
V-L2-104	9-Jun	12:02	10-Jun	00:00	168-03E	18-22S	1.36	23.8
V-L2-105	10-Jun	00:02	10-Jun	12:00	167-35E	18-34S	1.37	22.5
V-L2-106	10-Jun	12:03	11-Jun	00:00	166-35E	19-00S	1.36	24.0

V-L2-107	11-Jun	00:02	11-Jun	12:00	165-29E	19-29S	1.36	23.5
V-L2-108	11-Jun	12:02	12-Jun	00:00	164-40E	19-50S	1.37	18.0
V-L2-109	12-Jun	00:02	12-Jun	12:11	163-47E	18-57S	1.39	19.2
V-L2-110	12-Jun	12:13	13-Jun	00:00	163-25E	20-02S	1.34	19.2
V-L2-111	13-Jun	00:02	13-Jun	12:00	164-12E	20-56S	1.44	18.0
V-L2-112	13-Jun	12:02	14-Jun	00:00	163-15E	21-18S	1.44	17.0
V-L2-113	14-Jun	00:05	14-Jun	12:32	161-33E	21-58S	1.87	19.0
V-L2-114	14-Jun	12:34	15-Jun	00:00	160-04E	22-33S	1.72	14.2
V-L2-115	15-Jun	00:03	15-Jun	12:00	158-38E	23-07S	2.16	20.0
V-L2-116	15-Jun	12:01	15-Jun	23:55	157-11E	23-41S	2.13	25.0
V-L2-117	16-Jun	00:00	16-Jun	12:00	155-48E	24-14S	1.80	22.2
V-L2-118	16-Jun	12:01	17-Jun	00:00	154-56E	24-34S	1.79	17.8
V-L2-119	17-Jun	00:02	17-Jun	12:00	153-45E	25-00S	1.80	18.0
V-L2-120	17-Jun	12:02	18-Jun	00:09	153-35E	25-20S	1.83	21.0
V-L2-121	18-Jun	00:12	18-Jun	12:11	153-26E	25-54S	1.81	20.2

V-L3-125	20-Jun	12:10	21-Jun	00:01	154-34E	21-55S	1.77	23.8
V-L3-126	21-Jun	00:05	21-Jun	12:00	154-44E	19-14S	1.78	24.8
V-L3-127	21-Jun	12:04	22-Jun	00:00	154-44E	16-14S	1.79	23.0
V-L3-128	22-Jun	00:04	22-Jun	12:00	154-44E	13-26S	1.74	26.8
V-L3-129	22-Jun	12:05	22-Jun	23:57	154-34E	10-36S	1.57	26.2
V-L3-130	23-Jun	00:03	23-Jun	12:00	153-59E	07-40S	1.28	24.2
V-L3-131	23-Jun	12:03	23-Jun	23:01	153-29E	05-08S	1.18	22.8
V-L3-132	24-Jun	13:13	25-Jun	00:00	150-33E	00-07N	1.16	22.4
V-L3-133	25-Jun	00:03	25-Jun	12:00	148-52E	02-24N	1.29	25.8
V-L3-134	25-Jun	12:03	26-Jun	00:00	147-03E	04-48N	1.26	24.8
V-L3-135	26-Jun	00:08	26-Jun	12:00	145-13E	07-18N	1.23	24.6
V-L3-136	26-Jun	12:03	26-Jun	23:58	143-27E	09-36N	— (0.00)	24.4
V-L3-137	27-Jun	00:03	27-Jun	12:00	141-44E	11-56N	1.20	24.0
V-L3-138	27-Jun	12:05	28-Jun	00:02	140-29E	14-09N	1.20	23.8
V-L3-139	28-Jun	00:05	28-Jun	12:00	139-43E	16-14N	1.20	24.0
V-L3-140	28-Jun	12:04	29-Jun	00:00	138-45E	18-48N	1.21	24.6

V-L3-141	29-Jun	00:03	29-Jun	12:00	137-48E	21-17N	1.21	24.2
V-L3-142	29-Jun	12:03	30-Jun	00:00	136-51E	23-46N	1.21	24.6
V-L3-143	30-Jun	00:04	30-Jun	12:00	135-52E	26-13N	1.21	24.4
V-L3-144	30-Jun	12:02	1-Jul	00:23	134-57E	28-35N	1.19	24.2
V-L3-145	1-Jul	00:27	1-Jul	12:00	133-59E	30-54N	1.16	26.0
V-L3-146	1-Jul	12:04	2-Jul	00:00	132-19E	32-42N	1.18	23.6
V-L3-147	2-Jul	00:03	2-Jul	12:00	131-22E	33-45N	1.19	18.0
V-L3-148	2-Jul	12:03	2-Jul	23:48	131-00E	33-58N	1.17	18.4

Table 2.10-2 Summary of precipitation sampling for isotope analysis.

	Date	**Time (UT)**	**Lon**	**Lat**	**Date**	**Time (UT)**	**Lon**	**Lat**	**Rain (mm)**
R-L1-1	17-Apr	23:40	075-10.2W	15-35.0S	26-Apr	06:51	090-00.0W	16-45.0S	0.6
R-L1-2	26-Apr	06:52	090-00.0W	16-45.0S	26-Apr	16:03	090-51.2W	16-44.7S	1.6
R-L1-3	26-Apr	16:06	090-52.5W	16-44.9S	26-Apr	17:00	091-06.5W	16-44.9S	1.8
R-L1-4	26-Apr	17:08	091-08.6W	16-44.9S	27-Apr	06:50	092-40.2W	16-44.8S	3.7
R-L1-5	27-Apr	06:50	092-40.2W	16-44.8S	27-Apr	15:51	093-41.4W	16-44.5S	4.2
R-L1-6	27-Apr	15:51	093-41.4W	16-44.5S	27-Apr	23:28	094-40.2W	16-44.9S	2.2
R-L1-7	27-Apr	23:28	094-40.2W	16-44.9S	28-Apr	13:30	096-04.0W	16-44.8S	5.5
R-L1-8	28-Apr	13:30	096-04.0W	16-44.8S	28-Apr	15:36	096-36.7W	16-44.9S	1.3
R-L1-9	28-Apr	15:36	096-36.7W	16-44.9S	1-May	13:49	104-38.4W	16-44.9S	1.1
R-L1-10	1-May	13:50	104-38.5W	16-49.0S	1-May	20:11	105-21.6W	16-45.2S	2.0
R-L1-11	1-May	20:11	105-21.6W	16-45.2S	2-May	21:33	107-19.9W	16-44.9S	1.5
R-L1-12	2-May	21:33	107-19.9W	16-44.9S	3-May	12:15	108-00.3W	16-45.0S	1.3
R-L1-13	3-May	12:15	108-00.3W	16-45.0S	4-May	23:52	112-00.2W	15-45.3S	17.6
R-L1-14	4-May	23:52	112-00.2W	16-45.3S	5-May	12:31	114-00.0W	16-45.0S	4.3
R-L1-15	5-May	12:31	114-00.0W	16-45.0S	11-May	03:15	130-39.6W	16-45.8S	4.7
R-L1-16	11-May	03:15	130-39.6W	16-45.8S	11-May	21:41	132-51.6W	16-45.5S	6.7
R-L1-17	11-May	21:41	132-51.6W	16-45.5S	12-May	01:05	133-20.2W	16-45.1S	10.8
R-L1-18	12-May	01:05	133-20.2W	16-45.1S	12-May	05:25	133-33.7W	16-52.2S	18.2
R-L1-19	12-May	05:25	133-33.7W	16-52.2S	12-May	17:29	134-39.8W	16-45.6S	0.7
R-L2-20	21-May	18:00	149-34.2W	17-32.9S	23-May	03:36	152-59.6W	17-30.2S	8.7
R-L2-21	25-May	18:00	149-34.2W	17-32.2S	31-May	15:10	167-40.2W	17-29,8S	0.8
R-L2-22	31-May	15:10	167-40.2W	17-29,8S	2-Jun	00:20	170-59.4W	17-29.8S	3.0
R-L2-23	2-Jun	00:20	170-59.4W	17-29.8S	4-Jun	02:09	174-56.5W	17-29.5S	3.1

R-L2-24	4-Jun	02:09	174-56.5W	17-29.5S	11-Jun	15:30	165-14.8E	19-34.7S	4.2
R-L2-25	11-Jun	15:30	165-14.8E	19-34.7S	11-Jun	23:43	164-39.6E	19-49.5S	4.7
R-L2-26	11-Jun	23:43	164-39.6E	19-49.5S	12-Jun	07:39	164-20.6E	19-44.4S	1.1
R-L2-27	12-Jun	07:39	164-20.6E	19-44.4S	17-Jun	11:45	153-44.5E	24-59.8S	6.6
R-L2-28	17-Jun	11:45	153-44.5E	24-59.8S	17-Jun	15:05	153-52.0S	24-57.1S	4.8
R-L2-29	17-Jun	15:05	153-52.0S	24-57.1S	18-Jun	07:37	153-29.0E	25-40.0S	N.A.
R-L2-30	18-Jun	07:37	153-29.0E	25-40.0S	18-Jun	21:29	153-11.1E	26-46.9S	N.A.
R-L3-31	20-Jun	04:30	153-24.2E	26-25.1S	20-Jun	12:01	153-57.7E	24-39.8S	1.9
R-L3-32	20-Jun	12:01	153-57.7E	24-39.8S	23-Jun	12:10	153-58.0E	07-36.9S	6.6
R-L3-33	25-Jun	00:00	150-33.5E	00-06.8N	27-Jun	05:47	142-37.6E	10-44.8N	2.5
R-L3-34	27-Jun	05:47	142-37.6E	10-44.8N	28-Jun	23:43	138-46.3E	18-44.9N	5.7
R-L3-35	28-Jun	23:50	138-45.8E	18-46.3N	29-Jun	01:21	138-38.0E	19-04.6N	4.4
R-L3-36	29-Jun	01:23	138-37.8E	19-05.1N	29-Jun	06:44	138-12.8E	20-11.8N	3.7
R-L3-37	29-Jun	06:50	138-12.4E	20-13.0N	29-Jun	20:39	137-07.7E	23-03.8N	1.0
R-L3-38	29-Jun	20:42	137-07.5E	23-04.3N	1-Jul	23:20	132-27.4E	32-35.9N	11.1

* Rainfall shows collected amount (ml).

Table 2.10-3 Summary of surface seawater sample taken from 4m depths

Sampling No.		Date	Time	Position	
			(UTC)	LON	LAT
MR09-01 Leg1 O-	1	14-Apr	17:01	078.56.0W	16-44.7S
MR09-01 Leg1 O-	2	15-Apr	17:00	081-17.3W	16-44.9S
MR09-01 Leg1 O-	6	21-Apr	17:00	081-40.2W	16-44.5S
MR09-01 Leg1 O-	7	22-Apr	17:00	083-19.4W	16-44.3S
MR09-01 Leg1 O-	8	23-Apr	17:00	085-00.0W	16-44.8S
MR09-01 Leg1 O-	9	24-Apr	16:58	086-59.5W	16-43.7S
MR09-01 Leg1 O-	10	25-Apr	17:00	089-00.0W	16-44.4S
MR09-01 Leg1 O-	11	26-Apr	17:59	091-20.1W	16-45.1S
MR09-01 Leg1 O-	12	27-Apr	18:11	093-59.9W	16-44.7S
MR09-01 Leg1 O-	13	28-Apr	18:00	096-40.0W	16-44.2S
MR09-01 Leg1 O-	14	29-Apr	18:00	099-38.2W	16-44.6S
MR09-01 Leg1 O-	15	30-Apr	17:58	102-40.2W	16-45.0S
MR09-01 Leg1 O-	16	1-May	19:00	105-20.2W	16-45.3S
MR09-01 Leg1 O-	17	2-May	19:00	107-09.5W	16-44.8S
MR09-01 Leg1 O-	18	3-May	19:00	108-40.8W	16-45.4S
MR09-01 Leg1 O-	19	4-May	19:00	111-23.5W	16-45.0S

MR09-01 Leg1 O-	20	5-May	18:59	114-40.1W	16-45.3S
MR09-01 Leg1 O-	21	6-May	19:00	118-00.1W	16-45.0S
MR09-01 Leg1 O-	22	7-May	20:00	121-05.1W	16-45.0S
MR09-01 Leg1 O-	23	8-May	19:58	124-00.2W	16-45.1S
MR09-01 Leg1 O-	24	9-May	20:00	127-04.3W	16-45.2S
MR09-01 Leg1 O-	25	10-May	20:00	130-00.0W	16-45.1S
MR09-01 Leg1 O-	26	11-May	19:59	132-39.7W	16-45.3S
MR09-01 Leg1 O-	27	12-May	21:00	135-17.2W	16-45.0S
MR09-01 Leg1 O-	28	13-May	21:10	137-59.8W	16-45.1S
MR09-01 Leg1 O-	29	14-May	21:00	141-19.8W	16-44.7S
MR09-01 Leg1 O-	30	15-May	21:01	143-50.0W	17-30.0S
MR09-01 Leg1 O-	31	16-May	22:00	146-30.4W	17-29.7S
MR09-01 Leg1 O-	32	17-May	22:07	148-59.7W	17-29.8S
MR09-01 Leg2 O-	33	21-May	22:00	149-57.4W	17-30.1S
MR09-01 Leg2 O-	34	22-May	22:00	152-20.2W	17-30.1S
MR09-01 Leg2 O-	35	23-May	22:07	153-48.7W	17-30.1S
MR09-01 Leg2 O-	36	25-May	22:03	150-20.4W	17-26.1S
MR09-01 Leg2 O-	37	26-May	22:05	155-13.9W	17-29.7S
MR09-01 Leg2 O-	38	27-May	22:00	157-51.4W	17-29.8S
MR09-01 Leg2 O-	39	28-May	22:02	160-32.7W	17-29.6S
MR09-01 Leg2 O-	40	29-May	22:01	163-14.7W	17-29.7S
MR09-01 Leg2 O-	41	30-May	23:03	165-47.9W	17-29.6S
MR09-01 Leg2 O-	42	31-May	23:05	168-21.0W	17-30.6S
MR09-01 Leg2 O-	43	1-Jun	23:01	170-59.6W	17-29.8S
MR09-01 Leg2 O-	44	2-Jun	23:06	172-19.5W	17-28.6S
MR09-01 Leg2 O-	45	3-Jun	23:04	174-20.0W	17-24.9S
MR09-01 Leg2 O-	46	4-Jun	23:03	177-43.8W	17-31.6S
MR09-01 Leg2 O-	47	6-Jun	00:16	178-59.0E	18-24.8S
MR09-01 Leg2 O-	48	7-Jun	00:00	176-45.8E	17-50.1S
MR09-01 Leg2 O-	49	8-Jun	00:05	173-14.9E	17-50.1S
MR09-01 Leg2 O-	50	9-Jun	00:01	169-59.9E	17-49.8S
MR09-01 Leg2 O-	51	10-Jun	00:00	168-02.8E	18-22.2S
MR09-01 Leg2 O-	52	11-Jun	01:01	166-20.6E	19-06.9S
MR09-01 Leg2 O-	53	12-Jun	01:01	164-29.0E	19-53.7S
MR09-01 Leg2 O-	54	13-Jun	01:01	163-33.3E	20-11.8S
MR09-01 Leg2 O-	55	14-Jun	01:01	163-10.3E	21-19.8S

MR09-01 Leg2 O-	56	15-Jun	01:02	159-56.9E	22-35.9S
MR09-01 Leg2 O-	57	16-Jun	01:01	157-10.8E	23-40.7
MR09-01 Leg2 O-	58	17-Jun	01:04	154-39.4E	24-39.7S
MR09-01 Leg3 O-	59	21-Jun	02:08	154-39.0E	21-25.5S
MR09-01 Leg3 O-	60	22-Jun	03:00	154-44.2E	15-30.0S
MR09-01 Leg3 O-	61	23-Jun	03:07	154-23.7E	09-48.0S
MR09-01 Leg3 O-	62	25-Jun	03:03	150-07.6E	00-42.5N
MR09-01 Leg3 O-	63	26-Jun	03:00	146-37.3E	05-25.8N
MR09-01 Leg3 O-	64	27-Jun	03:01	143-01.9E	10-11.8N
MR09-01 Leg3 O-	65	28-Jun	04:31	140-14.5E	14-47.1N
MR09-01 Leg3 O-	66	29-Jun	03:04	138-30.6E	19-25.6N
MR09-01 Leg3 O-	67	30-Jun	03:01	136-37.1E	24-23.2N
MR09-01 Leg3 O-	68	1-Jul	03:00	134-43.8E	29-05.3N

Table 2.10-4 Summary of surface seawater sample taken by bucket sampling

Sampling No.		Date	Time	Position	
			(UTC)	LON	LAT
MR09-01 Leg1 O-	B1	14-Apr	18:50	079-20.1W	16-45.1S
MR09-01 Leg1 O-	B2	15-Apr	17:35	081-20.2W	16-44.6S
MR09-01 Leg1 O-	B6	21-Apr	18:57	082-00.1W	16-44.7S
MR09-01 Leg1 O-	B7	22-Apr	15:04	083-19.7W	16-44.8S
MR09-01 Leg1 O-	B8	23-Apr	16:20	085-00.0W	16-44.9S
MR09-01 Leg1 O-	B9	24-Apr	14:27	086-59.8W	16-44.7S
MR09-01 Leg1 O-	B10	25-Apr	15:42	089-00.2W	16-44.9S
MR09-01 Leg1 O-	B11	26-Apr	18:11	091-20.0W	16-44.8S
MR09-01 Leg1 O-	B12	27-Apr	17:20	093-59.9W	16-45.0S
MR09-01 Leg1 O-	B13	28-Apr	16:06	096-40.0W	16-44.8S
MR09-01 Leg1 O-	B14	29-Apr	19:42	100-00.1W	16-44.8S
MR09-01 Leg1 O-	B15	30-Apr	17:43	102-40.2W	16-45.0S
MR09-01 Leg1 O-	B16	1-May	18:02	105-20.2W	16-45.2S
MR09-01 Leg1 O-	B17	3-May	17:48	108-40.4W	16-45.2S
MR09-01 Leg1 O-	B18	4-May	21:45	112-00.0W	16-45.2S
MR09-01 Leg1 O-	B19	5-May	17:22	114-40.1W	16-45.1S
MR09-01 Leg1 O-	B20	6-May	19:10	118-00.4W	16-45.1S
MR09-01 Leg1 O-	B21	7-May	21:17	121-20.1W	16-45.0S
MR09-01 Leg1 O-	B22	8-May	18:16	124-00.0W	16-45.0S

MR09-01 Leg1 O-	B23	9-May	21:19	127-20.4W	16-45.1S
MR09-01 Leg1 O-	B24	10-May	19:19	130-00.0W	16-45.0S
MR09-01 Leg1 O-	B25	11-May	18:13	132-39.7W	16-45.0S
MR09-01 Leg1 O-	B26	12-May	21:29	135-20.0W	16-45.1S
MR09-01 Leg1 O-	B27	13-May	20:19	138-59.9W	16-45.1S
MR09-01 Leg1 O-	B28	14-May	20:44	141-19.8W	16-44.8S
MR09-01 Leg1 O-	B29	15-May	21:08	143-50.2W	17-29.6S
MR09-01 Leg1 O-	B30	16-May	20:48	146-30.5W	17-29.6S
MR09-01 Leg1 O-	B31	17-May	21:57	148-59.9W	17-29.8S
MR09-01 Leg2 O-	B32	5.18	21:04	149-57.4W	17-30.1S
MR09-01 Leg2 O-	B33	5.21	20:49	152-20.2W	17-30.1S
MR09-01 Leg2 O-	B34	5.22	0:05	155-40.0W	17-30.0S
MR09-01 Leg2 O-	B35	5.27	18:19	157-40.1W	17-29.6S
MR09-01 Leg2 O-	B36	5.28	18:10	160-20.4W	17-29.7S
MR09-01 Leg2 O-	B37	5.29	23:58	163-40.2W	17-29.9S
MR09-01 Leg2 O-	B38	5.30	19:10	166-40.7W	17-29.5S
MR09-01 Leg2 O-	B39	5.31	20:39	168-20.5W	17-30.3S
MR09-01 Leg2 O-	B40	6.1	21:27	171-00.0W	17-29.2S
MR09-01 Leg2 O-	B41	6.2	15:13	172-20.2W	17-29.9S
MR09-01 Leg2 O-	B42	6.3	22:30	174-20.2W	17-25.0S
MR09-01 Leg2 O-	B43	6.4	21:09	177-40.2W	17-29.9S
MR09-01 Leg2 O-	B44	6.5	22:35	179-00.1E	18-25.0S
MR09-01 Leg2 O-	B45	6.6	22:01	177-00.0E	17-50.0S
MR09-01 Leg2 O-	B46	6.8	1:19	172-59.8E	17-50.0S
MR09-01 Leg2 O-	B47	6.9	0:58	169-49.8E	17-49.9S
MR09-01 Leg2 O-	B48	6.9	23:05	168-03.0E	18-22.2S
MR09-01 Leg2 O-	B49	6.11	1:40	166-17.9E	19-08.0S
MR09-01 Leg2 O-	B50	6.12	2:07	164-21.1E	19-56.8S
MR09-01 Leg2 O-	B51	6.14	2:55	162-45.9E	21-29.1S
MR09-01 Leg2 O-	B52	6.15	0:43	159-57.0E	22-35.9S
MR09-01 Leg2 O-	B53	6.16	0:12	157-10.8E	23-40.8S
MR09-01 Leg2 O-	B54	6.17	2:25	154-23.0E	24-25.9S

2.11 Volatile organic matters

(1) Personnel

Yoko Yokouchi (National Institute for Environmental Studies)

(2) Objectives

To know the distribution of volatile organic compounds emitted from marine biota.

(3) Measured compounds

- Dibromomethane
- Methyl iodide
- Methyl chloride
- Methyl bromide
- Dimethyl sulfide
- Carbonyl sulfide
- Isoprene
- Chloroform

(4) Methods

Air samples were taken on board forward of any potential contamination from the stack, at the front of the uppermost deck on the Mirai. Samples were collected every 3 degree longitude between [16°45’S, 111°W] and [17°30’S, 147°W](4 May – 16 May) in Leg 1, and every 4 degree longitude between [17°30’S, 153°W] and [25°S, 154°E] (23 May – 17 June) in Leg 2. Evacuated 6-L stainless steel canisters with inert surfaces were used for the collection.

Samples will be analyzed using a preconcentration/capillary gas chromatographic/mass spectrometer (GC/MS) after the cruise.

(5) Results

2.12. Physical and chemical properties of marine aerosol and atmospheric deposition: Hemispherical and latitudinal distribution and impact to marine biogeochemical cycles in the western North and South Pacific Oceans

(1) Participated Personnel

[1]Hiroshi Furutani, [2]Jinyoung Jung, [3]Kazuhiko Miura, and [4]Mitsuo Uematsu

[1,2,4]Ocean Research Institute, University of Tokyo; [3]Science University of Tokyo

(2) Background and Objectives

Increased marine primary production is considered to increase emission of particulate matter and/or gaseous precursors (e.g., dimethyl sulfide and isoprene) from ocean to atmosphere, which is expected to lead a creation of new atmospheric aerosols through a nucleation process and/or growth of existing atmospheric aerosols through condensation of the gas precursors to the existing aerosols. On the other hand, depositions of atmospheric aerosols, precipitation, and trace gases into ocean surface supply essential nutrients for marine primary producers (e.g., iron, phosphorus, and nitrate) and further enhance their primary production. This suggests that atmospheric aerosols and marine biota are linked and the linkage is an important part of the global climate system since ocean covers about 70 % of the earth's surface. To estimate the impact of the atmospheric aerosols to the marine biota and vice versa, it is essential to understand the physiochemical properties of atmospheric aerosols and their geological distribution and compare them with marine biological properties. To understand the mutual relationship, it is desired to conduct atmospheric observation in the distant open ocean regions where impact of the anthropogenic matter is limited and effect of the linkage is expected more pronounced.

The MR09-01 cruise provides a unique opportunity for the study of the linkage: The MR09-01 cruise encompasses both south and north hemispheres (from 25°S to 35°N) and travels regions which are distant from the areas with heavy human activity.

Our objectives in the MR09-01 cruise are

A) To observe physical and chemical properties of atmospheric aerosols, such as size distribution, number concentration, cloud condensation nuclei (CCN) concentration, chemical compositions (ionic composition, trace metals, phosphorous, nitrogen, and organic compositions) and their size distribution and mixing states, including composition of precipitations.

B) To observe hemispherical and latitudinal distribution of the physical and chemical properties of atmospheric aerosols and depositions mentioned above.
C) To estimate the flux of the atmospheric depositions into ocean and their hemispherical and latitudinal distribution based on the present aerosol and rain observations.
D) To evaluate a potential impact of the atmospheric depositions to marine primary production.

(3) Methods and Observations

Table 2.12.1 summarizes observations carried out during MR09-01 cruise (leg 3, 6/20/2009 ~ 7/3/2009) and their methods, sampling time resolutions and frequencies. All observation instruments were installed in the three places on the R/V Mirai, (i) a newly constructed container laboratory installed in the #1 storage (Plate 2.12.1), (ii) compass deck (Plate 2.12.2), and (iii) general purpose observation room. The container lab in the #1 storage was constructed to accommodate aerosol measurement instruments which were newly introduced in this cruise (ATOFMS, CCN and CN counters). Aerosol measurements are generally divided into two different types of observation/analysis. One is a *real-time* and *in-situ* observation/analysis with a high time resolution from 1 second to 2 hours (*e.g.*, ATOFMS, CCN, CN, SMPS, OPC, nitrate monitor), while another is an aerosol collection followed by further detailed *off-line* chemical analysis with a relatively low time resolution from 1 ~ 3 days (*e.g.*, all aerosol sampling with filter collection method, mist-chamber total sampler). The combination of two different types of observations allows more comprehensive and better understanding of atmospheric aerosol properties. Aerosol collection, which was continued for a longer time period (from 12 hours to 2 weeks) by the aerosol samplers, was controlled by a wind sector system to avoid a contamination of engine exhaust from the funnel of the R/V Mirai. Aerosol samplers were activated only when wind blew in a direction from the fore of the ship with a certain wind speed (> 1 m/s).

(4) Preliminary Results and Further Analysis

Figure 2.12.1 shows temporal variations of selected *in-situ* measurements from 6/20/2009 to 7/2/2009. There are several clear periods with different aerosol properties. From 6/20/09~6/21/09, SMPS size distribution measurement showed that atmospheric aerosols were mainly in the diameter (D) < 50 nm, reflecting that the Mirai was in the vicinity of the area with increased human activity (anthropogenic aerosol sources around Brisbane area in Australia). Concentrations of CO, nitrate, and CN were also high in the period due to the influence of the anthropogenic aerosol sources. During 6/21/09 to 6/25/2009, which corresponds to the transect from Brisbane area to the equator, the SMPS size measurement showed that the peak diameter in the smaller size (< 50 nm) shifted from D = 20 nm to 40 nm. After 6/22/09, the second size mode appeared around D = 150 nm which accompanied by the increase in aerosol total concentration (CN), CO, and nitrate. The secondary size mode is indicative that the air parcel encountered during the period was not a freshly impacted by the aerosol sources but well-aged (spent longer time

period and underwent significant physicochemical transformation after emitted from aerosol sources). This continued till 6/29/09 except for the period from 6/26/09~6/27/09, in which period aerosol entire size distribution shifted toward larger size, suggesting a different type of air parcel was observed. On 6/29/09, CN concentration abruptly increased by a factor of 2.5 and remained high, which was also associated by the increase of CO and nitrate, reflecting that influence of continental aerosol sources began to join. Currently, detailed laboratory chemical analysis and data analysis are underway. Results from these atmospheric observations and their temporal/spatial/latitudinal variations will be further compared with temporal variations in nutrient concentrations and/or amount of biomass at the surface of ocean. A potential linkage between atmospheric aerosols and marine primary production will be evaluated.

We would like to thank principle investigators of the MR09-01 cruise, Dr. Kenichi Sasaki and Dr. Akihiko Murata, for their kind help and patient support for our rather complicated setting up. HF and JJ also would like to thank the captain and the crew in the R/V Mirai, and Takao Oshima (GODI) for their kind help and assistance during cruise and preparation.

Table 2.12.1. List of aeorosol and atmospheric measurements conducted during MR09-01 cruise (Leg 3, 6/20/09 - 7/3/09).

Categoly	Type of Meas.	Meas. Range / Property	Time Res.	Instrument / Analysis	Installed Location*
Atmospheric Aerosols	Size Distribution	(1) 10~500 nm	3 min	SMPS	CN-Lab
		(2) 100~500 nm	1 min	OPC 1	Cmp-Deck
		(3) 0.5 ~ 5 μm	1 min	OPC 2	Cmp-Deck
	Number Conc.	(4) Total number conc.	1 sec	CPC	CN-Lab
		(5) Cloud Concendation Nuclei	1 sec	CCN Counter	CN-Lab
	Composition	(6) Inorganic/organic/total phosphorus, nitrogen, and carbon	3~5 days	Filter sampling Laboratry analysis 1	Cmp-Deck
		(7) Trace metal, ionic comp.	3~5 days	Filter sampling Laboratry analysis 2	Cmp-Deck
		(8)Trace metal, ionic comp.	12 h	Filter sampling Laboratry analysis 3	Cmp-Deck
		(9) Size-resolved phosphorus, nitrogen, carbon, and ionic comp.	14 days	Filter sampling Laboratry analysis 4	Cmp-Deck
		(10) Water soluble total gas and aerosol comp.	1 day	Mist chamber total gas/aerosol collector	Cmp-Deck
		(11) d = 100~2500 nm, Single particle analysis, Organic, inorganic, and metal comp.	Real time	Aerosol Time-Of-Flight Mass Spectrometer (ATOFMS)	CN-Lab
		(12) Total nitrate conc.	10 min	Nitrate monitor	Cmp-Deck
Rain	Composition	Dissolved Matter: Ionic comp. / Total phosporus / Total nitrogen	While raining	Collection and laboratory analysis	Cmp-Deck
Atmosheric Gases	Concentration	O_3	1 min		GP-ObsRM
		CO			
		SO_2			

*CN-Lab: *Container Laboratory* in #1 storage, Cmp-Deck: Compass Deck, GP-ObsRM: General Purpose Observation Room

Plate 2.12.1. Installation of a newly constructed container laboratory to #1 storage in R/V Mirai; inside the container laboratory during MR08-06 cruise; air sampling inlet for the instruments in the container laboratory (blue arrow).

Plate 2.12.2. Aerosol instruments installed on compass deck.

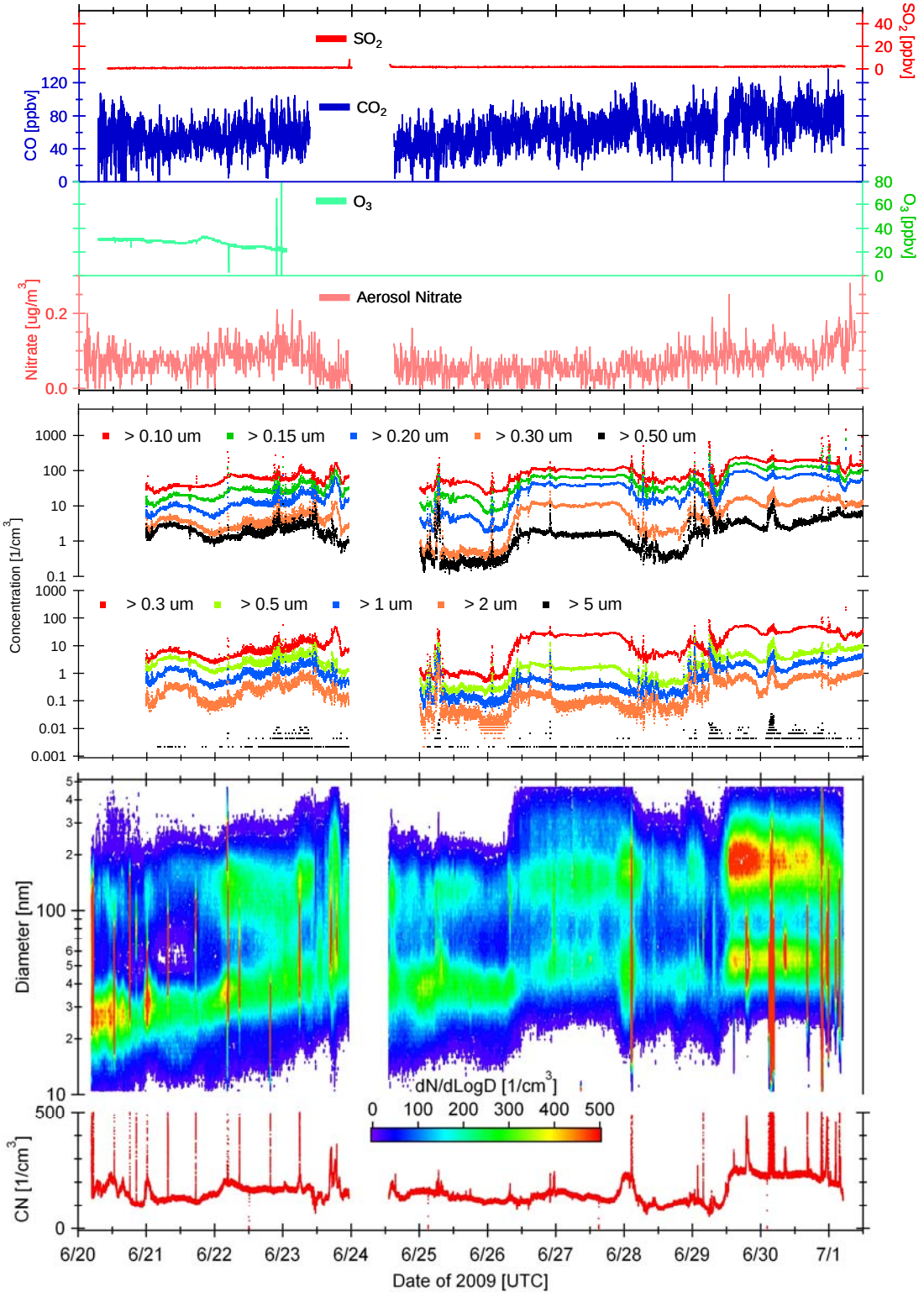
SO2
CO2
O3
Aerosol Nitrate
SO2 [ppbv]
CO [ppbv]
O3 [ppbv]
Nitrate [ug/m3]
> 0.10 um
> 0.15 um
> 0.20 um
> 0.30 um
> 0.50 um
> 0.3 um
> 0.5 um
> 1 um
> 2 um
> 5 um
Concentration [1/cm3]
Diameter [nm]
dN/dLogD [1/cm3]
CN [1/cm3]
6/20
6/21
6/22
6/23
6/24
6/25
6/26
6/27
6/28
6/29
6/30
7/1
Date of 2009 [UTC]

2.13. Surface seawater biology

(1) Personnel

Taketoshi KODAMA (The University of Tokyo)
Hiroyuki KUROTORI (The University of Tokyo)
Takuhei SHIOZAKI (The University of Tokyo)
Satoshi KITAJIMA (The University of Tokyo)
Shigenobu TAKEDA (The University of Tokyo)
Ken FURUYA (The University of Tokyo)

See,

2.14 Sea surface gravity

(1) Personnel

Takeshi Matsumoto	*(University of the Ryukyus)*	*: Principal investigator / Not on-board*
Masao Nakanishi	*(Chiba University)*	*: Principal investigator / Not on-board*
Shinya Okumura	*(GODI)*	*: Leg.1*
Satoshi Okumura	*(GODI)*	*: Leg.2*
Souichiro Sueyoshi	*(GODI)*	*: Leg.3*
Ryo Kimura	*(GODI)*	*: Leg.1, Leg.3*
Yousuke Yuuki	*(GODI)*	*: Leg.1*
Kazuho Yoshida	*(GODI)*	*: Leg.2*
Harumi Ota	*(GODI)*	*: Leg.2*

(2) Introduction

The difference of local gravity is an important parameter in geophysics and geodesy. We collected gravity data at the sea surface during the cruise.

(3) Data Period

Leg1: from 14 April 2009 to 18 May 2009

Leg2: from 21 May 2009 to 18 June 2009

Leg3: from 20 June 2009 to 03 July. 2009.

(4) Parameters

Relative Gravity [mGal] = Data reading value [CU] * coef.

Converting Relative Gravity coefficient: coef. = 0.9946

(5) Data Acquisition

We have measured relative gravity using on-board gravity meter (Micro-g LaCoste Air-sea gravity meter S-116) during this cruise. To calculate the absolute gravity, we measured at gravity reference points of Sekinehama and Moji, using portable gravity meter (Scintrex gravity meter CG-3M).

(6) Preliminary Results

Absolute gravity table is shown in Table 2.14.

Table 2.14 Absolute gravity table MR09-01 cruise

No.	Date	UTC	Port	Absolute Gravity (mGal)	Sea Level (cm)	Draft (cm)	Gravity at Sensor[*1] (mGal)	L&R[*2] (mGal)
1[*3]	14/Janualy/2009	06:04	Sekinehama	980371.94	233	620	980372.70	12634.85
2	06/July/2009	00:46	Moji	979673.29	278	550	979674.16	11944.96

*1: Gravity at Sensor= Absolute Gravity + Sea Level*0.3086/100 + (Draft-530)/100*0.0431

*2: Micro-g LaCoste air-sea gravity meter S-116

*3: MR08-06 cruise

Differential	G at sensor	L&R value
No.1 －No.2	-698.54 mGal ---(a)	-689.89 mGal ---(b)

L&R drift value (b)-(a)	8.648 mGal	/	173.78 days
Daily drift ratio	0.0498 mGal/day		

(6) Data Archive

Gravity data obtained during this cruise was submitted to the Data Integration and Analysis Group (DIAG) of JAMSTEC, and archived there.

(7) Remarks

1. We did not collect data in the territorial waters and the EEZ at following terms.

The territorial waters and the EEZ of Peru: 00:00UTC 13 Apr. 2009 to 12:40UTC 14 Apr. 2009
06:00UTC 16 Apr. 2009 to 00:15UTC 21 Apr. 2009

The territorial waters of Papua New Guinea: 23:10UTC 23 Jun. 2009 to 13:06UTC 24 Jun. 2009

2.15 On-board geomagnetic measurement

(1) Personnel

Takeshi Matsumoto	*(University of the Ryukyus)*	*: Principal investigator / Not on-board*
Masao Nakanishi	*(Chiba University)*	*: Principal investigator / Not on-board*
Shinya Okumura	*(GODI)*	*: Leg.1*
Satoshi Okumura	*(GODI)*	*: Leg.2*
Souichiro Sueyoshi	*(GODI)*	*: Leg.3*
Ryo Kimura	*(GODI)*	*: Leg.1, Leg.3*
Yousuke Yuuki	*(GODI)*	*: Leg.1*
Kazuho Yoshida	*(GODI)*	*: Leg.2*
Harumi Ota	*(GODI)*	*: Leg.2*

(2) Introduction

Measurement of magnetic force on the sea is required for the geophysical investigations of marine magnetic anomaly caused by magnetization in upper crustal structure. We measured geomagnetic field using a three-component magnetometer during the cruise.

(3) Method

A shipboard three-component magnetometer system (Tierra Tecnica SFG1214) is equipped on-board R/V Mirai. Three-axes flux-gate sensors with ring-cored coils are fixed on the fore mast. Outputs from the sensors are digitized by a 20-bit A/D converter (1 nT/LSB), and sampled at 8 times per second. Ship's heading, pitch and roll are measured by the Inertial Navigation System (INS). Ship's position (GPS) and speed data are received through LAN every second.

The relation between a magnetic-field vector observed on-board, Hob, (in the ship's fixed coordinate system) and the geomagnetic field vector, F, (in the Earth's fixed coordinate system) is expressed as:

$$\mathbf{H}\text{ob} = \mathbf{A}\,\mathbf{R}\,\mathbf{P}\,\mathbf{Y}\,\mathbf{F} + \mathbf{H}\text{p} \qquad \text{(a)}$$

where **R**, **P** and **Y** are the matrices of rotation due to roll, pitch and heading of a ship, respectively. $\tilde{\mathbf{A}}$ is a 3 x 3 matrix which represents magnetic susceptibility of the ship, and **H**p is a magnetic field vector produced by a permanent magnetic moment of the ship's body. Rearrangement of Eq. (a) makes

$$\mathbf{B}\,\mathbf{H}\text{ob} + \mathbf{H}\text{bp} = \mathbf{R}\,\mathbf{P}\,\mathbf{Y}\,\mathbf{F} \qquad \text{(b)}$$

where **B** = A-1, and **H**bp = -B **H**p. The magnetic field, **F**, can be obtained by measuring **R**, **P**, **Y** and **H**ob, if **B** and **H**bp are known. Twelve constants in **B** and **H**bp can be determined by measuring variation of **H**ob with **R**, **P** and **Y** at a place where the geomagnetic field, **F**, is known.

(4) Data Archive

Magnetic force data obtained during this cruise was submitted to the Data Integration and Analysis Group (DIAG) of JAMSTEC, and archived there.

(5) Remarks

1. For calibration of the ship's magnetic effect, we made a "figure-eight" turn (a pair of clockwise and anti-clockwise rotation). This calibration was carried out as below.

   Leg1: 17:19UTC 02 May. 2009 to 17:52UTC 02 May. 2009 about at 16-44.2S, 107-04.9W

   Leg3: 04:27UTC 22 Jun. 2009 to 04:48UTC 22 Jun. 2009 about at 16-44.2S, 107-04.9E
   02:15UTC 28 Jun. 2009 to 02:47UTC 28 Jun. 2009 about at 14-25.4N, 140-22.5E
   21:24UTC 30 Jun. 2009 to 21:51UTC 30 Jun. 2009 about at 28-09.0N, 135-07.0E

2. We did not collect data in the territorial waters and the EEZ at following terms.

The territorial waters and the EEZ of Peru:	00:00UTC 13 Apr. 2009 to 12:40UTC 14 Apr. 2009
	06:00UTC 16 Apr. 2009 to 00:15UTC 21 Apr. 2009
The territorial waters of Papua New Guinea:	23:10UTC 23 Jun. 2009 to 13:06UTC 24 Jun. 2009

2.16 Proton magnetometer

(1) Personnel

Takeshi Matsumoto	*(University of the Ryukyus)*	*: Principal investigator / Not on-board*
Masao Nakanishi	*(Chiba University)*	*: Principal investigator / Not on-board*
Shinya Okumura	*(GODI)*	*: Leg.1*
Satoshi Okumura	*(GODI)*	*: Leg.2*
Souichiro Sueyoshi	*(GODI)*	*: Leg.3*
Ryo Kimura	*(GODI)*	*: Leg.1, Leg.3*
Yousuke Yuuki	*(GODI)*	*: Leg.1*
Kazuho Yoshida	*(GODI)*	*: Leg.2*
Harumi Ota	*(GODI)*	*: Leg.2*

(2) Introduction

Measurement of magnetic force on the sea is required for the geophysical investigations of marine magnetic anomaly caused by magnetization in upper crustal structure. We measured total geomagnetic field using a proton magnetometer (GEOMETRICS, G811) during the MR09-01 Leg3 cruise.

(3) Data Period

02:09UTC 28 Jun. 2009 - 00:14UTC 01 Jul. 2009

(4) Specification

1. Setting:	Total Cycle time;	10sec
	Sensitivity;	0.2nT
2. Dynamic Operating Range:		17,000 to 95,000 gammas
3. Noise Level:		90% of all readings to be within selected sensitivity envelope
4. Accuracy:		+0.5 gamma or less as determined by the magnetic cleanliness of sensor materials and the known accuracy of the proton gyromagnetic constant.

(5) Data Archive

Total magnetic force data obtained during this cruise was submitted to the Data Integration and Analysis Group (DIAG) of JAMSTEC, and archived there.

3. Station Observation

3.1 $CTDO_2$ Measurements

September 8, 2009

(1) Personnel

Hiroshi Uchida (JAMSTEC)
Wolfgang Schneider (University of Concepcion, Chile)
Leg 1 and leg 2a
Kenichi Katayama (MWJ)
Shinsuke Toyoda (MWJ)
Hirokatsu Uno (MWJ)
Hiroyuki Hayashi (MWJ)
Leg 2b
Tomoyuki Takamori (MWJ)
Hiroshi Matsunaga (MWJ)
Masayuki Fujisaki (MWJ)
Shungo Oshitani (MWJ)
Satoshi Ozawa (MWJ)

(2) Winch arrangements

The CTD package was deployed by using 4.5 Ton Traction Winch System (Dynacon, Inc., Bryan, Texas, USA), which was installed on the R/V Mirai in April 2001 (Fukasawa et al., 2004). Primary system components include a complete CTD Traction Winch System with up to 8000 m of 9.53 mm armored cable (Rochester Wire & Cable).

(3) Overview of the equipment

The CTD system was SBE 911plus system (Sea-Bird Electronics, Inc., Bellevue, Washington, USA). The SBE 911plus system controls 36-position SBE 32 Carousel Water Sampler. The Carousel accepts 12-litre Niskin-X water sample bottles (General Oceanics, Inc., Miami, Florida, USA). The SBE 9plus was mounted horizontally in a 36-position carousel frame. SBE's temperature (SBE 3) and conductivity (SBE 4) sensor modules were used with the SBE 9plus underwater unit. The pressure sensor is mounted in the main housing of the underwater unit and is ported to outside through the oil-filled plastic capillary tube. A modular unit of underwater housing pump (SBE 5T) flushes water through sensor tubing at a constant rate independent of the CTD's motion, and pumping rate (3000 rpm) remain nearly constant over the entire input voltage range of 12-18 volts DC. Flow speed of pumped water in standard TC duct is about 2.4 m/s. Two sets of temperature and conductivity modules were used. An SBE's dissolved oxygen sensor (SBE 43) was placed between the primary conductivity sensor and the pump module. Auxiliary sensors, a Deep Ocean Standards Thermometer (SBE 35), an altimeter (PSA-916T; Teledyne Benthos, Inc., North Falmous, Massachusetts, USA), three oxygen optodes (Oxygen Optode 3830 and 4330F; Aanderaa Data Instruments AS, Bergen, Norway, and RINKO-III; JFE Alec Co., Ltd, Kobe Hyogo, Japan), a fluorometer (Seapoint sensors, Inc., Kingston, New Hampshire, USA), and a transmissometer (C-Star Transmissometer; WET Labs, Inc., Philomath, Oregon, USA) were also used with the SBE 9plus underwater unit. To minimize motion of the CTD package, a heavy stainless frame (total weight of the CTD package without sea water in the bottles is about 1000 kg) was used with an aluminum plate (54 × 90 cm).

Summary of the system used in this cruise

Deck unit:

SBE 11plus, S/N 0272

Under water unit:

SBE 9plus, S/N 79511 (Pressure sensor: S/N 0677)

Temperature sensor:

SBE 3plus, S/N 4815 (primary)

SBE 3, S/N 1525 (secondary)

Conductivity sensor:

SBE 4, S/N 2854 (primary)

SBE 4, S/N 1203 (secondary: stations from P21_14_1 to P21_86_1)

SBE 4, S/N 3261 (secondary: stations from P21_87_1 to P21_288_1)

Oxygen sensor:

SBE 43, S/N 0394 (stations from P21_14_1 to P21_76_1)

SBE 43, S/N 0330 (stations from P21_X18_1 to P21_288_1)

AANDERAA Oxygen Optode 3830, S/N 612 (foil batch no. 1707)

AANDERAA Oxygen Optode 4330F, S/N 143 (foil batch no. 2808F)

JFE Alec RINKO-III, S/N 006 (foil batch no. 131002A)

Pump:

SBE 5T, S/N 4598 (primary)

SBE 5T, S/N 4595 (secondary)

Altimeter:

PSA-916T, S/N 1100

Deep Ocean Standards Thermometer:

SBE 35, S/N 0045

Fluorometer:

Seapoint Sensors, Inc., S/N 3054

Transmissometer:

C-Star, S/N CST-207RD

Carousel Water Sampler:

SBE 32, S/N 0391

Water sample bottle:

12-litre Niskin-X model 1010X (no TEFLON coating)

* without Oxygen Optode 4330F, fluorometer, and transmissometer at station P21_200_1

(4) Pre-cruise calibration

i. Pressure

The Paroscientific series 4000 Digiquartz high pressure transducer (Model 415K-187: Paroscientific, Inc., Redmond, Washington, USA) uses a quartz crystal resonator whose frequency of oscillation varies with pressure induced stress with 0.01 per million of resolution over the absolute pressure range of 0 to 15000 psia (0 to 10332 dbar). Also, a quartz crystal temperature signal is used to compensate for a wide range of temperature changes at the time of an observation. The pressure sensor has a nominal accuracy of 0.015 % FS (1.5 dbar), typical stability of 0.0015 % FS/month (0.15 dbar/month), and resolution of 0.001 % FS (0.1 dbar). Since the pressure sensor measures the absolute value, it inherently includes atmospheric pressure (about 14.7 psi). SEASOFT subtracts 14.7 psi from computed pressure automatically.

Pre-cruise sensor calibrations for linearization were performed at SBE, Inc.

S/N 0677, 4 May 2007

The time drift of the pressure sensor is adjusted by periodic recertification corrections against a dead-weight piston gauge (Model 480DA, S/N 23906; Bundenberg Gauge Co. Ltd., Irlam, Manchester, UK). The corrections are performed at JAMSTEC, Yokosuka, Kanagawa, Japan by Marine Works Japan Ltd. (MWJ), Yokohama, Kanagawa, Japan, usually once in a year in order to monitor sensor time drift and linearity.

S/N 0677, 9 December 2008

slope = 0.99977580

offset = –0.02383

Result of the pre-cruise pressure sensor calibration against the dead-weight piston gauge is shown in Fig. 3.1.1.

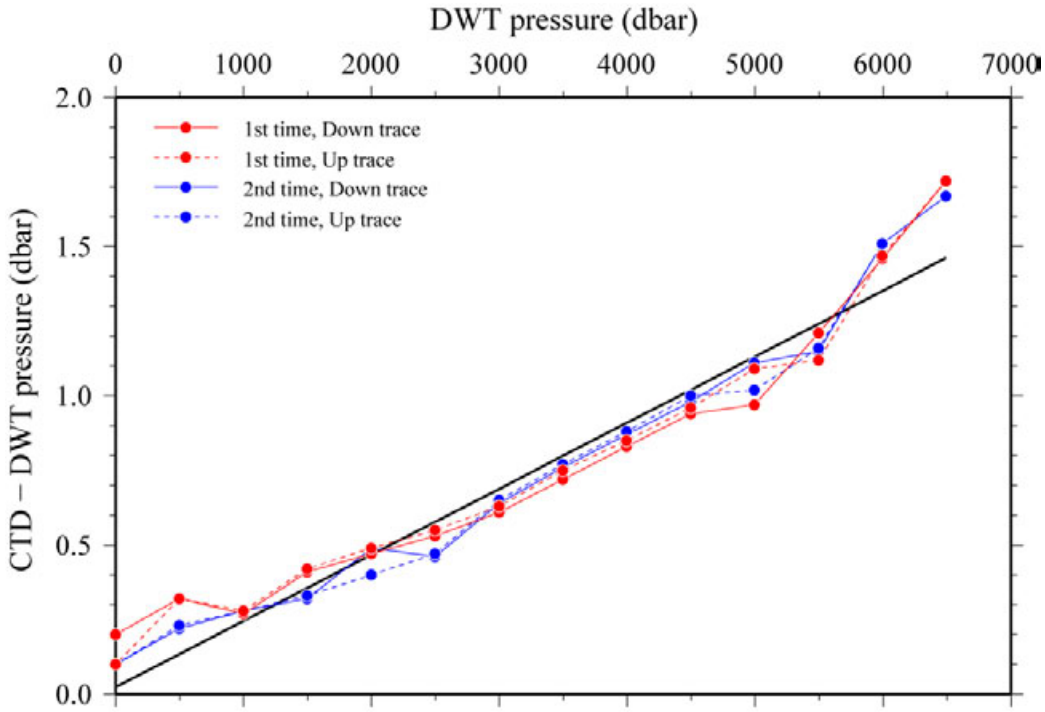

Fig. 3.1.1 Difference between the dead-weight piston gauge and the CTD pressure. The calibration line (black line) is also shown.

ii. Temperature (SBE 3)

The temperature sensing element is a glass-coated thermistor bead in a stainless steel tube, providing a pressure-free measurement at depths up to 10500 (6800) m by titanium (aluminum) housing. The SBE 3 thermometer has a nominal accuracy of 1 mK, typical stability of 0.2 mK/month, and resolution of 0.2 mK at 24 samples per second. The premium temperature sensor, SBE 3plus, is a more rigorously tested and calibrated version of standard temperature sensor (SBE 3).

Pre-cruise sensor calibrations were performed at SBE, Inc.

S/N 4815, 26 November 2008

S/N 1525, 25 November 2008

Pressure sensitivity of SBE 3 was corrected according to a method by Uchida et al. (2007), for the following sensor.

S/N 4815, –3.45974716e–7 [°C/dbar]

S/N 1525, 5.92243e–9 [°C/dbar]

Time drift of the SBE 3 temperature sensors based on the laboratory calibrations is shown in Fig. 3.1.2.

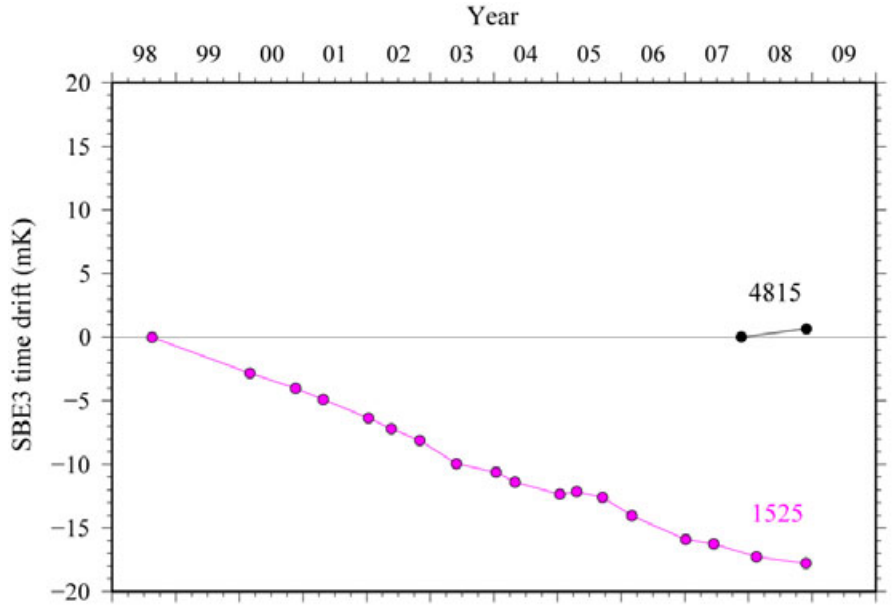

Fig. 3.1.2 Time drift of SBE 3 temperature sensors based on laboratory calibrations.

iii. Conductivity (SBE 4)

The flow-through conductivity sensing element is a glass tube (cell) with three platinum electrodes to provide in-situ measurements at depths up to 10500 (6800) m by titanium (aluminum) housing. The SBE 4 has a nominal accuracy of 0.0003 S/m, typical stability of 0.0003 S/m/month, and resolution of 0.00004 S/m at 24 samples per second.

Pre-cruise sensor calibrations were performed at SBE, Inc.

S/N 2954, 25 November 2008 (new cell preventing a stress concentration)

S/N 1203, 12 December 2008 (new cell preventing a stress concentration)

S/N 3261, 17 December 2008 (new cell preventing a stress concentration)

The value of conductivity at salinity of 35, temperature of 15 °C (IPTS-68) and pressure of 0 dbar is 4.2914 S/m.

iv. Oxygen (SBE 43)

The SBE 43 oxygen sensor uses a Clark polarographic element to provide in-situ measurements at depths up to 7000 m. The range for dissolved oxygen is 120 % of surface saturation in all natural waters, nominal accuracy is 2 % of saturation, and typical stability is 2 % per 1000 hours.

Pre-cruise sensor calibrations were performed at SBE, Inc.

S/N 0394, 20 December 2008

S/N 0330, 20 December 2008

v. Deep Ocean Standards Thermometer

Deep Ocean Standards Thermometer (SBE 35) is an accurate, ocean-range temperature sensor that can be standardized against Triple Point of Water and Gallium Melt Point cells and is also capable of measuring temperature in the ocean to depths of 6800 m. The SBE 35 was used to calibrate the SBE 3 temperature sensors in situ (Uchida et al., 2007).

Pre-cruise sensor linearization was performed at SBE, Inc.

S/N 0045, 27 October 2002

Then the SBE 35 is certified by measurements in thermodynamic fixed-point cells of the TPW (0.01 °C) and GaMP (29.7646 °C). The slow time drift of the SBE 35 is adjusted by periodic recertification corrections. Pre-cruise sensor calibration was performed at SBE, Inc.

S/N 0045, 23 December 2008 (slope and offset correction)

The time required per sample = 1.1 × NCYCLES + 2.7 seconds. The 1.1 seconds is total time per an acquisition cycle. NCYCLES is the number of acquisition cycles per sample and was set to 4. The 2.7 seconds is required for converting the measured values to temperature and storing average in EEPROM.

When using the SBE 911 system with SBE 35, the deck unit receives incorrect signal from the under water unit for confirmation of firing bottle #16. In order to correct the signal, a module (Yoshi Ver. 1; EMS Co. Ltd., Kobe, Hyogo, Japan) was used between the under water unit and the deck unit.

Time drift of the SBE 35 based on the fixed point calibrations is shown in Fig. 3.1.3.

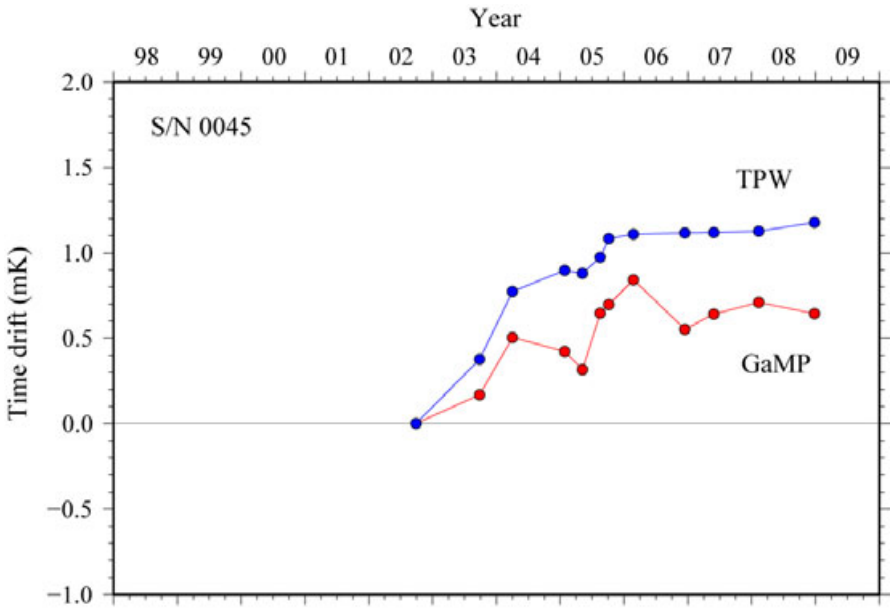

Fig. 3.1.3 SBE35 time drift based on laboratory fixed point calibrations (triple point of water, TPW and gallium melt point, GaMP) performed by SBE, Inc.

vi. Altimeter

Benthos PSA-916T Sonar Altimeter (Teledyne Benthos, Inc.) determines the distance of the target from the unit by generating a narrow beam acoustic pulse and measuring the travel time for the pulse to bounce back from the target surface. It is rated for operation in water depths up to 10000 m. The PSA-916T uses the nominal speed of sound of 1500 m/s.

vii. Oxygen Optode

(a) Oxygen Optode 3830

Oxygen Optode 3830 (Aanderaa Data Instruments AS) is based on the ability of selected substances to act as dynamic fluorescence quenchers. In order to use with the SBE 911plus CTD system, an analog adaptor (3966) is connected to the oxygen optode (3830). The analog adaptor is packed into titanium housing made by Alec Electronics Co., Ltd. The sensor is designed to operate down to 6000 m. The range for dissolved oxygen is 120 % of surface saturation in all natural waters, nominal accuracy is less than 8 μM or 5 % of saturation which ever is greater and setting time (63%) is shorter than 25 seconds.

(b) Oxygen Optode 4330F

Oxygen Optode 4330F (Aanderaa Data Instruments AS) is based on the ability of selected substances to act as dynamic fluorescence quenchers. In order to use with the SBE 911plus CTD system, an analog adaptor (3966) with titanium housing for Oxygen Optode 3975 is connected to the oxygen optode (4330F). The sensor is designed to operate down to 6000 m. The range for dissolved oxygen is 150 % of surface saturation in all natural waters, nominal accuracy is less than 8 μM or 5 % of saturation which ever is greater and setting time (63%) is shorter than 8 seconds.

(c) RINKO

RINKO (JFE Alec Co., Ltd.) is based on the ability of selected substances to act as dynamic fluorescence quenchers. RINKO model III is designed to use with a CTD system which accept an auxiliary analog sensor, and is designed to operate down to 7000 m.

Outputs from Optode 3830 and RINKO are the raw phase shift data. Raw phase shift data for Optode 4330F can be back calculated from the outputs (oxygen concentration and temperature). The optode oxygen can be calibrated by the Stern-Volmer equation, according to a method by Uchida et al. (2008) with slight modification:

$$O_2\ (\mu mol/l) = (P_0 / P - 1) / K_{sv}$$

where P is phase shift, P_0 is phase shift in the absence of oxygen and K_{sv} is Stern-Volmer constant. The P_0 and the K_{sv} are assumed to be functions of temperature as follows.

$$K_{sv} = C_0 + C_1 \times T + C_2 \times T^2$$

$$P_0 = 1 + C_3 \times T$$

$$P = C_4 + C_5 \times P_b$$

where T is CTD temperature (°C) and P_b is raw phase measurement (degrees). P_0 and P are normalized by the phase shift in the absence of oxygen at 0°C. The oxygen concentration is calculated using temperature data from the first responding CTD temperature sensor instead of temperature data from slow responding optode temperature sensor. The pressure-compensated oxygen concentration O_{2c} can be calculated as follows.

$$O_{2c} = O_2\ (1 + C_p p / 1000)^{1/3}$$

where p is CTD pressure (dbar) and C_p is the compensation coefficient. Since the sensing foil of the optode is permeable only to gas and not to water, the optode oxygen must be corrected for salinity. The salinity-compensated oxygen can be calculated by multiplying the factor of the effect of salt on the oxygen solubility (García and Gordon, 1992). García and Gordon (1992) have recommended the use of the solubility coefficients derived from the data of Benson and Krause.

The calibration coefficients were preliminary determined by using the bottle oxygen data obtained in this cruise, and used during the cruise.

viii. Fluorometer

The Seapoint Chlorophyll Fluorometer (Seapoint Sensors, Inc., Kingston, New Hampshire, USA) provides in-situ measurements of chlorophyll-a at depths up to 6000 m. The instrument uses modulated blue LED lamps and a blue excitation filter to excite chlorophyll-a. The fluorescent light emitted by the chlorophyll-a passes through a red emission filter and is detected by a silicon photodiode. The low level signal is then processed using synchronous demodulation circuitry, which generates an output voltage proportional to chlorophyll-a concentration.

ix. Transmissometer

The C-Star Transmissometer (WET Labs, Inc., Philomath, Oregon, USA) measures light transmittance at a single wavelength over a know path. In general, losses of light propagating through water can be attributed to two primary causes: scattering and absorption. By projecting a collimated beam of light through the water and placing a focused receiver at a known distance away, one can quantify these losses. The ratio of light gathered by the receiver to the amount originating at the source is known as the beam transmittance. Suspended particles, phytoplankton, bacteria and dissolved organic matter contribute to the losses sensed by the instrument. Thus, the instrument provides information both for an indication of the total concentrations of matter in the water as well as for a value of the water clarity.

(5) Data collection and processing

i. Data collection

CTD system was powered on at least 20 minutes in advance of the data acquisition and was powered off at least two minutes after the operation in order to acquire pressure data on the ship's deck.

The package was lowered into the water from the starboard side and held 10 m beneath the surface in order to activate the pump. After the pump was activated, the package was lifted to the surface and lowered at a rate of 1.0 m/s to 200 m (or 300 m when significant wave height is high) then the package was stopped to operate the heave compensator of the crane. The package was lowered again at a rate of 1.2 m/s to the bottom. For the up cast, the package was lifted at a rate of 1.1 m/s except for bottle firing stops. At each bottle firing stops, the bottle was fired after waiting from the stop for 30 seconds (20 seconds from station P21_23_1) and the package was stayed at least 5 seconds for measurement of the SBE 35. At 200 m (or 300 m) from the surface, the package was stopped to stop the heave compensator of the crane.

Water samples were collected using a 36-bottle SBE 32 Carousel Water Sampler with 12-litre Niskin-X bottles. Before a cast taken water for CFCs, the 36-bottle frame and Niskin-X bottles were wiped with acetone.

Data acquisition software

SEASAVE-Win32, version 7.18c

ii. Data collection problems

(a) Temperature and conductivity sensors

Since differences of temperature-salinity relationship calculated from the secondary sensors between downcast and upcast were larger than that calculated from the primary sensors, the secondary conductivity sensor S/N 1203 was replaced with the conductivity sensor S/N 3261 after the station P21_86_1. However, the differences were still larger than that calculated from the primary sensors. The results suggest that the secondary temperature sensor S/N 1525 may have a pressure hysteresis relatively larger than the primary temperature sensor.

At the station P21_16_1, the primary temperature and conductivity data were noisy probably due to jellyfish in the primary TC duct. Therefore, the second cast P21_16_2 was carried out.

At the station P21_26_1, the primary temperature and conductivity data were noisy probably due to jellyfish in the primary TC duct. Since the second cast was not carried out, the secondary temperature and conductivity data must be used for this station.

(b) SBE43 oxygen sensor

Since differences between downcast and upcast profiles near the surface gradually became large, the SBE43 oxygen sensor S/N 0394 was replaced with the oxygen sensor S/N 0330 after the station P21_76_1.

(c) Miss trip and miss fire

Niskin bottles did not trip correctly at the following stations.

Miss trip	Miss fire
P21_33_1, #13	P21_61_1, #14
P21_18_1, #13	P21_69_1, #15
P21_36_1, #15	P21_177_1, #21
	P21_185_1, #21
	P21_188_1, #21
	P21_255_1, #33

(d) Problem of the Niskin bottle #13

Discrepancies between CTD salinity and bottle sampled salinity data for the bottle #13 (about 3000 dbar) were slightly larger (about 0.001) than that obtained from neighboring bottles during leg 1. Bottle salinity data were obtained from a different bottle at the same depth of following stations, and were compared with the bottle salinity data obtained from the bottle #13.

Bottle #2 of P21_47_1

Bottle #3 of P21_131_1, P21_132_1, P21_133_1, P21_135_1, P21_137_1

Bottle #9 of P21_136_1

Mean difference with standard error between CTD salinity and bottle salinity data are −0.0021 ± 0.0002 and −0.0013 ± 0.0001 for the bottle #13 and for the duplicate bottles, respectively. Salinity data from bottle #13 were significantly smaller than the other bottles probably due to slight leakage, although leak was not found for the bottle #13 at the water sampling. Therefore, the Niskin bottle #13 (S/N X12013) was replaced with the Niskin bottle S/N X12014 after the station P21_141_1, and the bottle flags of #13 for stations from P21_29_1 to P21_141_1 were set to 7 (unknown problem). For the other water sampling parameters, significant difference was not detected for the duplicate bottle comparison (#2 and #13) at the station P21_47_1.

(e) Other incidents of note

At the station P21_200_1, Oxygen Optode 4330F, fluorometer, and transmissometer were removed from the CTD system, because the maximum pressure (6500 dbar) for the cast was beyond the proof pressure of these sensors (6000 m).

To gain more observation time, the bottle was fired after waiting from the stop for 20 seconds at each bottle firing stops from station P21_23_1. Immediately after the bottle firing stop, water around the instruments can be contaminated by the wake effect (Uchida et al., 2007). Although the wake effect is usually large within the first 20 seconds of the stop, the data may somewhat contaminated by the wake effect.

At the station P21_97_1, the cast was aborted at 285 dbar of the down cast due to a bad condition of the winch system, and the second cast P21_97_2 was carried out. At the station P21_118_1, the cast was aborted at 54 dbar of the down cast due to a mistake of the parameter setting for the LADCP, and the second cast P21_118_2 was carried out.

iii. Data processing

SEASOFT consists of modular menu driven routines for acquisition, display, processing, and archiving of oceanographic data acquired with SBE equipment. Raw data are acquired from instruments and are stored as unmodified data. The conversion module DATCNV uses instrument configuration and calibration coefficients to create a converted engineering unit data file that is operated on by all SEASOFT post processing modules. The following are the SEASOFT and original software data processing module sequence and specifications used in the reduction of CTD data in this cruise.

Data processing software

SEASOFT-Win32, version 7.18c

DATCNV converted the raw data to engineering unit data. DATCNV also extracted bottle information where scans were marked with the bottle confirm bit during acquisition. The duration was set to 4.4 seconds, and the offset was set to 0.0 second. The hysteresis correction for the SBE 43 data (voltage) was applied for both profile and bottle information data.

TCORP (original module, version 1.1) corrected the pressure sensitivity of the SBE 3 for both profile and bottle information data.

RINKOCOR (original module, version 1.0) corrected the time-dependent, pressure-induced effect (hysteresis) of the RINKO for both profile data.

RINKOCORROS (original module, version 1.0) corrected the time-dependent, pressure-induced effect (hysteresis) of the RINKO for bottle information data by using the hysteresis-corrected profile data.

BOTTLESUM created a summary of the bottle data. The data were averaged over 4.4 seconds.

ALIGNCTD converted the time-sequence of sensor outputs into the pressure sequence to ensure that all calculations were made using measurements from the same parcel of water. For a SBE 9plus CTD with the ducted temperature and conductivity sensors and a 3000-rpm pump, the typical net advance of the conductivity relative to the temperature is 0.073 seconds. So, the SBE 11plus deck unit was set to advance the primary and the secondary conductivity for 1.73 scans (1.75/24 = 0.073 seconds). Oxygen data are also systematically delayed with respect to depth mainly because of the long time constant of the oxygen sensor and of an additional delay from the transit time of water in the pumped plumbing line. This delay was compensated by 5 seconds advancing oxygen sensor output (voltage) relative to the temperature data. Delay of the RINKO data was also compensated by 1 second advancing sensor output (voltage) relative to the temperature data.

WILDEDIT marked extreme outliers in the data files. The first pass of WILDEDIT obtained an accurate estimate of the true standard deviation of the data. The data were read in blocks of 1000 scans. Data greater than 10 standard deviations were flagged. The second pass computed a standard deviation over the same 1000 scans excluding the flagged values. Values greater than 20 standard deviations were marked bad. This process was applied to pressure, temperature, conductivity and SBE 43 output.

CELLTM used a recursive filter to remove conductivity cell thermal mass effects from the measured conductivity. Typical values used were thermal anomaly amplitude alpha = 0.03 and the time constant 1/beta = 7.0.

FILTER performed a low pass filter on pressure with a time constant of 0.15 seconds. In order to produce zero phase lag (no time shift) the filter runs forward first then backwards.

WFILTER performed as a median filter to remove spikes in fluorometer and transmissometer data. A median value was determined by 49 scans of the window.

SECTIONU (original module, version 1.1) selected a time span of data based on scan number in order to reduce a file size. The minimum number was set to be the start time when the CTD package was beneath the sea-surface after activation of the pump. The maximum number was set to be the end time when the depth of the package was 1 dbar below the surface. The minimum and maximum numbers were automatically calculated in the module.

LOOPEDIT marked scans where the CTD was moving less than the minimum velocity of 0.0 m/s (traveling backwards due to ship roll).

DESPIKE (original module, version 1.0) removed spikes of the data. A median and mean absolute deviation was calculated in 1-dbar pressure bins for both down- and up-cast, excluding the flagged values. Values greater than 4 mean absolute deviations from the median were marked bad for each bin. This process was performed 2 times for temperature, conductivity, SBE 43, Optode 3830, and RINKO output.

DERIVE was used to compute oxygen (SBE 43).

BINAVG averaged the data into 1-dbar pressure bins. The center value of the first bin was set equal to the bin size. The bin minimum and maximum values are the center value plus and minus half the bin size. Scans with pressures greater than the minimum and less than or equal to the maximum were averaged. Scans were interpolated so that a data record exist every dbar.

OPTBACKCAL (original module, version 1.0) calculated raw phase shift data of the Optode 4330F from the Optode 4330F outputs (oxygen concentration and temperature data). For bottle information data, this module was applied before applying the module BOTTLESUM.

DERIVE was re-used to compute salinity, potential temperature, and density (σ_θ).

SPLIT was used to split data into the down cast and the up cast.

Remaining spikes in the CTD data were manually eliminated from the 1-dbar-averaged data. The data gaps resulting from the elimination were linearly interpolated with a quality flag of 6.

(6) Post-cruise calibration

i. Pressure

The CTD pressure sensor offset in the period of the cruise was estimated from the pressure readings on the ship deck. For best results the Paroscientific sensor was powered on for at least 20 minutes before the operation. In order to get the calibration data for the pre- and post-cast pressure sensor drift, the CTD deck pressure was averaged over first and last one minute, respectively. Then the atmospheric pressure deviation from a standard atmospheric pressure (14.7 psi) was subtracted from the CTD deck pressure. The atmospheric pressure was measured at the captain deck (20 m high from the base line) and sub-sampled one-minute interval as a meteorological data. Time series of the CTD deck pressure is shown in Fig. 3.1.4.

The CTD pressure sensor offset was estimated from the deck pressure obtained above. Mean of the pre- and the post-casts data over the whole period gave an estimation of the pressure sensor offset from the pre-cruise calibration. Mean residual pressure between the dead-weight piston gauge and the calibrated CTD data at 0 dbar of the pre-cruise calibration was subtracted from the mean deck pressure. Estimated mean offset of the pressure data is listed in Table 3.1.1. The post-cruise correction of the pressure data is not deemed necessary for the pressure sensor.

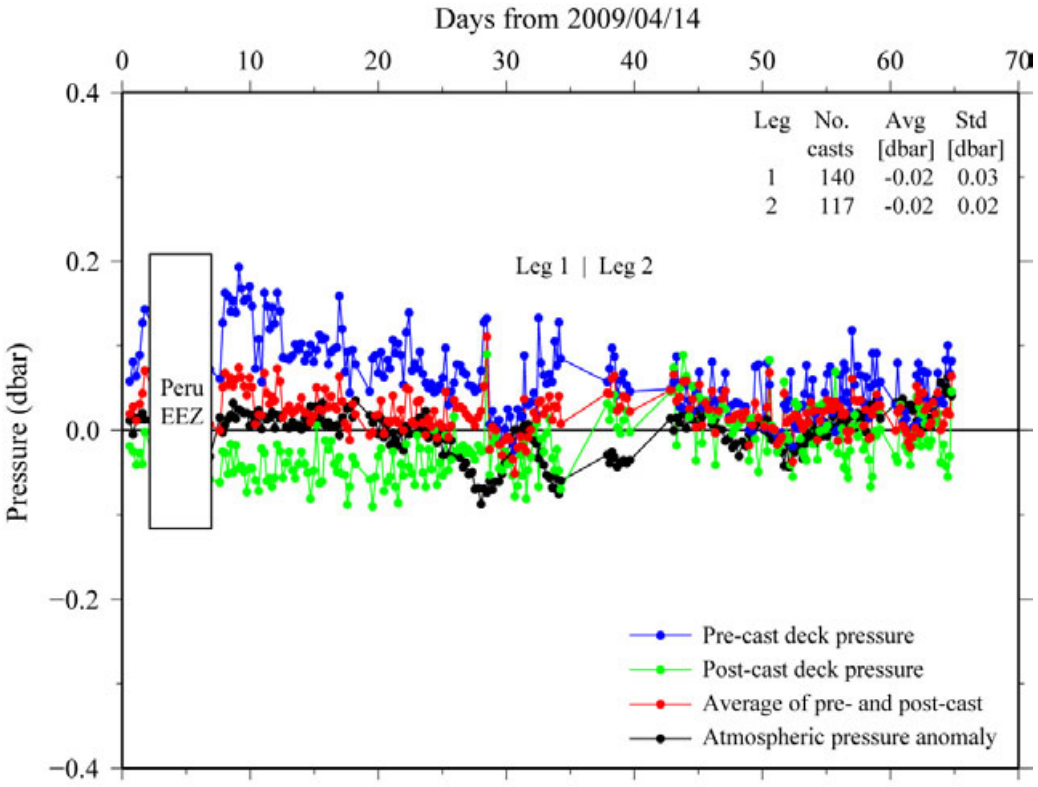

Fig. 3.1.4 Time series of the CTD deck pressure. Black dot indicates atmospheric pressure anomaly. Blue and green dots indicate pre- and post-cast deck pressures, respectively. Red dot indicates an average of the pre- and the post-cast deck pressures.

Table 3.1.1 Offset of the pressure data. Mean and standard deviation are calculated from time series of the average of the pre- and the post-cast deck pressures.

Number of cast	Mean deck pressure [dbar]	Standard deviation [dbar]	Residual pressure [dbar]	Estimated offset [dbar]
Leg 1				
140	0.02	0.03	0.13	–0.11
Leg 2				
117	0.02	0.02	0.13	–0.11

ii. Temperature

The CTD temperature sensors (SBE 3) were calibrated with the SBE 35 under the assumption that discrepancies between SBE 3 and SBE 35 data were due to pressure sensitivity, the viscous heating effect, and time drift of the SBE 3, according to a method by Uchida et al. (2007).

Post-cruise sensor calibration for the SBE 35 was performed at SBE, Inc.

S/N 0045, 19 August 2009 (2nd step: fixed point calibration)

Slope = 1.000013

Offset = –0.001173

Offset of the SBE 35 data from the pre-calibration was estimated to be smaller than 0.1 mK for temperature smaller than 4.5C. So the post-cruise correction of the SBE 35 temperature data was not deemed necessary for the SBE 35.

The CTD temperature was preliminary calibrated as

$$\text{Calibrated temperature} = T - (c_0 \times P + c_1 \times t + c_2)$$

where T is CTD temperature in °C, P is pressure in dbar, t is time in days from pre-cruise calibration date of the CTD temperature and c_0, c_1, and c_2 are calibration coefficients. The coefficients were determined using the data for the depths deeper than 1950 dbar.

The primary temperature data were basically used for the post-cruise calibration. The secondary temperature sensor was also calibrated and used instead of the primary temperature data for the station P21_26_1. The number of data used for the calibration and the mean absolute deviation from the SBE 35 are listed in Table 3.1.2 and the calibration coefficients are listed in Table 3.1.3. The results of the post-cruise calibration for the CTD temperature are summarized in Table 3.1.4 and shown in Figs. 3.1.6 and 3.1.7.

Table 3.1.2 Number of data used for the calibration (pressure ≥ 1950 dbar) and mean absolute deviation between the CTD temperature and the SBE 35.

Leg	Serial number	Number	Mean absolute deviation	Note
1	4815	1315	0.1 mK	
1	1525	1315	0.1 mK	for station P21_26_1
2	4815	834	0.1 mK	
2	1525	834	0.1 mK	Not used

Table 3.1.3 Calibration coefficients for the CTD temperature sensors.

Leg	Serial number	c_0 (°C/dbar)	c_1 (°C/day)	c_2 (°C)
1	4815	1.03996e–8	2.23793e–6	–0.0000
1	1525	–7.61078e–9	1.76847e–6	0.0005
2	4815	–4.16502e–8	3.67354e–7	–0.0003
2	1525	1.76844e–8	–1.01065e–5	0.0024

Table 3.1.4 Difference between the CTD temperature and the SBE 35 after the post-cruise calibration. Mean and standard deviation (Sdev) are calculated for the data below and above 1950 dbar. Number of data used is also shown.

Serial number	Pressure ≥ 1950 dbar			Pressure < 1950 dbar		
	Number	Mean (mK)	Sdev (mK)	Number	Mean (mK)	Sdev (mK)
Leg 1						
4815	1315	–0.01	0.2	2647	–0.03	8.7
1525	1315	–0.01	0.2	2647	0.46	9.8
Leg 2						
4815	834	–0.00	0.3	2171	–0.42	4.8
1525	834	–0.02	0.5	2171	–0.00	5.2

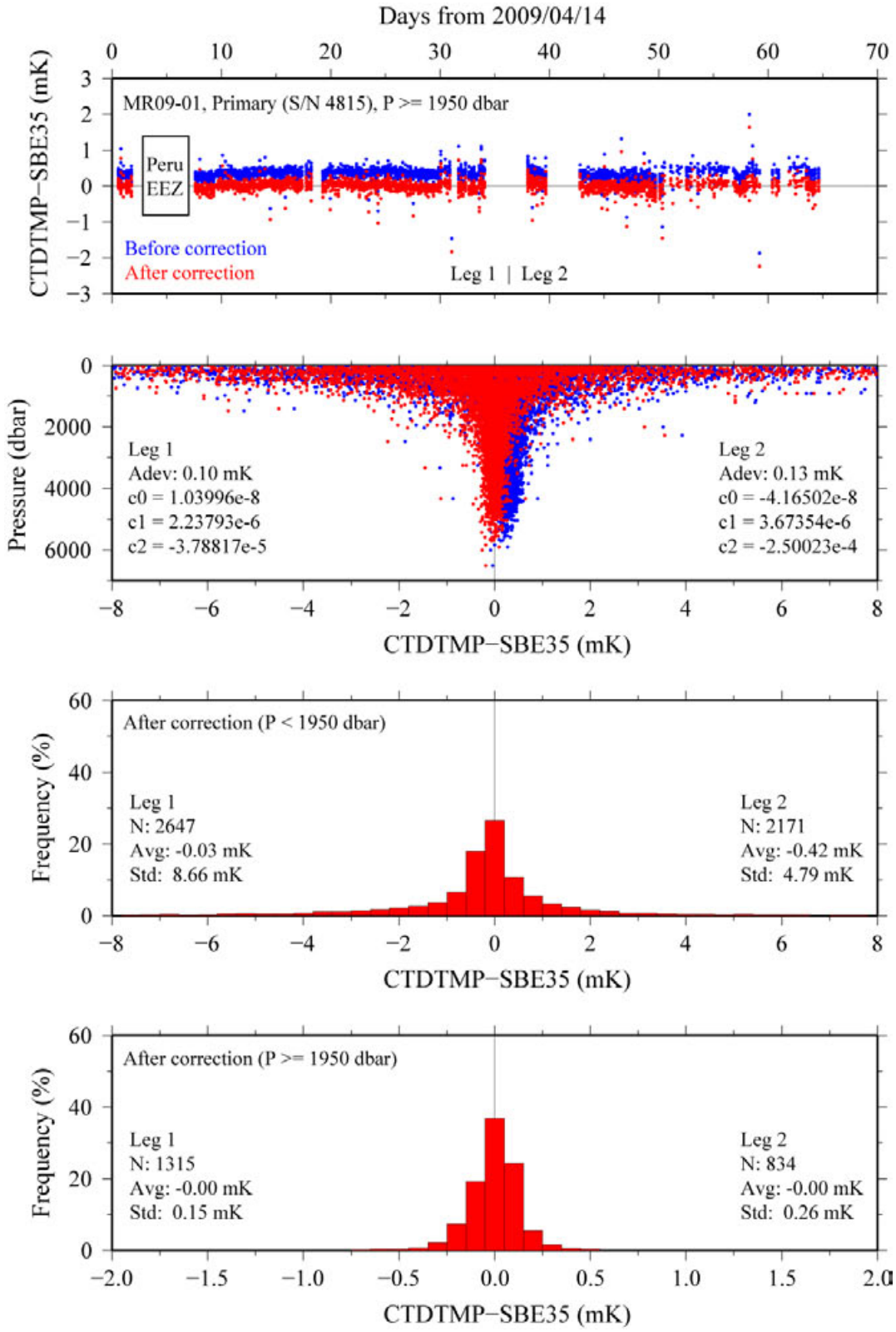

Fig. 3.1.5 Difference between the CTD temperature and the SBE 35. Blue and red dots indicate before and after the post-cruise calibration using the SBE 35 data, respectively. Lower two panels show histogram of the difference after the calibration. Results from the primary temperature sensor (S/N 4815) are shown.

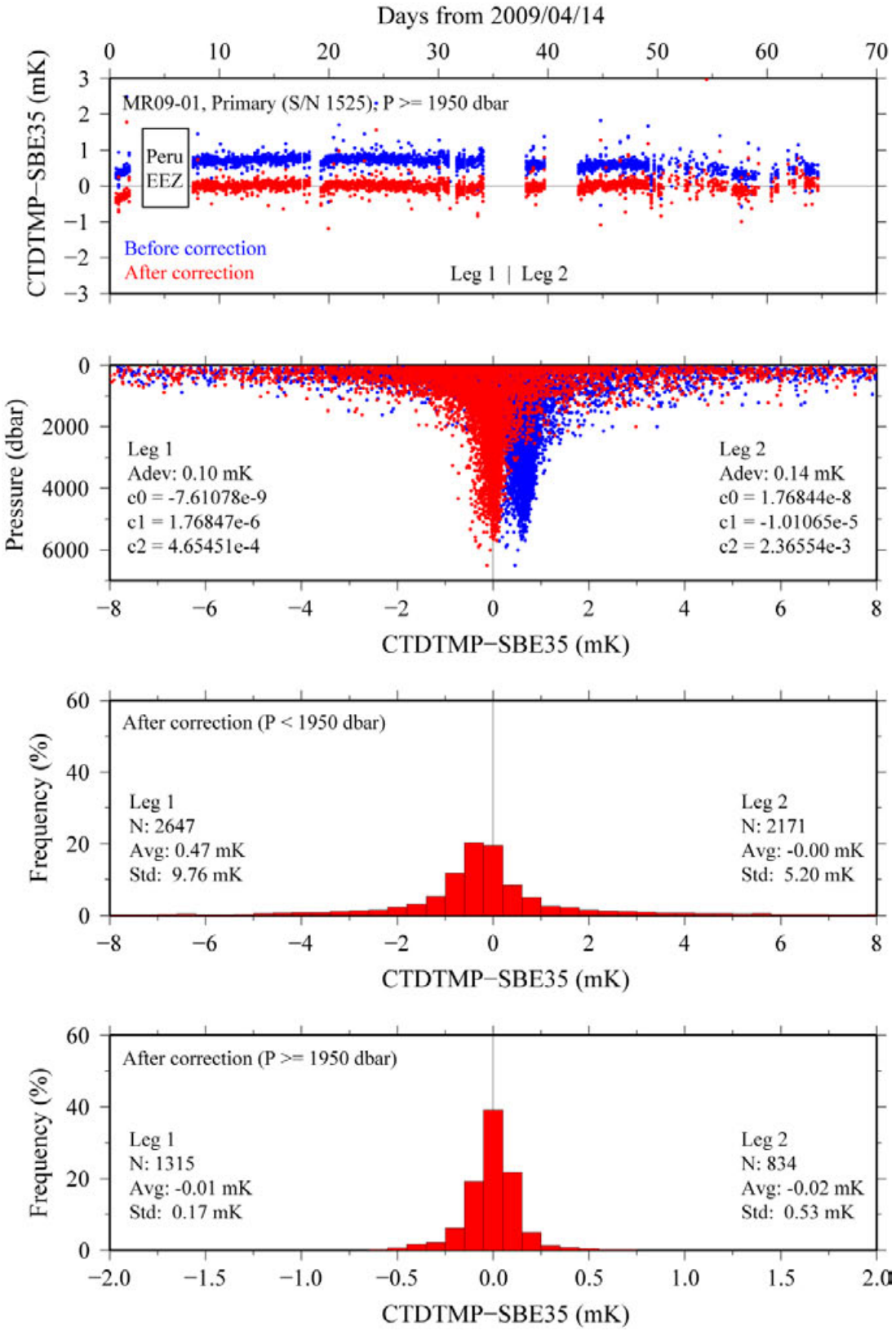

Fig. 3.1.6 Same as Fig. 3.1.5, but for the secondary temperature sensor (S/N 1525).

iii. Salinity

The discrepancy between the CTD conductivity and the conductivity calculated from the bottle salinity data with the CTD temperature and pressure data is considered to be a function of conductivity, pressure and time. The CTD conductivity was calibrated as

$$\text{Calibrated conductivity} = c_0 \times C + c_1 \times P + c_2 \times C \times P + c_3 \times t + c_4$$

where C is CTD conductivity in S/m, P is pressure in dbar, t is time in days from 14 April 2009 and c_0, c_1, c_2, c_3 and c_4 are calibration coefficients. The best fit sets of coefficients were determined by a weighted least square technique to minimize the deviation from the conductivity calculated from the bottle salinity data. The revised quasi-Newton method (FORTRAN subroutine DMINF1 from the Scientific Subroutine Library II, Fujitsu Ltd., Kanagawa, Japan) was used to determine the sets. The weight was given as a function of pressure as

$$\text{Weight} = \min[100, \exp\{\log(100) \times P / PR\}]$$

where PR is threshold of the pressure (950 dbar). When pressure is large (small), the weight is large (small) at maximum (minimum) value of 100 (1).

The primary conductivity data created by the software module ROSSUM were basically used after the post-cruise calibration for the temperature data. For the station P21_26_1, the secondary conductivity data was used, because the primary conductivity data was not able to be used for the station. Data from the station P21_14_1 to P21_27_1 were used for the calibration of the secondary conductivity. The coefficients were determined for each leg. The calibration coefficients are listed in Table 3.1.5. The results of the post-cruise calibration for the CTD salinity are summarized in Table 3.1.6 and shown in Fig. 3.1.7.

Table 3.1.5 Calibration coefficients for the CTD conductivity sensors.

Number	c_0	c_1 [S/(m dbar)]	c_2 (1/dbar)	c_3 [S/(m day)]	c_4 (S/m)	Note
Leg 1						
3743	1.00015	3.00883e–8	–9.60863e–8	4.24710e–6	–4.86614e–4	S/N 2854
330	0.999985	1.87529e–7	–6.74291e–8	5.33449e–5	–9.41355e–5	S/N 1203
Leg 2						
2849	1.00021	–3.50016e–8	5.62948e–9	–1.22961e–6	–4.63040e–4	S/N 2854

Table 3.1.6 Difference between the CTD salinity and the bottle salinity after the post-cruise calibration. Mean and standard deviation (Sdev) (in 10^{-3}) are calculated for the data below and above 950 dbar. Number of data used is also shown.

Leg (Serial no.)	Pressure ≥ 950 dbar			Pressure < 950 dbar		
	Number	Mean	Sdev	Number	Mean	Sdev
Leg 1 (2854)	1933	–0.02	0.42	1810	0.15	5.57
Leg 1 (1203)	163	–0.00	0.40	167	0.13	3.20
Leg 2 (2854)	1347	0.00	0.39	1502	0.05	4.58

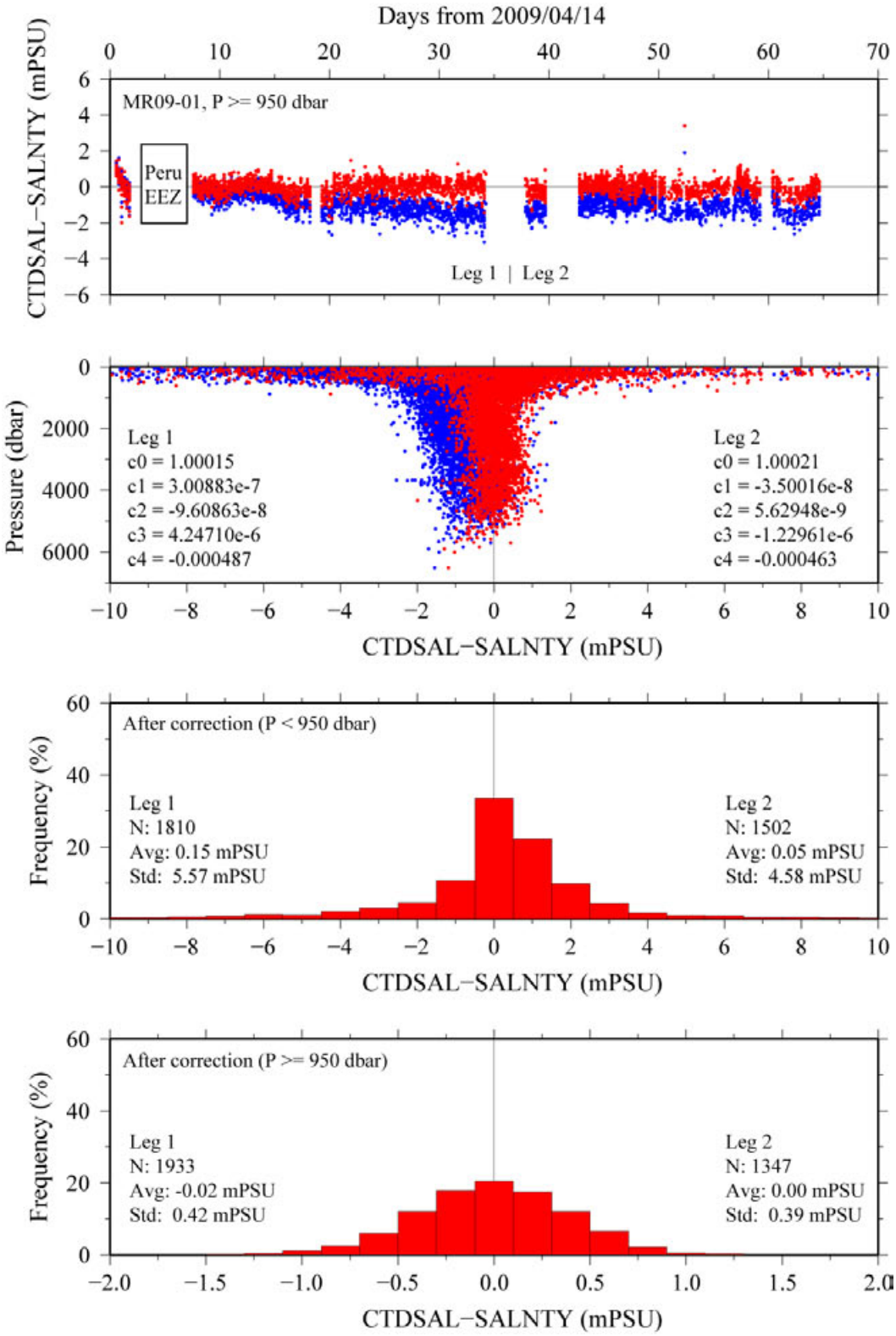

Fig. 3.1.7 Difference between the CTD salinity and the bottle salinity. Blue and red dots indicate before and after the post-cruise calibration, respectively. Lower two panels show histogram of the difference after the calibration. Results from the primary conductivity sensor (S/N 2854) are shown.

iv. Oxygen

The RINKO oxygen optode was calibrated and used as the CTD oxygen data, since the RINKO has a fast time response. However, the time-dependent, pressure-induced effect on the sensing foil was large for the RINKO, as was observed for the SBE 43. Data from the RINKO was corrected for the time-dependent, pressure-induced effect by means of the same method as that developed for the SBE 43 (Sea-Bird Electronics, 2009). The calibration coefficients, H1 (amplitude of hysteresis correction), H2 (curvature function for hysteresis), and H3 (time constant for hysteresis) were determined empirically as:

H1 = 0.0065

H2 = 5000 dbar

H3 = 2000 seconds.

Difference between the up and down cast oxygen was quite small for the pressure-hysteresis corrected RINKO data (Fig. 3.1.8).

The pressure-hysteresis corrected RINKO data was calibrated by the Stern-Volmer equation, basically according to a method by Uchida et al. (2008) with slight modification:

$$[O_2]\ (\mu mol/l) = (V_0 / V - 1) / K_{sv}$$

and

$$K_{sv} = C_0 + C_1 \times T + C_2 \times T^2$$

$$V_0 = 1 + C_3 \times T$$

$$V = C_4 + C_5 \times V_b + C_6 \times t + C_7 \times t \times V_b$$

where V_b is the RINKO output (voltage), V_0 is voltage in the absence of oxygen, T is temperature in °C, and t is time (days). Time drift of the RINKO output was corrected. The pressure-compensation coefficient (Cp) was estimated to be 0.058. The coefficient for the V_0 (C_3 = –0.00076) was estimated from laboratory experiments on August 6, 2009. The remaining seven coefficients (C0, C1, C2, C4, C5, C6, and C7) were determined by minimizing the sum of absolute deviation with a weight from the bottle oxygen data. The revised quasi-Newton method (DMINF1) was used to determine the sets. The weight was given as a function of pressure as

$$\text{Weight} = \min[10, \exp\{\log(10) \times P / PR\}]$$

where PR is threshold of the pressure (950 dbar).

The post-cruise calibrated temperature and salinity data were used for the calibration. The coefficients were determined for some groups of the CTD stations. The calibration coefficients are listed in Table 3.1.7. The results of the post-cruise calibration for the RINKO oxygen are summarized in Table 3.1.8 and shown in Fig. 3.1.9.

(7) Preliminary results

Vertical sections for potential temperature, CTD salinity and CTD oxygen are shown in Figs. 3.1.10 to 3.1.12. The post-cruise calibrated data were used.

References

Fukasawa, M., T. Kawano and H. Uchida (2004): Blue Earth Global Expedition collects CTD data aboard Mirai, BEAGLE 2003 conducted using a Dynacon CTD traction winch and motion-compensated crane, *Sea Technology*, 45, 14–18.

García, H. E. and L. I. Gordon (1992): Oxygen solubility in seawater: Better fitting equations. *Limnol. Oceanogr.*, 37 (6), 1307–1312.

Sea-Bird Electronics (2009): SBE 43 dissolved oxygen (DO) sensor – hysteresis corrections, Application note no. 64-3, 7 pp.

Uchida, H., K. Ohyama, S. Ozawa, and M. Fukasawa (2007): In situ calibration of the Sea-Bird 9plus CTD thermometer, *J. Atmos. Oceanic Technol.*, 24, 1961–1967.

Uchida, H., T. Kawano, I. Kaneko, and M. Fukasawa (2008): In situ calibration of optode-based oxygen sensors, *J. Atmos. Oceanic Technol.*, 25, 2271–2281.

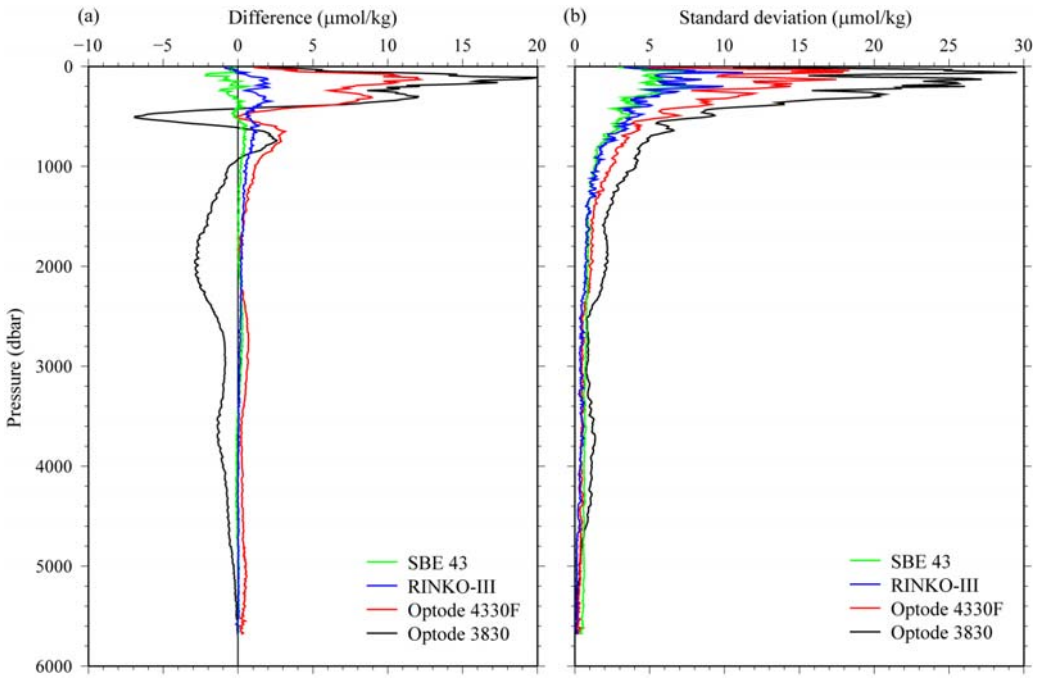

Fig. 3.1.8 Difference between the up and down cast oxygen profiles from RINKO, SBE 43, Optode 4330F, and Optode 3830. (a) mean and (b) standard deviation calculated from all CTD data.

Table 3.1.7 Calibration coefficients for the RINKO oxygen sensor.

Group	C_0	C_1	C_2	C_4	C_5	C_6	C_7
Leg 1							
A	4.15059e–3	1.47144e–4	3.05621e-6	–0.206232	0.297228	–5.79920e–3	3.53189e–3
B	4.14546e–3	1.57668e–4	2.66849e–6	–0.217899	0.300001	–8.77281e–5	1.07190e–3
C	4.18851e–3	1.48916e–4	3.48902e–6	–0.223606	0.303905	–4.66944e–4	8.79272e–4
D	4.12146e–3	1.53674e–4	2.91170e–6	–0.213679	0.303022	–5.17204e–4	7.76309e–4
E	4.07941e–3	1.53031e–4	2.82122e–6	–0.200688	0.303989	–9.83979e–4	6.80893e–4
F	3.43121e–3	1.36075e–4	1.50920e–6	–0.136717	0.284063	–1.10206e–3	1.06424e–3
Leg 2							
G	3.49508e–3	1.37615e–4	1.53061e–6	–0.223159	0.330024	1.22271e–3	–2.66367e–4
H	3.69011e–3	1.41356e–4	2.15466e–6	–0.171280	0.304838	–7.56518e–4	5.06191e–4

Group of CTD stations A: 29_1–33_1, B: 14_1–28_1, C: 41_1–68_1, D: 69_1–86_1, E: 87_1–148_1, F: 149_1–156_1, G: 164_1–172_1, H: 173_1–288_1

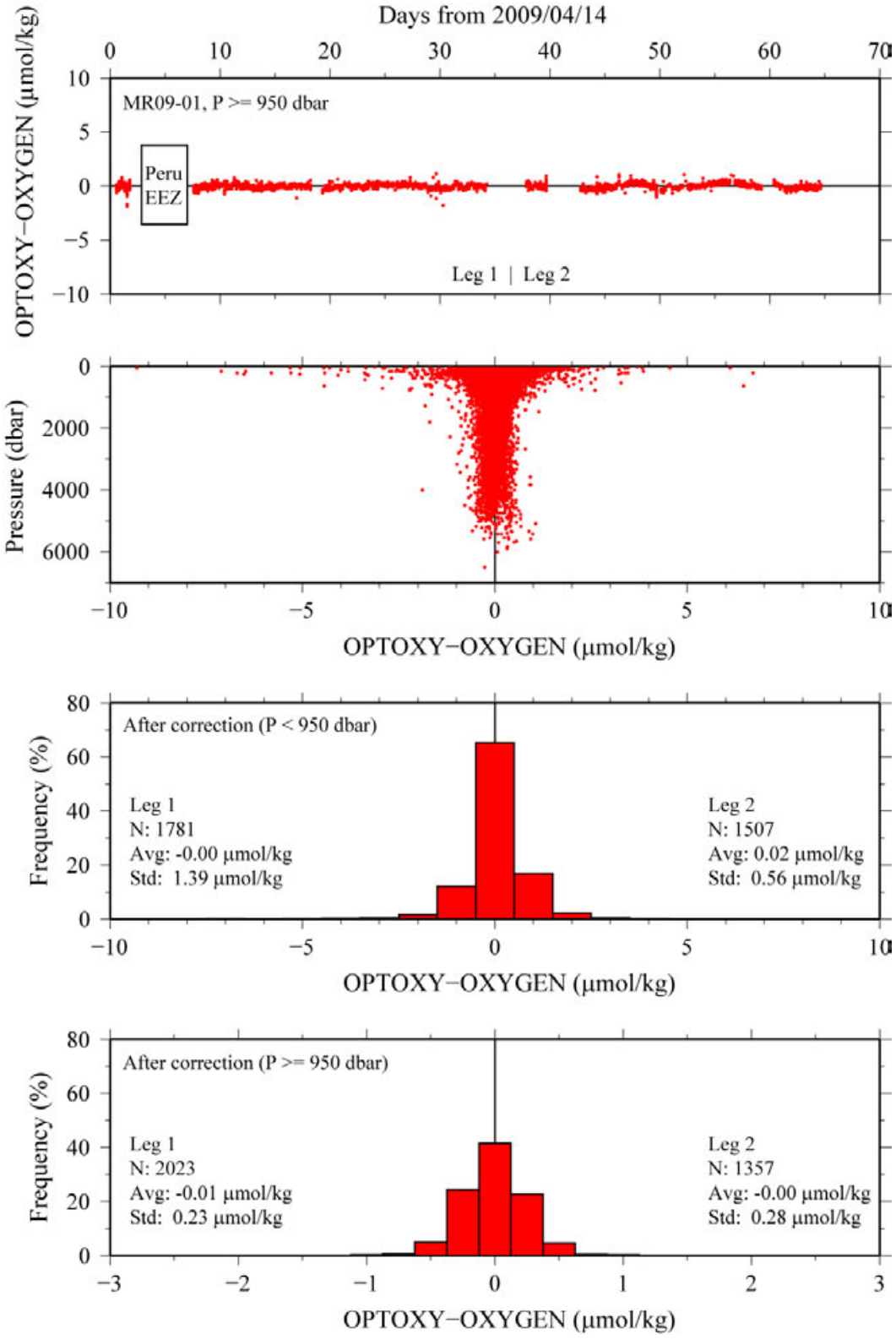

Fig. 3.1.9 Difference between the RINKO oxygen and the bottle oxygen after the post-cruise calibration. Lower two panels show histogram of the difference.

Table 3.1.8 Difference between the RINKO oxygen and the bottle oxygen after the post-cruise calibration. Mean and standard deviation (Sdev) are calculated for the data below and above 950 dbar. Number of data used is also shown.

Leg	Pressure ≥ 950 dbar			Pressure < 950 dbar		
	Number	Mean (μmol/kg)	Sdev (μmol/kg)	Number	Mean (μmol/kg)	Sdev (μmol/kg)
Leg 1	2023	–0.01	0.23	1781	–0.00	1.39
Leg 2	1357	–0.00	0.28	1507	0.02	0.56

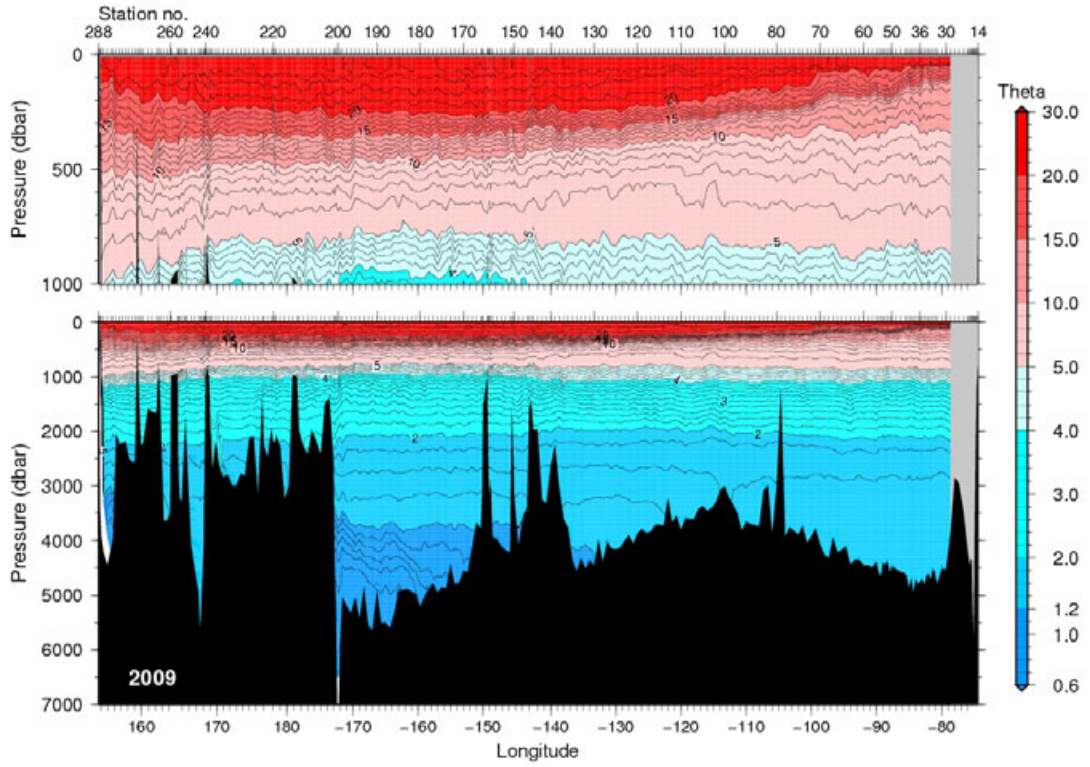

Fig. 3.1.10 Vertical section of potential temperature.

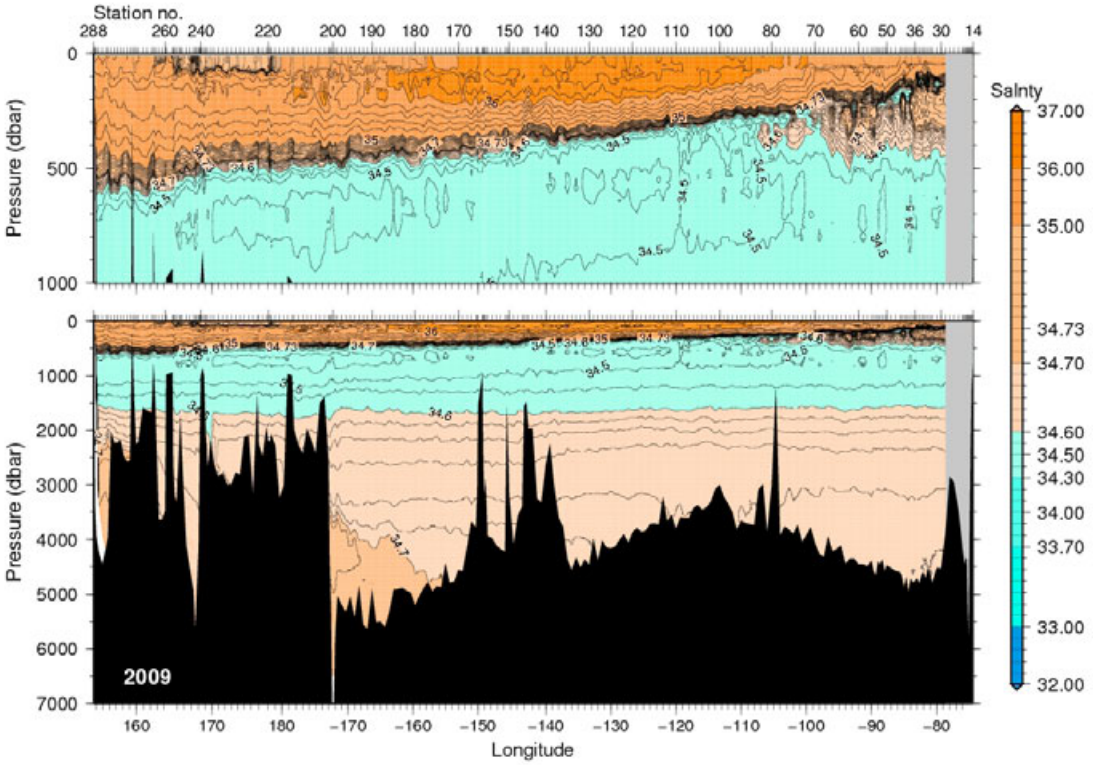

Fig. 3.1.11 Same as Fig. 3.1.10, but for CTD salinity.

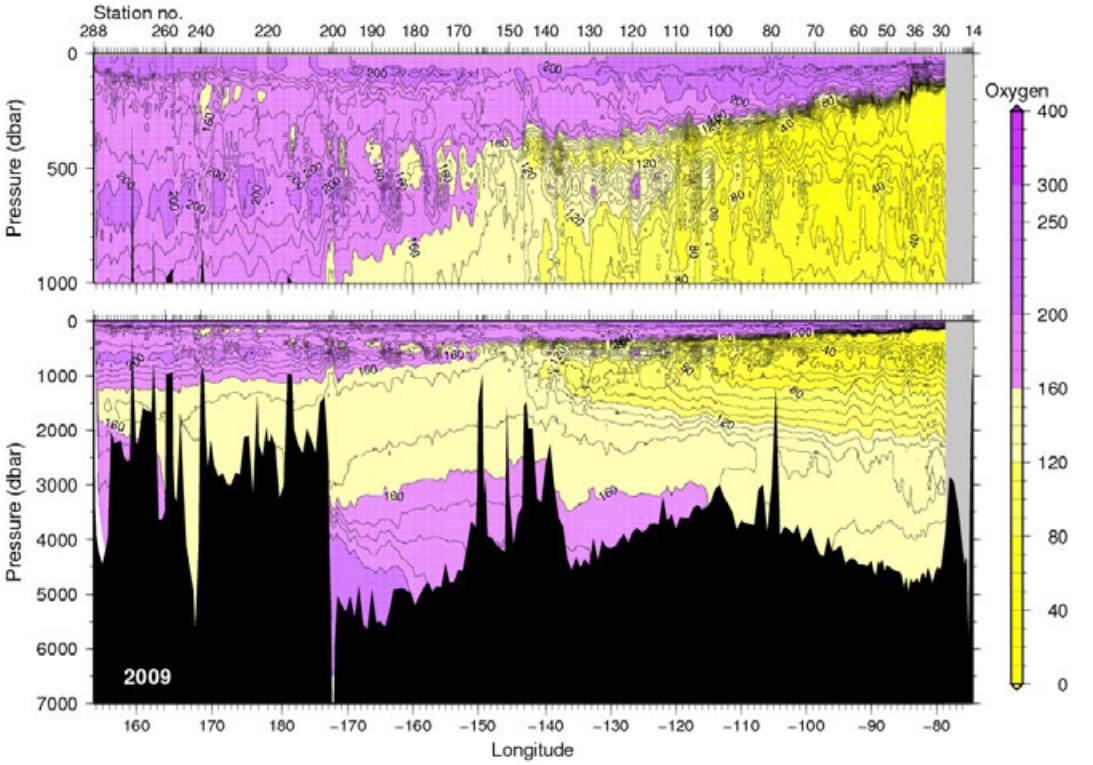

Fig. 3.1.12 Same as Fig. 3.1.10, but for CTD oxygen.

3.2 Bottle Salinity

(1) Personnel

Takeshi Kawano (JAMSTEC)
Fujio Kobayashi (MWJ)
Tatsuya Tanaka (MWJ)
Akira Watanabe (MWJ)
Kenichi Katayama (MWJ)

(2) Objectives

Bottle salinities were measured to compare with CTD salinities for calibrating CTD salinities and for identifying leaking bottles.

(3) Instrument and Method

i. Salinity Sample Collection

The bottles in which the salinity samples are collected and stored are 250 ml Phoenix brown glass bottles with screw caps. Each bottle was rinsed three times with sample water and was filled to the shoulder of the bottle. The caps were also thoroughly rinsed. Salinity samples were stored more than 12 hours in the same laboratory as the salinity measurement was made.

ii. Instruments and Method

The salinity analysis was carried out on Guildline Autosal salinometer model 8400B (S/N 62556), which was modified by adding an Ocean Scientific International Ltd. peristaltic-type sample intake pump and two Guildline platinum thermometers model 9450. One thermometer monitored an ambient temperature and the other monitored a bath temperature. The resolution of the thermometers was 0.001 deg C. The measurement system was almost same as Aoyama *et al*. (2002). The salinometer was operated in the air-conditioned laboratory of the ship at a bath temperature of 24 deg C.

An ambient temperature varied from approximately 20 deg C to 24 deg C, while a bath temperature is very stable and varied within +/- 0.002 deg C on rare occasion. A measure of a double conductivity ratio of a sample is taken as a median of 31 readings. Data collection was started after 10 seconds and it took about 10 seconds to collect 31 readings by a personal computer. Data were sampled for the sixth and seventh filling of the cell. In case where the difference between the double conductivity ratio of this two fillings is smaller than 0.00002, the average value of the two double conductivity ratios is used to calculate the bottle salinity with the algorithm for practical salinity scale, 1978 (UNESCO, 1981). If the difference is grater than or equal to the 0.00003, we measure another additional filling of the cell. In case where the double conductivity ratio of the additional filling does not satisfy the criteria above, we measure other additional fillings of the cell within 10 fillings in total. In case where the number of fillings is 10 and those fillings do not satisfy the criteria above,, the median of the double conductivity ratios of five fillings are used to calculate the bottle salinity.

The measurement was conducted about from 12 to 20 hours per day and the cell was cleaned with soap after the measurement of the day. We measured more than 8,500 samples in total.

(4) Preliminary Result

i. Standard Seawater

Leg1 and Leg2a

Standardization control was set to 649 during Leg1 and Leg2a. The value of STANDBY was 5491 +/- 0002 and that of ZERO was 0.00000 +/- 0.00001. We used IAPSO Standard Seawater batch P150 which conductivity ratio was 0.99978 (double conductivity ratio is 1.99956) as the standard for salinity. We measured 219 bottles of P150 during routine measurement. Fig.3.2.1 shows the history of double conductivity ratio of the Standard Seawater batch P150 during Leg1 and Leg2a.

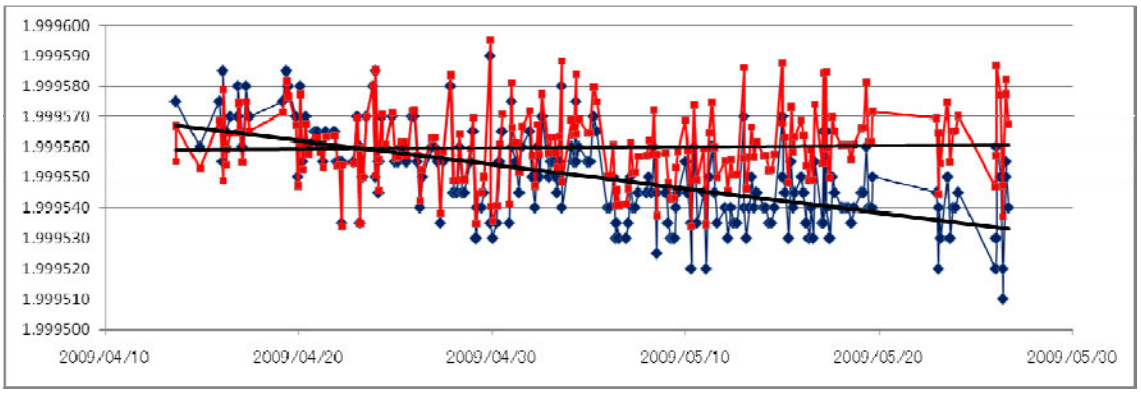

Fig.3.2.1 History of Double conductivity ratio of P150 during Leg1 and Leg2a. X and Y axes represents date and double conductivity ratio, respectively. Blue diamond is raw data and red rectangular is corrected data.

Drifts were calculated by fitting data from P150 to the equation obtained by the least square method (solid lines). Correction for the double conductivity ration of the sample was made to compensate for the drift. After correction, the average of double conductivity ratio became 1.99956 and the standard deviation was 0.00001, which is equivalent to 0.0002 in salinity.

Leg2b

As the drift of this salinometer had been significant, the re-standardization was done on 27 May, and standardization control was set to 652 during Leg2b. The value of STANDBY was 5492 +/- 0001 and that of ZERO was .00000 +/- 0.00001. We used IAPSO Standard Seawater batch P150 which conductivity ratio was 0.99978 (double conductivity ratio is 1.99956) as the standard for salinity. We measured 137 bottles of P150 during routine measurement. Fig.3.2.2 shows the history of double conductivity ratio of the Standard Seawater batch P150 during Leg2b.

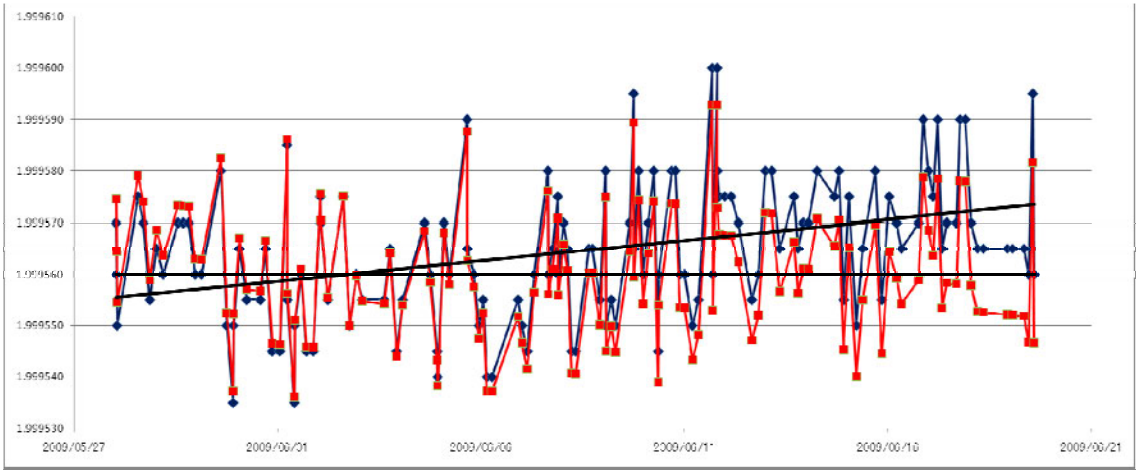

Fig.3.2.2 History of Double conductivity ratio of P150 during Leg2b. X and Y axes represents date and double conductivity ratio, respectively. Blue diamond is raw data and red rectangular is corrected data.

Drifts were calculated by fitting data from P150 to the equation obtained by the least square method (solid lines). Correction for the double conductivity ration of the sample was made to compensate for the drift. After correction, the average of double conductivity ratio became 1.99956 and the standard deviation was 0.00001, which is equivalent to 0.0002 in salinity.

ii. Sub-Standard Seawater

We also used sub-standard seawater which was deep-sea water filtered by pore size of 0.45 micrometer and stored in a 20 liter cubitainer made of polyethylene and stirred for at least 24 hours before measuring. It was measured every six samples in order to check the possible sudden drift of the salinometer. During the whole measurements, there was no detectable sudden drift of the salinometer.

iii. Replicate Samples

Leg1

We took 819 pairs of replicate during Leg1. Fig.3.2.3 shows the histogram of the absolute difference between replicate samples. There was 1 bad measurement of replicate samples. Excluding these bad measurements, the standard deviation of the absolute deference of 818 pairs of replicate samples was 0.00023 in salinity.

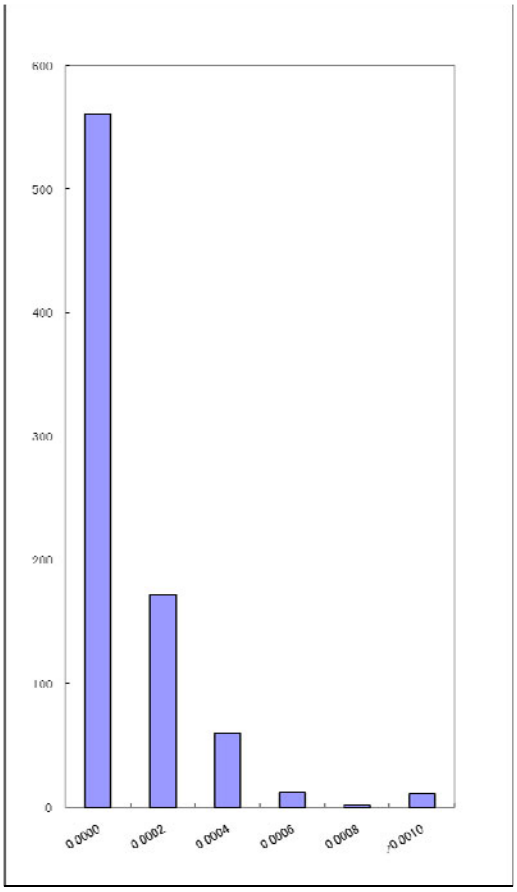

Fig.3.2.3 The histogram of the absolute difference between replicate samples in Leg1. X axis is absolute difference in salinity and Y axis is frequency.

Leg2

We took 613 pairs of replicate during Leg2. Fig.3.2.4 shows the histogram of the absolute difference between replicate samples. There was 1 bad measurement of replicate samples. Excluding these bad measurements, the standard deviation of the absolute deference of 612 pairs of replicate samples was 0.00019 in salinity.

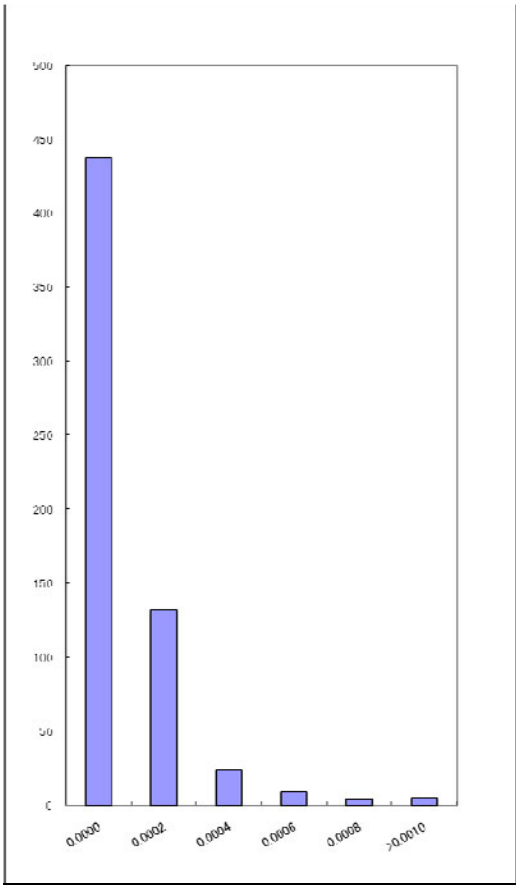

Fig.3.2.4 The histogram of the absolute difference between replicate samples in Leg2.
X axis is absolute difference in salinity and Y axis is frequency.

(5) Further data quality check

All the data will be checked once again in detail with other parameters such as dissolved oxygen and nutrients.

(6) Reference

Aoyama, M., T. Joyce, T. Kawano and Y. Takatsuki : Standard seawater comparison up to P129. Deep-Sea Research, I, Vol. 49, 1103～1114, 2002

UNESCO : Tenth report of the Joint Panel on Oceanographic Tables and Standards. UNESCO Tech. Papers in Mar. Sci., 36, 25 pp., 1981

3.3 Oxygen

July 06, 2009

(1) Personnel

Yuichiro KUMAMOTO [1)]**,** ***Miyo IKEDA*** [2)]**,** ***Fuyuki SHIBATA*** [2)]**,** ***Masanori ENOKI*** [2)]**, and** ***Misato KUWAHARA*** [2)]

1) Japan Agency for Marine Earth Science and Technology (JAMSTEC)

2) Marine Works Japan Co. Ltd

(2) Objectives

Dissolved oxygen is one of good tracers for the ocean circulation. Recent studies indicated that the oxygen minimum layers in the tropical region have expanded (Stramma et al., 2008). Climate models predict a decline in oceanic dissolved oxygen concentration and a consequent expansion of the oxygen minimum layers under global warming conditions, which results mainly from decreased interior advection and ongoing oxygen consumption by remineralization. The mechanism of the decrease, however, is still unknown During MR09-01, we measured dissolved oxygen concentration from surface to bottom layers at all the hydrocast stations along approximately 18°S in the tropical South Pacific. These stations reoccupied the WOCE Hydrographic Program P21 stations in 1994. Our purpose is to evaluate temporal change in dissolved oxygen concentration in the tropical South Pacific between the 1994 and 2009.

(3) Reagents

Pickling Reagent I: Manganous chloride solution (3M)

Pickling Reagent II: Sodium hydroxide (8M) / sodium iodide solution (4M)

Sulfuric acid solution (5M)

Sodium thiosulfate (0.025M)

Potassium iodate (0.001667M)

CSK standard of potassium iodate: Lot TSK3952, Wako Pure Chemical Industries Ltd., 0.0100N

(4) Instruments

Burette for sodium thiosulfate and potassium iodate;

APB-510 manufactured by Kyoto Electronic Co. Ltd. / 10 cm^3 of titration vessel

Detector;

Automatic photometric titrator, DOT-01 manufactured by Kimoto Electronic Co. Ltd.

(5) Seawater sampling

Following procedure is based on a determination method in the WHP Operations Manual (Dickson, 1996). Seawater samples were collected from 12-liters Niskin sampler bottles attached to the CTD-system. Seawater for bottle oxygen measurement was transferred from the Niskin sampler bottle to a volume calibrated glass flask (ca. 100 cm^3). Three times volume of the flask of seawater was overflowed. Sample temperature was measured by a thermometer during the overflowing. Then two reagent solutions (Reagent I, II) of 0.5 cm^3 each were added immediately into the sample flask and the stopper was inserted carefully into the flask. The sample flask was then shaken vigorously to mix the contents and to disperse the precipitate finely throughout. After the precipitate has settled at least halfway down the flask, the flask was shaken again to disperse the precipitate. The sample flasks containing pickled samples were stored in a laboratory until they were titrated.

(6) Sample measurement

At least two hours after the re-shaking, the pickled samples were measured on board. A magnetic stirrer bar and 1 cm^3 sulfuric acid solution were added into the sample flask and stirring began. Samples were titrated by sodium thiosulfate solution whose molarity was determined by potassium iodate solution. Temperature of sodium thiosulfate during titration was recorded by a thermometer. We measured dissolved oxygen concentration using two sets of the titration apparatus, named DOT-1 and DOT-2. Dissolved oxygen concentration ($\mu mol\ kg^{-1}$) was calculated by the sample temperature during the sampling, CTD salinity, flask volume, and titrated volume of the sodium thiosulfate solution. When we measured suboxic samples (oxygen concentration less than about 40 $\mu mol\ kg^{-1}$), titration procedure was adjusted manually. In case of anoxic sample measurements (oxygen concentration less than about 6 $\mu mol\ kg^{-1}$), titration volume of sodium thiosulfate was not corrected using an empirical equation of burette calibration.

(7) Standardization

Concentration of sodium thiosulfate titrant (ca. 0.025M) was determined by potassium iodate solution. Pure potassium iodate was dried in an oven at 130°C. 1.7835 g potassium iodate weighed out accurately was dissolved in deionized water and diluted to final volume of 5 dm^3 in a calibrated volumetric flask (0.001667M). 10 cm^3 of the standard potassium iodate solution was added to a flask using a volume-calibrated dispenser. Then 90 cm^3 of deionized water, 1 cm^3 of sulfuric acid solution, and 0.5 cm^3 of pickling reagent solution II and I were added into the flask in order. Amount of titrated volume of sodium thiosulfate (usually 5 times measurements average) gave the molarity of the sodium thiosulfate titrant. Table 3.3.1 shows result of the standardization during this cruise. Error (C.V.) of the standardization was 0.02±0.01 %, c.a. 0.05 $\mu mol\ kg^{-1}$.

(8) Determination of the blank

The oxygen in the pickling reagents I (0.5 cm^3) and II (0.5 cm^3) was assumed to be 3.8×10^{-8} mol (Murray *et al.*, 1968). The blank from the presence of redox species apart from oxygen in the reagents (the pickling reagents I, II, and the sulfuric acid solution) was determined as follows. 1 and 2 cm^3 of the standard potassium iodate solution were added to two flasks respectively. Then 100 cm^3 of deionized water, 1 cm^3 of sulfuric acid solution, and 0.5 cm^3 of pickling reagent solution II and I each were added into the two flasks in order. The blank was determined by difference between the two times of the first (1 cm^3 of KIO_3) titrated volume of the sodium thiosulfate and the second (2 cm^3 of KIO_3) one. The results of 3 times blank determinations were averaged (Table 3.3.1). The averaged blank values for DOT-1 and DOT-2 were –0.002±0.001 (S.D., n=27) and –0.000±0.001 (S.D., n=27) cm^3, respectively.

Table 3.3.1 Results of the standardization and the blank determinations during MR09-01.

	KIO_3 No.		$Na_2S_2O_3$ No.	DOT-1		DOT-2		Stations
(UTC)	#	ID No.		E.P.	blank	E.P.	blank	
2009/4/13	1	20081203-11-02	20080704-2-1	3.957	-0.001	3.957	-0.001	029,030,031,032,040,033
2009/4/18		20081203-11-03	20080704-2-1	3.958	0.001	3.959	0.003	014,015
2009/4/18		20081203-11-04	20080704-2-2	3.958	-0.002	3.957	-0.002	017,018,019,021,022,023,024,025,026,027,028
2009/4/21		20081203-11-05	20080704-2-2	3.956	-0.001	3.956	0.001	041,034,042,035
2009/4/22		20081203-11-07	20080704-3-1	3.960	-0.002	3.960	-0.001	043,036,044,037,045,038,046,039
2009/4/24	2	20081203-12-02	20080704-3-1	3.962	-0.002	3.962	-0.001	047,X19,049,050
2009/4/25		20081203-12-03	20080704-3-2	3.961	-0.002	3.964	0.001	054,051,055,056,053,057,058,059,060,061,062,063,064,065
2009/4/26		20081203-12-04	20080704-3-2	3.962	-0.002	3.961	0.000	052
2009/4/28		20081203-12-06	20080704-4-1	3.963	-0.002	3.962	0.000	066,067,068,069,070,071,072,073,074,075,076,X18,077,078
2009/5/1		20081203-12-08	20080704-4-2	3.963	-0.002	3.964	-0.001	079,080,085,086,087,088,089,090,095,096,097-2,098,099,100
2009/5/5		20081203-12-10	20080704-5-1	3.964	-0.002	3.964	0.000	101,102,103,104,105,106
2009/5/6	3	20081203-13-01	20080704-5-1	3.962	-0.001	3.962	0.000	107,108,109,110,111,112,113,114
2009/5/8		20081203-13-02	20080704-5-2	3.965	-0.002	3.964	-0.001	115,116,117,118,119,120,121,122,123,124,125,126,127
2009/5/11		20081203-13-04	20080704-6-1	3.964	-0.001	3.964	0.000	128,129,130,X17,131,132,133,134,135,136,137
2009/5/14		20081203-13-06	20080704-6-2	3.964	-0.002	3.964	-0.001	138,139,140,141,142,143,144,145,146,147,148,149,150,151,152
2009/5/16		20081203-13-08	20080704-7-1	3.963	-0.001	3.965	0.000	153,154,155,160,159,158,157,156

Table 3.3.1 continued.

	KIO_3 No.		$Na_2S_2O_3$ No.	DOT-1		DOT-2		Stations
(UTC)	#	ID No.		E.P.	blank	E.P.	blank	
2009/5/21	4	20081203-14-01	20080704-7-2	3.963	-0.003	3.965	-0.003	164,165,X16,167,168,169, 170,171,172
2009/5/26		20081203-14-03	20080704-8-1	3.968	-0.001	3.971	0.001	173,174,175,176,177,178, 179,180,181,182,183
2009/5/29		20081203-14-05	20080704-8-2	3.968	-0.001	3.969	-0.001	184,185,186,187,188,189, 190,191,192
2009/6/1		20081203-14-07	20080704-9-1	3.965	-0.001	3.965	-0.001	193,194,195,196,197,198, 199,200,201,203,204,205
2009/6/3		20081203-14-09	20080704-9-2	3.965	-0.002	3.966	0.000	206,207,208,209,210,211, 212,213
2009/6/5	5	20081203-15-01	20080704-9-2	3.963	-0.002	3.964	0.000	214,215,216,217,218,220, 221,222
2009/6/6		20081203-15-03	20080704-10-1	3.975	-0.001	3.976	0.001	223,224,225,226,227,228, 229,230,231,232,233
2009/6/9		20081203-15-05	20080704-10-2	3.977	-0.001	3.978	0.002	234,235,236,237,238,239, 240,241,243,244,245,246
2009/6/10		20081203-15-07	20080704-11-1	3.965	-0.001	3.965	0.000	247,248,249,250,251,252, 253,255,254
2009/6/13	6	20081204-16-01	20080704-11-2	3.967	-0.002	3.968	0.000	260,261,262,263,264,265, 266,267,268,269,270,271, 272,273,274,275,276
2009/6/16		20081204-16-03	20080704-12-1	3.966	-0.002	3.967	0.000	277,278,279,280,281,282, 283,285,287,286,288

Batch number of the KIO_3 standard solution

(9) Replicate sample measurement

Replicate samples were taken from every CTD cast. Total amount of the replicate sample pairs of good measurement (flagged 2) was 686. The standard deviation of the replicate measurement was 0.09 μmol kg^{-1} that was calculated by a procedure (SOP23) in DOE (1994). The replicate measurements depended on neither sampling depth (Fig. 3.3.1) nor measurement date (Fig.3.3.2). In the hydrographic data sheet, a mean of replicate sample pairs will be presented with the flag 2 (see section 12).

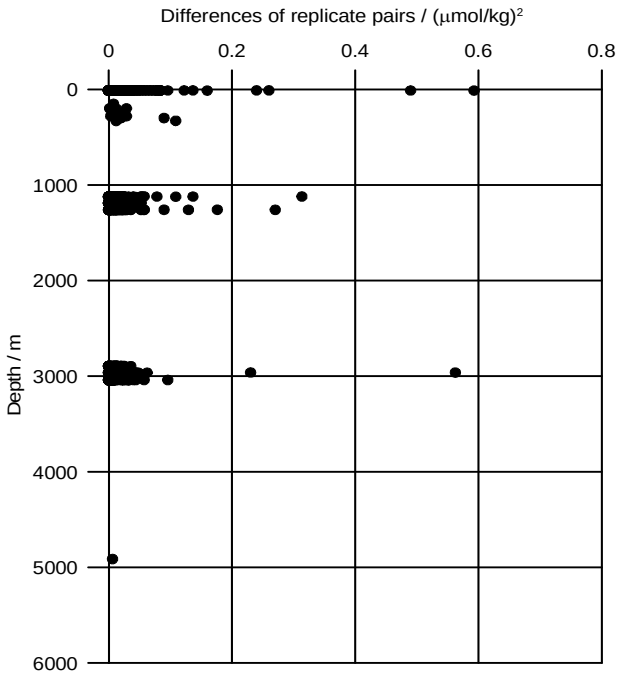

Figure 3.3.1 Differences of replicate sample pairs against sampling depth.

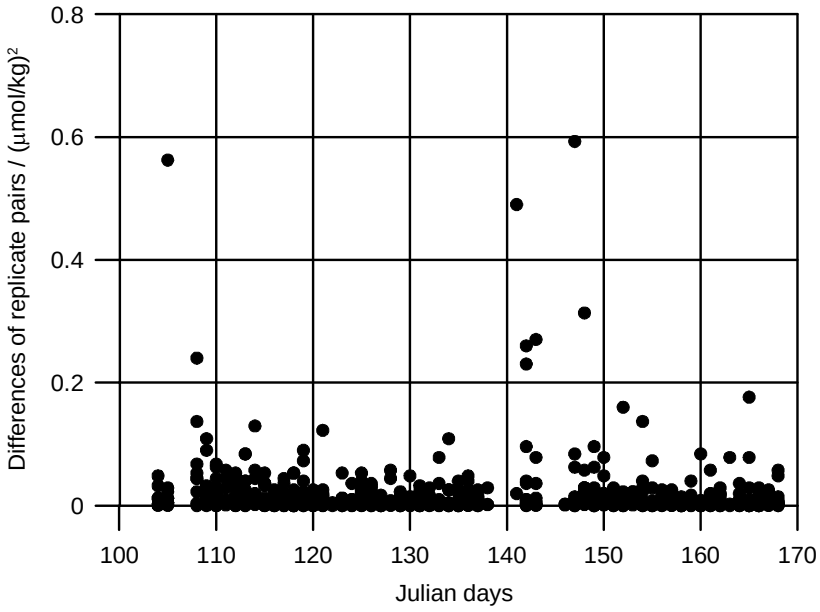

Figure 3.3.2 Differences of replicate sample pairs against measurement date (Julian days).

(10) Duplicate sample measurement

Duplicate samples were taken from 27 CTD casts during this cruise. Niskin numbers and sampling pressure of the duplicate pairs at the 27 stations are shown in Table 3.3.2. The standard deviation of the duplicate measurements was calculated to be 0.07 μmol kg^{-1} that was equivalent with that of the replicate measurements (see section 9).

Table 3.3.2 Results of the duplicate sampling during MR09-01.

	Leg	Stations	Pres.(db)	#1 Niskin	#1 Oxygen [umol/kg]	#2 Niskin	#2 Oxygen [umol/kg]
1	1	P21-31	4485	1	154.75	2	154.74
2	1	P21-41	4420	3	154.94	7	154.97
3	1	P21-42	4330	4	153.53	8	153.54
4	1	P21-36	4080	5	151.06	9	150.99
5	1	P21-37	3750	6	147.47	10	147.36
6	1	P21-38	3420	2	140.99	11	141.06
7	1	P21-39	3330	2	143.32	12	143.39
8	1	P21-47	2930	2	138.61	13	138.77
9	1	P21-49	2870	2	142.88	14	142.90
10	1	P21-51	2670	2	141.81	15	141.61
11	1	P21-52	2400	2	138.11	16	138.03
12	1	P21-53	2130	2	126.28	17	126.37
13	1	P21-60	2000	2	119.85	18	119.89
14	2	P21-175	4858	1	188.49	2	188.51
15	2	P21-177	4500	3	185.99	7	185.88
16	2	P21-179	4670	4	190.16	6	190.18
17	2	P21-181	4330	5	184.64	8	184.53
18	2	P21-184	4080	2	183.66	9	183.89
19	2	P21-186	3750	2	175.59	10	175.61
20	2	P21-190	3580	2	165.39	11	165.44
21	2	P21-192	3250	2	160.98	12	160.93
22	2	P21-194	2930	2	151.66	13	151.61
23	2	P21-197	2730	2	145.70	14	145.63
24	2	P21-201	2600	2	142.29	15	142.14
25	2	P21-215	2470	2	149.94	16	149.91
26	2	P21-217	2200	2	149.93	17	150.00
27	2	P21-226	1930	2	147.32	18	147.15

(11) CSK standard measurements

The CSK standard is a commercial potassium iodate solution (0.0100 N) for analysis of dissolved oxygen. We titrated the CSK standard solutions (Lot TSK3952) against our KIO_3 standards as samples before and during this cruise (Table 3.3.3). A good agreement among them confirms that there was no systematic shift in our oxygen analyses from preparation of our KIO_3 standards onshore to sample measurements on board. In addition, we also confirmed an agreement of titrated values between the current (TSK3952) and former (EWL3818) batches of the CSK standard solutions. This agreement indicates comparability in the oxygen measurements between this cruise (MR09-01) and our previous cruises in 2007 (MR07-04 and MR07-06) because the concentration of the former CSK solutions (EWL3818) was certified during the previous cruises.

Table 3.3.3 Results of the CSK standard (Lot TSK3952) measurements on board.

Date (UTC)	KIO_3 ID No.	DOT-1		DOT-2		Remarks
		Conc. (N)	error (N)	Conc. (N)	error (N)	
2009/04/10	20081203-11-01	0.010003	0.000002	0.010008	0.000001	MR09-01 Leg-1
2009/05/18	20081203-13-09	0.010008	0.000001	0.010003	0.000003	MR09-01 Leg-1
2009/06/18	20081204-16-04	0.010005	0.000007	0.010002	0.000002	MR09-01 Leg-2
Date (UTC)	KIO_3 ID No.	DOT-3		−		Remarks
		Conc. (N)	error (N)	−	−	
2008/12/08	20081203-11-12	0.010000	0.000002	−	−	before cruise
2008/12/08	20081203-12-12	0.010001	0.000002	−	−	before cruise
2008/12/08	20081203-13-12	0.010001	0.000002	−	−	before cruise
2008/12/08	20081203-14-12	0.009999	0.000002			before cruise
2008/12/08	20081203-15-12	0.009999	0.000002	−	−	before cruise
2008/12/09	20081203-16-12	0.010001	0.000003	−	−	before cruise

(12) Quality control flag assignment

Quality flag values were assigned to oxygen measurements using the code defined in Table 0.2 of WHP Office Report WHPO 91-1 Rev.2 section 4.5.2 (Joyce *et al*., 1994). Measurement flags of 2 (good), 3 (questionable), 4 (bad), and 5 (missing) have been assigned (Table 3.3.4). The replicate data were averaged and flagged 2 if both of them were flagged 2. If either of them was flagged 3 or 4, a datum with "younger" flag was selected. Thus we did not use flag of 6 (replicate measurements). For the choice between 2, 3, or 4, we basically followed a flagging procedure as listed below:

a. Bottle oxygen concentration at the sampling layer was plotted against sampling pressure. Any points not lying on a generally smooth trend were noted.
b. Difference between bottle oxygen and CTD oxygen (Optode-2 sensor) was then plotted against sampling pressure. If a datum deviated from a group of plots, it was flagged 3.
c. Vertical sections against pressure and potential density were drawn. If a datum was anomalous on the section plots, datum flag was degraded from 2 to 3, or from 3 to 4.
d. If there was problem in the measurement, the datum was flagged 4.
e. If the bottle flag was 4 (did not trip correctly), a datum was flagged 4 (bad). In case of the bottle flag 3 (leaking) or 5 (unknown problem), a datum was flagged based on steps a, b, c, and d.

Table 3.3.4 Summary of assigned quality control flags.

Flag	Definition	
2	Good	6668
3	Questionable	40
4	Bad	32
5	Not report (missing)	0
	Total	6740

(12) Problems

i. Unknown problem

At station 31, there was a large disagreement between bottle and sensor oxygen concentration at 4670 dbar (Niskin #6). The cause of this disagreement is unknown. The datum was flagged 4.

ii. Oxygen measurements for anoxic seawater.

We failed to measure oxygen concentration in some of anoxic samples (oxygen concentration less than 2 μmol kg^{-1}) collected in the coastal region off Peru. In the most cases, a slope of titration curve became gradual, resulting in a positive bias of about 1 μmol kg^{-1} against the oxygen concentration measured using the sensor. We measured "seawater blank*" in order to verify its contribution to the positive bias. The measured seawater blanks were less than 1 μmol kg^{-1} and a relationship between the seawater blank and the positive bias was uncertain. These data were flagged 3 or 4.

*Method of the seawater blank

Seawater sample was collected in the volume calibrated glass flask (ca. 100 cm^3) without the pickling. Then 1 cm^3 of the standard potassium iodate solution, 1 cm^3 of sulfuric acid solution, and 0.5 cm^3 of pickling reagent solution II and I each were added into the flask in order. In addition, a flask contained 1 cm^3 of the standard potassium iodate solution, 100 cm^3 of deionized water, 1 cm^3 of sulfuric acid solution, and 0.5 cm^3 of pickling reagent solution II and I was prepared. The difference of the titrant volumes of the seawater flask and the deionized water one gave the seawater blank.

iii Contamination from remaining deposit in the bottle

Due to stain in the sample bottles, some measurements of bottle oxygen at stations 176 and 178 were positively biased by about 3 μmol kg^{-1}. In the case, bottle washing without acid solution was inadequate and deposit of manganese hydroxide remained in the bottles. The data were flagged 4.

(13) Preliminary Results

i. Comparison with oxygen measurements at the cross point of MR07-06.

During this cruise, we compared vertical profile of oxygen concentration at a cross point of MR07-06, 18.75°S/177.83°E. The first and second hydrocasts were conducted on 13-Dec.-2007 (MR07-06_P14C-049) and 06-Jun.-2009 (MR09-01_P21-221), respectively. Below 1500 dbar, we got a good agreement between the first and second measurements (Fig. 3.3.3).

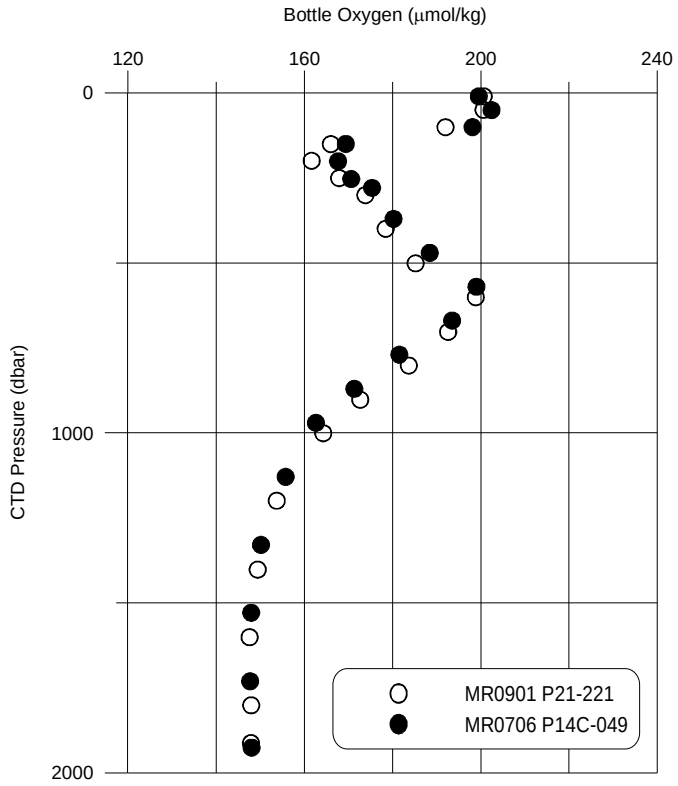

Figure 3.3.3 Vertical profiles of bottle oxygen concentration at a cross point (18.75°S/177.83°E) during MR07-06 and MR09-01 cruises.

ii. Distribution of dissolved oxygen along WHP-P21 in 2009

Dissolved oxygen concentration below the main pycnocline off Peru is very low (anoxic), which corresponds to the southward Peru-Chile undercurrent. This current originates in the equatorial subsurface water, which experiences vigorous oxygen consumption. A tongue-shaped oxygen minima centered around 500 – 1000 m east of about 140°W also comes from the equatorial zone. West of 150°W, subsurface (around 500 – 1000 m) oxygen maxima were obvious. The maxima were traced by about 100°W. These oxygen maxima were derived from Antarctic Intermediate Water (AAIW). Another high-oxygen water found in bottom water of the Southwestern Pacific Basin around 150°W – 170°W, which corresponds the Circumpolar Deep Water (CDW). The deep part of the New Caledonia Trough and New Hebrides Trench (around 165°E) are blocked by the topography to the south and is therefore filled by flow from the north. Similarly, the North Fiji Basin (around 170°E) is filled from the north and probably from the southeast over a sill north of New Zealand. On the other hand, deep water in the Tasman Sea (around 155°E) is oxygen-riched due to inflow of CDW from south.

iii. Decadal changes in dissolved oxygen along WHP-P21 from 1994 and 2009

Along the P21 line, dissolved oxygen above 500 m depth decreased. West of around 170°E, oxygen concentration in the oxygen maximum centered around 500 – 1000 m increased. Another oxygen increase was found in deep water (around 500 – 2000 m) between 140°W and 115°W. East of this increase, oxygen concentration between 115°W and 90°W in the deep water decreased. In the Southwestern North Pacific, decreases of dissolved oxygen up to 5 μmol kg^{-1} were found in deep and bottom waters (1000 – 5500 m). Striped pattern of the oxygen decreases in the bottom water implies temporal change of oxygen concentration due to internal waves. Oxygen decreases were also found in deep water (– 3000 m) of the North Fiji Basin.

References

Dickson, A. (1996) Determination of dissolved oxygen in sea water by Winkler titration, in WHPO Pub. 91-1 Rev. 1, November 1994, Woods Hole, Mass., USA.

DOE (1994) Handbook of methods for the analysis of the various parameters of the carbon dioxide system in sea water; version 2. A.G. Dickson and C. Goyet (eds), ORNL/CDIAC-74.

Joyce, T., and C. Corry, eds., C. Corry, A. Dessier, A. Dickson, T. Joyce, M. Kenny, R. Key, D. Legler, R. Millard, R. Onken, P. Saunders, M. Stalcup (1994) Requirements for WOCE Hydrographic Programme Data Reporting, WHPO Pub. 90-1 Rev. 2, May 1994 Woods Hole, Mass., USA.

Murray, C.N., J.P. Riley, and T.R.S. Wilson (1968) The solubility of oxygen in Winkler reagents used for determination of dissolved oxygen, Deep-Sea Res., 15, 237-238.

Stramma, L., G. C. Johnson, J. Sprintall, V. Mohrholz (2008) Expanding Oxygen-Minimum Zones in the Tropical Oceans, Science, 320, 655-668.

3.4 Nutrients

13 July 2009

(1) Personnel

MR0901 cruise

Michio AOYAMA (Meteorological Research Institute / Japan Meteorological Agency, Principal Investigator)

LEG 1

Ayumi TAKEUCHI (Department of Marine Science, Marine Works Japan Ltd.)
Shinichiro YOKOGAWA (Department of Marine Science, Marine Works Japan Ltd.)
Kohei MIURA (Marine Works Japan Ltd.)

LEG 2

Junji MATSUSHITA (Department of Marine Science, Marine Works Japan Ltd.)
Ayumi TAKEUCHI (Department of Marine Science, Marine Works Japan Ltd.)
Kohei MIURA (Marine Works Japan Ltd.)

(2) Objectives

The objectives of nutrients analyses during the R/V Mirai MR0901 cruise, WOCE P21 revisited cruise in 2009, in the North Pacific are as follows;

- Describe the present status of nutrients concentration with excellent comparability.
- The determinants are nitrate, nitrite, phosphate and silicate.
- Study the temporal and spatial variation of nutrients concentration based on the previous high quality experiments data of WOCE previous P21 cruises in 1994, GOESECS, IGY and so on.
- Study of temporal and spatial variation of nitrate: phosphate ratio, so called Redfield ratio.
- Obtain more accurate estimation of total amount of nitrate, phosphate and silicate in the interested area.
- Provide more accurate nutrients data for physical oceanographers to use as tracers of water mass movement.

(3) Summary of nutrients analysis

We made 247 TRAACS800 runs for the samples at 257 stations in MR0901. The total amount of layers of the seawater sample reached up to 6574 for MR0901. We made duplicate measurement at all layers.

(4) Instrument and Method

(4.1) Analytical detail using TRAACS 800 systems (BRAN+LUEBBE)

The phosphate analysis is a modification of the procedure of Murphy and Riley (1962).
Molybdic acid is added to the seawater sample to form phosphomolybdic acid which is in turn reduced to phosphomolybdous acid using L-ascorbic acid as the reductant.

Nitrate + nitrite and nitrite are analyzed according to the modification method of Grasshoff (1970). The sample nitrate is reduced to nitrite in a cadmium tube inside of which is coated with metallic copper. The sample stream with its equivalent nitrite is treated with an acidic, sulfanilamide reagent and the nitrite forms nitrous acid which reacts with the sulfanilamide to produce a diazonium ion. N-1-Naphthylethylene-diamine added to the sample stream then couples with the diazonium ion to produce a red, azo dye. With reduction of the nitrate to nitrite, both nitrate and nitrite react and are measured; without reduction, only nitrite reacts. Thus, for the nitrite analysis, no reduction is performed and the alkaline buffer is not necessary. Nitrate is computed by difference.

The silicate method is analogous to that described for phosphate. The method used is essentially that of Grasshoff et al. (1983), wherein silicomolybdic acid is first formed from the silicate in the sample and added molybdic acid; then the silicomolybdic acid is reduced to silicomolybdous acid, or "molybdenum blue," using ascorbic acid as the reductant. The analytical methods of the nutrients during this cruise are same as the methods used in (Kawano et al. 2009). We, though, changed the rate of NED in channel 2 from WHT/WHT to RED/RED to increase stability of the analysis. We also made slight change in NED regent that we add Triton(R)X-100 as shown in (4.3) Nitrite Regents. The flow diagrams and reagents for each parameter are shown in Figures 3.4.1 to 3.4.4.

(4.2) Nitrate Reagents

Imidazole (buffer), 0.06 M (0.4 % w/v)

Dissolve 4 g imidazole, $C_3H_4N_2$, in ca. 1000 ml DIW; add 2 ml concentrated HCl. After mixing, 1 ml Triton(R)X-100 (50 % solution in ethanol) is added.

Sulfanilamide, 0.06 M (1 % w/v) in 1.2M HCl

Dissolve 10 g sulfanilamide, 4-$NH_2C_6H_4SO_3H$, in 900 ml of DIW, add 100 ml concentrated HCl. After mixing, 2 ml Triton(R)X-100 (50 %f solution in ethanol) is added.

N-1-Napthylethylene-diamine dihydrochloride, 0.004 M (0.1 %f w/v)

Dissolve 1 g NEDA, $C_{10}H_7NHCH_2CH_2NH_2 \cdot 2HCl$, in 1000 ml of DIW and add 10 ml concentrated HCl. After mixing, 1 ml Triton(R)X-100 (50 %f solution in ethanol) is added.

Stored in a dark bottle.

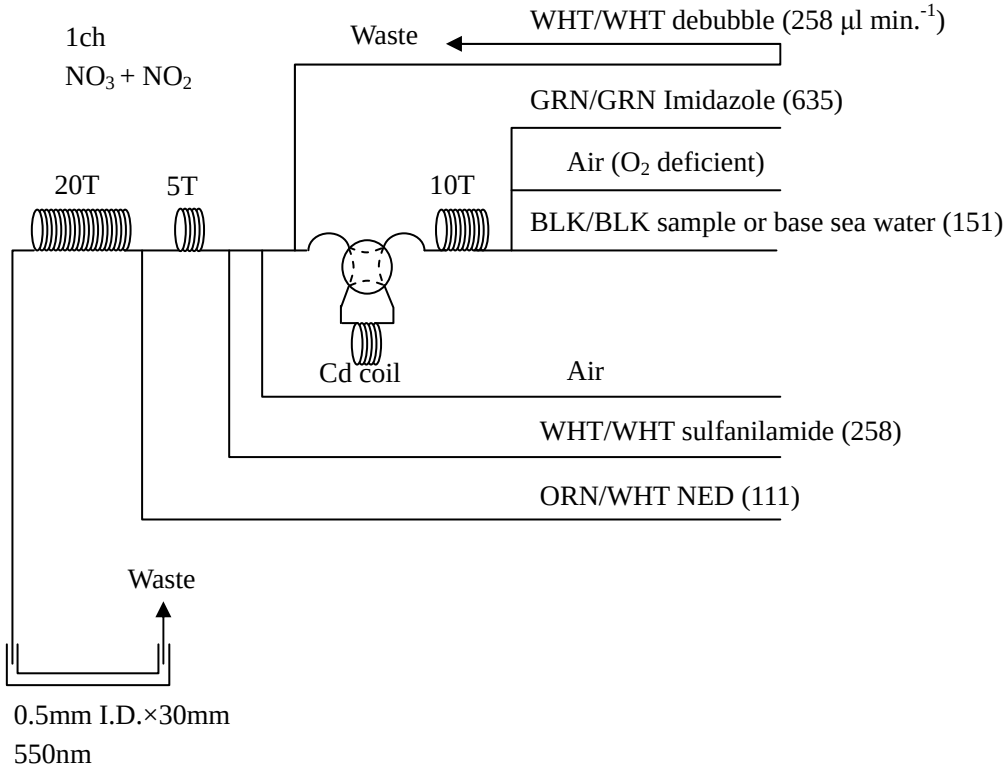

Figure3.4.1: 1ch. (NO_3+NO_2) Flow diagram.

(4.3) Nitrite Reagents

Sulfanilamide, 0.06 M (1 % w/v) in 1.2 M HCl

Dissolve 10g sulfanilamide, 4-$NH_2C_6H_4SO_3H$, in 900 ml of DIW, add 100 ml concentrated HCl. After mixing, 2 ml Triton(R)X-100 (50 % solution in ethanol) is added.

N-1-Napthylethylene-diamine dihydrochloride, 0.004 M (0.1 % w/v)

Dissolve 1 g NEDA, $C_{10}H_7NHCH_2CH_2NH_2 \cdot 2HCl$, in 1000 ml of DIW and add 10 ml concentrated HCl.

After mixing, 1 ml Triton(R)X-100 (50 %f solution in ethanol) is added.

Stored in a dark bottle.

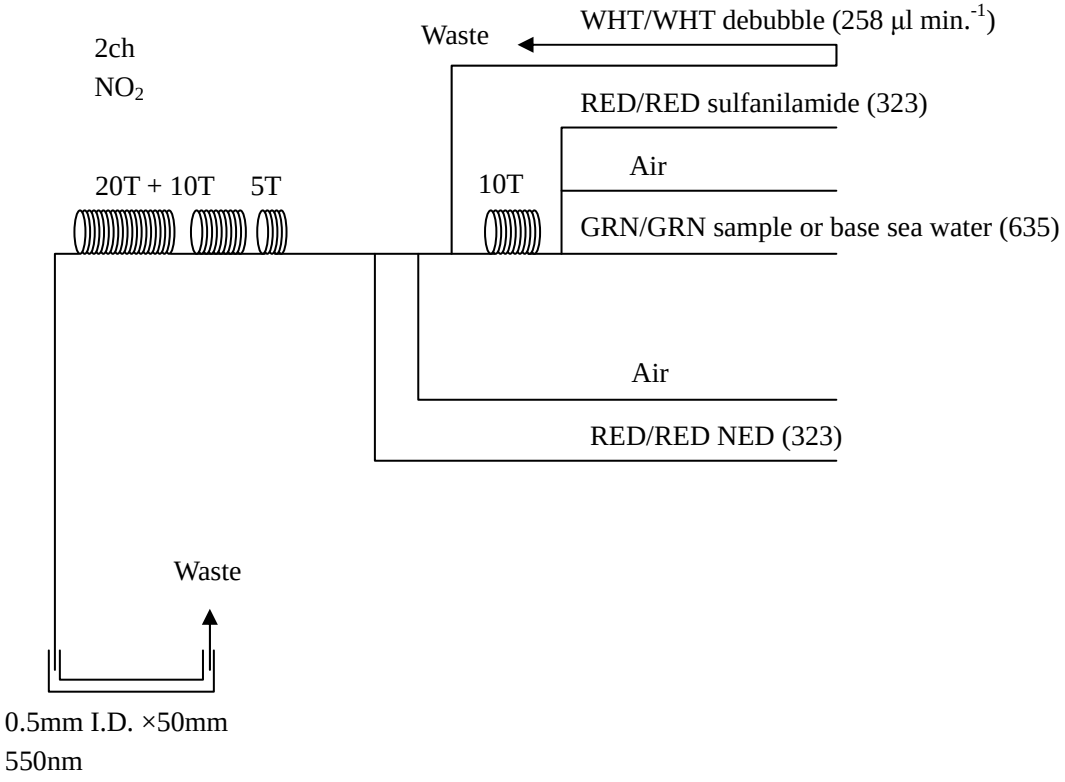

Figure3.4.2: 2ch. (NO_2) Flow diagram.

(4.4) Silicate Reagents

Molybdic acid, 0.06 M (2 % w/v)

Dissolve 15 g Disodium Molybdate(VI) Dihydrate, $Na_2M_oO_4 \cdot 2H_2O$, in 980 ml DIW, add 8 ml concentrated H_2SO_4. After mixing, 20 ml sodium dodecyl sulphate (15 % solution in water) is added.

Oxalic acid, 0.6 M (5 % w/v)

Dissolve 50g Oxalic Acid Anhydrous, HOOC: COOH, in 950 ml of DIW.

Ascorbic acid, 0.01M (3 % w/v)

Dissolve 2.5g L (+)-Ascorbic Acid, $C_6H_8O_6$, in 100 ml of DIW. Stored in a dark bottle and freshly repared before every measurement.

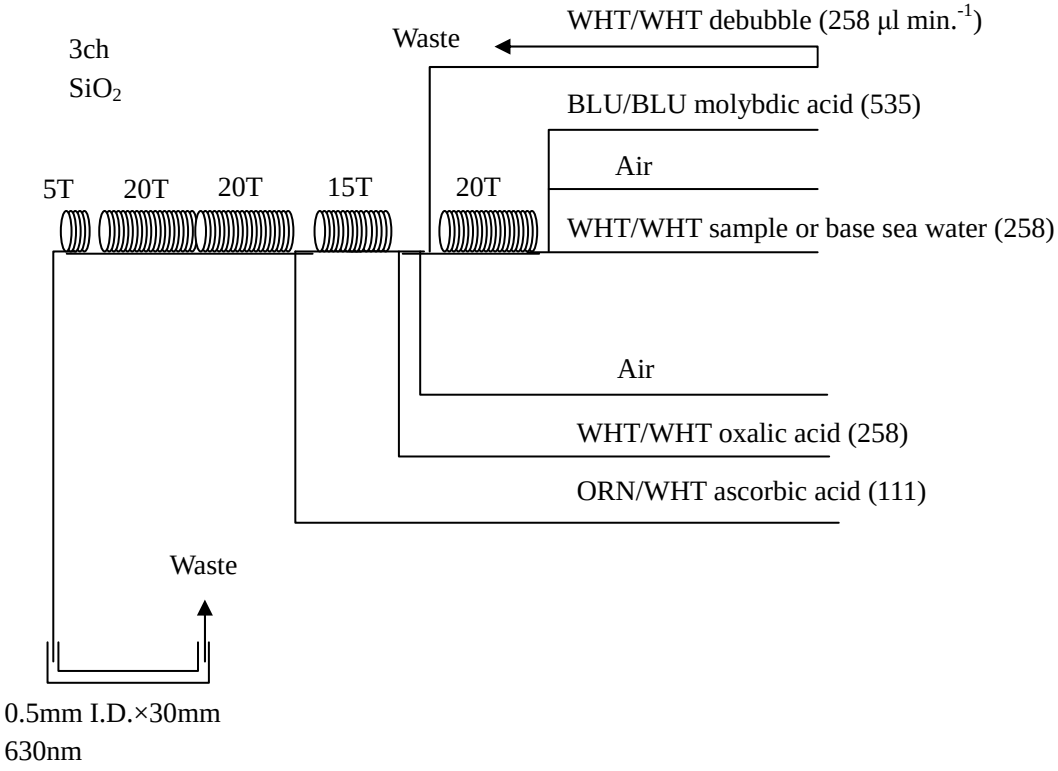

Figure3.4.3: 3ch. (SiO_2) Flow diagram.

(4.5) Phosphate Reagents

Stock molybdate solution, 0.03M (0.8 % w/v)

Dissolve 8 g Disodium Molybdate(VI) Dihydrate, $Na_2M_oO_4 \cdot 2H_2O$, and 0.17 g Antimony Potassium Tartrate, $C_8H_4K_2O_{12}Sb_2 \cdot 3H_2O$, in 950 ml of DIW and add 50 ml concentrated H_2SO_4.

Mixed Reagent

Dissolve 0.8 g L (+)-Ascorbic Acid, $C_6H_8O_6$, in 100 ml of stock molybdate solution. After mixing, 2 ml sodium dodecyl sulphate (15 % solution in water) is added. Stored in a dark bottle and freshly prepared before every measurement.

Reagent for sample dilution

Dissolve Sodium Hydrate, NaCl, 10 g in ca. 950 ml of DIW, add 50 ml Acetone and 4 ml concentrated H_2SO_4. After mixing, 5 ml sodium dodecyl sulphate (15 % solution in water) is added.

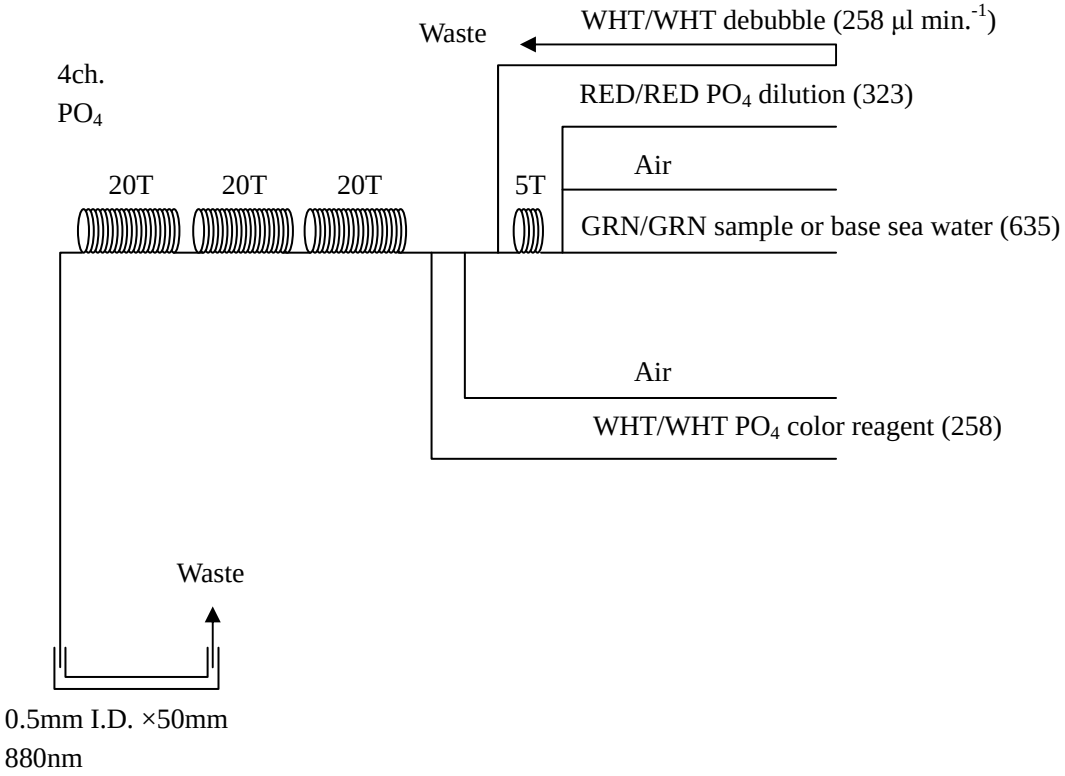

Figure3.4.4: 4ch. (PO_4) Flow diagram.

(4.6) Sampling procedures

Sampling of nutrients followed that oxygen, trace gases and salinity. Samples were drawn into two of virgin 10 ml polyacrylates vials without sample drawing tubes. These were rinsed three times before filling and vials were capped immediately after the drawing. The vials are put into water bath adjusted to ambient temperature, 25 ± 1deg. C, in 10 to 20 minutes before use to stabilize the temperature of samples in MR0901.

No transfer was made and the vials were set an auto sampler tray directly. Samples were analyzed after collection basically within 17 hours in MR0901.

(4.7) Data processing

Raw data from TRAACS800 were treated as follows;

- Check baseline shift.
- Check the shape of each peak and positions of peak values taken, and then change the positions of peak values taken if necessary.
- Carry-over correction and baseline drift correction were applied to peak heights of each samples followed by sensitivity correction.
- Baseline correction and sensitivity correction were done basically using liner regression.
- Load pressure and salinity from CTD data to calculate density of seawater.
- Calibration curves to get nutrients concentration were assumed second order equations.

(5) Nutrients standards

(5.1) Volumetric Laboratory Ware of in-house standards

All volumetric glass ware and polymethylpentene (PMP) ware used were gravimetrically calibrated. Plastic volumetric flasks were gravimetrically calibrated at the temperature of use within 0 to 4 K.

Volumetric flasks

Volumetric flasks of Class quality (Class A) are used because their nominal tolerances are 0.05 % or less over the size ranges likely to be used in this work. Class A flasks are made of borosilicate glass, and the standard solutions were transferred to plastic bottles as quickly as possible after they are made up to volume and well mixed in order to prevent excessive dissolution of silicate from the glass. High quality plastic (polymethylpentene, PMP, or polypropylene) volumetric flasks were gravimetrically calibrated and used only within 0 to 4 K of the calibration temperature.

The computation of volume contained by glass flasks at various temperatures other than the calibration temperatures were done by using the coefficient of linear expansion of borosilicate crown glass.

Because of their larger temperature coefficients of cubical expansion and lack of tables constructed for these materials, the plastic volumetric flasks were gravimetrically calibrated over the temperature range of intended use and used at the temperature of calibration within 0 to 4 K. The weights obtained in the calibration weightings were corrected for the density of water and air buoyancy.

Pipettes and pipettors

All pipettes have nominal calibration tolerances of 0.1 % or better. These were gravimetrically calibrated in order to verify and improve upon this nominal tolerance.

(5.2) Reagents, general considerations

Specifications

For nitrate standard, “potassium nitrate 99.995 suprapur” provided by Merck, CAS No. : 7757-91-1, was used.

For phosphate standard, “potassium dihydrogen phosphate anhydrous 99.995 suprapur” provided by Merck, CAS No. : 7778-77-0, was used.

For nitrite standard, “sodium nitrate” provided by Wako, CAS No. : 7632-00-0, was used. And assay of nitrite was determined according JIS K8019 and assays of nitrite salts were 98.04 %. We use that value to adjust the weights taken.

For the silicate standard, we use “Silicon standard solution SiO_2 in NaOH 0.5 mol/l CertiPUR” provided by Merck, CAS No. : 1310-73-2, of which lot number is HC751838 is used. The silicate concentration is certified by NIST-SRM3150 with the uncertainty of 0.5 %.

Ultra pure water

Ultra pure water (MilliQ water) freshly drawn was used for preparation of reagents, higher concentration standards and for measurement of reagent and system blanks.

Low-Nutrient Seawater (LNSW)

Surface water having low nutrient concentration was taken and filtered using 0.45 μm pore size membrane filter. This water is stored in 20 liter cubitainer with paper box. The concentrations of nutrient of this water were measured carefully in Jul 2008.

(5.3) Concentrations of nutrients for A, B and C standards

Concentrations of nutrients for A, B and C standards are set as shown in Table 3.4.1. The C standard is prepared according recipes as shown in Table 3.4.2. All volumetric laboratory tools were calibrated prior the cruise as stated in chapter (i). Then the actual concentration of nutrients in each fresh standard was calculated based on the ambient, solution temperature and determined factors of volumetric lab. wares.

The calibration curves for each run were obtained using 6 levels, C-1, C-2, C-3, C-4, C-5 and C-6. For the 10 stations from station 233 to station 245, we used only five levels, from C-1 to C-5 because silicate concentration of C-6 for these stations might be higher rather than target concentration. For the 19 runs, we used only five levels because nutrients concentration of one of the RMs was outliter.

Table 3.4.1 Nominal concentrations of nutrients for A, B and C standards.

	A	B	C-1	C-2	C-3	C-4	C-5	C-6
NO_3(μM)	45000	900	AS	BJ	AX	BE	AZ	55
NO_2(μM)	4000	20	AS	BJ	AX	BE	AZ	1.2
SiO_2(μM)	36000	2880	AS	BJ	AX	BE	AZ	170
PO_4(μM)	3000	60	AS	BJ	AX	BE	AZ	3.6

Table 3.4.2 Working calibration standard recipes.

C Std.	B-1 Std.	B-2 Std.
C-6	30 ml	30 ml

B-1 Std.: Mixture of nitrate, silicate and phosphate

B-2 Std.: Nitrite

(5.4) Renewal of in-house standard solutions.

In-house standard solutions as stated in (iii) were renewed as shown in Table 3.4.3(a) to (c).

Table 3.4.3(a) Timing of renewal of in-house standards.

NO_3, NO_2, SiO_2, PO_4	Renewal
A-1 Std. (NO_3)	maximum 1 month
A-2 Std. (NO_2)	maximum 1 month
A-3 Std. (SiO_2)	commercial prepared solution
A-4 Std. (PO_4)	maximum 1 month
B-1 Std. (mixture of NO_3, SiO_2, PO_4)	8 days
B-2 Std. (NO_2)	8 days

Table 3.4.3(b) Timing of renewal of in-house standards.

C Std.	Renewal
C-6 Std. (mixture of B-1 and B-2 Std.)	24 hours

Table 3.4.3(c) Timing of renewal of in-house standards.

Reduction estimation	Renewal
D-1 Std. (7200μM NO_3)	when A-1 Std. renewed
43μM NO_3	when C Std. renewed
47μM NO_2	when C Std. renewed

(6) Reference material of nutrients in seawater

To get the more accurate and high quality nutrients data to achieve the objectives stated above, huge numbers of the bottles of the reference material of nutrients in seawater (hereafter RMNS) are prepared (Aoyama et al., 2006, 2007, 2008). In the previous world wide expeditions, such as WOCE cruises, the higher reproducibility and precision of nutrients measurements were required (Joyce and Corry, 1994). Since no standards were available for the measurement of nutrients in seawater at that time, the requirements were described in term of reproducibility. The required reproducibility was 1 %, 1 to 2 %, 1 to 3 % for nitrate, phosphate and silicate, respectively. Although nutrient data from the WOCE one-time survey was of unprecedented quality and coverage due to much care in sampling and measurements, the differences of nutrients concentration at crossover points are still found among the expeditions (Aoyama and Joyce, 1996, Mordy et al., 2000, Gouretski and Jancke, 2001). For instance, the mean offset of nitrate concentration at deep waters was 0.5 μmol kg^{-1} for 345 crossovers at world oceans, though the maximum was 1.7 μmol kg^{-1} (Gouretski and Jancke, 2001). At the 31 crossover points in the Pacific WHP one-time lines, the WOCE standard of reproducibility for nitrate of 1 % was fulfilled at about half of the crossover points and the maximum difference was 7 % at deeper layers below 1.6 deg. C in potential temperature (Aoyama and Joyce, 1996).

(6.1) RMNSs for this cruise

RMNS lots AS, BJ, AX, BE and AZ, which cover full range of nutrients concentrations in the western North Pacific Ocean are prepared. 160 sets of AS, BJ, AX, BE and AZ are prepared.

Three hundred ten bottles of RMNS lot BI and 200 bottles of RMNS lot AV are prepared for MR0901. Lot BI was used at 99 stations from 14 to 120 and lot AV was used at 158 stations from 121 to 288, respectively. These RMNS assignment were completely done based on random number. The RMNS bottles were stored at a room in the ship, REAGENT STORE, where the temperature was maintained around 24 deg. C.

(6.2) Assigned concentration for RMNSs

We assigned nutrients concentrations for RMNS lots AS, BJ, AX, BE, AZ, BI and AV as shown in Table 3.4.4.

Table 3.4.4 Assigned concentration of RMNSs.

unit: μmol kg^{-1}

	Nitrate	Phosphate	Silicate	Nitrite
AS*	0.11	0.077	1.58	0.02
BJ*	7.74	0.628	31.04	0.02
AX**	21.42	1.619	58.06	0.35
BE*	36.70	2.662	99.20	0.03
AZ*	42.36	3.017	133.93	0.03
BI*	41.36	2.576	147.51	0.02
AV**	33.36	2.516	154.14	0.10

* The value in the Table is result of measurement on 6 January. 2009.

** The value in the Table is result of measurement on 7 October. 2007.

(6.3) The homogeneity of RMNSs

The homogeneity of lot AV and AZ used in MR0901 cruise and analytical precisions are shown in Table 3.4.5. These are for the assessment of the magnitude of homogeneity of the RMNS bottles those are used during the cruise. As shown in Table 3.4.5 homogeneity of RMNS lot AV and AZ for nitrate, phosphate and silicate are the same magnitude of analytical precision derived from fresh raw seawater in January 2009.

Table 3.4.5 Homogeneity of lot AV and AZ derived from simultaneous 297 samples measurements and analytical precision onboard R/V Mirai in MR0901.

	Nitrate CV %	Phosphate CV %	Silicate CV %
AV	**0.09**	**0.12**	**0.08**
AZ	**0.13**	**0.15**	**0.08**
Precision	**0.08**	**0.10**	**0.07**

AV: N=297 AZ: N=244

We can see history of homogeneity of several lots of RMNS as shown in Table 3.4.6. The homogeneity of phosphate in old lots such as lot AH and K were relatively larger than those of recent lots, BI and BC. The homogeneities of nitrate and silicate, we also see progress from lot K to recent lots.

Table 3.4.6 History of homogeneity of lot BI and previous lots derived from simultaneous 30 samples measurements and analytical precision onboard R/V Mirai in January 2009.

	Nitrate CV %	Phosphate CV %	Silicate CV %
BI	**0.19**	**0.21**	**0.08**
BC*	**0.22**	**0.32**	**0.19**
AH*	**0.39**	**0.83**	**0.13**
K*	**0.3)**	**1.0**	**0.2**
Precision	**0.18**	**0.14**	**0.07**

* Table 3.4.5 in WHP P01, P14 REVISIT DATA BOOK (Kawano et al. 2009)

(6.4) Comparability of RMNSs during the periods from 2003 to 2009

Cruise-to-cruise comparability has examined based on the results of the previous results of RMNSs measurements obtained among cruises, and RMNS international comparison experiments in 2003 and 2009. The uncertainties for each value were obtained similar method described in 7.1 in this chapter at the measurement before each cruise and inter-comparison study, shown as precruise and intercomparison, and mean of uncertainties during each cruise, only shown cruise code, respectively. As shown in Table 3.4.7, the nutrients concentrations of RMNSs were in good agreement among the measurements during the period from 2003 to 2009. For the silicate measurements, we show lot numbers and chemical company names of each cruise/measurement in the footnote. As shown in Table 3.4.7, there shows less comparability among the measurements due to less comparability among the standard solutions provided by chemical companies in the silicate measurements.

Table 3.4.7 (a) Comparability for nitrate.

unit: µmol kg^{-1}

Cruise / Lab.	RM Lots													
	AH	unc.	AZ	unc.	BA	unc.	AX	unc.	AV	unc.	BC	unc.	BE	unc.
			Nitrate											
2003														
2003intercomp_repeorted	35.23	0.06					21.39							
MR03-K04 Leg1	35.25													
MR03-K04 Leg2	35.37													
MR03-K04 Leg4	35.37													
MR03-K04 Leg5	35.34													
2005														
MR05-02			42.30		0.07	0.02	21.45	0.07	33.35	0.06	40.70	0.06		
MR05-05_1 precruise	35.65	0.05	42.30	0.10	0.07	0.00	21.41	0.01	33.41	0.02	40.76	0.03		
MR05-05_1			42.33		0.07	0.01	21.43	0.05	33.36	0.05	40.73	0.85		
MR05-05_2 precruise			42.33		0.08	0.00	21.39	0.02	33.36	0.05	40.72	0.03		
MR05-05_2			42.34		0.07	0.01	21.44	0.05	33.36	0.05	40.73	0.06		
MR05-05_3 precruise			42.35		0.06	0.00	21.49	0.01	33.39	0.01	40.79	0.01		
MR05-05_3			42.36		0.07	0.01	21.44	0.04	33.37	0.05	40.75	0.05		
2006														
2006intercomp			42.24	0.04	0.04	0.00	21.40	0.02	33.32	0.03	40.63	0.04		
2003intercomp_revisit	35.40	0.03												
2007														
MR07-04_1 precruise	35.74	0.03			0.07	0.00	21.59	0.02	33.49	0.03	40.83	0.03		
MR07-04_2 precruise	35.80	0.01			0.08	0.00	21.60	0.01	33.47	0.01	40.92	0.02		

Cruise / Lab.	RM Lots													
	AH	unc.	AZ	unc.	BA	unc.	AX	unc.	AV	unc.	BC	unc.	BE	unc.
							Nitrate							
MR07-04					0.08	0.01	21.41	0.06	33.38	0.05	40.77	0.05		
MR07-06_1 precruise	35.61	0.02			0.07	0.00	21.44	0.01	33.43	0.02	40.79	0.02		
MR07-06_2 precruise	35.61	0.04			0.06	0.00	21.43	0.02	33.54	0.04	40.79	0.05		
MR07-06_1					0.08	0.01	21.44	0.03	33.41	0.05	40.81	0.04		
MR07-06_2					0.09	0.01	21.44	0.03	33.39	0.06	40.81	0.04		
2008														
2008intercomp_report					0.08	0.00	21.44	0.02						
2006intercomp_revisit			42.27	0.04	0.07	0.00	21.47	0.02	33.34	0.03				
2003intercomp_revisit	35.35	0.04												
2009														
MR09-01_0 precruise			42.36	0.02	0.07	0.00	21.43	0.01	33.42	0.02	40.81	0.02	36.70	0.02
MR09-01_1			42.42	0.06	0.11	0.01	21.51	0.04	33.53	0.04	40.82	0.11	36.74	0.04
MR09-01_2			42.43	0.05			21.54	0.03	33.53	0.03			36.74	0.03
INSS stability test_1	35.76	0.22			0.08	0.01	21.49	0.02	33.45	0.03				

Table 3.4.7 (b) Comparability for nitrate.

unit: µmol kg^{-1}

Cruise / Lab.	RM Lots													
	AH	unc.	AZ	unc.	BA	unc.	AX	unc.	AV	unc.	BC	unc.	BE	unc.
			Phosphate											
2003														
2003intercomp	2.141	0.001												
MR03-K04 Leg1	2.110													
MR03-K04 Leg2	2.110													
MR03-K04 Leg4	2.110													
MR03-K04 Leg5	2.110													
2005														
MR05-02			3.010		0.061	0.010	1.614	0.008	2.515	0.008	2.778	0.010		
MR05-05_1 precruise	2.148	0.006	3.020	0.010	0.045	0.000	1.620	0.001	2.517	0.002	2.781	0.002		
MR05-05_1			3.016		0.063	0.007	1.615	0.006	2.515	0.007	2.778	0.033		
MR05-05_2 precruise			3.015		0.066	0.000	1.608	0.001	2.510	0.001	2.784	0.002		
MR05-05_2			3.018		0.064	0.005	1.614	0.004	2.515	0.005	2.782	0.006		
MR05-05_3 precruise			3.020		0.060	0.000	1.620	0.001	2.517	0.002	2.788	0.002		
MR05-05_3			3.016		0.061	0.004	1.618	0.005	2.515	0.004	2.779	0.008		
2006														
2006intercomp			3.018	0.002	0.071	0.000	1.623	0.001	2.515	0.001	2.791	0.001		
2003intercomp_revisit	2.141	0.001												
2007														
MR07-04_1 precruise	2.140	0.002			0.062	0.000	1.620	0.001	2.512	0.002	2.782	0.002		
MR07-04_2 precruise	2.146	0.002			0.056	0.000	1.620	0.001	2.517	0.002	2.788	0.002		

Cruise / Lab.	RM Lots													
	AH	unc.	AZ	unc.	BA	unc.	AX	unc.	AV	unc.	BC	unc.	BE	unc.
							Phosphate							
MR07-04_2 precruise	2.146	0.002			0.056	0.000	1.620	0.001	2.517	0.002	2.788	0.002		
MR07-04					0.066	0.004	1.617	0.005	2.513	0.004	2.781	0.007		
MR07-06_1 precruise	2.144	0.001			0.066	0.000	1.617	0.001	2.517	0.001	2.790	0.001		
MR07-06_2 precruise	2.146	0.002			0.067	0.000	1.620	0.001	2.517	0.002	2.789	0.002		
MR07-06_1					0.064	0.004	1.620	0.003	2.515	0.003	2.783	0.005		
MR07-06_2					0.066	0.004	1.619	0.005	2.515	0.003	2.785	0.006		
2008														
2008intercomp_report					0.068	0.000	1.615	0.005						
2006intercomp_revisit			3.014	0.008	0.065	0.000	1.627	0.005	2.513	0.007				
2003intercomp_revisit	2.131	0.006												
2009														
MR09-01_0 precruise			3.017	0.001	0.074	0.000	1.619	0.001	2.520	0.001	2.790	0.001	2.662	0.001
MR09-01_1			3.019	0.005	0.072	0.002	1.623	0.004	2.528	0.003	2.783	0.004	2.668	0.005
MR09-01_2			3.018	0.004			1.625	0.003	2.527	0.003			2.668	0.003
INSS stability test_1	2.134	0.008			0.069	0.001	1.606	0.001	2.512	0.003				

Table 3.4.7 (C) Comparability for phosphate.

unit: μmol kg^{-1}

Cruise	RM Lots													
	AH	unc.	AZ	unc.	BA	unc.	AX	unc.	AV	unc.	BC	unc.	BE	unc.
			Silicate											
2003														
2003intercomp *	130.51	0.20												
MR03-K04 Leg1 **	132.01													
MR03-K04 Leg2 **	132.26													
MR03-K04 Leg4 **	132.28													
MR03-K04 Leg5 **	132.19													
2005														
MR05-02 #			133.69		1.61	0.05	58.04	0.11	153.92	0.19	155.93	0.19		
MR05-05_1 precruise ##	132.49	0.13	133.77	0.02	1.51	0.00	58.06	0.03	153.97	0.09	15.65	0.09		
MR05-05_1 ##			133.79		1.59	0.07	58.01	0.12	154.01	0.26	156.08	0.36		
MR05-05_2 precruise ##			133.78		1.58	0.00	57.97	0.04	154.07	0.09	156.21	0.10		
MR05-05_2 ##			133.88		1.59	0.06	58.00	0.09	154.05	0.16	156.14	0.15		
MR05-05_3 precruise ##			134.02		1.57	0.00	58.05	0.05	154.07	0.14	156.11	0.14		
MR05-05_3 ##			133.79		1.60	0.05	57.98	0.09	153.98	0.18	156.08	0.13		
2006														
2006intercomp $			133.83	0.07	1.64	0.00	58.20	0.03	154.16	0.08	156.31	0.08		
2003intercomp_revisit $	132.55	0.07												
2007														
MR07-04_1 precruise $$	133.38	0.06			1.61	0.00	58.46	0.03	154.82	0.07	156.98	0.07		
MR07-04_2 precruise $$	133.15	0.12			1.69	0.00	58.44	0.05	154.87	0.14	156.86	0.14		

Cruise	RM Lots													
	AH	unc.	AZ	unc.	BA	unc.	AX	unc.	AV	unc.	BC	unc.	BE	unc.
							Silicate							
MR07-04 $$					1.62	0.07	58.11	0.11	154.45	0.21	156.62	0.48		
MR07-06_1 precruise $$	133.02	0.09			1.64	0.00	58.50	0.04	155.06	0.11	156.33	0.11		
MR07-06_2 precruise $$	132.70	0.07			1.56	0.00	58.25	0.03	154.39	0.08	156.57	0.08		
MR07-06_1 $$					1.61	0.04	58.13	0.08	154.48	0.13	156.64	0.08		
MR07-06_2 $$					1.58	0.07	58.04	0.10	154.38	0.16	156.61	0.13		
2008														
2008intercomp ¥					1.64	0.00	58.17	0.05						
2006intercomp_re ¥			134.11	0.11	1.65	0.00	58.26	0.05	154.36	0.12				
2003intercomp_re ¥	132.11	0.11												
2009														
MR09-01_0 precruise ¥			133.93	0.04	1.57	0.00	58.06	0.02	154.23	0.05	156.16	0.05	99.20	0.03
MR09-01_1 ¥			133.97	0.11	1.34	0.11	58.15	0.08	154.48	0.09	155.89	0.13	99.24	0.08
MR09-01_2 ¥			133.96	0.11			58.19	0.08	154.42	0.12			99.23	0.08
INSS stability test_1 ¥¥	132.40	0.35			1.69	0.02	58.18	0.02	154.43	0.09				

List of lot numbers: *: Kanto 306F9235; **: Kanto 402F9041; #: Kanto 507F9205; ##: Kanto 609F9157; $: Merck OC551722; $$: Merck HC623465; ¥: Merck HC751838; ¥¥: HC814662

(7) Quality control

(7.1) Precision of nutrients analyses during the cruise

Precision of nutrients analyses during the cruise was evaluated based on the 9 to 11 measurements, which are measured every 10 to 13 samples, during a run at the concentration of C-6 std. There is exception for the number of the measurements that are used to evaluate analytical precision of silicate at 10 runs from stations 233 to 245 where we evaluate analytical precision based on 6 to 8 measurements. Summary of precisions are shown as shown in Table 3.4.8 and Figures 3.4.5 to 3.4.7, the precisions for each parameter are generally good considering the analytical precisions estimated from the simultaneous analyses of 14 samples in January 2009 as shown in Table 3.4.6. Analytical precisions previously evaluated were 0.18 % for nitrate, 0.14 % for phosphate and 0.08 % for silicate, respectively. During this cruise, analytical precisions were 0.08 % for nitrate, 0.10 % for phosphate and 0.07 % for silicate in terms of median of precision, respectively. Then we can conclude that the analytical precisions for nitrate, phosphate and silicate were maintained throughout this cruise. The time series of precision are shown in Figures 3.4.5 to 3.4.7.

Table 3.4.8 Summary of precision based on the replicate analyses.

	Nitrate CV %	Phosphate CV %	Silicate CV %
Median	**0.08**	**0.10**	**0.07**
Mean	**0.08**	**0.10**	**0.08**
Maximum	**0.18**	**0.17**	**0.14**
Minimum	**0.02**	**0.03**	**0.02**
N	**279**	**279**	**277**

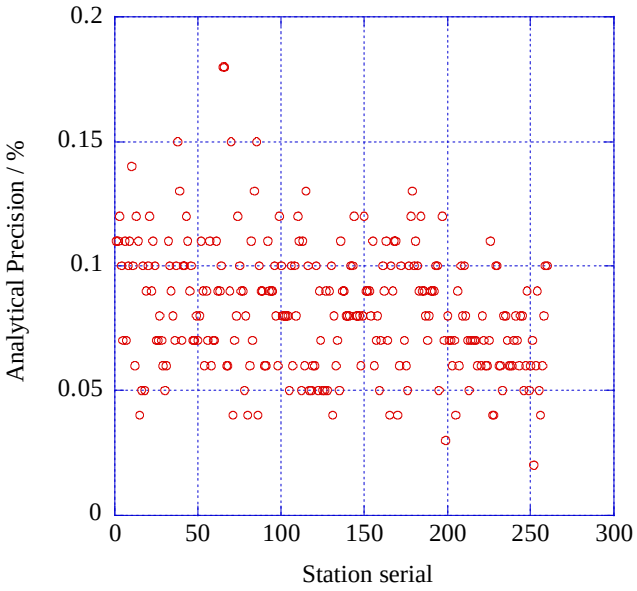

Figure 3.4.5 Time series of precision of nitrate for MR0901.

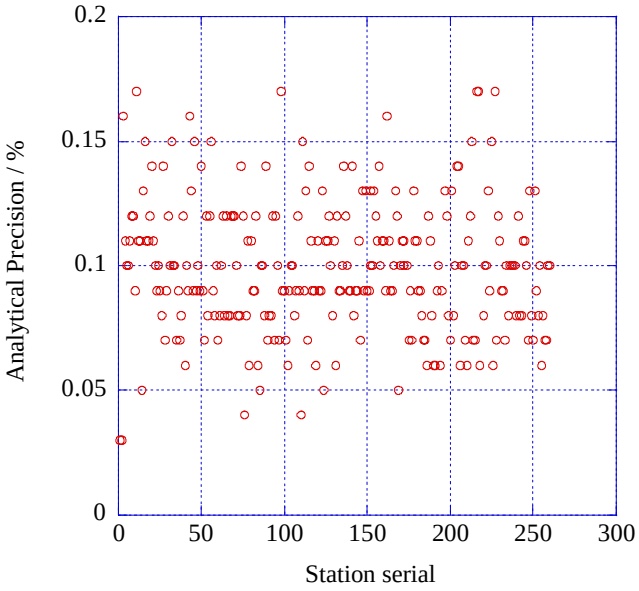

Figure 3.4.6 Time series of precision of phosphate for MR0901.

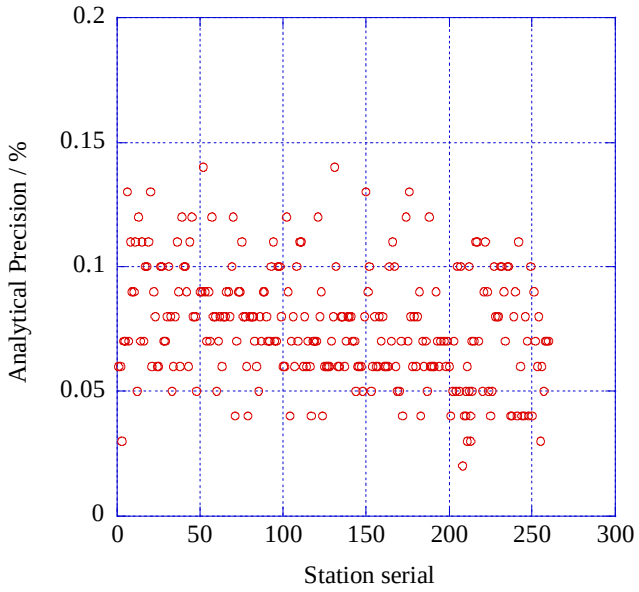

Figure 3.4.7 Time series of precision of silicate for MR0901.

(7.2) Carry over

We can also summarize the magnitudes of carry over throughout the cruise. These are small enough within acceptable levels as shown in Table 3.4.10.

Table 3.4.10 Summary of carry over through out MR0901 cruise.

	Nitrate CV %	Phosphate CV %	Silicate CV %
Median	**0.21**	**0.24**	**0.20**
Mean	**0.22**	**0.23**	**0.20**
Maximum	**0.40**	**0.53**	**0.33**
Minimum	**0.03**	**0.01**	**0.03**
N	**250**	**250**	**248**

(7.3) Dilution for shallower samples by lot AZ.

We decided to dilute 107 samples from shallower layers as shown Table 3.4.11 due to higher nitrite concentration which exceed 2 μmol kg^{-1}. We add 5 ml of lot AZ to 0.5 ml of sample. Therefore, uncertainties of the nutrients concentration of diluted samples were larger compared with non-diluted samples.

Table 3.4.11 Summary of diluted samples.

Station	Pressure (dbar)
14	**10, 50, 100, 150, 200, 250, 300, 400**
15	**10, 50, 100, 150, 200, 250, 330, 430**
16	**150, 200, 250, 280, 370**
17	**10, 50, 100, 150, 200, 250, 300, 400**
18	**100, 150, 200, 250**
19	**100, 150, 200, 250**
21	**200, 250, 300**
22	**200, 250**
23	**200, 250, 280**
24	**250, 300**
25	**100, 150, 200, 250, 330**
26	**100, 150, 200, 250, 280**
27	**250**
29	**10, 50, 100, 150, 200, 250, 280**
30	**10, 50, 100, 150, 200, 250, 300**
31	**10, 50, 100, 150, 200, 250, 330**
32	**150, 200, 250, 280**
35	**280**

Station	Pressure (dbar)
40	**150, 200, 250, 300**
41	**250, 280**
43	**250, 300**
46	**200, 250**
51	**100**
67	**100**
68	**100**
143	**150**
144	**150**

(7.4) Possible concentration change of lot AV

We found that nutrients concentrations of RM-AV were about 0.5% higher rather than those we assigned before cruise as shown in Table 3.4.4. The reasons of this increase are not clear yet, it might occur depend on the storage history of this RM-AV.

(8) Problems/improvements occurred and solutions.

No problem occurred during this cruise.

References

Aminot, A. and Kerouel, R. 1991. Autoclaved seawater as a reference material for the determination of nitrate and phosphate in seawater. Anal. Chim. Acta, 248: 277-283.

Aminot, A. and Kirkwood, D.S. 1995. Report on the results of the fifth ICES intercomparison exercise for nutrients in sea water, ICES coop. Res. Rep. Ser., 213.

Aminot, A. and Kerouel, R. 1995. Reference material for nutrients in seawater: stability of nitrate, nitrite, ammonia and phosphate in autoclaved samples. Mar. Chem., 49: 221-232.

Aoyama M., and Joyce T.M. 1996, WHP property comparisons from crossing lines in North Pacific. In Abstracts, 1996 WOCE Pacific Workshop, Newport Beach, California.

Aoyama, M., 2006: 2003 Intercomparison Exercise for Reference Material for Nutrients in Seawater in a Seawater Matrix, Technical Reports of the Meteorological Research Institute No.50, 91pp, Tsukuba, Japan.

Aoyama, M., Susan B., Minhan, D., Hideshi, D., Louis, I. G., Kasai, H., Roger, K., Nurit, K., Doug, M., Murata, A., Nagai, N., Ogawa, H., Ota, H., Saito, H., Saito, K., Shimizu, T., Takano, H., Tsuda, A., Yokouchi, K., and Agnes, Y. 2007. Recent Comparability of Oceanographic Nutrients Data: Results of a 2003 Intercomparison Exercise Using Reference Materials. Analytical Sciences, 23: 1151-1154.

Aoyama M., J. Barwell-Clarke, S. Becker, M. Blum, Braga E. S., S. C. Coverly,E. Czobik, I. Dahllof, M. H. Dai, G. O. Donnell, C. Engelke, G. C. Gong, Gi-Hoon Hong, D. J. Hydes, M. M. Jin, H. Kasai, R. Kerouel, Y. Kiyomono, M. Knockaert, N. Kress, K. A. Krogslund, M. Kumagai, S. Leterme, Yarong Li, S. Masuda, T. Miyao, T. Moutin, A. Murata, N. Nagai, G.Nausch, M. K. Ngirchechol, A. Nybakk, H. Ogawa, J. van Ooijen, H. Ota, J. M. Pan, C. Payne, O. Pierre-Duplessix, M. Pujo-Pay, T. Raabe, K. Saito,K. Sato, C. Schmidt, M. Schuett, T. M. Shammon, J. Sun, T. Tanhua, L. White, E.M.S. Woodward, P. Worsfold, P. Yeats, T. Yoshimura, A.Youenou, J. Z. Zhang, 2008: 2006 Intercomparison Exercise for Reference Material for Nutrients in Seawater in a Seawater Matrix, Technical Reports of the Meteorological Research Institute No. 58, 104pp.

Gouretski, V.V. and Jancke, K. 2001. Systematic errors as the cause for an apparent deep water property variability: global analysis of the WOCE and historical hydrographic data・REVIEW ARTICLE, Progress In Oceanography, 48: Issue 4, 337-402.

Grasshoff, K., Ehrhardt, M., Kremling K. et al. 1983. Methods of seawater anylysis. 2nd rev. Weinheim: Verlag Chemie, Germany, West.

Joyce, T. and Corry, C. 1994. Requirements for WOCE hydrographic programmed data reporting. WHPO Publication, 90-1, Revision 2, WOCE Report No. 67/91.

Kawano, T., Uchida, H. and Doi, T. WHP P01, P14 REVISIT DATA BOOK, (Ryoin Co., Ltd., Yokohama, 2009).

Kirkwood, D.S. 1992. Stability of solutions of nutrient salts during storage. Mar. Chem., 38 : 151-164.

Kirkwood, D.S. Aminot, A. and Perttila, M. 1991. Report on the results of the ICES fourth intercomparison exercise for nutrients in sea water. ICES coop. Res. Rep. Ser., 174.

Mordy, C.W., Aoyama, M., Gordon, L.I., Johnson, G.C., Key, R.M., Ross, A.A., Jennings, J.C. and Wilson. J. 2000. Deep water comparison studies of the Pacific WOCE nutrient data set. Eos Trans-American Geophysical Union. 80 (supplement), OS43.

Murphy, J., and Riley, J.P. 1962. Analytica chim. Acta 27, 31-36.

Uchida, H. & Fukasawa, M. WHP P6, A10, I3/I4 REVISIT DATA BOOK Blue Earth Global Expedition 2003 1, 2, (Aiwa Printing Co., Ltd., Tokyo, 2005).

3.5. Chlorofluorocarbons

(1) Personnel

Ken'ichi Sasaki (JAMSTEC)
Katsunori Sagishima (MWJ)
Yuichi Sonoyama (MWJ)
Shoko Tatamisashi (MWJ)
Hideki Yamamoto (MWJ)

(2) Objectives

Chlorofluorocarbons (CFCs), solely man-made compounds, are chemically and biologically stable gases and have been accumulated in the atmosphere since 1930s. The atmospheric CFCs can slightly dissolve in sea surface water by air-sea gas exchange and the dissolved CFCs are spread into the ocean interior. Three chemical species of CFCs, CFC-11 (CCl_3F), CFC-12 (CCl_2F_2), and CFC-113 ($C_2Cl_3F_3$), can be used as transient chemical tracers for the ocean circulation on timescale of several decades. We measured concentrations of these compounds in seawater on board.

(3) Apparatus

Dissolved CFCs were measured by an electron capture detector (ECD) – gas chromatograph attached with a purging & trapping system.

Table 3-5-1 Instruments

Gas Chromatograph:	GC-14B (Shimadzu Ltd.)
Detector:	ECD-14 (Shimadzu Ltd)
Analytical Column:	
Pre-column:	Silica Plot capillary column [i.d.: 0.53mm, length: 8 m, film thickness: 0.25μm]
Main column:	Connected two capillary columns (Pola Bond-Q [i.d.: 0.53mm, length: 9 m, film thickness: 6.0μm] followed by Silica Plot [i. d.: 0.53mm, length: 14 m, film thickness: 0.25μm])
Purging & trapping:	Developed in JAMSTEC. Cold trap columns are 1/16" SUS tubing packed with Porapak T.

(4) Procedures

i. Sampling

Seawater sub-samples for CFC measurements were collected from 12 litter Niskin bottles to 250 ml glass bottles designed in JAMSTEC. The bottles were filled by pure nitrogen gas before sampling. Three times of the bottle volumes of seawater sample were overflowed. The bottles filled by seawater sample were kept in water bathes roughly controlled at sample temperature. The CFCs concentrations were determined as soon as possible after sampling (usually within 24 hours).

In order to confirm CFC concentrations of standard gases and their stabilities and also to check CFC saturation levels in sea surface water, CFC mixing ratios in background air were periodically analyzed. Air samples were continuously led into laboratory by 10 mm OD Dekaron® tubing. The end of the tubing was put on a head of the compass deck and another end was connected onto a macro air pump in the laboratory. The tubing was relayed by a T-type union which had a small stop cock. Air sample was collected from the flowing air into a 200ml glass cylinder attached on the cock.

ii. Analysis

The analytical system was modified from the original design of Bullister and Weiss (1988). Constant volume of sample water (50ml) was taken into a sample loop. The sample was send into stripping chamber and dissolved CFCs were de-gassed by N_2 gas purging for 8 minutes. The gas sample was dried by magnesium perchlorate desiccant and concentrated on a trap column cooled to -50 degree centigrade. Stripping efficiencies of CFCs were frequently confirmed by re-stripping of surface layer samples and more than 99.5 % of dissolved CFCs were extracted on the first purge. Following purging & trapping, the trap column was isolated and electrically heated to 140 degree centigrade. CFCs were desorbing by the heating, and lead into the pre-column. CFCs are roughly separated from other compounds on the pre-column and are sent onto main analytical column. And then the pre-column was switched to back flush line and cleaned by counter flow of pure nitrogen gas. CFCs sent into main column were separated further and detected by an electron capture detector (ECD). Nitrogen gases used in this system was filtered by N2 gas purifier (P300-1, VICI Mat/Sen Inc.) and gas purifier tube packed with Molecular Sieve 13X (MS-13X).

Table 3-5-2 Analytical conditions of dissolved CFCs in seawater.

Temperature	
Analytical Column:	95 deg-C
Detector (ECD):	240 deg-C
Trap column:	-50 deg-C (at adsorbing) & 140 deg-C (at desorbing)
Mass flow rate of nitrogen gas (99.99995%)	
Carrier gas:	15 ml/min
Detector make-up gas:	22 ml/min
Back flush gas:	20 ml/min
Sample purge gas:	130 ml/min
Standard gas (Japan Fine Products co. ltd.)	
Base gas:	Nitrogen
CFC-11:	300 ppt (v/v)
CFC-12:	160 ppt (v/v)
CFC-113:	30 ppt (v/v)

(5) Performance

The analytical precisions are estimated from replicate sample analyses. The precisions of CFCs measurements are calculated as ± 0.004 pmol/kg (n = 607 pairs), ± 0.003 pmol/kg (n = 608 pairs) and ± 0.005 pmol/kg (n = 390 pairs) for CFC-11, -12 and -113, respectively. Unknown compounds interfered determining CFC-113 in near surface water and data flag of “4” or “5” was given in case that correction of the chromatogram was impossible.

The standard gases used in this cruise will be calibrated with respect to SIO scale standard gases after the cruise, and then the data will be corrected.

(6) Preliminary Results

Concentrations of CFC-11 and -12 in sea surface water closed to equilibrium value with respect to the atmospheric CFC mixing ratios. Maximum concentrations of CFC-11 and -12 were found in several hundred meter depths. No CFC signals were detected in almost deep and bottom water samples except several regions.

Significant CFC-11 concentration was found in bottom water of 80-85°W, deep and bottom water of 140-175°W, and bottom water around 155°E. Especially, CFC concentrations in bottom water of 140-175 °W were so high (maximum concentration of CFC-11 was ~ 0.08 pmol kg^{-1}). These CFC signals indicate that the water masses contain younger components than the atmospheric CFC histories.

3.5.6 Reference

Bullister, J.L and Weiss R.F. 1988. Determination of CCl_3F and CCl_2F_2 in seawater and air. Deep Sea Research, 35, 839-853.

3.6. Carbon items

(1) Personnel

Akihiko Murata (JAMSTEC)
Minoru Kamata (MWJ)
Tomonori Watai (MWJ)
Yoshiko Ishikawa (MWJ)
Ayaka Hatsuyama (MWJ)
Yasuhiro Arii (MWJ)

(2) Objectives

Concentrations of CO_2 in the atmosphere are now increasing at a rate of 1.9 ppmv y^{-1} owing to human activities such as burning of fossil fuels, deforestation, and cement production. It is an urgent task to estimate as accurately as possible the absorption capacity of the oceans against the increased atmospheric CO_2, and to clarify the mechanism of the CO_2 absorption, because the magnitude of the anticipated global warming depends on the levels of CO_2 in the atmosphere, and because the ocean currently absorbs 1/3 of the 6 Gt of carbon emitted into the atmosphere each year by human activities.

In this cruise, we were aimed at quantifying how much anthropogenic CO_2 absorbed in the ocean are transported and redistributed in the South Pacific. For the purpose, we measured CO_2-system parameters such as dissolved inorganic carbon (C_T), total alkalinity (A_T) and pH.

(3) Apparatus

i. C_T

Measurements of C_T was made with two total CO_2 measuring systems (systems A and C; Nippon ANS, Inc.), which were slightly different from each other. The systems comprised of a seawater dispensing system, a CO_2 extraction system and a coulometer. In this cruise, we used new coulometers constructed by Nippon ANS. Each of the two systems had almost a same specification as follows:

> The seawater dispensing system had an auto-sampler (6 ports), which took seawater in a 300 ml borosilicate glass bottle and dispensed the seawater to a pipette of nominal 20 ml volume by PC control. The pipette was kept at 20 °C by a water jacket, in which water from a water bath set at 20 °C was circulated. CO_2 dissolved in a seawater sample was extracted in a stripping chamber of the CO_2 extraction system by adding phosphoric acid (10 % v/v). The stripping chamber was made approx. 25 cm long and had a fine frit at the bottom. The acid was added to the stripping chamber from the bottom of the chamber by pressurizing an acid bottle for a given time to push out the right amount of acid. The pressurizing was made with nitrogen gas (99.9999 %). After the acid was transferred to the stripping chamber, a seawater sample kept in a pipette was introduced to the stripping chamber by the same method as in adding an acid. The seawater reacted with phosphoric acid was stripped of CO_2 by bubbling the nitrogen gas through a fine frit at the bottom of the stripping chamber. The CO_2 stripped in the chamber was carried by the nitrogen gas (flow rates is 140 ml min^{-1}) to the coulometer through a dehydrating module. The modules of systems A and C consisted of two electric dehumidifiers (kept at 1 - 2 °C) and a chemical desiccant ($Mg(ClO_4)_2$).

The measurement sequence such as system blank (phosphoric acid blank), 2 % CO_2 gas in a nitrogen base, sea water samples (6) was programmed to repeat. The measurement of 2 % CO_2 gas was made to monitor response of coulometer solutions (from UIC, Inc.) or laboratory-made.

ii. A_T

Measurement of A_T was made based on spectrophotometry using a custom-made system (Nippon ANS, Inc.). The system comprises of a water dispensing unit, an auto-burette (765 Dosimat, Metrohm), and a spectrophotometer (Carry 50 Bio, Varian), which were automatically controlled by a PC. The water dispensing unit had a water-jacketed pipette and a water-jacketed titration cell. The spectrophotometer had a water-jacketed quartz cell, length and volume of which were 8 cm and 13 ml, respectively. To circulate sample seawater between the titration and the quartz cells, PFA tubes were connected to the cells.

A seawater of approx. 40 ml was transferred from a sample bottle (borosilicate glass bottle; 130 ml) into the water-jacketed (25 ºC) pipette by pressurizing the sample bottle (nitrogen gas), and was introduced into the water-jacketed (25 ºC) titration cell. The seawater was circulated between the titration and the quartz cells by a peristaric pump to rinse the route. Then, Milli-Q water was introduced into the titration cell, and was circulated in the route twice to rinse the route. Next, a seawater of approx. 40 ml was weighted again by the pipette, and was transferred into the titration cell. The weighted seawater was introduced into the quartz cell. Then, for seawater blank, absorbances were measured at three wavelengths (750, 616 and 444 nm). After the measurement, an acid titrant, which was a mixture of approx. 0.05 M HCl in 0.65 M NaCl and bromocresol green (BCG) was added (about 2 ml) into the titration cell. The seawater + acid titrant solution was circulated for 6 minutes between the titration and the quartz cells, with stirring by a stirring tip and bubbling by wet nitrogen gas in the titration cell. Then, absorbances at the three wavelengths were measured again.

Calculation of A_T was made by the following equation:

$$A_T = (-[H^+]_T V_{SA} + M_A V_A) / V_S,$$

where M_A is the molarity of the acid titrant added to the seawater sample, $[H^+]_T$ is the total excess hydrogen ion concentration in the seawater, and V_S, V_A and V_{SA} are the initial seawater volume, the added acid titrant volume, and the combined seawater plus acid titrant volume, respectively. $[H^+]_T$ is calculated from the measured absorbances based on the following equation (Yao and Byrne, 1998):

$$\begin{aligned} pH_T = -\log[H^+]_T = {} & 4.2699 + 0.002578(35 - S) + \log((R - 0.00131)/(2.3148 - 0.1299R)) \\ & - \log(1 - 0.001005S), \end{aligned}$$

where S is the sample salinity, and R is the absorbance ratio calculated as:

$$R = (A_{616} - A_{750})/(A_{444} - A_{750}),$$

where A_i is the absorbance at wavelength *i* nm.

The HCl in the acid titrant was standardized on land. The concentrations of BCG were estimated to be approx. 2.0×10^{-6} M in the sample seawater, respectively.

iii. pH

Measurement of pH was made by a pH measuring system (Nippon ANS, Inc.). For the detection of pH, spectrophotometry was adopted. The system comprised of a water dispensing unit and a spectrophotometer (Carry 50 Scan, Varian). For an indicator, *m*-cresol purple (2 mM) was used.

Seawater was transferred from borosilicate glass bottle (300 ml) to a sample cell in the spectrophotometer. The length and volume of the cell were 8 cm and 13 ml, respectively, and the sample cell was kept at 25.00 ± 0.05 ºC in a

thermostated compartment. First, absorbances of seawater only were measured at three wavelengths (730, 578 and 434 nm). Then the indicator was injected and circulated for about 4 minutes. to mix the indicator and seawater sufficiently. After the pump was stopped, the absorbances of seawater + indicator were measured at the same wavelengths. The pH was calculated based on the following equation (Clayton and Byrne, 1993):

$$pH = pK_2 + \log\left(\frac{A_1/A_2 - 0.00691}{2.2220 - 0.1331(A_1/A_2)}\right),$$

where A_1 and A_2 indicate absorbances at 578 and 434 nm, respectively, and pK_2 is calculated as a function of water temperature and salinity.

(4) Performances

i. C_T

The two systems worked well without a major malfunction. Replicate analysis was made approximately on every about 9th seawater sample. During the leg 1, the repeatability for systems A and C were estimated to be 0.7 ± 0.7 (n = 115 pairs) and 0.8 ± 0.7 (n = 96 pairs) μmol kg^{-1}, respectively. The combined result was 0.7 ± 0.7 μmol kg^{-1} (n = 211 pairs). During the leg 2, they were 0.7 ± 0.6 (n = 73 pairs) and 0.5 ± 0.5 (n = 92 pairs) μmol kg^{-1}, respectively. The combined result was 0.6 ± 0.6 μmol kg^{-1} (n = 165 pairs). Through the two legs, repeatability was 0.7 ± 0.7 μmol kg^{-1} (n = 188 pairs) and 0.6 ± 0.6 μmol kg^{-1} (n = 188 pairs) for systems A and C, respectively. The combined result was 0.7 ± 0.7 μmol kg^{-1} (n = 376 pairs).

ii. A_T

The system showed a very good precision compared to systems used in previous studies. A few replicate samples were taken on every stations. During the leg 1, the repeatability was estimated to be 0.5 ± 0.4 μmol kg^{-1} (n = 200 pairs), while during the leg 2, it was estimated to be 0.6 ± 0.5 μmol kg^{-1} (n = 164 pairs). Through the two legs, the combined result was 0.5 ± 0.5 μmol kg^{-1} (n = 364 pairs).

iii. pH

The system worked well with no troubles. The average of absolute differences between replicate samples were 0.0004 ± 0.0004 (n = 263 pairs) and 0.0004 ± 0.0004 (n = 205) pH unit for legs 1 and 2, respectively. Through the two legs, the combined result was 0.0004 ± 0.0004 (n = 468) pH unit.

(5) Results

Cross sections of C_T, pH, and A_T along WOCE P21 line are illustrated in Figs. 3.6.1, 3.6.2 and 3.6.3, respectively.

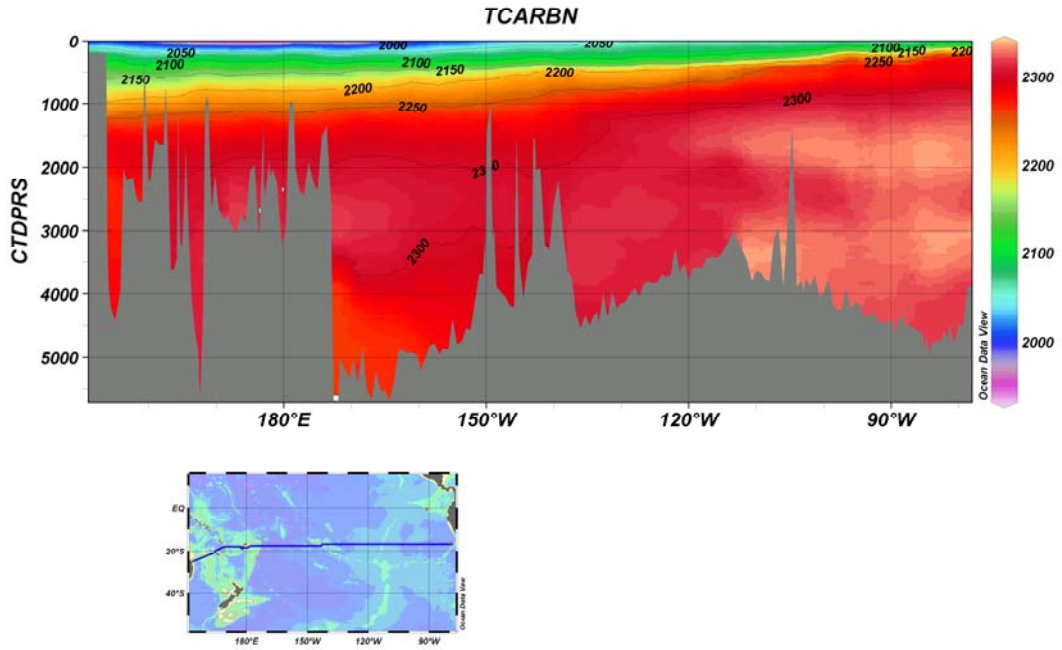

Fig. 3.6.1. Distributions of C_T along the P21 line.

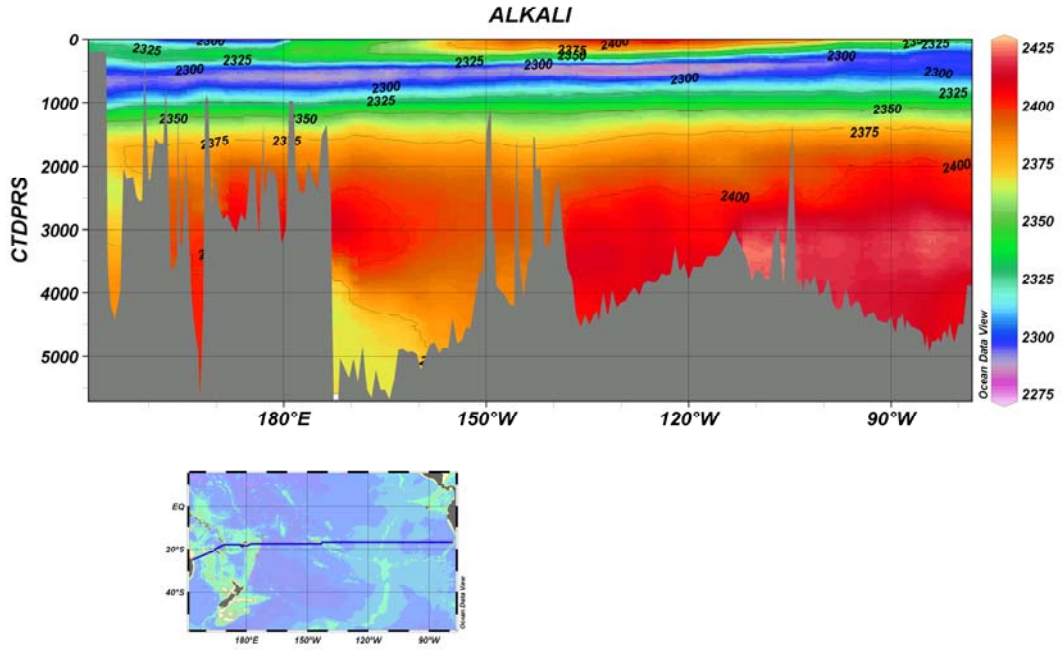

Fig. 3.6.2. Distributions of A_T along the P21 line.

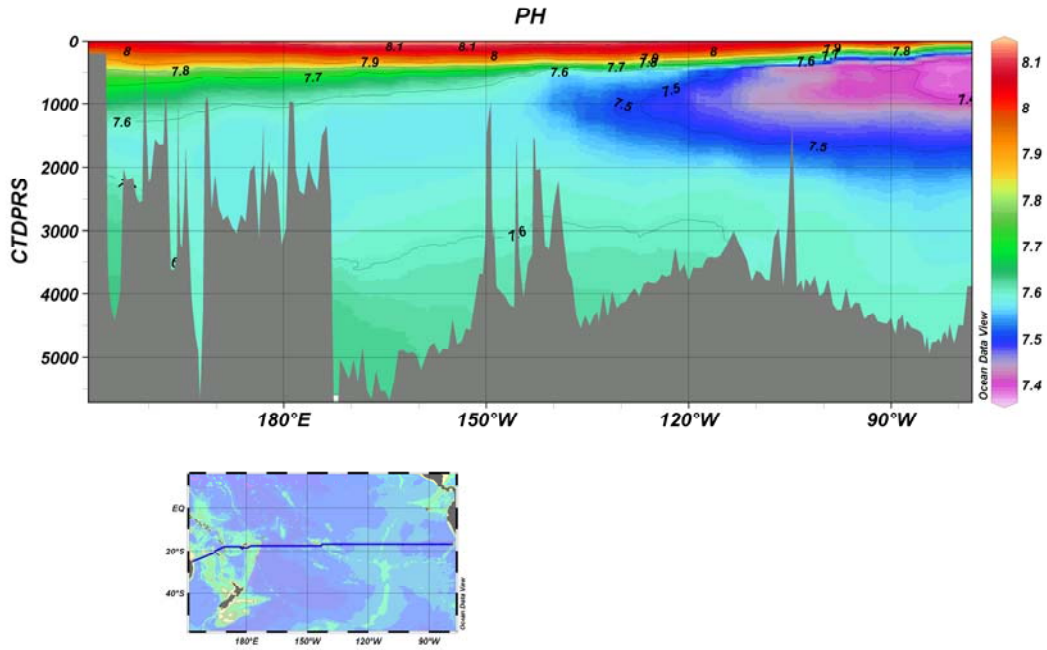

Fig. 3.6.3. Distributions of pH along the P21 line.

References

Clayton T.D. and R.H. Byrne (1993) Spectrophotometric seawater pH measurements: total hydrogen ion concentrtaion scale calibration of m-cresol purple and at-sea results. Deep-Sea Research 40, 2115-2129.

Yao W. and R. H. Byrne (1998) Simplified seawater alkalinity analysis: Use of linear array spectrometers. Deep-Sea Research I 45, 1383-1392.

3.7 Carbon isotopes

July 06, 2009

(1) Personnel

Yuichiro KUMAMOTO

Japan Agency for Marine Earth Science and Technology (JAMSTEC)

(2) Objective

In order to investigate the water circulation and carbon cycle in the South Pacific, seawaters for carbon-14 (radiocarbon) and carbon-13 (stable carbon isotope) of total dissolved inorganic carbon (TDIC) were collected by the hydrocasts from surface to near bottom during MR09-01 cruise.

(3) Sample collection

The sampling stations and number of samples are summarized in Table 3.7.1. All samples for carbon isotope ratios (total 807 samples) were collected at 27 stations using 12-liter Niskin-X bottles. The seawater sample was siphoned into a 250 cm^3 glass bottle with enough seawater to fill the glass bottle 2 times. Immediately after sampling, 10 cm^3 of seawater was removed from the bottle and poisoned by 0.1 cm^3 μl of saturated $HgCl_2$ solution. Then the bottle was sealed by a glass stopper with Apiezon grease M and stored in a cool and dark space on board.

(4) Sample preparation and measurements

In our laboratory, dissolved inorganic carbon in the seawater samples will be stripped cryogenically and split into three aliquots: radiocarbon measurement (about 200 μmol), carbon-13 measurement (about 100 μmol), and archive (about 200 μmol). The extracted CO_2 gas for radiocarbon will be then converted to graphite catalytically on iron powder with pure hydrogen gas. The carbon-13 of the extracted CO_2 gas will be measured using Finnigan MAT252 mass spectrometer. The carbon-14 in the graphite sample will be measured by Accelerator Mass Spectrometry (AMS).

Table 3.7.1 The sampling stations and number of samples for carbon isotope ratios.

Station	No. samples	No. replicate samples	Max. sampling depth /m
P21-018	34	2	5468
P21-032	32	2	4692
P21-X19	30	2	4481
P21-059	30	2	4385
P21-068	29	2	4112
P21-X18	29	2	3971
P21-088	27	2	3630
P21-100	24	1	2969
P21-108	27	2	3533
P21-116	27	2	3634
P21-123	29	2	3936
P21-X17	29	2	4206
P21-137	27	2	3543
P21-144	19	1	1824
P21-154	28	2	3987
P21-X16	27	2	3589
P21-176	32	2	4870
P21-183	32	2	4851
P21-191	35	2	5552
P21-195	32	2	4955
P21-210	22	1	2411
P21-220	20	1	2133
P21-231	24	1	2916
P21-245	35	2	5590
P21-262	27	2	3558
P21-273	22	1	2502
P21-282	30	2	4362
Total	759	48	

3.8. Nutrients dynamics and its association with primary productivity

(1) Personnel

Taketoshi KODAMA (The University of Tokyo)
Hiroyuki KUROTORI (The University of Tokyo)
Takuhei SHIOZAKI (The University of Tokyo)
Satoshi KITAJIMA (The University of Tokyo)
Shigenobu TAKEDA (The University of Tokyo)
Ken FURUYA (The University of Tokyo)

(2) Objectives

Concentrations of nitrogenous and phosphorus inorganic nutrients in the tropical and subtropical oligotrophic region are usually below the detection limits of conventional analytical methods. Recent studies on nutrient dynamics using highly sensitive analytical methods have shown that dissolved inorganic N and P are variable at nanomolar levels in the basin scale associated with physical and biological processes (Karl, 2007). N2 fixation is one of the most important processes causing phosphate depletion. In the western North Pacific subtropical gyre, where a large scale phosphorus exhaustion occurs (Hashihama *et al*., 2009), it is suggested that N2 fixation activity is high because of favorable iron supply due to high atmospheric dust deposition (Kitajima *et al*., 2009; Shiozaki *et al*., 2009). In contrast, the eastern South Pacific subtropical gyre, where phosphorus supply is in excess, nitrogen fixation is reported to be extremely low (Raimbault *et al*., 2008) and dust deposition is calculated to be much less than the North Pacific (Jickells *et al*., 2005). Therefore, the western North Pacific and the eastern South Pacific are likely in contrastive biogeochemical regimes each other. However, available information is extremely limited for comparative analysis of the both regions. Thus, we conducted following experiments during this cruise, with particular attention to nutrients distribution and its association with phytoplankton abundance, primary productivity and nitrogen fixation.

(3) Materials and Methods

Semi- and continuous measurement of nutrients and hydrography in the surface water

Seawater ample was continuously collected by pumping up from the bottom of the ship during cruising. Concentrations of nitrate+nitrite (N+N), soluble reactive phosphorus (SRP), and ammonium were determined using a highly sensitive colorimetric method whose detection limit was 3nM. Temperature and salinity were measured continuously by Ocean Seven 301 (Idronaut) and chlorophyll fluorescence by a fluorometer (Chelsea).

Nutrients, pigments and abundance of phytoplankton, and isotopic composition of particulate organic nitrogen (PON) and carbon (POC)

Water samples for nutrients, chlorophyll a, phytoplankton abundance and isotopic composition of PON and POC were collected from 0–200m using an acid-cleaned bucket for the surface and Niskin-X bottles for subsurface layers. Concentrations of nitrate, nitrite, and SRP were determined by a conventional colorimetry using a TRAACS-800TM (Bran+Luebbe) analyzer. When the nutrients concentrations were <0.1 μM, the concentrations of N+N and SRP were analyzed using the highly sensitive colorimetric method. Samples for chlorophyll a were measured fluorometrically with a Turner Design 10-AU fluorometer after extraction in N, N-dimethylformamide. Samples for phytoplankton abundance were fixed with 1% glutaraldehyde and frozen immediately in liquid nitrogen, or fixed with 0.6% Lugol solution for later analysis on land. Samples of 4.5L collected for natural 15N and 13C abundance of PON and POC were filtered immediately on pre-combusted GF/F filters.

Samples for pigments for HPLC analysis and nitrogen isotope abundance in zooplankton were taken from the pumped-up experimental seawater.

N2 fixation activity, primary production, and abundance of diazotrophs

Samples for N2 fixation activity and primary production, and abundance of diazotrophs were also collected from 0–200m in an acid-cleaned bucket and Niskin-X bottles. Subsamples for abundance of diazotrophic were filtered onto 10-μm and 0.2-μm polycarbonate filters, and frozen immediately at -80°C until later analysis on land.

N_2 fixation activities were determined by two methods; ^{15}N tracer technique and acetylene reduction assay. Samples for the ^{15}N tracer experiment were only taken from the surface and were introduced into triplicate acid-cleaned 4.5 L polycarbonate bottles. ^{13}C-labeled sodium bicarbonate (99 atom% ^{13}C; Cambridge Isotope Lab.) was added to each bottle at a final tracer concentration of 200 μM before sealed with a thermoplastic elastomer cap. Then, using a gas-tight syringe, 2 ml of $^{15}N_2$ gas (99.8 atom% ^{15}N; Shoko) was added into each bottle. The samples were incubated in an on-deck incubator, and the incubation was terminated after 24 hours.

For the acetylene reduction assay, triplicates or duplicates of samples of 550-mL seawater were poured into three or two 1200-mL polyethylene-terephthalate bottles. After sealed with a butyl rubber stopper, 120 mL of acetylene was injected into each bottle by replacing the same volume of headspace. The samples were incubated for 24 hours in the on-deck incubator. For the samples taken at the surface, size fractionation was made using a 10-μm nylon mesh and a 2-μm polycarbonate filter. These fractionated samples were incubated in the same manner as the whole-water samples. Subsamples of headspace were taken several times during the incubation, and measured by a gas chromatograph (GC-17A, Shimadzu). After the incubation, samples were recovered into polyethylene bottles and fixed with Lugol solution, or filtered onto 0.2-μm polycarbonate membrane filter for further analysis on land.

Along with the water sampling, plankton net (20-μm mesh) samples were also collected at the surface to examine the occurrence of microplanktonic diazotrophs.

(4) References

Hashihama, F., K. Furuya, S. Kitajima, S. Takeda, T. Takemura, and J. Kanda, 2009: Macro-scale exhaustion of surface phosphate by N2 fixation in the western North Pacific. *Geophysical Research Letters*., VOL. 36, L03610, doi:10.1029/2008GL036866

Jickells, T. D., Z. S. An, K. Andersen, R. Baker, G. Bergametti, N. Brooks, J. J. Cao, P. W. Boyd, R.A.Duce, K. A. Hunter, H. Kawahata, N. Kubilay, J. laRoche, P. S. Liss, N.Mahowald, J. M. Prospero, A. J. Ridgwell, I. Tegen, and R. Torres, 2005 Global Iron Connections Between Desert Dust, Ocean Biogeochemistry, and Climate. *Science*., VOL. 308, 67-71

Karl, D. M., 2007: Microbial oceanography: Paradigms, processes and promise, *Nat. Rev. Microbiol.*, VOL. 5, 759–769.

Kitajima, S., K. Furuya, F. Hashihama, S. Takeda, and J. Kanda, 2009: Latitudinal distribution of diazotrophs and their nitrogen fixation in the tropical and subtropical western North Pacific *Limnology and Oceanography*.

Shiozaki, T., K. Furuya, T. Kodama, and S. Takeda, 2009: Contribution of N2 fixation to new production in the western North Pacific along 155°E. *Marine Ecology Progress Series*.

Raimbault, P., and N. Garcia, 2008: Evidence for efficient regenerated production and dinitrogen fixation in nitrogen-deficient waters of the South Pacific Ocean: impact on new and export production estimates. *Biogeosciences*., VOL. 5:323-338

3.9. Methane (CH_4), Nitrous oxide (N_2O), Carbonyl sulfide (COS), and related substances

July 3, 2009

(1) Personnel

Osamu Yoshida[1,2*], Sakae Toyoda[3], Taku Watanabe[3], Sho Imai[2], Chiho Kubota[2], Keita Yamada[3]
Chisato Yoshikawa[3,4], and Naohiro Yoshida[3]

[1] Faculty of Environment Systems, Rakuno Gakuen University

[2] Graduate School of Dairy Science, Rakuno Gakuen University

[3] Interdisciplinary Graduate School of Science and Engineering, Tokyo Institute of Technology

[4] Japan Society for the Promotion of Science

** Principal Investigator*

(2) Sampling elements

All sampling elements of Tokyo Institute of Technology and Rakuno Gakuen University group at hydrographic stations are listed below.

Table 1. Parameters and hydrographic station numbers for samples collection in Legs 1 and 2.

Parameters	Hydrographic station Numbers (WHP-P21)
1. Dissolved CH_4 (concentration)	14, 18, 25, 33, X19, 59, 66, 73, 85, 96, 104, 112, 121, 128, 134, 141, 145, 152, X16, 174, 183, 189, 198, 209, 216, 229, 236, 247, 255, 273, 285
2. Dissolved CH_4 (carbon isotope ratio)	14, 25, X19, 66, 85, 104, 121, 134, 152, 174, 189, 209, 229, 255, 285
3. Dissolved CH_4 (hydrogen isotope ratio)	14, 25, X19, 66, 85, 104, 121, 134, 152, 174, 189, 209, 229, 255, 285
4. Dissolved N_2O (concentration)	14, 18, 25, 33, X19, 59, 66, 73, 85, 96, 104, 112, 121, 128, 134, 141, 145, 152, X16, 174, 183, 189, 198, 209, 216, 229, 236, 247, 255, 273, 285
5. Dissolved N_2O (nitrogen and oxygen isotopomers)	14, 25, X19, 66, 85, 104, 121, 134, 152, 174, 189, 209, 229, 255, 285
6. NO_3^- (isotope ratios)	14, 18, 25, 33, X19, 59, 66, 73, 85, 96, 104, 121, 134, 152, 174, 189, 209, 229, 236, 247, 255, 273, 285
7. On-board incubation experiments (N_2O and CH_4)	25, 120, 189, 254, 283
8. Chlorophyll *a*	14, 25, X19, 66, 85, 104, 121, 134, 152, 174, 189, 209, 229, 255, 285
A. Air samples for air-sea flux of CH_4 and N_2O	14, 24, X19, 66, 85, 104, 121, 134, 152, 174, 189, 209, 229, 255, 285
B. Concentration and sulfur isotope ratio of COS in the maritime air	14, 103, 173, 285

Table 2. Parameters and sampling locations in Leg 3.

Parameters	Station numbers (lattitude, longitude)
A. Concentration and isotope ratios of CH_4 and N_2O in the maritime air	TIT-RGU-32 (15.08S 154.43E), TIT-RGU-33 (9.27S 154.19E), TIT-RGU-34 (5.44N 146.23E), TIT-RGU-35(10.28N 142.49E), TIT-RGU-36 (19.42N 138.24E), TIT-RGU-37 (29.16N 134.39E)
B. Concentration and sulfur isotope ratio of COS in the maritime air	TIT-RGU-32~36

(3) Methane

Methane concentration and stable isotopic distribution as indicators of biogenic methane dynamics in the South Pacific Ocean

i. Dissolved CH_4

i-a Introduction

Atmospheric methane (CH_4) is a trace gas playing an important role in the global carbon cycle as a greenhouse gas. Its concentration has increased by about 1050 ppbv from 700 ppbv since the pre-industrial era (IPCC, 2007). In order to understand the current global methane cycle, it is necessary to quantify its sources and sinks. At present, there remain large uncertainties in the estimated methane fluxes from sources to sinks. The ocean's source strength for atmospheric methane should be examined in more detail, even though it might be a relatively minor source, previously reported to be 0.005 to 3% of the total input to the atmosphere (Cicerone and Oremland, 1988; Bange et al., 1994; Lelieveld et al., 1998).

To estimate an accurate amount of the methane exchange from the ocean to the atmosphere, it is necessary to explore widely and vertically. Distribution of dissolved methane in surface waters from diverse locations in the world ocean is often reported as a characteristic subsurface maximum representing a supersaturation of several folds (Yoshida et al., 2004). Although the origin of the subsurface methane maximum is not clear, some suggestions include advection and/or diffusion from local anoxic environment nearby sources in shelf sediments, and in situ production by methanogenic bacteria, presumably in association with suspended particulate materials (Karl and Tilbrook, 1994; Katz et al., 1999). These bacteria are thought to probable live in the anaerobic microenvironments supplied by organic particles or guts of zooplankton (Alldredge and Cohen, 1987).

So, this study investigates in detail profile of methane concentration and stable isotopic distribution in the water column in the South Pacific Ocean to clarify methane dynamics and estimate the flux of methane to the atmosphere.

i-b Materials and methods

Seawater samples are taken by CTD-CAROUSEL system attached Niskin samplers of 12 L at 8-22 layers and surface layer taken by plastic bucket at 15-31 hydrographic stations as shown in Table 1. Each sample was carefully subsampled into 30, 125, 600 ml glass vials to avoid air contamination for analysis of methane concentration, carbon isotope ratio, and hydrogen isotope ratio respectively. The seawater samples were poisoned by 20 μl (30 and 125 ml vials) or 100 μl (600 ml vial) of mercuric chloride solution (Tilbrook and Karl, 1995; Watanabe et al., 1995), and were closed with rubber and aluminum caps. These were stored in a dark and cool place until we got to land, where we conducted gas chromatographic analysis of methane concentration and mass spectrometric analysis of carbon and hydrogen isotopic composition at the laboratory.

The analytical method briefly described here: The system consists of a purge and trap unit, a desiccant unit, rotary valves, a gas chromatograph equipped with a flame ionization detector for concentration of methane, GC/C/IRMS for carbon isotope ratio of methane, GC/TC/IRMS for hydrogen isotope ratio of methane, and data acquisition units. The entire volume of seawater in each glass vial was processed all at once to avoid contamination and loss of methane. Precisions obtained from replicate determinations of methane concentration, and carbon and hydrogen isotope ratios were estimated to be better than 5%, and 0.3‰ and 3‰, respectively, for the usual concentration of methane in seawater.

i-c Expected results

Subsurface maximum concentrations of methane (>3 nmol kg^{-1}) were expected to be observed in the North Pacific Ocean. A commonly-encountered distribution in the upper ocean with a methane peak within the pycnocline (e.g., Ward et al., 1987; Owens et al., 1991; Watanabe et al., 1995). Karl and Tilbrook (1994) suggested the suboxic conditions would further aid the development of microenvironments within particles in which methane could be produced. The organic particles are accumulated in the pycnocline, and methane is produced in the micro reducing environment by

methanogenic bacteria. Moreover, in situ microbial methane production in the guts of zooplankton can be expected (e.g., Owens et al., 1991; de Angelis and Lee, 1994; Oudot et al., 2002; Sasakawa et al., 2008). Watanabe et al. (1995) pointed out that the diffusive flux of methane from subsurface maxima to air-sea interface is sufficient to account for its emission flux to the atmosphere. In the mixed layer above its boundary, the methane is formed and discharged to the atmosphere in part, in the below its boundary, methane diffused to the bottom vertically. By using concentration and isotopic composition of methane and hydrographic parameters for vertical water samples, it is possible to clarify its dynamics such as production and/or consumption in the water column.

Kelley and Jeffrey (2002) observed in the equatorial upwelling region of 10 and 20% supersaturated methane. Rehder et al. (2002) reported that the enhancement of methane fluxes to the atmosphere in regions of coastal upwelling is likely to occur on a global scale. In this study, the combination of in situ methane production and coastal upwelling result in the property distributions and large methane flux in the eastern North Pacific can be expected.

Tsurushima et al. (1996) reported that methane flux in the East China Sea was somewhat larger than the oceanic usual values. Remarkable supersaturation in coastal regions, including continental shelf zones, has been expected related to biological productivity, advection from nearby sources in shelf sediments, and diffusion and/or advection from local anoxic environments.

ii. CH_4 on-board incubation experiments

ii-a Introduction

Typical methane (CH_4) concentrations in open ocean waters are nanomolar throughout the depth distribution and are maximum in surface mixed layer above the pycnocline. Supersaturation in the mixed layer maximum with respect to the atmosphere have been observed widely (e.g., Lamontagne et al., 1973; Burke et al., 1983). The supersaturations observed in the open ocean indicate the CH_4 production in the surface mixed layer. Bacterial CH_4 production occurs only under strict anoxic condition, so CH_4 supersaturation in the mixed layer is termed the “Ocean Methane Paradox” (Kiene, 1991). Methanogenic bacteria with the potential to produce CH_4 under anoxic conditions were observed in fish intestines and plankton samples (Oremland, 1979), and in sinking particulate matter and zooplankton fecal pellets (Bianchi et al., 1992, Marty, 1993). On the basis of these observations, at present, a mechanism for producing CH_4 in anoxic microenvironment of fecal pellet and releasing CH_4 into the ocean mixed layer is suggested for CH_4 supersaturation in the mixed layer (e.g., Karl and Tilbrook, 1994, Holmes et al., 2000). The fecal pellet microenvironment hypothesis provides a good first-order explanation of the mixed layer CH_4 maximum, but a number of questions remain.

Alternatively, non-biological CH_4 production in seawater via a photochemical pathway has been argued. Wilson et al. (1970) investigated photochemical CH_4 production in seawater and distilled water augmented with natural dissolved organic carbon, but found CH_4 production in only 2 out of 15 experiments. Tilbrook and Karl (1995) observed CH_4 production in irradiation experiments with sea water from the Pacific Ocean and ascribed this CH_4 formation to an as yet unknown, possibly photochemical, production pathway. Bange and Uher (2005) conducted irradiation experiments with marine water to investigate the possibility of photochemical CH_4 formation. They concluded that photochemical formation is negligible in the present ocean, based on their results indicating that CH_4 photoproduction was undetectable under oxic conditions or in the absence of methyl radical precursors.

In this study, we reevaluate the potential for photochemical CH_4 formation by conducting on-board incubation experiments using surface seawater. Recently, CH_4 production under aerobic conditions was found for terrestrial ecosystems (Keppler et al., 2006). This finding is our motivation to reevaluate the potential for photochemical CH_4 formation in surface sea water.

ii-b Materials and methods

Water samples for on-board incubation experiments were collected at the depths of chlorophyll *a* maximum. The samples are divided into three 125 ml glass vials.

Two vials are sterilized with mercury chloride. One vial is stored at dark place until analyses ($Vial_{CH4\text{-}dark}$), and

the other is irradiated for ~7-10 days and then stored at dark place until analyses ($Vial_{CH4\text{-}irradiated}$). Dissolved CH_4 concentrations and its carbon isotopic compositions will be measured by GC/C/IRMS.

2 ml of distilled water saturated with CH_2F_2 is added to the remaining one vial due to deactivate bacterial CH_4 oxidation. After 7 days incubation, the vial is sterilized with mercury chloride and stored at dark place until analyses ($Vial_{CH4\text{-}ox\text{-}deactivated}$).

ii-c Expected results

First, the difference in concentration for $Vial_{CH4\text{-}dark}$ and $Vial_{CH4\text{-}irradiated}$ will be analyzed to determine the potential for photochemical CH_4 formation. If the difference can be recognized, carbon isotopic measurement will be performed to determine the isotopic signature for photochemical CH_4.

Second, the difference in concentration for $Vial_{CH4\text{-}dark}$, $Vial_{CH4\text{-}irradiated}$ and $Vial_{CH4\text{-}ox\text{-}deactivated}$ will be analyzed to determine the net bacterial CH_4 production. If the difference can be recognized, carbon isotopic measurement will be performed to determine the isotopic signature for bacterial CH_4.

ii-d References

Alldredge, A. A., Y. Cohen: Can microscale chemical patches persist in the sea? Microelectrode study of marine snow, fecal pellets, Science, 235, 689-691, 1987.

Bange, H. W., U. H. Bartell, S. Rapsomanikis, and M. O. Andreae: Methane in the Baltic and the North seas and a reassessment of the marine emissions of methane, Global Biogeochem. Cycles, 8, 465–480, 1994.

Bange, H.W., and G. Uher: Photochemical production of methane in natural waters: implications for its present and past oceanic source, Chemosphere, 58, 177-183, 2005.

Burke, R.J., Jr., D.F. Reid, J.M. Brooks, and D.M. Lavoie: Upper water column methane geochemistry in the eastern tropical North Pacific, Limnol. Oceanogr., 28, 19–32, 1983.

Cicerone, R. J., and R. S. Oremland: Biogeochemical aspects of atmospheric methane, Global Biogeochem. Cycles, 2, 299–327, 1988.

de Angelis, M. A., and C. Lee: Methane production during zooplankton grazing on marine phytoplankton, Limnol. Oceanogr., 39, 1298-1308, 1994.

Holmes, E., F.J. Sansone, T.M. Rust, and B.N. Popp: Methane production, consumption, and air-sea exchange in the open ocean: An evaluation based on carbon isotopic ratios. Global Biogeochem. Cycles, 14, 1-10, 2000.

Intergovermental Panel on Climate Change (2007), Couplings Between Change in the Climate System and Biogeochemistry, in Climate Change 2007: The Physical Science Basis: Contribution of Working Group I to the Fourth Assessment Report of the Intergovernment Panel on Climate Change, edited by S. Solomon, et al., pp. 501-568, Cambridge University Press, Cambridge, United Kingdom and New York, NY, USA.

Karl, D. M., and B. D. Tilbrook: Production and transport of methane in oceanic particulate organic matter, Nature, 368, 732–734, 1994.

Katz, M. E., D. K. Pak, G. R. Dickkens, and K. G. Miller (1999), The source and fate of massive carbon input during the latest Paleocene thermal maximum, Scince, 286, 1531–1533.

Kelley C. A. and Jeffrey, W. H.: Dissolved methane concentration profiles and air-sea fluxes from 41S to 27N. Global. Biogeochem. Cycle, 16, No.3, 10.1029/2001GB001809, 2002.

Keppler, F., J.T.G. Hamilton, M. Brass, and T. Roeckmann: Methane emissions from terrestrial plants under aerobic conditions, Nature, 439, 187-191, 2006.

Kiene, R.P.: Production and consumption of methane in aquatic systems, In Microbial Production and Consumption of Greenhouse Gases: Methane, Nitrogen Oxide, Halomethanes; Rogeres, J.E., Whitman, W.B., Eds., American Society for Microbiology, Washinfton, DC, 111-146, 1991.

Lamontagne, R.A., J.W. Swinnerton, V.J. Linnenbom, and W.D. Smith: Methane concentration in various marine environment, J. Geophys. Res., 78, 5317–5324, 1973.

Lelieveld, J., P. J. Crutzen, and F. J. Dentener (1998), Changing concentration, lifetime and climate forcing of

atmospheric methane, Tellus Ser. B, 50, 128–150.
Oremland, R.S.: Methanogenlc activity in plankton samples and fish intestines: A mechanisms for*in situ* methanogenesis in oceanic surface water , Limnol. Oceanogr., 24, 1136–1141, 1979.
Oudot, C., P. Jean-Baptiste, E. Fourre, C. Mormiche, M. Guevel, J-F. Ternon, and P. L. Corre: Transatlantic equatorial distribution of nitrous oxide and methane, Deep-Sea Res., Part I, 49, 1175–1193, 2002.
Owens, N. J. P., C. S. Law, R. F. C. Mantoura, P. H. Burkill, and C. A. Llewellyn: Methane flux to the atmosphere from the Arabian Sea, Nature, 354, 293–296, 1991.
Rehder, G., R. W. Collier, K. Heeschen, P. M. Kosro, J. Barth, and E. Suess: Enhanced marine CH4 emissions to the atmosphere off Oregon caused by coastal upwelling, Global Biogeochem. Cycles, 16, 10.1029/2000GB001391, 2002.
Sasakawa, M., U. Tsunogai, S. Kameyama, F. Nakagawa, Y. Nojiri, and A. Tsuda (2008), Carbon isotopic characterization for the origin of excess methane in subsurface seawater, J. Geophys. Res., 113, C03012, doi: 10.1029/2007JC004217.
Tilbrook, B. D., and D. M. Karl: Methane sources, distributions and sinks from California coastal waters to the oligotrophic North Pacific gyre, Mar. Chem., 49, 51–64, 1995.
Tsurushima, N., S. Watanabe, N. Higashitani, and S. Tsunogai: Methane in the East China Sea water, J. Oceanogr., 52, 221–233, 1996.
Ward, B. B., K. A. Kilpatrick, P. C. Novelli, and M. I. Scranton: Methane oxidation and methane fluxes in the ocean surface layer and deep anoxic waters, Nature, 327, 226–229, 1987.
Watanabe, S., N. Higashitani, N. Tsurushima, and S. Tsunogai: Methane in the western North Pacific, J. Oceanogr., 51, 39–60, 1995.
Wilson, D.F., J.W. Swinnerton, and R.A. Lamontagne: Production of carbon monoxide and gaseous hydrocarbons in seawater: relation to dissolved organic carbon. Science, 168, 1577-1579, 1970.
Yoshida, O., H. Y. Inoue , S. Watanabe, S. Noriki, M. Wakatsuchi: Methane in the western part of the Sea of Okhotsk in 1998-2000, J. Geophys. Res., 109, C09S12, doi:10.1029/2003JC001910, 2004.

(4) Nitrous oxide and related substances

Production, consumptions and air-sea flux of N_2O in the South Pacific Ocean

i. Introduction

Recently considerable attention has been focused on emission of biogenic trace gases from ecosystems, since the gases contain a significant amount of greenhouse gases such as carbon dioxide (CO_2), methane (CH_4) and nitrous oxide (N_2O). Isotopic signatures of these gases are well recognized to provide constraints for relative source strength and information on reaction dynamics concerning their formation and biological pathways. Nitrous oxide is a very effective heat-trapping gas in the atmosphere because it absorbs outgoing radiant heat in infrared wavelengths that are not captured by the other major greenhouse gases, such as water vapor and CO_2. The annual input of N_2O into the atmosphere is estimated to be about 16 Tg N_2O-N yr^{-1}, and the oceans are believed to contribute more than 20% of the total annual input (IPCC, 2007).

N_2O is produced by the biological processes of nitrification and denitrification (Dore et al., 1998; Knowles et al., 1981; Rysgaard et al., 1993; Svensson, 1998; Ueda et al., 1993). Depending on the redox conditions, N_2O is produced from inorganic nitrogenous compounds (NH_4 or NO_3^-), with subsequently different isotopic fractionation factors. The isotopic signatures of N_2O confer constraints on the relative source strength, and the reaction dynamics of N_2O biological production pathways are currently under investigation. Furthermore, isotopomers of N_2O contain more easily interpretable biogeochemical information as to their sources than obtained from conventional bulk ^{15}N and ^{18}O measurements (Yoshida and Toyoda, 2000).

The Pacific Ocean is the largest of the world's five oceans (followed by the Atlantic Ocean, Indian Ocean,

Southern Ocean, and Arctic Ocean) (CIA, www) and expected to be important for the biogeochemical and biological cycles. Thus, the study of N_2O production and nutrients dynamics are very important to examine the origins of N_2O in seawater and to estimate the inventory of N_2O from this region with respect to the troposphere.

ii. Materials and methods

Samples were collected in the framework of MR09-01 research expedition on the *R/V Mirai* from April 10 to July 3, 2009. The purpose of the expedition was to study on the heat and material transports and their variability of the general ocean circulation and a study on chemical environment and its changes in the ocean. In order to investigate the production and consumption of dissolved N_2O in South Pacific, seawater samples for dissolved N_2O concentration/isotopomer ratio analysis and those for nitrate isotope ratio analysis were collected at total 15-31 and 23 stations, respectively (Table 1). Air samples were also collected into pre-evacuated stainless-steel canisters (total 21 stations, Tables 1 and 2).

ii-a Air-sea flux measurement

Concentration of N_2O at the surface water and ambient air will be measured using GC/ECD at Rakuno Gakuen University and/or GC/IRMS at Tokyo Institute of Technology.

ii-b N_2O concentration and isotope analyses

Seawater samples collected by CTD-CAROUSEL system was subsampled into three glass vials: one 30-ml vial for concentration analysis and two 125 or 225 ml glass vials for isotopomer ratio analysis. The subsamples were then sterilized with saturated $HgCl_2$ solution (about 20 μL per 100 ml seawater). The vials were sealed with butyl-rubber septa and aluminum caps, taking care to avoid bubble formation, and then brought back to the laboratory and stored at 4˚C until analysis. Dissolved N_2O concentrations and its isotopic compositions will be measured by GC/ECD and/or GC/IRMS.

ii-c. N_2O on-board incubation experiments

Water samples for on-board incubation experiments were collected at the depths of chlorophyll *a* maximum. The samples are divided into 18 vials of 125 mL volume. The subsamples were incubated in a water bath (~10°C) after the following treatments: (a) control incubation (no operation), (b) addition of 1-μL of 0.2 mol L^{-1}-$^{15}NH_4Cl$ solution (15N atomic fraction: 99 %), and (c) addition of 5-μL of 0.1 mol L^{-1}-$Na^{15}NO_3$ solution (15N atomic fraction: 99 %). At the elapsed time of 0, 24, and 48 hours, microbial activity was stopped by adding 0.5-mL of saturated $HgCl_2$ solution. The concentration and isotopomer ratios of N_2O dissolved in each vial will be determined as described above. Then, N_2O production rate will be calculated from isotopomer ratios obtained without incubation (t = 0) and the raw mass spectroscopic data obtained from ^{15}N-added incubation, assuming the statistical transfer of ^{15}N from the substrate to N_2O (Toyoda et al., 2009).

ii-d Isotope ratios of NO_3^-

Water sample was collected into a 50-ml syringe equipped with a DISMIC® filter (pore size: 0.45 μm). The sample was then filtrated and divided into five polypropylene tubes. One of the tubes was stored at -40ºC until analysis. The rest of the tubes were stored at room temperature after adding 0.5 mL of 1 mol L^{-1} NaOH. Isotope ratios of NO_3^- will be measured by denitrifer method (Sigman et al., 2001) in which N_2O converted from nitrate is measured by using GC/IRMS.

iii. Expected results

In the surface layer, N_2O concentration of water affects the sea-air flux directly (Dore et al., 1998). However the pathway of N_2O production in surface layer is still unresolved. In the surface layer, N_2O is predominantly produced by nitrification, but also by denitrification if oxygen concentration is low (Maribeb and Laura, 2004). Moreover, it was

reported that N_2O production by nitrification is photo-inhibited (Olson, 1981). Therefore, concentration and isotopomer ratios of N_2O/nitrate together with N_2O production rate from ammonium/nitrate obtained by this study will reveal the pathway of N_2O production and N_2O production rate in the surface layer (especially euphotic zone).

In deeper layer, N_2O could be produced through *in situ* biological processes of settling particles or fecal pellets derived from phytoplankton or zooplankton, and N_2O maximum was indeed observed at 600-800 m depth in the North Pacific (Popp et al., 2002; Toyoda et al., 2002). However, following problems have not been resolved: (i) what the major pathway for the N_2O maximum is and (ii) whether the N_2O is produced *in situ* or transported from other area. Although there is a report on distribution of concentration and isotopomer ratio of N_2O in the central and eastern South Pacific (Charpentier et al., 2007), this study will be the first one which reveals the distribution and production pathway of N_2O in the whole subtropical South pacific including the western part.

iv. References

Charpentier, J., L. Farias, N. Yoshida, N. Boontanon, and P. Raimbault: Nitrous oxide distribution and its origin in the central and eastern South Pacific Subtropical Gyre, Biogeosciences, 4 (5), 729-741, 2007.

Dore, J.E., Popp, B.N., Karl, D.M. and Sansone, F.J.: A large source of atmospheric nitrous oxide from subtropical North Pacific surface water, Nature, 396, 63-66, 1998.

IPCC, Climate Change 2007: The Physical Science Basis. Contribution of Working Group I to the Fourth Assessment Report of the Intergovernmental Panel on Climate Change, edited by S. Solomon et al., pp. 996, Cambridge University Press, Cambridge, United Kingdom and New York, NY, USA, 2007.

Knowles, R., Lean, D.R.S. and Chan, Y.K.: Nitrous oxide concentrations in lakes: variations with depth and time, Limnology and Oceanography, 26, 855-866, 1981.

Maribeb, C.-G. and Laura, F.: N_2O cycling at the core of the oxygen minimum zone off northern Chile, Marine Ecology Progress Series, 280, 1-11, 2004.

Olson, R.J.: Differential photoinhibition of marine nitrifying bacteria: a possible mechanism for the formation of the primary nitrite maximum, Journal of Marine Research, 39, 227-238, 1981.

Popp, B. N., et al.: Nitrogen and oxygen isotopomeric constraints on the origins and sea-to-air flux of N_2O in the oligotrophic subtropical North Pacific gyre, Global Biogeochem. Cycles, 16(4), 1064, 2002. doi: 10.1029/2001GB001806.

Rysgaard, S., Risgaard-Petersen, N., Nielsen, L.P. and Revsbech, N.P.: Nitrification and denitrification in lake and estuarine sediments measured by the ^{15}N dilution technique and isotope pairing, Applied and Environmental Microbiology, 59, 2093-2098, 1993.

Sigman, D. M., K. L. Casciotti, M. Andreani, C. Barford, M. Galanter, and J. K. Boehlke: A bacterial method for the nitrogen isotopic analysis of nitrate in seawater and freshwater, Anal. Chem., 73, 4145-4153, 2001.

Svensson, J.M.: Emission of N_2O, nitrification and denitrification in a eutrophic lake sediment bioturbated by Chironomus plumosus, Aquatic Microbial Ecology, 14, 289-299, 1998.

Toyoda, S., H. Iwai, K. Koba, and N. Yoshida: Isotopomeric analysis of N_2O dissolved in a river in the Tokyo metropolitan area, Rapid Commun. Mass Spectrom., 23 (6), 809-821, 2009. doi: 10.1002/rcm.3945.

Toyoda, S., N. Yoshida, T. Miwa, Y. Matsui, H. Yamagishi, U. Tsunogai, Y. Nojiri, and N. Tsurushima: Production mechanism and global budget of N_2O inferred from its isotopomers in the western North Pacific, Geophys. Res. Lett., 29 (3), 7-1-7-4, 2002.

Ueda, S., Ogura, N. and Yoshinari, T.: Accumulation of nitrous oxide in aerobic ground water, Water Research, 27, 1787-1792, 1993

www.cia.gov/cia/publications/factbook/geos/zn.html

Yoshida, N. and Toyoda, S.: Constraining the atmospheric N_2O budget from intramolecular site preference in N_2O isotopomers, Nature, 405, 330-334, 2000.

(5) Carbonyl sulfide

i. Introduction

Carbonyl sulfide (COS) is the most abundant (about 500 pptv) and most stable (life time is about 16 years) gaseous sulfur species in the background (remote) atmosphere. It is oxidized in the stratosphere to form sulfate aerosols which may influence the radiation budget at the Earth's surface and the stratospheric ozone cycle (Crutzen, 1976). It is emitted from natural sources such as microbial metabolism of sulfur in the ocean and terrestrial environment and anthropogenic sources such as sulfur industry and combustion of fossil fuel and biomass (Chin and Davis, 1993; Watts, 2000; Kettle et al., 2002). Its major sinks are considered to be soil and plant uptake, reaction with OH and O radials, and photolysis in the stratosphere. However, estimated fluxes of the sources have large uncertainty because they are based on limited observations of COS concentration, and COS budget has not been closed yet. Therefore, isotopic study of COS may provide constraints for relative source strength as well as information on reaction pathways in its formation and destruction processes. Sulfur isotope ratio of COS in the atmosphere or source gasses has not been reported so far, although there is a study on sulfur isotope fractionation in the stratospheric COS which suffers from low analytical precision by balloon-born infrared spectroscopy (Leung et al., 2002).

In this study, we are developing a high-sensitive, high-precision, and rapid analytical system for concentration and sulfur isotope ratios of COS that is applicable to trace COS in environment. Our purpose of this cruise is to collect maritime air samples which contain background COS or COS emitted from nearby oceanic sources for the isotopic analysis.

ii. Materials and methods

Air samples were collected at 10 stations listed in Tables 1 and 2. At each station, ambient air near the bridge (about 10 m above sea level) was pressurized into two stainless-steel canisters (6L) at 5 atm (absolute pressure) using a sampling device which consists of a diaphragm pump, a back-pressure regulating valve, a desiccant tube packed with $Mg(ClO_4)_2$, and stainless tubes and connectors. Inner surface of the SS canisters are deactivated to prevent COS adsorption or decomposition during sample storage.

iii. Expected results

First, concentration analysis will be performed to determine the sample size and detail procedure for isotopic measurement. Then, stability of COS in the glass bottle and canister will be checked by periodic analysis of concentration using an aliquot of the same sample. Finally, sulfur isotope ratio will be measured by the newly developed analytical system. If succeeded, sulfur isotope ratio of atmospheric COS will be revealed for the first time.

iv. References

Crutzen, P. J.: The possible importance of OCS for the sulfate layer of the stratosphere, Geophys. Res. Lett., 3, 73-76, 1976.

Chin, M., and D. D. Davis: Global sources and sinks of OCS and CS2 and their distributions, Global Biogeochem. Cycles, 7 (2), 321-337, 1993.

Kettle, A. J., U. Kuhn, M. von Hobe, J. Kesselmeier, and M. O. Andreae: Global budget of atmospheric carbonyl sulfide: Temporal and spatial variations of the dominant sources and sinks, J. Geophys. Res., 107 (D22), 4658, 2002.

Leung, F.-Y., A. J. Colussi, and M. R. Hoffmann: Isotopic fractionation of carbonyl sulfide in the atmosphere: Implications for the sources of background stratospheric sulfate aerosol, Geophys. Res. Lett., 29 (10), 1474, 2002.

Watts, S. F.: The mass budgets of carbonyl sulfide, dimethyl sulfide, carbon disulfide and hydrogen sulfide, Atmos. Environ., 34, 761-779, 2000.

(6) Chlorophyll *a*

i. Objective

Chlorophyll *a* is one of the most convenient indicators of phytoplankton stock, and has been used extensively for the estimation of phytoplankton abundance in various aquatic environments. The object of this study is to investigate the vertical distribution of phytoplankton in various light intensity depth.

ii. Sampling elements

Chlorophyll *a*

iii. Materials and Methods

Seawater samples were collected 0.5 L at 6 depths from surface to about 200 m with Niskin bottles, except for the Surface water, which was taken by the bucket. The samples were gently filtrated by low vaccum pressuer (<15 cmHg) through Whatman GF/F filter (diameter 25 mm) in the dark room. Phytoplankton pigments were immediately extracted in 7 ml of N,N-dimethylformamide (DMF) after filtration and then, the samples were stored at –20°C under the dark condition to extract chlorophyll *a* for 24 hours or more. The extracted samples are measured the fluorescence by Turner fluorometer (10-AU-005, TURNER DESIGNS) which was previously calibrated against a pure chlorophyll *a* (Sigma chemical Co.). We applied the fluorometric “Non-acidification method” (Welschmeyer, 1994)

iv. Results

The results of Chlorophyll *a* were shown in Figure 1.

v. Data archives

All processed Chlorophyll *a* data were submitted to Principal Investigator according to the data management policy of JAMSTEC.

vi. Reference

Welschmeyer, N. A.: Fluorometric analysis of chlrophyll *a* in the presence of chlorophyll *b* and pheopigments. Limno. Oceanogr., 39, 1985-1992, 1994.

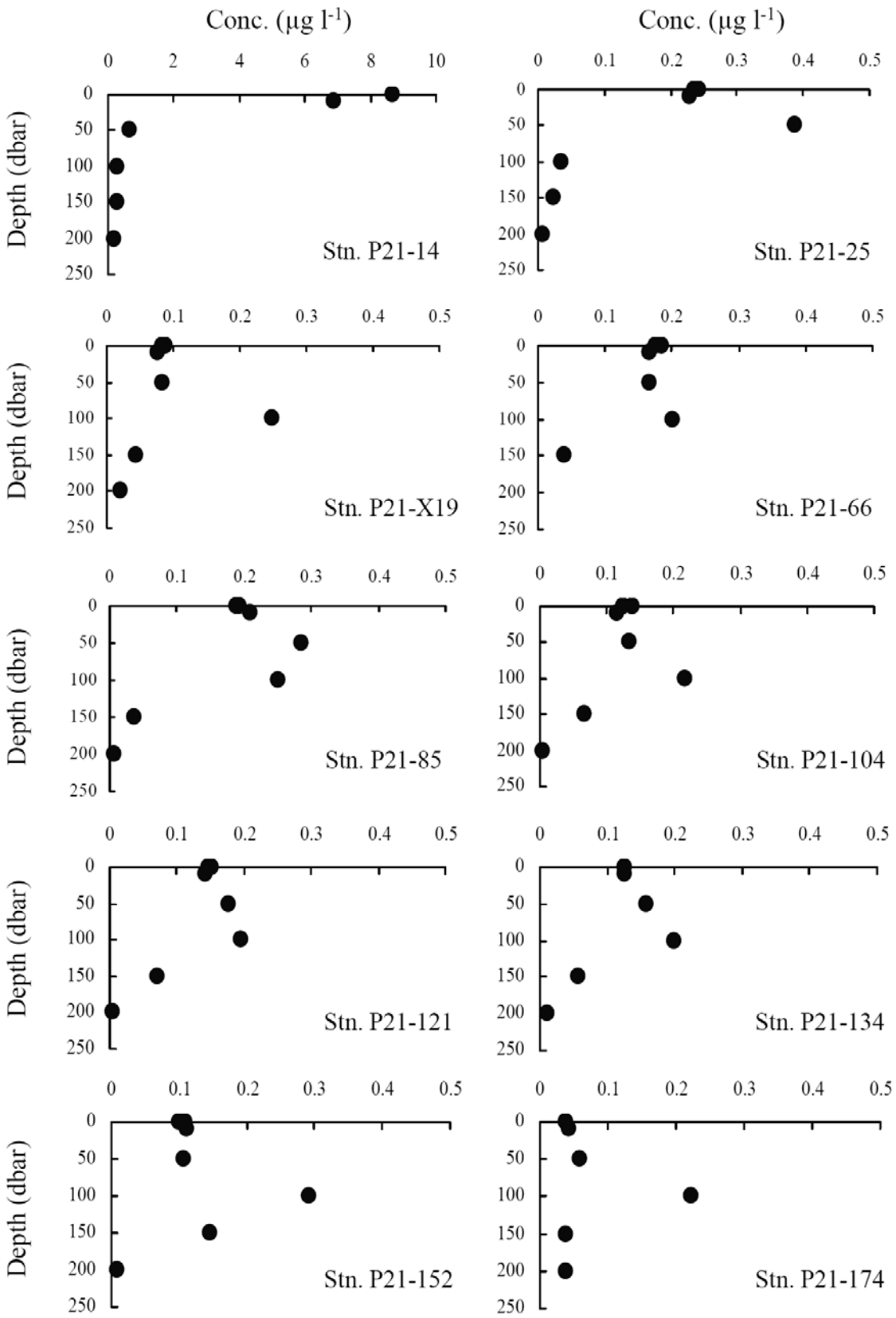

Figure 1. The vertical distributions of chlorophyll *a* at MR09-01.

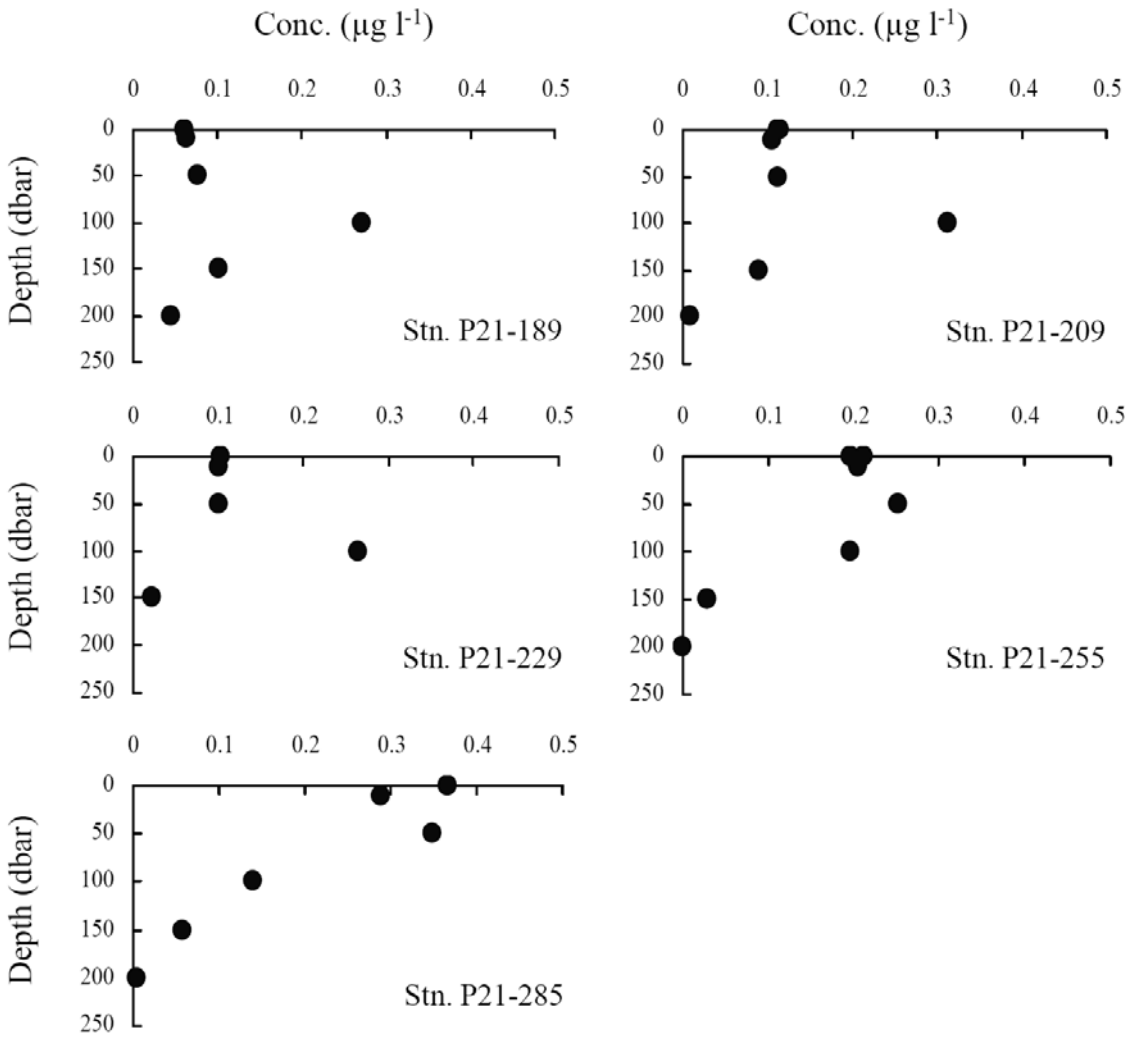

Figure 1. Continued.

3.10. LADCP

(1) Personnel

Shinya Kouketsu (JAMSTEC)
Hiroshi Uchida (JAMSTEC)
Katsurou Katsumata (JAMSTEC)
Toshimasa Doi (JAMSTEC)

(2) Overview of the equipment

An acoustic Doppler current profiler (ADCP) was integrated with the CTD/RMS package. The lowered ADCP (LADCP), Workhorse Monitor WHM300 (Teledyne RD Instruments, San Diego, California, USA), which has 4 downward facing transducers with 20-degree beam angles, rated to 6000 m. The LADCP makes direct current measurements at the depth of the CTD, thus providing a full profile of velocity. The LADCP was powered during the CTD casts by a 50.4 volts rechargeable Ni-Cd battery pack. The LADCP unit was set for recording internally prior to each cast. After each cast the internally stored observed data was uploaded to the computer on-board. By combining the measured velocity of the sea water and bottom with respect to the instrument, and shipboard navigation data during the CTD cast, the absolute velocity profile can be obtained (e.g., Visbeck, 2002).

The instrument used in this cruise was as follows.

Teledyne RD Instruments, WHM300
S/N 11853 (CPU firmware ver. 50.32, ver. 50.35, with pressure sensor)
S/N 8484 (CPU firmware ver. 50.32, ver. 50.35)
S/N 1512 (CPU firmware ver. 50.35)

(3) Data collection

In this cruise, data were collected with the following configuration.

Bin size: 8 m
Number of bins: 14
Pings per ensemble: 1
Ping interval: 1 sec

At the following stations, the CTD cast was carried out without the LADCP, because maximum pressure was beyond the pressure-proof of the LADCP (6000 m).

Station P21-200

(4) Data collection problems

We changed the instruments many times due to various troubles. The log of changing instruments is as follows.

Station P21-120: from S/N 11853 (firmware ver. 50.32) to S/N 8484 (firmware ver. 50.32)
Station P21-132: from S/N 8484 (firmware ver. 50.32) to S/N 8484 (firmware ver. 50.35)
Station P21-141: from S/N 8484 (firmware ver. 50.35) to S/N 11853 (firmware ver. 50.35)
Station P21-174: from S/N 11853 (firmware ver. 50.35) to S/N 1512 (firmware ver. 50.35)
Station P21-181: from S/N 1512 (firmware ver. 50.35) to S/N 11853 (firmware ver. 50.35)
Station P21-182: from S/N 11853 (firmware ver. 50.35) to S/N 1512 (firmware ver. 50.35)

Until the Station 120, data recording was intermittently stopped during a cast due to the firmware (ver. 50.32) bug. Because the beam 2 of S/N 8484 became weak at the Station 139, we changed instruments from S/N 8484 to S/N

11853. The beam 2 of the instrument (S/N 11853) also didn't work well at the Station 173 and the instrument was changed to S/N 1512. Since the beam 3 of the instrument (S/N 1512) became weak at the Station 180, we tried the S/N 11853 again at the Station 181 to compare the echo intensities. Since the instrument of S/N 1512 worked better than S/N 11853, the S/N 1512 was used after the Station 182 (see Fig. 3.10.1).

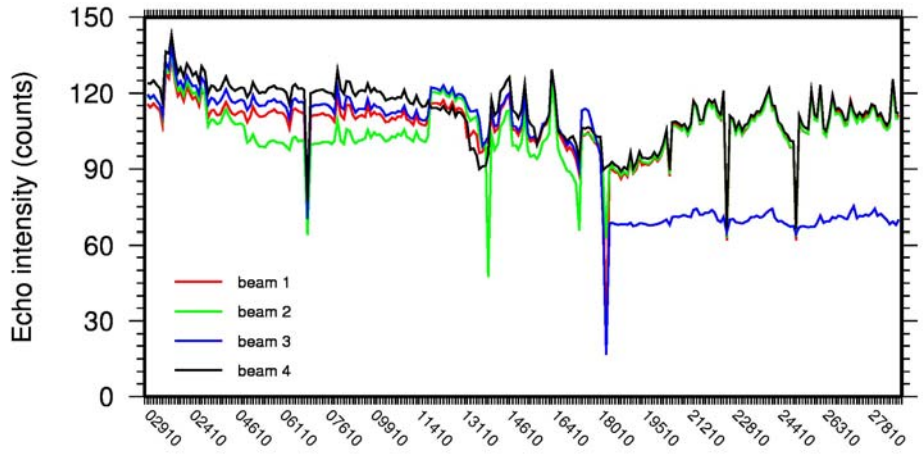

Fig. 3.10.1. Cast-averaged echo intensities at 3rd bin

(4) Data process

Vertical profiles of velocity are obtained by the inversion method (Visbeck, 2002). Since the first bin from LADCP is influenced by the turbulence generated by CTD frame, the weight for the inversion is set to 0.1. GPS navigation data and the bottom-track data are used in the calculation of the reference velocities. Shipboard ADCP data averaged for 1 minutes are also included in the calculation. The CTD data are used for the sound speed and depth calculation. The directions of velocity are corrected using the magnetic deviation estimated with International Geomagnetic reference field data.

However, the inversion method doesn't work well due to no-good velocity data due to the instrument problems as well as weak echo intensity at deep layers. We again plan to process carefully after the cruise.

Reference

Visbeck, M. (2002): Deep velocity profiling using Lowered Acoustic Doppler Current Profilers: Bottom track and inverse solutions. *J. Atmos. Oceanic Technol.*, 19, 794-807.

3.11 XCTD

August 27, 2009

(1) Personnel

Hiroshi Uchida (JAMSTEC)
Leg 1
Shinya Okumura (GODI)
Ryo Kimura (GODI)
Yosuke Yuki (GODI)
Leg 2
Satoshi Okumura (GODI)
Kazuho Yoshida (GODI)
Harumi Ota (GODI)

(2) Objectives

In this cruise, XCTD (eXpendable Conductivity, Temperature and Depth profiler) measurements were carried out to examine short-term changes in temperature and salinity profiles, and to evaluate fall rate equations by comparing with CTD (Conductivity, Temperature and Depth profiler) measurements and bottom topography measurements.

(3) Instrument and Method

The XCTDs used were XCTD-1 and XCTD-2 (Tsurumi-Seiki Co., Ltd., Yokohama, Kanagawa, Japan) with an MK-130 deck unit (Tsurumi-Seiki Co., Ltd.). The manufacturer's specifications are listed in Table 3.11.1. In this cruise, seven XCTD-1 probes and twenty-three XCTD-2 probes were deployed by using 8-loading automatic launcher (Tsurumi-Seiki Co., Ltd.) (Table 3.11.2). Ship's speed was slowed down to 3 knot during the XCTD-2 measurement. For the comparison with CTD, XCTD was deployed at about 5 minutes for XCTD-1 and at about 10 minutes for XCTD-2 after the beginning of the down cast of the CTD.

Table 3.11.1. Manufacturer's specifications of XCTD-1 and XCTD-2.

Parameter	Range	Accuracy
Conductivity	0 ~ 60 mS cm^{-1}	±0.03 mS cm^{-1}
Temperature	–2 ~ 35 °C	±0.02 °C
Depth	0 ~ 1000 m (for XCTD-1)	5 m or 2%, whichever is greater *
	0 ~ 1850 m (for XCTD-2)	5 m or 2%, whichever is greater *

* Depth error is shown in Kizu et al (2008).

(4) Data Processing and Quality Control

The XCTD data were processed and quality controlled based on a method by Uchida and Imawaki (2008) with slight modification. The followings are the data processing sequence used in the reduction of XCTD data.

1. Raw temperature and conductivity data from the first 32 scans (about 4.3 m) of the XCTD data were deleted, and data after the probe contacts to the bottom and spikes were manually removed.
2. Missing data by the above editing was linearly interpolated when the data gap was within 15 scans (about 2 m).
3. Temperature and conductivity data were low-pass filtered (running mean with a window of 15 scans).
4. The conductivity data was advanced for 1.5 scans (about 0.2 m), instead of 2 scans described in Uchida and Imawaki (2008), relative to the temperature data to correct mismatch of response time of the sensors.

5. Pressure was calculated by vertical integration of density multiplied by gravitational acceleration. The gravitational acceleration is a function of pressure and location (latitude).
6. Salinity was calculated from the pressure, temperature and conductivity data by using the reference conductivity of 42.896 mS cm^{-1} at salinity of 35, temperature of 15 °C and pressure of 0 dbar. The reference conductivity value is used in the manufacturer's data processing software.
7. The data were sampled at 1-dbar interval.
8. Salinity biases of the XCTD data were estimated by using temperature and salinity relationships in the deep ocean obtained from the post-cruise calibrated CTD data (Table 3.11.2). For the XCTD data of the station P21_29_1, salinity bias could not be estimated because the maximum depth was too shallow to estimate the salinity bias.

(5) Preliminary results

Vertical section of potential temperature is shown in Fig. 3.11.1 for stations between 29 and 33. Comparison with the CTD data shows short-term fluctuation in temperature between the observation periods 6 days apart.

Result of comparison of bottom depth estimated from XCTD data with that measured by multi narrow beam echo sounder (MNBES) is shown in Fig. 3.11.2. Bottom depth measured by MNBES is the gridded data set. Bottom depth estimated from maximum depth of the CTD data plus height above bottom measured by altimeter is also shown in Fig. 3.11.2. The bottom depth estimated from XCTD data agree with independent estimates of the bottom depth within the manufacturer's specification. However, the estimation from XCTD data is systematically smaller than the other estimates. Mean difference with standard error for the eleven comparisons was –21.6 ± 5.0 m for the comparison with the MNBES data and –18.2 ± 4.2 m for the comparison with the CTD data. More precise, temperature dependent coefficients for the fall rate equation of the XCTD (Kizu et al., 2008) will be used for the evaluation of the XCTD measurements. Direct comparisons of temperature and salinity profiles between XCTD and CTD will also be made.

Reference

Kizu, S., H. Onishi, T. Suga, K. Hanawa, T. Watanabe, and H. Iwamiya (2008): Evaluation of the fall rates of the present and developmental XCTDs. *Deep-Sea Res I*, **55**, 571–586.

Uchida, H. and S. Imawaki (2008): Estimation of the sea level trend south of Japan by combining satellite altimeter data with in situ hydrographic data. *J. Geophys. Res.*, **113**, C09035, doi:10.1029/2008JC004796.

Table 3.11.2. Serial number and probe type of the XCTD. Water depth, ship intake temperature (SST) and salinity (SSS; not corrected), and maximum pressure for the XCTD data are shown. Salinity offset applied to the XCTD data and reference salinity estimated from the CTD data are also shown.

Station	Serial number (type)	Depth [m]	SST [°C]	SSS [PSU]	Max pressure [dbar]	Salinity offset [PSU]	Reference salinity [PSU]
Leg 1							
29_1 *	08112315 (2)	3798	23.759	35.444	187 **	–	NA
29_2 *	08112312 (2)	3816	23.725	35.430	1967	0.009	34.6215 @ 2.5°C
30_1 *	08112308 (2)	4462	24.249	35.432	1967	0.021	34.6215 @ 2.5°C
31_1 *	08112304 (2)	4441	24.815	35.497	1913	0.022	34.6215 @ 2.5°C
32_1 *	08112309 (2)	4713	23.453	35.480	1917	0.007	34.6215 @ 2.5°C
33_1 *	08112306 (2)	4442	23.787	35.538	1967	0.014	34.6215 @ 2.5°C
41_1	03022164 (1)	4659	23.975	35.456	1036	0.023	34.5219 @ 4.5°C
41_2	08112305 (2)	4659	23.977	35.455	1967	0.007	34.6215 @ 2.5°C
34_1	08112307 (2)	4536	24.030	35.505	1967	0.012	34.6215 @ 2.5°C
34_2	07022711 (1) ***	4537	24.029	35.505	1037	0.000	34.5219 @ 4.5°C
42_1	03022159 (1)	4558	23.544	35.584	1037	–0.017	34.5219 @ 4.5°C
42_2	08112310 (2)	4572	23.547	35.585	1967	0.015	34.6215 @ 2.5°C
96_1	03022156 (1)	3732	25.612	36.217	1036	–0.005	34.5219 @ 4.5°C
96_2	08112311 (2)	3751	25.610	36.218	1967	0.007	34.6215 @ 2.5°C
97_1	03022162 (1)	3462	25.592	36.166	1037	0.012	34.5219 @ 4.5°C
97_2	08112313 (2)	3453	25.591	36.166	1967	0.010	34.6215 @ 2.5°C
98_1	03022157 (1)	3287	25.649	36.149	1037	0.002	34.5219 @ 4.5°C
98_2	08112314 (2)	3297	25.659	36.162	1967	0.010	34.6215 @ 2.5°C
145_1	08112319 (2)	1505	28.117	36.244	1464	0.007	34.5665 @ 3.0°C
146_1	08112316 (2)	1530	27.918	36.291	1520	0.020	34.5665 @ 3.0°C
151_1	08112322 (2)	1531	28.009	36.315	1518	0.005	34.5665 @ 3.0°C
156_1	03022155 (1)	943	28.339	36.223	943	0.008	34.4726 @ 4.5°C
Leg 2							
205_1	08112325 (2)	1365	28.097	35.430	1356	0.014	34.4781 @ 3.5°C
206_1	08112317 (2)	1484	27.978	35.548	1470	0.037	34.5512 @ 3.0°C
209_1	08112318 (2)	1924	27.032	35.260	1286 **	0.008	34.4911 @ 3.5°C
213_1	08112327 (2)	991	26.979	35.232	985	0.016	34.4238 @ 4.5°C
221_1	08112320 (2)	1883	26.466	34.783	1911	–0.004	34.6094 @ 2.5°C
250_1	08112321 (2)	1716	25.045	34.938	1700	0.013	34.5710 @ 3.0°C
266_1	08112324 (2)	1638	24.094	34.950	1631	–0.001	34.5860 @ 3.0°C
268_1	08112323 (2)	1562	23.496	35.227	1551	0.014	34.5860 @ 3.0°C

* Not for simultaneous measurements with CTD

** Failure of measuremets due to noise or lost contact

*** Relatively large (about 30 minutes) time difference between CTD and XCTD measurements

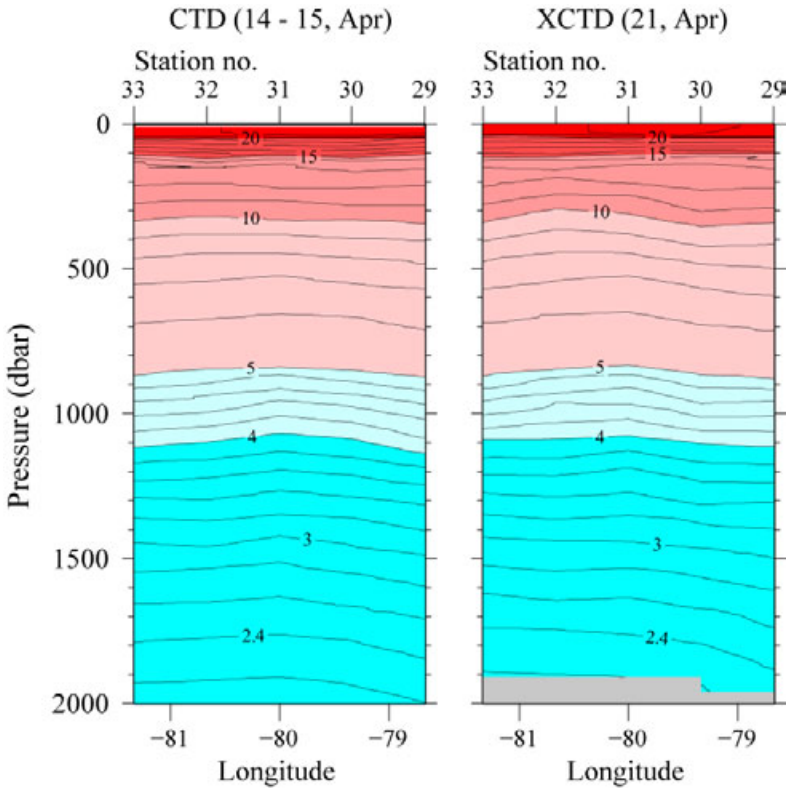

Figure 3.11.1. Vertical sections of potential temperature measured by CTD (left) and XCTD (right).

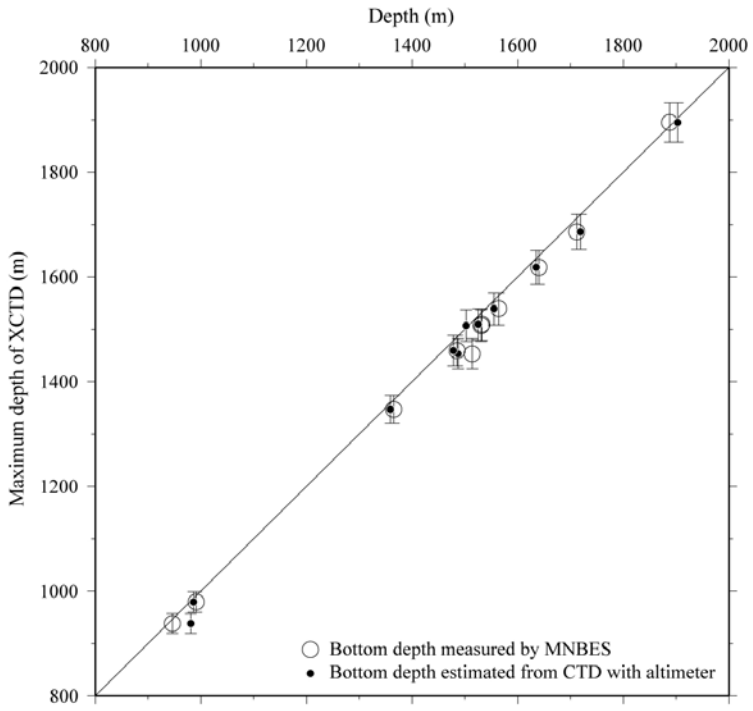

Figure 3.11.2. Comparison of bottom depth estimated from XCTD data with that measured by multi narrow beam echo sounder (MNBES). Comparison with bottom depth estimated from maximum depth from CTD data plus height above bottom measured by altimeter is also shown. Vertical bars show depth error of the manufacturer's specification.

3.12. Expendable Microstructure Profiler

(1) Personnel

K. Katsumata (JAMSTEC)

(2) Objectives

Turbulence mixing in the ocean has been a difficult quantity to measure directly despite its important role in the ocean energy budget and general circulation dynamics. Recent improvements on materials such as optic fibre and on sensors as high precision shear sensor now enable the measurement using the newly developed expendable microstructure profiler (XMP)

(3) Apparatus

XMP probe and its deck unit are manufactured by Rockland Scientific International, Canada. The expendable sensor has a cylindrical shape with the length of about 152 cm and a diameter of 18 cm. Two shear sensors, one temperature sensor, a pressure sensor, and an accelerometer are mounted on the deeper tip of the cylinder. The tail is fringed with plastic drag brushes to stabilise its drop rate.

The shear sensors measure the shear with $2.5\times10^{-3}\,s^{-1}$ rms resolution. Least squares fit of the shear spectrum to the Nasmyth theoretical curve yields an estimate of the turbulent kinetic energy dissipation rate. The instrument oscillation is measured by the accelerometer and corrected during the spectrum estimation

The measured data are transmitted to the deck unit through an optic fibre. Twlelve kilometre of the fibre on a spool is mounted on a bike stand and the fibre freely comes off the spool as the instrument falls underwater.

The turbulent kinetic energy dissipation rate ϵ is estimated by

$$\varepsilon = \frac{15}{2}\nu\overline{u_z^2},$$

where ν is the kinematic molecular viscosity of water and u_z is the vertical derivative of the horizontal velocity and the overbar denotes a spatial or ensemble averaging. Detailed description of the principle and sensors can also be found in Lueck *et al.*, (2002).

(4) Deployments

Five probes were deployed at three different CTD stations right after the CTD cast. Serial numbers 8 and 9 were deployed at the CTD station 172, Serial numbers 7 and 10 were at the Station 205. Serial number 11 at Station 264. The time below is in UT and in the year of 2009.

Serial number	Lat	Lon	Water depth (m)	Time (UT)
8	17-30.43°S	154-19.72°W	4723	23 May 17:52
9	17-30.65°S	154-19.72°W	4726	23 May 18:39
7	17-29.81°S	173-40.32°W	1364	3 June 18:35
10	17-30.08°S	173-39.88°W	1362	3 June 19:07
11	21-29.05°S	162-46.03°W	1556	14 June 04:14

(5) Results

All probes lost connection before they reach the bottom. Noisy record on Serial Number 8 suggests water leakage. Other probes returned good data. Figs 3.12.1 shows the vertical distribution of the eddy kinetic energy dissipation rate. The method for estimating the dissipation rate follows that of Lueck *et al.* (2002).

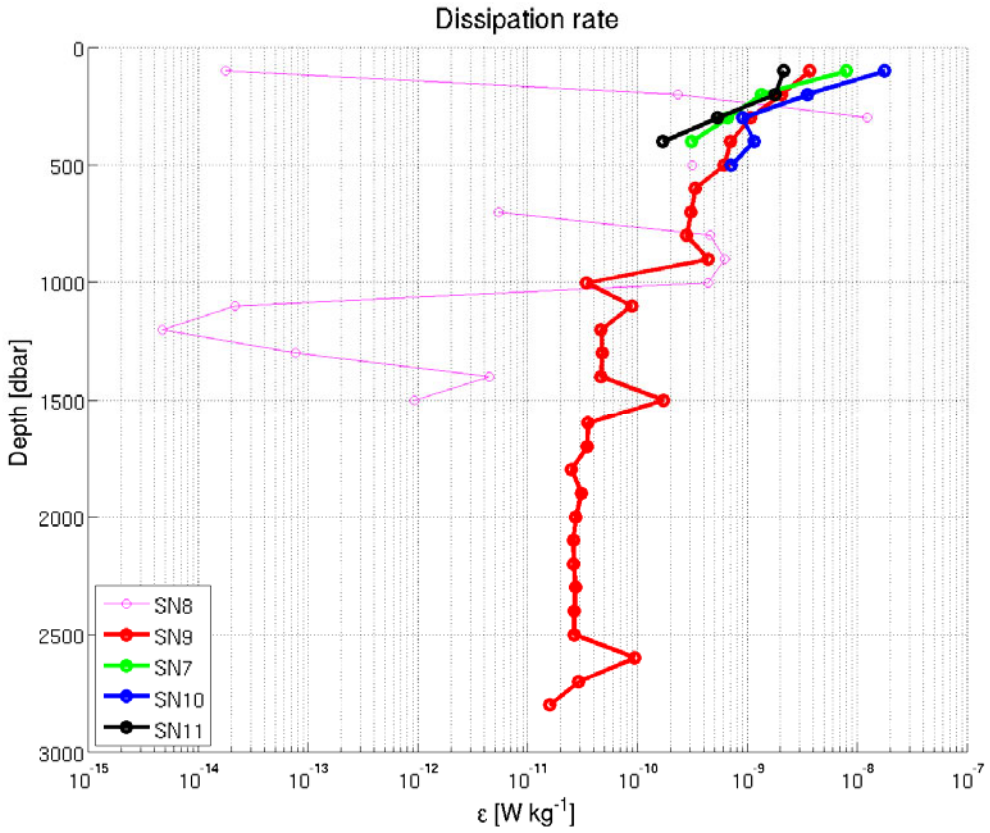

Fig. 3.12.1. Kinetic energy dissipation rate estimated at intervals of 50-150 dbar, 150-250 dbar, 250-350 dbar, and so forth. SN8 probably suffered from water leakage.

References

Lueck, R.G., F. Wolk, and H. Yamazaki (2002) Oceanic Velocity Microstructure Measurements in the 20th Century. Journal of Oceanography 58, 153-174.

4. Floats, Drifters and Moorings

4.1 Argo floats

(1) Personnel

Toshio Suga	***(JAMSTEC/IORGC):Principal Investigator (not on board)***
Shigeki Hosoda	***(JAMSTEC/IORGC):not on board***
Kanako Sato	***(JAMSTEC/IORGC):not on board***
Mizue Hirano	***(JAMSTEC/IORGC):not on board***
Kenichi Katayama	***(MWJ):Technical Staff (Operation Leader of Leg 1)***
Shinsuke Toyoda	***(MWJ) :Technical Staff***
Tetsuo Aoki	***(MWJ) :Technical Staff***

(2)Objectives

The objective of deployment is to clarify the structure and temporal/spatial variability of water masses in the South Pacific such as the Eastern Subtropical Mode Water and the Antarctic Intermediate Water.

The two type of profiling floats are launched in this cruise: one measures vertical profiles of temperature and salinity automatically every two days, the other measures every ten days. The data from the floats will enable us to understand the phenomenon mentioned above with time/spatial scales much smaller than in previous studies.

(3) Parameters

Water temperature, salinity, and pressure

(4) Methods

i. Profiling float deployment

We launched APEX floats manufactured by Webb Research Ltd. These floats equip an SBE41 CTD sensor manufactured by Sea-Bird Electronics Inc.

Five floats were launched from 105W to 115W along the cruise track (Table 4.1-1). The floats usually drift at a depth of 1000 dbar (called the parking depth), diving to a depth of 2000 dbar and rising up to the sea surface by decreasing and increasing their volume and thus changing the buoyancy. During the ascent, they measure temperature, salinity, and pressure. The floats shading in Table 4.1-1 measures these parameters every two days, the others measures every ten days. They stay at the sea surface for approximately ten hours, transmitting the CTD data to the land via the ARGOS system, and then return to the parking depth by decreasing volume. The status of two types of floats and their launches are shown in Table 4.1-1.

(5) Preliminary Result

The time series of vertical profiles of sea-water temperature and salinity observed every two days are shown in Fig. 4.1-1. The salinity maximum and minimum are observed in the surface layer and below 350m. The salinity minimum shown in Fig. 4.1-1 is the upper part of salinity minimum layer distributed around the center of 700m shown in Fig. 4.1-2. This salinity minimum water seems to be the Antarctic Intermediate Water.

(6) Data archive

The real-time data are provided to meteorological organizations, research institutes, and universities via Global Data Assembly Center (GDAC: http://www.usgodae.org/argo/argo.html, http://www.coriolis.eu.org/) and Global Telecommunication System (GTS), and utilized for analysis and forecasts of sea conditions.

Table 4.1-1 Status of JAMSTEC floats and their launches

Float 1(shading in launches table)

Float Type	**APEX floats manufactured by Webb Research Ltd.**
CTD sensor	**SBE41 manufactured by Sea-Bird Electronics Inc.**
Cycle	**10 days (approximately 9 hours at the sea surface)**
ARGOS transmit interval	**30 sec**
Target Parking Pressure	**1000 dbar**
Sampling layers	**124 (2000, 1900, 1800, 1700, 1600, 1500, 1400, 1300, 1200, 1100, 1000, 900, 800, 700, 600, 590, 580, 570, 560, 550, 540, 530, 520, 510, 500, 495, 490, 485, 480, 475, 470, 465, 460, 455, 450, 445, 440, 435, 430, 425, 420, 415, 410, 405, 400, 395, 390, 385, 380, 375, 370, 365, 360, 355, 350, 345, 340, 335, 330, 325, 320, 315, 310, 305, 300, 295, 290, 285, 280, 275, 270, 265, 260, 255, 250, 245, 240, 235, 230, 225, 220, 215, 210, 205, 200, 195, 190, 185, 180, 175, 170, 165, 160, 155, 150, 145, 140, 135, 130, 125, 120, 115, 110, 105, 100, 95, 90, 85, 80, 75, 70, 65, 60, 55, 50, 45, 40, 35, 30, 25, 20, 15, 10, 4 or surface dbar)**

Float 2 (non-shading in launches table)

Float Type	**APEX floats manufactured by Webb Research Ltd.**
CTD sensor	**SBE41 manufactured by Sea-Bird Electronics Inc.**
Cycle	**10 days (approximately 9 hours at the sea surface)**
ARGOS transmit interval	**30 sec**
Target Parking Pressure	**1000 dbar**
Sampling layers	**115 (2000, 1950, 1900, 1850, 1800, 1750, 1700, 1650, 1600, 1550, 1500, 1450, 1400, 1350, 1300, 1250, 1200, 1150, 1100, 1050, 1000, 980, 960, 940, 920, 900, 880, 860, 840, 820, 800, 780, 760, 740, 720, 700, 680, 660, 640, 620, 600, 580, 560, 540, 520, 500, 490, 480, 470, 460, 450, 440, 430, 420, 410, 400, 390, 380, 370, 360, 350, 340, 330, 320, 310, 300, 290, 280, 270, 260, 250, 240, 230, 220,210, 200, 195, 190, 185, 180, 175, 170, 165, 160, 155, 150, 145, 140, 135, 130, 125, 120, 115, 110, 105, 100, 95, 90, 85, 80, 75, 70, 65, 60, 55, 50, 45, 40, 35, 30, 25, 20, 15, 10, 4 or surface dbar)**

Launches

Float S/N	ARGOS ID	Date and Time of Reset (UTC)	Date and Time of Launch (UTC)	Location of Launch	CTD St. No.
4099	**86536**	**2009/05/01 18:45**	**2005/05/01 20:03**	**16-45.21 [S] 105-20.41[W]**	**P21-080**
4042	**86510**	**2005/05/03 08:16**	**2009/05/03 09:15**	**16-44.51 [S] 107-19.90[W]**	**P21-087**
4101	**86537**	**2009/05/04 05:54**	**2009/05/04 06:35**	**16-45.05 [S] 109-59.34[W]**	**P21-095**
4043	**86511**	**2009/05/05 04:05**	**2009/05/04 04:52**	**16-44.99 [S] 112-41.19[W]**	**P21-099**
4102	**86538**	**2009/05/05 18:37**	**2009/05/05 19:37**	**16-45.33 [S] 114-40.55[W]**	**P21-102**

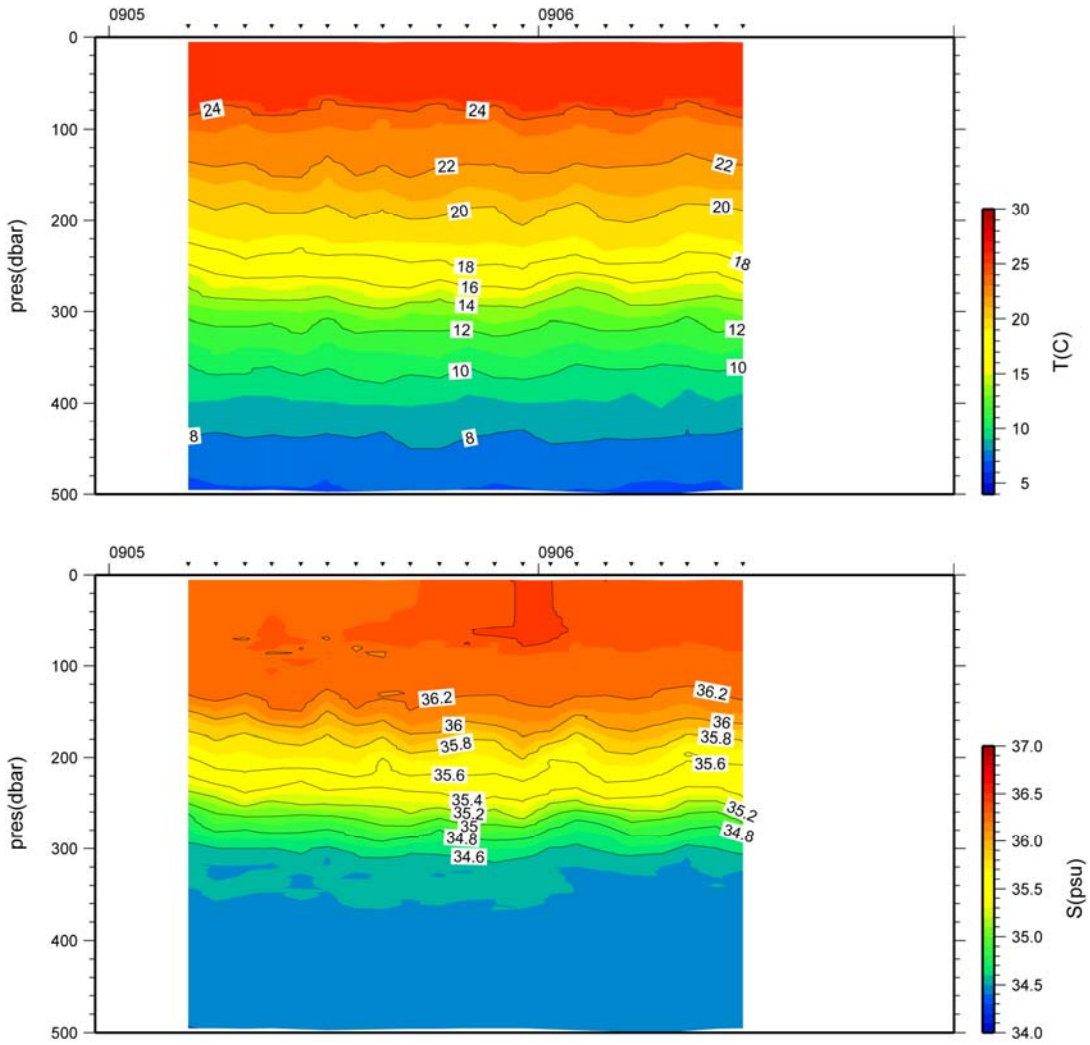

Figure 4.1-1 The time series of vertical profiles of sea-water temperature (top) and salinity (bottom) observed every two days by the floats whose WMO_ID is 3900858.

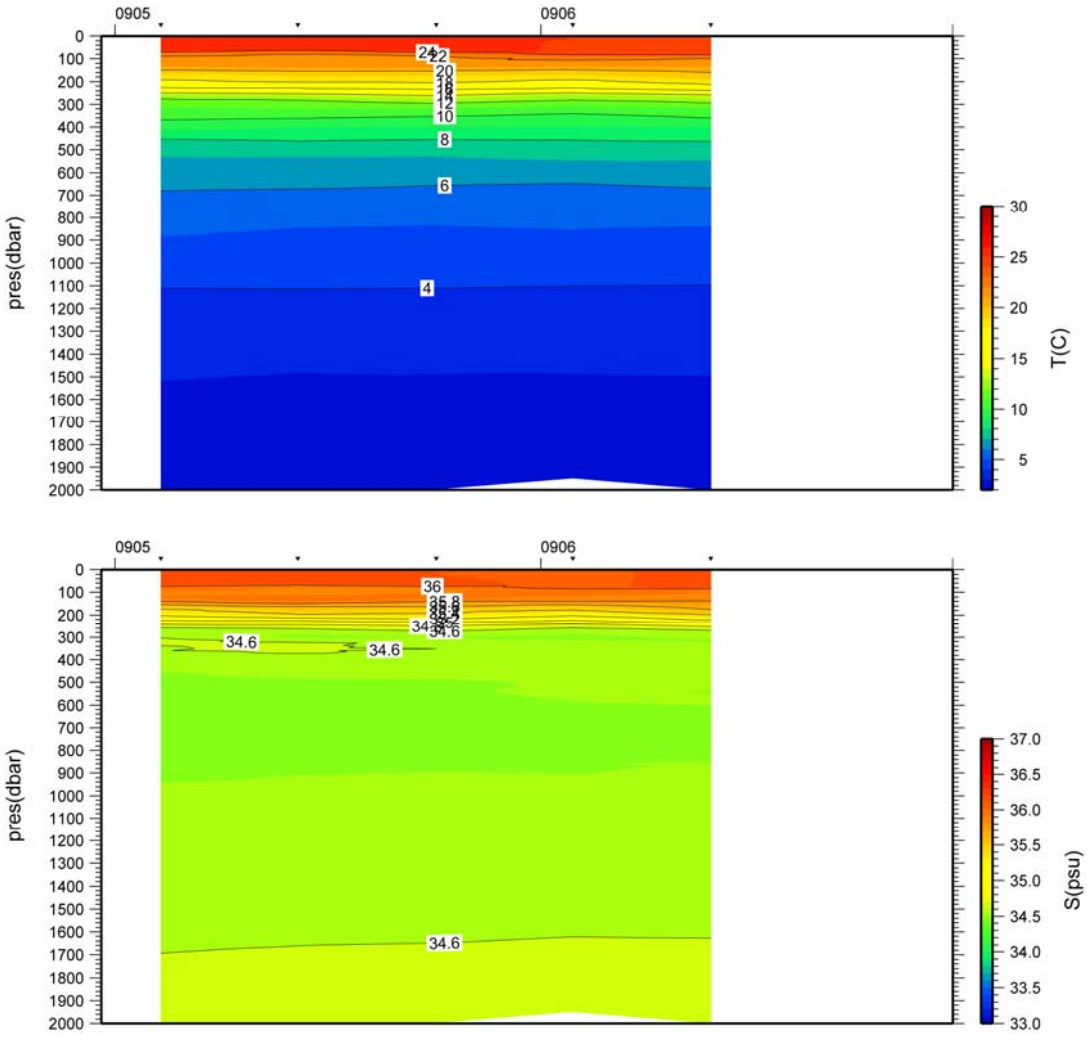

Figure 4.1-2 The time series of vertical profiles of sea-water temperature (top) and salinity (bottom) observed every ten days by the floats whose WMO_ID is 3900855.

III. Notice on Using

This cruise report is a preliminary documentation as of the end of the cruise. It may not be corrected even if changes on content (i.e. taxonomic classifications) are found after publication. It may also be changed without notice. Data on the cruise report may be raw or not processed. Please ask the Chief Scientist for the latest information before using.

Users of data or results of this cruise are requested to submit their results to Data Integration and Analysis Group (DIAG), JAMSTEC.